UNLV University Libraries
University of Nevada, Las Vegas

UNLV Theses, Dissertations, Professional Papers, and Capstones

12-2010

Improving ensemble streamflow prediction using interdecadal/ interannual climate variability

Kenneth W. Lamb
University of Nevada, Las Vegas, kwlamb@csupomona.edu

Follow this and additional works at: https://digitalscholarship.unlv.edu/thesesdissertations

Part of the Civil and Environmental Engineering Commons, Climate Commons, Environmental Monitoring Commons, and the Water Resource Management Commons

Repository Citation

Lamb, Kenneth W., "Improving ensemble streamflow prediction using interdecadal/interannual climate variability" (2010). *UNLV Theses, Dissertations, Professional Papers, and Capstones*. 718.
https://digitalscholarship.unlv.edu/thesesdissertations/718

This Dissertation is protected by copyright and/or related rights. It has been brought to you by Digital Scholarship@UNLV with permission from the rights-holder(s). You are free to use this Dissertation in any way that is permitted by the copyright and related rights legislation that applies to your use. For other uses you need to obtain permission from the rights-holder(s) directly, unless additional rights are indicated by a Creative Commons license in the record and/or on the work itself.

This Dissertation has been accepted for inclusion in UNLV Theses, Dissertations, Professional Papers, and Capstones by an authorized administrator of Digital Scholarship@UNLV. For more information, please contact digitalscholarship@unlv.edu.

IMPROVING ENSEMBLE STREAMFLOW PREDICTION USING INTERDECADAL/INTERANNUAL CLIMATE VARIABILITY

by

Kenneth W. Lamb

Bachelor of Science, Civil Engineering
University of Nevada, Las Vegas
2003

Masters of Civil Engineering
Norwich University
2007

A dissertation submitted in partial fulfillments of
the requirements for the

Doctor of Philosophy in Engineering
Department of Civil and Environmental Engineering
Howard R. Hughes College of Engineering

Graduate College
University of Nevada, Las Vegas
December 2010

Copyright by Kenneth W. Lamb 2011
All Rights Reserved

UNLV
UNIVERSITY OF NEVADA LAS VEGAS

THE GRADUATE COLLEGE

We recommend the dissertation prepared under our supervision by

Kenneth W. Lamb

entitled

Improving Ensemble Streamflow Prediction Using Interdecadal/ Interannual Climate Variability

be accepted in partial fulfillment of the requirements for the degree of

Doctor of Philosophy in Engineering
Civil and Environmental Engineering

Thomas C. Piechota, Committee Chair

Jacimaria Batista, Committee Member

Sajjad Ahmad, Committee Member

Ashok K. Singh, Committee Member

Susanna Priest, Graduate Faculty Representative

Ronald Smith, Ph. D., Vice President for Research and Graduate Studies
and Dean of the Graduate College

December 2010

ABSTRACT

Improving Ensemble Streamflow Prediction Using Interdecadal/Interannual Climate Variability

by

Kenneth W. Lamb

Thomas C. Piechota, Examination Committee Chair
Professor of Civil Engineering
University of Nevada, Las Vegas

The National Weather Service's (NWS) river forecast centers provide long-term water resource forecasts for the main river basins in the U.S. The NWS creates seasonal streamflow forecasts using an ensemble prediction model called the Extended Streamflow Prediction (ESP) software. ESP creates runoff volume forecasts by taking the current observed soil moisture and snowpack conditions in the basin and applying them to historical temperature and precipitation scenarios. The ESP treats every historic input year as a likely scenario of future basin conditions. Therefore improving the knowledge about how long-term climate cycles impact streamflow can extend the forecast lead time and improve the quality of long-lead forecasts.

First, a study of the existing climate indices is carried out in Chapter 3 to establish which index shows a significant long-lead connection to the Colorado River Basin (CRB). Using Singular Value Decomposition (SVD) this step identifies a 1-year lagged relationship between the Pacific Ocean sea surface temperatures (SST) and CRB streamflow. A new SST region is identified in this analysis (named the Hondo region) and compared to the other established climate indices (e.g. SOI, PDO, NAO, AMO). The tests demonstrate Hondo performs better at longer lead times than the existing climate indices.

Second, Chapter 4 identifies the climate cycles impacting the CRB streamflow. The SVD analysis performed in Chapter 3 is extended to include the simultaneous (or 0-year lag) as well as the 2nd and 3rd year lag times. Because SST's and streamflow are basically independent data, this chapter explains the physical connection between them by analyzing the relationship between the ocean, atmosphere and CRB streamflow. This analysis, as well as recent research into the Pacific Quasi-Decadal Oscillation (PQDO), demonstrates that the CRB streamflow is dominated by a hierarchy of climate drivers. The Hondo is the secondary level which exists between the extreme impacts of the ENSO signal and the longer cyclical patters observed in the PQDO. The current research shows that the QDO cycle leads precipitation by three years, and the Hondo leads the CRB by one to two years.

Finally, the information from Chapter 4 reveals that the Hondo region can be used as a basis for weighing the ESP output. This is done because water resource managers create multi-year water plans that are utilized to project power generation supplies and water system improvements. In Chapter 5 several methods of weighing the ESP output based on the Hondo region are presented. Each method is assessed using parametric and non-parametric forecast skill metrics. The overall goal of this chapter is to identify a weighting technique, lag time, and season interval which show a marked improvement over simply using the 30-year mean as a streamflow predictor. From this analysis the forecast skill score is optimized when using the January – March average SST values as a basis for forecasting the streamflow for the following water year.

TABLE OF CONTENTS

ABSTRACT ... iii

LIST OF FIGURES ... viii

CHAPTER 1 INTRODUCTION ... 1
1.1 Research Problem ... 1
1.2 Long Lead Ensemble Streamflow Forecasting ... 2
1.3 Water Resource Planning Forecasts in the Colorado River Basin ... 3
1.3.1 CRB Forecasts and the 24-Month Study ... 5
1.4 Existing CRB-Climate Teleconnections ... 6
1.5 Research Questions ... 8
1.6 Research Tasks – Question 1 ... 9
1.6.1 Establishing a Long Lead Climate-Streamflow Teleconnection ... 9
1.6.2 Defining the SST-Streamflow Teleconnection ... 10
1.6.3 Inter-comparison of Climate Indices ... 12
1.6.4 Testing Forecast Potential ... 13
1.7 Research Tasks – Question 2 ... 14
1.7.1 Extended SVD and Correlation Analysis ... 14
1.7.2 Comparison With Current Research ... 15
1.8 Research Tasks – Question 3 ... 17
1.8.1 Weight Kernel Selection ... 17
1.8.2 Cross-Validation Forecast Skill ... 20

CHAPTER 2 LITERATURE REVIEW ... 22
2.1 Introduction ... 22
2.2 Streamflow Forecasting ... 22
2.3 Pacific Ocean Climate Indices ... 24
2.3.2 Pacific Decadal Oscillation ... 27
2.4 Atlantic Ocean Climate Indices ... 29
2.4.1 Northern Atlantic Oscillation ... 29
2.5 Global Gridded Climate Data ... 34
2.5.1 Sea Surface Temperature Data ... 34
2.5.2 Geopotential Height ... 38
2.5.3 Zonal Wind Field ... 38
2.6 Colorado River Basin Streamflow/Forecast Data ... 40
2.7 Summary of Data ... 42

CHAPTER 3 A BASIS FOR IMPROVING STREAMFLOW FORECASTING OF THE COLORADO RIVER BASIN ... 44
3.1 Introduction ... 44
3.2 Data 47
3.2.1 Naturalized Streamflow ... 47
3.2.2 SST and Climate Index Data ... 48
3.3 Methodology ... 50

3.3.1 Rank Sum Analysis 50
3.3.2 Combination of Indices 52
3.3.3 SVD Analysis of Pacific Ocean SSTs 53
3.3.4 Forecast Skill Comparison 56
3.4 Results 57
3.4.1 Climate Indices 57
3.4.2 Pacific Ocean SSTs 60
3.4.3 Forecast Skill Comparison Results 65
3.5 Conclusion 67

CHAPTER 4 CONNECTING THE PACIFIC OCEAN TO THE COLORADO RIVER BASIN 68
4.0 Introduction 68
4.1 Data 70
4.1.1 Streamflow Data 70
4.1.2 Climate Data 71
4.2 Methodology 72
4.3 Analysis Results 74
4.4 Discussion 83
4.4.1 Climatology 83
4.4.2 The Lagged Relationship 87
4.5 Summary and Conclusions 90

CHAPTER 5 TESTING A POST-ANALYSIS WEIGHTING TECHNIQUE TO IMPROVE lONG-LEAD FORECASTS OF THE COLORADO RIVER BASIN 92
5.1 Introduction 92
5.2 Data 94
5.2.1 Streamflow Data 94
5.2.1 Sea Surface Temperature Data 95
5.3 Methodology 97
5.3.1 Weighting Kernels 98
5.3.2 Forecast Development 100
5.3.3 Forecast Skill Scores 101
5.3.4 Average Skill Score 103
5.4 Results 104
5.4.1 Forecast Skill Results Summary 104
5.4.2 Forecast Skill Maps 107
5.4.3 Forecast Time Series 109
5.5 Conclusions and Recommendations 116

CHAPTER 6 CONCLUSIONS AND RECOMMENDATIONS 118
6.1 Contributions 118
6.2 Recommendations for Future Work 120

APPENDIX 1 122

APPENDIX 2 220

REFERENCES 239

VITA ……..... 256

LIST OF FIGURES

Figure 1.1 Depiction of 3-month and 6-month lag-lead analysis 11
Figure 1.2 Combination rank sum testing using the SOI as a basis..... 13
Figure 1.3 Depiction of extended 3-month analysis of climate data 15
Figure 2.1 Mean SOI values 1951-2009 (monthly-grey / yearly-black)..... 26
Figure 2.2 Mean PDO values 1950-2007 (monthly-grey / yearly-black) 28
Figure 2.3 Mean NAO values 1950-2009 (monthly-grey / yearly-black)..... 31
Figure 2.4 Mean AMO values 1950-2009 (monthly-grey / yearly-black) 33
Figure 2.5 60S -60N ERSST Annual Anomaly (1880 – 2009) 35
Figure 2.6 Location Map showing the limits of the SST data. 37
Figure 2.7 Location map of 29 USGS streamflow gauges..... 41
Figure 3.1 Location map of 29 USGS streamflow gauges..... 49
Figure 3.2 Depiction of 3-month and 6-month lag-lead analysis 51
Figure 3.3 Combination rank sum testing using the SOI as a basin 53
Figure 3.4 Number of significant results of the rank sum test 59
Figure 3.5 6-month left and right heterogeneous correlation maps ($|r| \geq 0.27$)..... 61
Figure 3.6 3-month left and right heterogeneous correlation maps ($|r| \geq 0.27$)..... 62
Figure 3.7 Plots showing contribution of index to forecast skill. 66
Figure 4.1 Location map of 29 USGS streamflow gauges..... 71
Figure 4.2 Lagged analysis schematic 73
Figure 4.3 0-year and 1-year lag correlation maps from SVD analysis..... 75
Figure 4.4 2-year and 3-year lag correlation maps from SVD analysis..... 76
Figure 4.5 0-year and 1-year Z500 correlation maps..... 79
Figure 4.6 2-year and 3-year Z500 correlation maps..... 80
Figure 4.7 0-year and 1-year U200 correlation maps 81
Figure 4.8 2-year and 3-year U200 correlation maps 82
Figure 4.9 Zonal wind field (a) and sea level pressure (b) climatology maps. 84
Figure 4.10 Comparison between 1983 and 2003 ENSO Events..... 86
Figure 5.1 Location map of 29 USGS streamflow gauges..... 96
Figure 5.2 Schematic showing how P_f and P_o are obtained from the eCDF..... 103
Figure 5.3 Maps showing average skill score results..... 108
Figure 5.4 Scatterplots from Alternative 2 (Observed vs. Forecast) 110
Figure 5.5 Scatterplots from Alternative 3 (Observed vs. Forecast) 111
Figure 5.6 0-year lag forecast relative errors for eight gauge locations..... 112
Figure 5.7 1-year lag forecast relative errors for eight gauge locations..... 113
Figure 5.8 2-year lag forecast relative errors for eight gauge locations..... 114

CHAPTER 1

INTRODUCTION

1.1 Research Problem

This dissertation seeks to improve the quality and length of lead time used in ensemble forecasts of streamflow. The basic concept of ensemble forecasting can be explained as the use of some initial states (observed climate data) being applied as input into numerical weather models which simulate climate patterns. The process produces various model outputs, or traces, which are the result of answering the question: what would have happened in the past if the current initial conditions had been present? The number of traces created by the ensemble forecast model produces a probability distribution of time series data, from which, the mean trace or 95% confidence limits can be extracted.

The use of ensemble forecasting has been developing for several decades. Gleeson (1961, 1970) introduced the concept of defining the probability space of a given climate field while using quantum mechanics and statistical mechanics to define a final distribution, or ensemble, of forecast values. Epstein (1969) also provided some theoretical and practical approaches to handle the issue of uncertainty in numerical weather prediction (NWP) forecasts. However, the theoretical equations proved to be extremely complicated and still were not capable of capturing enough of the atmospheric uncertainty to generate a reliable forecast. Building upon this research Leith (1974) proposed and tested the skill of approximating the stochastic dynamic forecasting technique introduced by Epstein by using Monte-Carlo methods. Since Monte-Carlo

methods are used to generate ensemble forecasts, the improvement in computing resources has automatically improved the frequency and quality of the forecasts.

In the short term (3 – 7 days) ensemble forecasts have demonstrated good accuracy, but more importantly, the uncertainty of these forecasts is fairly well known. Once there is a shift from short-term to mid-term (10 – 30 days) forecasts, as well as long-term forecasts (monthly – seasonal) the significant autocorrelation of the climate states is eliminated and the model becomes heavily dependent upon the accuracy of the initial condition's estimate and the NWP model (Wilks, 2006).

1.2 Long Lead Ensemble Streamflow Forecasting

The use of ensemble forecasts for climate forecasts is virtually the same for making streamflow forecasts, except that streamflow forecasts require a hydrologic modeling component to convert the forecasted temperature and precipitation data into surface runoff or snow pack. Therefore the first step to increasing the forecast lead time is to incorporate knowledge of how the volume of water stored as snowpack contributes to runoff in the spring. Whether using an ensemble streamflow forecasting technique or not, understanding the relationship between a basin's snowpack and spring runoff can extend the forecast lead time (Miller et al, 2006; Grantz et al., 2005; Simpson et al., 2004; Cayan and Peterson, 1989).

A second method to extending streamflow forecast lead times is to utilized climate data which demonstrates interannual, or even interdecadal persistence. In this scenario, a climate event must have the ability to remain in an anomalous phase (observations which are significantly higher or lower than the expected seasonal values) for much longer than the forecast lead time. There are many climate indices that have

been defined to represent persistent climate variability including the Pacific Decadal Oscillation (PDO), El Niño Southern Oscillation (ENSO), North Atlantic Oscillation (NAO) and the Atlantic Multi-decadal Oscillation (AMO). While the discussion of how each of these climate indices has been used in research is given in Chapter 2, it is important to point out that this list is not exhaustive, nor is it impossible to expect that there are other climate patterns not currently defined by a climate index which may improve long-lead forecasts.

1.3 Water Resource Planning Forecasts in the Colorado River Basin

For stakeholders of the Colorado River Basin (CRB), having a better estimate of the streamflow before the spring runoff begins is necessary for them to make effective water management decisions. Water resource projection generated prior to a given water year are typically heavily dependent upon the historical average of runoff for the CRB, or historically ambivalent water-year outlooks which are modeled assuming all input years have equally probable impact on the coming year's streamflow. In order to assist water managers of the CRB, the National Weather Service's (NWS) Colorado Basin River Forecast Center (CBRFC) issues three different types of forecasts.

The first CBRFC water supply forecast is a 3-month forecast of monthly water volumes issued at the start of each month throughout the year. The second forecast is a 4-month lump sum water volume for the April – July runoff period. This forecast is issued starting January 1 of each year and updated monthly through July 1. The final forecast is actually referred to only as an "outlook" for the coming water year. While this water-year outlook is generated using the same tool as the April – July forecast, there is less confidence in the output value for several reasons, including: lack of research

supporting 12-month forecasts, and unknown uncertainty in the model. The outlook is issued on August 1 and then updated on October 1 (NWS CBRFC staff, personal communication, 2008).

All three forecasts are generated using the same analysis tool: the Extended Streamflow Prediction (ESP) software (Day, 1985). ESP forecasts are calibrated on the observed soil moisture, climate (Temperature and Precipitation) and runoff data from the 30 period of 1976-2005. The observed soil moisture conditions and snowpack measurements (if available) are used as the initial conditions for the ESP model. The ESP uses the initial conditions and creates a time series of daily streamflow values (also known as a "trace") by applying a time series of temperature and precipitation values from a year in the calibration period (e.g. 1976). In all, the ESP analysis creates 30 output traces: one for each calibration year. From these 30 values, the median is reported as the forecast value, and the 5^{th}, 10^{th}, 90^{th}, and 95^{th} quartiles are reported as different confidence intervals (NWS CBRFC staff, personal communication, 2009).

The April – July forecast is unique in that it is created in coordination with the National Resource Conservation Service (NRCS) who generate their own forecast for the runoff season (April-July) each year. Before the CBRFC forecast is officially issued to the CRB stakeholders, CBRFC and NRCS staff meet to discuss their separate forecast results before issuing the "coordinated" runoff forecast for the CRB (NWS CBRFC staff, personal communication, 2008).

After the ESP generates its forecast traces certain years can be assigned more significance than others based on climatic similarities between the forecast year and the calibrated historical years. Research related to finding a post-analysis weight method has

been done on the April – July forecasts while using the average November – January Niño3.4 index as a predictor of seasonal streamflow (Werner et al, 2004). Werner et al. were able to define a weighting technique for the April – Forecasts created by the ESP at two locations within the CRB, but because of the poor El Niño Southern Oscillation (ENSO) impact in the northern regions of the basin, the weighting technique was, predictably, non-significant. Also noticeably absent from this paper was any discussion about how this research can improve forecasts (or outlooks) created more than a few months ahead of the spring runoff. As such was the case, currently no research has been done to improve the water-year outlook created by the ESP.

1.3.1 CRB Forecasts and the 24-Month Study

Whether it is the 3-month forecasts, the April – July forecast, or the water year outlook, the forecast, and outlook, values are reported for a dozen locations in the upper CRB. The USBR uses the ESP and ESP/NRCS forecasts to create a 24-month projection of water resource storage and releases along the CRB by modeling the forecast inputs through the river basin modeling tool, RiverWare. The 24-month study uses the ESP-generated forecasts as the primary input into the RiverWare model for the first year of the study. The second year of the study uses the 30-year average (1976-2005) observed streamflow values to continue their release/storage projections based on the various treaties, compacts, laws, and court decisions which make up the "Law of the River". The 24-month study is then issued to all stakeholders of the Colorado River including fish and wildlife, power generation and water consumption managers, all of whom use this information in their operation plans (USBR staff, personal communication, 2009).

There are many studies which demonstrate the uses of the 24-month study with respect to CRB water resources. Background information into computer models used to manage storage and release schedules can be found in Schuster (1989), Fulp et al, (1991), and Zagona et al, (2001). Most of the research regarding modeling of CRB streamflow and the 24-month study, try to simulate policy decisions on future river conditions based on using the Law of the River as constraints in the 24-month study (Stevens, 1986; Booker, 1995; Sangoyomi and Harding, 1995; Fulp et al, 1991; Gilmore et al., 2000). One study touched on the inputs and assumptions of the 24-month study (Garrick, et al, 2008). However, there are no studies which examine the quality of the 24-month study inputs, or ways to improve them.

1.4 Existing CRB-Climate Teleconnections

Recent research has provided many tools for the climate scientist to understand the connection between large-scale climate inputs (for example, sea surface temperatures (SST) and sea level pressure) with surface climate over the United States (Ropelewski and Halpert, 1986, 1989; Latif and Barnett, 1994; McCabe and Dettinger, 1999; Rajagopalan et al., 2000; Hidalgo, 2004; McCabe et al., 2007). Due to the recent drought conditions in the desert southwest, much of this research focuses on ways to describe the changes Colorado River Basin (CRB) streamflow by observing large-scale climate variability over the Pacific Oceans (Grantz et al., 2005; Kim et al. 2006; Kim et al. 2007). The well known relationships between SST/SLP data and streamflow of the western United States are attributed to the El Niño Southern Oscillation (ENSO). However, there are limitations to what information the ENSO can provide water managers of the CRB (McCabe and Dettinger, 2002).

The first limitation is that the effects of the ENSO, while easily correlated with surface climate of the northwestern and southwestern areas of the United States (Ropelewski and Halpert, 1986), has a poor signal over a large area covering central California, Nevada, Utah, Colorado and Wyoming which does not respond consistently to ENSO variability (Hidalgo and Dracup, 2003; Kahya and Dracup, 1993; Kahya and Dracup 1994b). Clark et al. (2001) supposes that this region is a transition area between the positive ENSO-Streamflow correlation of the southwest, and the negative ENSO-Streamflow correlation of the northwest. Because of the focus on ENSO signals over larger regions of the U.S., there is no research that shows if any other climate index demonstrates significant correlation with the entire CRB.

Another limitation to the ENSO is that its effect on surface hydrology of the western U.S. has a lead time which does not lend itself to improving the long-lead forecasts used in the 24-month study. McCabe and Dettinger (2002), who tested a lagged response between ENSO and snowpack in the upper Rocky Mountains, found that summer-fall ENSO observations were correlated with snowpack measurements in the western U.S. Since snowpack measurements are well correlated with spring runoff (Clark et al., 2001), this provided the potential for forecasting the April – July runoff about 7 months before the predictand period. In order to improve the ESP outlook the research needs to show a relationship between the entire water year (October – September and not just April – July) volume, and the months leading up to that year. There are no studies which examine the limit of the lag response between the established climate indices and CRB streamflow.

1.5 Research Questions

The overall goal of the proposed research is to develop an approach which is capable of improving the existing ESP outlook by establishing a weight methodology that will be applied to the ESP output to generate a new forecast. This goal is broken down into the following three research questions:

Question 1: Which large-scale climate patterns demonstrate a long-lead connection to most of the streamflow in the CRB?

Hypothesis 1: A 1-year lagged teleconnection will be identified, but it will most likely not be associated with an established climate index.

Question 2: How does the Pacific Ocean climate impact streamflow in the Colorado River Basin?

Hypothesis 2: The Pacific Ocean – CRB connection will be explained through analysis of atmospheric data and demonstrate a significant correlation with streamflow gauges in the CRB

Question 3: Which climate lag-time and weight technique combination demonstrates the greatest potential for generating successful forecasts?

Hypothesis 3: The optimal forecasting approach will improve upon the use of climatology as a forecast value and provide a basis for testing the ESP output

1.6 Research Tasks – Question 1

1.6.1 Establishing a Long Lead Climate-Streamflow Teleconnection

Question No. 1: Which large-scale climate patterns demonstrate a long-lead connection to most of the streamflow in the CRB?

The most well understood atmospheric or oceanic patterns used in research include the El Niño Southern Oscillation (ENSO) as represented by the Southern Oscillation Index (SOI), the Pacific Decadal Oscillation (PDO), the Northern Atlantic Oscillation (NAO), and the Atlantic Multidecadal Oscillation (AMO). While there are many more climate indices representing different areas of the globe, these four are most often used in research when trying to define Climate-Hydrology teleconnections. Therefore these climate indices will form the foundation of the first question. Aside from the existing climate indices an SST index will be "created" for the CRB and then compared to the other established climate indices. All of the teleconnections are established using the climate data from a given water year with the streamflow volumes of the following water year. A full description of the data and the origin of each data set is given in Chapter 2.

The first step to find an answer to the first question is summarized into the following tasks:

1a) Define an SST region of the Pacific Ocean using Singular Value Decomposition (SVD).

1b) Compare the existing climate indices with the SVD results using Rank Sum testing

1c) Assess the forecast potential of the results from (1a) and (1b) by creating a sample forecast using a weighted kernel approach to optimize forecast skill score.

1.6.2 Defining the SST-Streamflow Teleconnection

Yarnall and Diaz (1986) suggested the potential to create basin-specific indices. In light of the suggestion, the basic concept of Singular Value Decomposition (SVD) is to provide an understanding of the covariance between two spatially distributed datasets (Prohaska, 1976). Therefore the application of this method can work for finding the contribution of one data field upon another, so long as the have the same number of observations. Since this is the case the application of this method has appeared widely in research whose aim is to describe the covariance of two meteorological data sets (Oikonomou et al., 2010; Grassi et al., 2009; Yang, 2009; Wu et al., 2007; Skinner et al., 2006; Tootle and Piechota, 2006; Xue et al., 2005; Shabbar and Skinner, 2004; Kim et al., 2002; George and Saunders, 2001; Cholaw and Liren, 1999; Nakamura, 1996). The utility of SVD was compared to other analysis techniques by Bretherton et al. (1992) and its companion paper Wallace et al. (1992). In general, SVD is ideal for climate analysis because it provides a non-parametric explanation of the climatic contribution of one dataset on another.

The use of SVD in the proposed work will use the 3-month average and 6-month average SST values of a 2º SST grid from 120º East to 80º West and 20º South to 60º North. These two monthly averages are chosen arbitrarily, but they are intended to reflect a season, or two seasons, of SST data. SVD analysis is run for various lag times to find the optimal long-lead lag time. Figure 1.1 shows how each lag time will be tested. Since the goal is to improve the forecasts for the following water year, the initial lag time

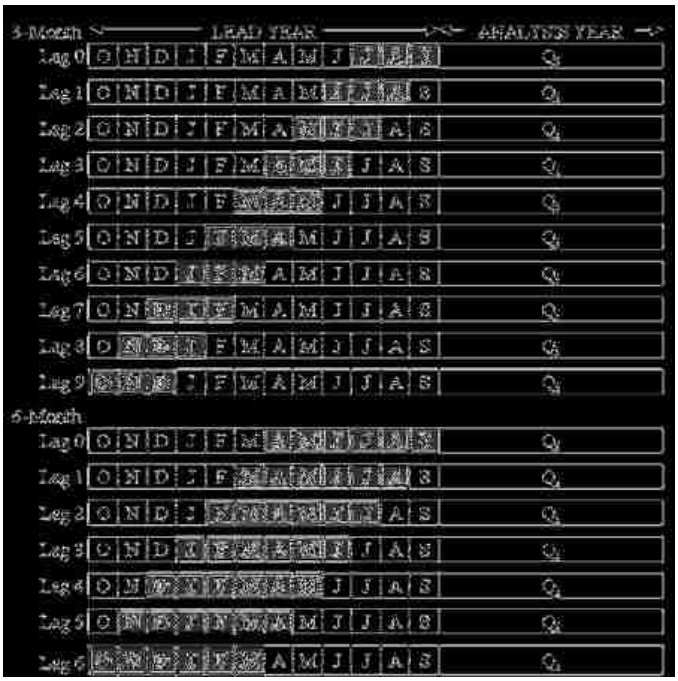

Figure 1.1 Depiction of 3-month and 6-month lag-lead analysis
(Qi = yearly total runoff measured at station i)

(lag 0) is the July-September SST average and the April – September SST average for the 3-month and 6-month analyses respectively. Therefore, Lag 1 is the June-August SST average and March-August SST average for the 3-month and 6-month analyses respectively. Each lag represents a one month step back in time, and there are lags generated until reaching the start of the previous water year (for example October-December for the 3-month, lag 9; and October-March for the 6-month, lag 6).

The output of the SVD analysis will be mapped to show regions where the covariance is significant ($\alpha = 0.05$) between the SST gird location and a given streamflow gauge in the CRB. These maps will help identify a specific region which represents the strongest covariance with CRB streamflow. In addition to the maps the SVD also provides a Temporal Expansion Series (TES) which resembles the properties of a

standardized climate index. The SVD TES can then used to compare its performance with the other existing climate indices using the Rank Sum Test.

1.6.3 Inter-comparison of Climate Indices

As mentioned earlier the comparison of the climate indices is performed using the two-sample Rank Sum test. This is a non-parametric test where the null hypothesis is that two datasets have the same distribution (Alder and Roessler, 1977; Mann and Whitney, 1947; Wilcoxon, 1945). By statistical proof, this test also shows that the median between two data sets are similar (Kvam and Vidakovic, 2007). This test has many applications across many fields. Therefore it is not surprising to find it used in climate data analysis (Timilsena et al., 2009; Miller and Piechota, 2008; Timilsena, et al., 2007; Baughman et al. 1976). The test is considered robust and resistant because it performs nearly as well as the t-test and it is not easily affected by outliers (Wilks, 2006).

The Rank Sum test is used in the proposed research to test if the positive or negative phase of a given climate variable has a significant impact on observed streamflow. Streamflow observed under an index's positive are compared to streamflow values observed under the negative phase to see if their median values are significantly different. Similar to the lagged SVD analysis the Rank sum testing will be completed for various lag intervals (See Figure 1.1) using the 3-month and 6-month average index values, for each of the four (4) existing climate indices (SOI, PDO, NAO, AMO).

After each climate index is tested alone, the rank sum testing is completed for the SOI-coupled variables. Here the positive and negative phases of the PDO, NAO and AMO are tested based on the positive and negative phase of the SOI. Figure 1.2 shows how the coupled analysis will take place. As an example, during input years where the

SOI was in a positive phase the streamflow observed under a positive PDO phase was compared to those observed under a PDO negative phase. A similar test is completed for the PDO-positive versus PDO-negative under the SOI negative phase. The coupled index analysis is performed because research has demonstrated that the phases of the PDO, AMO, and NAO can augment or dampen the effects of the ENSO based on its phase (Timilsena, 2007).

Six (6) coupled index testing scenarios are proposed along with four (4) stand-alone scenarios. These ten tests are then compared to the rank sum testing using the SVD's TES as a stand-alone index. In all, a total of 12 rank sum test scenarios are run for comparison purposes.

Figure 1.2 Combination rank sum testing using the SOI as a basis

1.6.4 Testing Forecast Potential

In order to determine the forecast potential of the results obtained thus far the three Pacific Ocean indices (SOI, PDO, SST) will be used in a forecasting technique designed by Piechota et al. (1998). The results of this technique demonstrate the contribution of each climate input to the overall forecast skill generated by assigning each input a weight between -1.0 and 1.0 to optimize the combined forecast skill score as

determined by the Linear Error in Probability Space (LEPS) score (more details about the LEPS score are provided below).

1.7 Research Tasks – Question 2

Question No. 2: How does the Pacific Ocean climate impact streamflow in the Colorado River Basin?

Since the analysis from Task 1 may solely be a statistical relationship, it is necessary to analyze further the physical connection linking Pacific Ocean Climate with Colorado River Streamflow. To accomplish this goal the following subtasks are proposed:

2a) Use SVD on datasets which represent atmospheric climate fields such as zonal wind, geopotential height, and/or sea level pressure to identify the physical connection between Pacific Ocean SSTs and CRB streamflow

2b) Compare the SVD analysis to current research into Pacific Ocean teleconnections with the intermountain west to identify common patterns between the proposed work and other research

1.7.1 Extended SVD and Correlation Analysis

This analysis will proceed in a similar manner with Task 1a. The difference here is that this analysis will take place over a period of four (4) lag years rather than just one (1). In order to compare this analysis with the results in Task 1a the SVD analysis of the SST-CRB relationship will also be extended to cover the same number of lag years as the climate research. This subtask aims to identify persistent ocean and climate patterns most closely associated with the CRB. The 3-month average SST, or climate values are compared with streamflow volumes from the "Analysis Water Year" (see Figure 1.3)

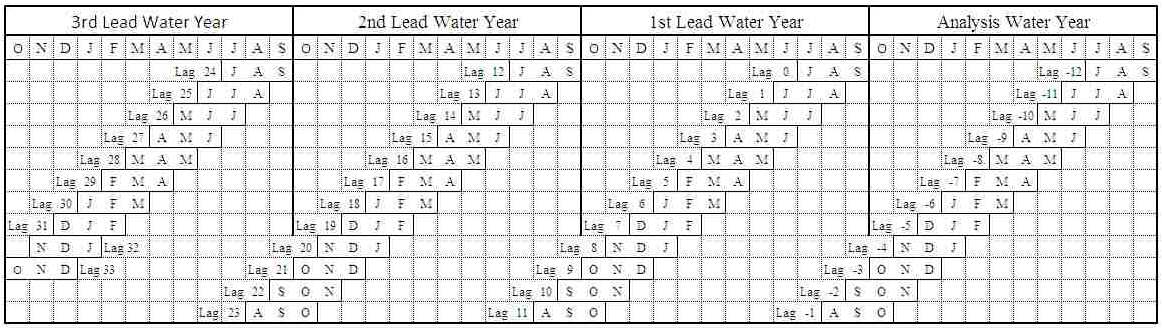

Figure 1.3 Depiction of extended 3-month analysis of climate data

The SVD on the SST – Streamflow covariance matrix gives three matrices [SVD(covarTS) = $U \Sigma V$], where V represents the decomposed covariance values closely associated with the streamflow. Therefore, given the decomposed matrix, V, and the original matrix of streamflow anomalies, S, the streamflow temporal expansion series (STES) is determined by the following equation: $STES = V'S'$. The result of this calculation is a series of values, one for each time period in V and S. Once calculated, the STES is then correlated with cell of the Z500 and U200 gridded data.

1.7.2 Comparison With Current Research

There are several studies by Wang et al. (2009, 2010a, 2010b, 2010c) that are significant to the proposed work trying to establish a connection between the Pacific Ocean and CRB Streamflow. These studies represent an analysis of the long-lead climate drivers of precipitation in the intermountain west region of the U.S. The reason these studies are of importance to the proposed work is that they identify the physical relationship between the Pacific Ocean cycles and the lagged response in precipitation.

According to several studies (Ely et al. 1994; Harnack et al., 1998; Schafer and Steenburgh 2008) the precipitation in the intermountain west is typically produced by transient synoptic activity (i.e. cyclone waves and the interaction of frontal passages with

orography - the spatial variation in the atmosphere). Wang et al (2009) identified that the Pacific Ocean SSTs have a 10-20 year cycle, and that this cycle leads a precipitation cycle of similar length by about 3-years. Wang et al (2010a) show that the Pacific Ocean cycles are actually closer to 12 years and are best represented by the central equatorial region of SSTs (essentially the Niño4 region: 5˚N-5˚S and 160˚E-150˚W). This study analyzed the water vapor flux data in order to identify the leading modes of the transient synoptic activity impacting the intermountain west. The results of this analysis showed that there is a 3-year lag between the first two principle components of the moisture flux data, and the first component is highly correlated with the Niño4 data and the second component is highly correlated with the precipitation cycle.

The work of Wang et al (2010c) analyzed the moisture flux potential data to determine the specific mechanism drawing storm activity into the intermountain west region. The second mode of the principle component analysis revealed the t short atmospheric wave pattern beginning in western tropical region (east of the Philippines) and ending off the coast of the pacific Northwest coast of the U.S. this wave track is the primary driver of the persistent climate anomalies toward the western U.S.

The works by Wang et al provide the proposed work with a foundation upon which to build. The circulation patterns and leading cycles identified will provide a basis for understanding the results generated in the proposed work. For example since the foundation identifies a 3-year lag time between Pacific Ocean SSTs and the precipitation in the intermountain west, then the proposed analysis should resemble this lag time as well. Also since the short wave track identifies several region of significance between

the tropical pacific and the western U.S. the proposed research should identify at least one of these regions as significant in the SVD analysis.

1.8 Research Tasks – Question 3

Question No. 3: Which climate lag-time and weight technique combination demonstrates the greatest potential for generating successful forecasts?

Building upon the results from the first question the approach to the second question is broken down into the following tasks:

3a) Calculate probability weights for years based on the three most significant SST regions identified in Task 1b using four (4) weighting kernels

3b) Assess forecast skill of kernel-interval input combination using weighted bootstrap technique to create a cross validation forecast for CRB streamflow from 1976-2005

3c) Using the best weight kernel-interval input combination from Task 2b, re-forecast streamflow for 1906 – 1974

1.8.1 Weight Kernel Selection

Four different kernels are selected to create forecast values. The kernel which results in the highest improvement in forecast skill is considered the optimal choice. The first weight kernel is taken from research by Rajagopalan and Lall (1999) which is used in a k-Nearest Neighbor (k-NN) technique to downscale climate data from yearly observations to daily data. The kernel is defined as follows:

$$W1_i = \frac{1/R_i}{\sum_{i=1}^{n} 1/R_i}$$

Here R_i, is the rank of a training year i. The kernel is designed to represent directly the probability of resampling as its weights have a possible values of 0 – 1. Since this weight kernel is based on the rank alone, there is some concern that regardless of the difference in Hondo values, there will always be a year which receives a weight of 1.

The second kernel selected is a linearly distributed proportion based on the absolute differences in SST values. W2 is defined as:

$$W2_i = 1 - \frac{|d_i|}{|d_{i,\max}|}$$

The values d_i and $d_{i,max}$ represent the distance between year i and the forecast year, and the maximum distance calculated from all years, respectively. The absolute value is taken because it does not matter if the training year is more or less than the test year. This kernel has two purposes. First, a given year could only have a resampling value of one if and only if the observed SST is the same as the target year SST. Second, each successive weight is distributed on a roughly linear, but negative, sloping line so that year i has only slightly more weight than year $i+1$. However, since the behavior of this kernel is a decreasing linear distribution of weights, then there is a chance that it will give too much weight to years which are not actually "near" to the target year.

The third weight, $W3$ is given as the inverse distance squared weight:

$$W3_i = \frac{1}{d_i^2}$$

Once again, d_i is the difference between the training year and the forecast year. Because the theoretical values of $W3$ range from $-\infty$ to ∞, the weights for each forecast year are proportioned so that values range between 0 and 1 and their sum is equal to 1. This weight kernel has a plotted behavior similar to $W1$ except that it gives even less weight to

observations with increasing values of d_i. Since this kernel does shift the majority of the weight to the first or second years some relevant information from other years may be ignored.

The final kernel, *W*4 is simply the inverse distance:

$$W4_i = \frac{1}{|d_i|}$$

Both *W*3 and *W*4 are commonly used kernels used in resampling and interpolating applications or as comparisons to other more sophisticated methods. *W*4 does not weigh the closest 1 or 2 as heavily as *W*1 or *W*3, but since it is not linear it also does not distribute the weights to too many of the other, adjacent observations.

Weights are calculated using the raw SST values. A test was run to see if there would be any difference between using raw data and calculating the Hondo anomalies which were used in the SVD analysis (Lamb et al. 2010, Aziz et al,. 2010). The results of this simple test demonstrated that there was no significant difference between the forecast skill score resulting from these two data sets. Additionally, using proportioned weights were compared to raw (un-proportioned) weights to see if the forecast skill is sensitive to either method. The results of this test demonstrated that there was no significant difference. From these two small tests the use of the raw Hondo data is selected for testing because it is simpler to employ, and the proportioned weights are used because they communicate the idea of resampling probability better than the raw weights.

The weighting kernels determine resampling probabilities for each of the 30 years in the analysis period. Since these are being applied to 30 years in the cross-validation analysis, a 30 x 30 matrix of values is created from a given weight kernel. Once matrix of probabilities is created for each weight kernel selected. Since the weight kernels are

also based on which 3-month average SST values are used (i.e. Dec-Feb, Jan-Mar, or Feb-Apr) a total of 12 probability matrices are calculated to generate the forecasts for Task 2b.

1.8.2 Cross-Validation Forecast Skill

Using the results from 2a, the forecasts are generated for each kernel-SST interval. This is done using a weighted bootstrap technique. The bootstrap technique was first developed by Efron (1979, 1982) in order to make estimates of population parameters from relatively small datasets. This method is selected because it, like the other statistical methods proposed in this research, is non-parametric. The current research proposed using the weighted (or generalized bootstrap) method to intentionally introduce a bias to the resampling process (Barbe and Bertail, 1995).

In order to preserve the ~1 year lag between the Pacific Ocean SST region and the streamflow observations the probability weights are actually calculated on the data set from 1975-2004, and then applied to the observed data from 176-2005. The 30 year period from 1976-2005 is significant because this is the current 30 period upon which the CBRFC ESP model is calibrated. Using this 30-year period will provide a better basis for comparison in future research tasks.

The forecast skill score is determined using the Linear Error in Probability Space (LEPS) score. This score was initially developed by Ward and Folland (1991) and further revised by Potts et al. (1996). The score measures the distance between the observed and forecast values in probability space. To do this the LEPS score requires that an empirical distribution function (EDF) be created for each streamflow gauge. The

probabilities for the observed and forecast values are read from the appropriate EDF and then inserted into the following equation developed by Potts et al.:

$$LEPS = 3(1 - |P_f - P_o| + P_f^2 - P_f + P_o^2 - P_v) - 1$$

After the forecast skill is calculated at each location for each year in the cross-validation analysis, the average skill score is determined for each location in the CRB. The average skill score is ranges from -1 to 1 with a score of 0 being as good as forecasting with the mean. Scores which are greater than 10% are considered as "good" skill. These results will help determine which weight kernel, applied to which 3-month average SST interval, was most successful.

CHAPTER 2

LITERATURE REVIEW

2.1 Introduction

The proposed dissertation is based upon several general topics, which include long-lead streamflow forecasting and the data typically used in such forecasting The following chapter describes the basis of research regarding the recent improvements to long-lead forecasting as well as the state of knowledge surrounding the data, which include the Southern Oscillation Index (SOI – measure of the ENSO signal), Pacific Decadal Oscillation (PDO), Atlantic Multi-decadal Oscillation (AMO), and North Atlantic Oscillation (NAO) datasets. Also included in the proposed research is sea surface temperature data, the naturalized/unimpaired streamflow data, and the historic forecast data.

2.2 Streamflow Forecasting

As noted in Chapter 1, the major goal of the proposed dissertation is to improve upon the current knowledge of long lead streamflow forecasting. For many years, deterministic forecasts generated by understanding the relationship between snowpack and spring runoff provided the only methodology to long-term streamflow forecasting (Druce, 2001). In 1975 the Hydraulic Research Laboratory of the NWS in initiated a program to create the Extended Streamflow Prediction (ESP) procedure. Day's (1985) work essentially marked the beginning of ensemble streamflow forecasting procedures even though it did not wholly supplant any other forecasting method then or since (e.g. Krzysztofowicz,1999; Kalra and Ahmad, 2009).

The application of the ESP is not focused on just streamflow forecasting, or has it been limited to the United States. For example Faber and Stedinger (2001) coupled the ESP with a dynamic optimization procedure to analysis optimal reservoir operation policies. Hamlet et al. (2002) used ESP to asses the economic impact of improved streamflow forecasting. As eluded to earlier the ESP has been applied to river basins in other countries such as Israel (Shentsis and Ben-Avi, 2001), Korea (Jeong and Kim, 2005), and Brazil (Souza Filho and Lall, 2003).

In addition to software improvements, some credit to improving long-term forecasting capability should be given to the El Niño event of 1982-1983. Prior to this event much of the research of the Pacific Ocean did not focus on the ENSO as the driving force of climate variability in the United States (Rasmusson and Wallace, 1983). However since this time it is hard to find interseasonal climate research in the Pacific Ocean basin which does not mention the ENSO cycle. The impact of the ENSO provided water resource researchers the tool to connect summer/fall sea surface temperatures in the equatorial Pacific Ocean with the snowpack expected the following winter. Building upon the existing knowledge of the snowpack-spring runoff connection, researchers began using the ENSO to extend the lead time for forecasting streamflow (Hamlet and Lettenmaier, 1999; Clark et al, 2001; McCabe and Dettinger 2002; Werner et al 2004; Grantz et al, 2005). After the ENSO connection was established, other climate indices were identified as having a measurable impact on streamflow in the United States such as the PDO (Hidalgo and Dracup, 2003; Hidalgo, 2004; Beebee and Manga, 2004, Tootle et al., 2005; Timilsena et al., 2009). Therefore the understanding that streamflow

forecasting could take place well in advance of the spring runoff season became a commonly accepted idea by the start of the last decade.

It should be pointed out here that the ESP tool and the use of large scale climate as predictors in long-term streamflow forecasting, have largely been developed without a comprehensive discussion about the model uncertainty (Krzysztofowicz,, 2001). Even thought the ESP output is often communicated in terms of probability (e.g. median forecast with 95% confidence limits), it does not discuss the sampling error imbedded in the model's initial states or the 30 calibrated years used to represent the population of precipitation and temperature time series. ESP and large-scale climate uncertainty is a large enough topic that it would warrant considerable work to fully address. However, for completeness' sake the limitations of the ESP are simply mentioned.

2.3 Pacific Ocean Climate Indices

Data from the Pacific Ocean has been logically linked with many hydrologic responses in the world and especially in the United States, as is demonstrated below. The two most widely used climate indices representing the Pacific Ocean include the Southern Oscillation Index (SOI), representing the ENSO signal, and the Pacific Decadal Oscillation (PDO). The SOI is a measurement of sea level pressure (SLP) and the PDO is a measurement of sea surface temperatures.

2.3.1 El Niño Southern Oscillation

The ENSO is perhaps the most widely known climate variable outside of academic circles. This acronym refers to both the warm and cool phases of the oscillation known as El Niño and La Niña respectively. It was initially observed by Sir Charles Todd, but not named, in the 1880's, but it was ultimately defined by Sir Gilbert

Walker and his collaborators in publications in 1923 and 1932 as a "seesaw" of sea-level pressure (Diaz and Markagraf, 1992). The increase in the South Pacific High diminishes the tradewinds pushing east towards South America which results in warming SST's. As SST's increase so does the evaporation and heating in the troposphere which improves the conditions for "convection and rainfall" (Diaz and Markagraf, 1992).

Currently there are several indices used to define the ENSO phenomenon. These indices include several sea surface temperature (SST) indices such as the Wright SST, Niño1&2, Niño3, Niño3.4 and Niño4. In addition to the SST indices there is an index created from sea level pressure (SLP), called the Southern Oscillation Index (SOI) and a composite wind, pressure, and temperature index called the Multivariate ENSO Index (MEI). Each has been used in various teleconnection studies and none is officially accepted as the only index to represent the ENSO. Figure 2.1 shows a time series plot of the SOI index from 1950 – 2010.

The proposed research uses the SOI to represent the ENSO which is maintained by the National Oceanic Atmospheric Administration's (NOAA) Climate Prediction Center (CPC) and it can be downloaded from their website (http://www.cpc.ncep.noaa.gov/data/indices/soi). The SOI dataset covers monthly values from 1951 through the current year. The SOI is defined as the difference between the standardized SLP anomalies at Tahiti and Darwin, Australia. These observations describe the seesaw event that Walker (1923) and Walker and Bliss (1932) divide. As SLP values increase in Darwin, there is a resulting decrease in SLP at Tahiti and vice versa. Therefore a positive SOI phase occurs when the Tahitian SLP anomaly is greater

than the observation at Darwin, and when Darwin is larger the SOI is in a negative phase. Positive SOI phases correspond to increased SST (El Niño) events.

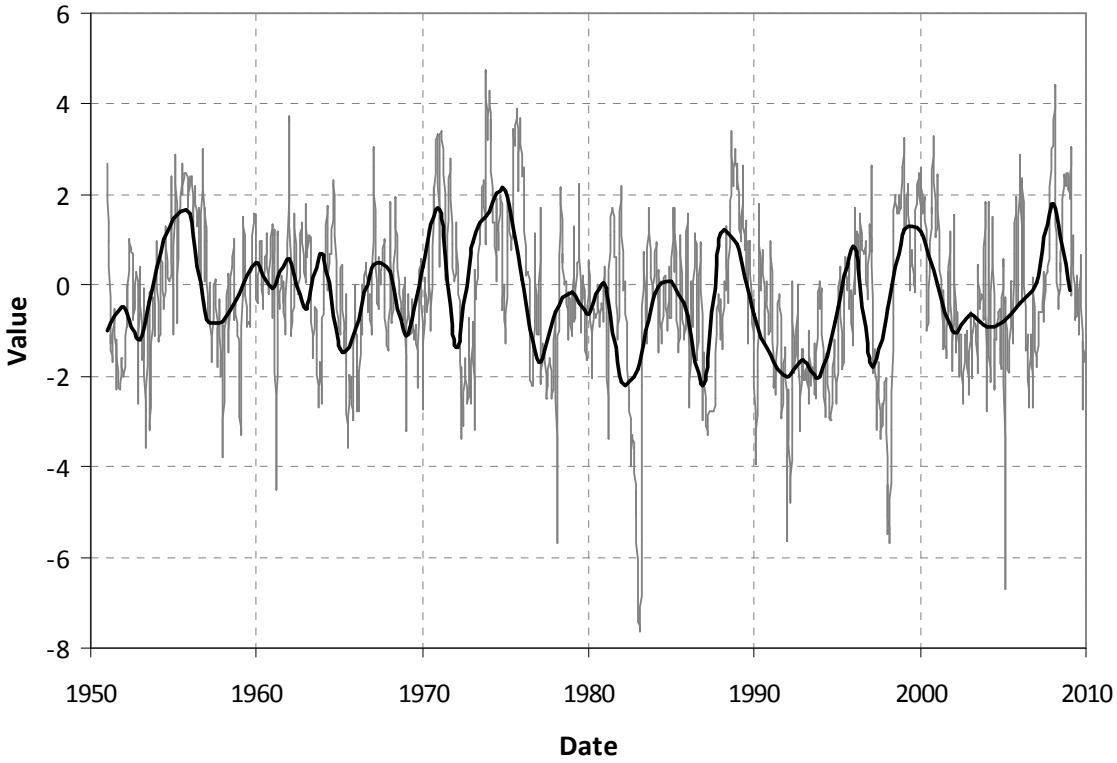

Figure 2.1 Mean SOI values 1951-2009 (monthly-grey / yearly-black)
Data obtained from Earth System Research Laboratory
http://www.esrl.noaa.gov/psd/data/climateindices

The effects of ENSO have been linked to hydrologic responses across the globe (Diaz and Markagraf, 2000). Aside from the studies already listed earlier there are many other studies which demonstrate ENSO teleconnections with U.S. hydrology (Kiladis and Diaz 1989, Cayan and Peterson, 1989, Redmond and Koch 1991, Hanson and Maul, 1991, Cayan and Webb, 1992, Dracup and Kahya, 1992; Kahya and Dracup, 1993; 1994a; 1994b; Piechota and Dracup, 1996; Shabbar et al., 1997; Piechota, et al., 1997; Zorn and Waylen, 1997; NRCS, 1997; Brandon, 1998; Hamlet and Lettenmaier, 1999;

Schmidt et al., 2001; Harshburger et al., 2002; Maurer and Lettenmaier, 2003; Hidalgo and Dracup, 2003; Hidalgo and Dracup, 2004; Beebee and Manga, 2004; Tootle and Piechota, 2004; Mauer, et al., 2004; Hidalgo, 2004; Twine et al., 2005). Despite the shortcomings of the ENSO already mentioned earlier, the ENSO-U.S. Hydrology teleconnection has been discussed enough that is included here as a way to show that the testing being done with the current research matches up with past research. It is expected that the ENSO signal will appear during the short lag times and for gauges located in the lower CRB. In the context of the current research, it is also expected to show the limit of the ENSO-CRB teleconnection.

2.3.2 Pacific Decadal Oscillation

When discussing the CRB, the second most common climate index is the Pacific Decadal Oscillation (PDO). The PDO is defined as the first mode of the principal component analysis of Pacific Ocean SSTs poleward of 20º N. The anomalies and the impacts of the PDO were initially observed by Nitta and Yamada (1989) and Trenbreth (1990). PDO fluctuations have a period between 50-70 years with a given warm or cool phase persisting for about 15 – 25 years (Chao et al., 2000; Minobe; 1997). The mechanism driving PDO variability is not known, but it is hypothesized by Trenberth and Hurell (1994), that the origins of the PDO can be found in the tropical Pacific Ocean. PDO data are available from the Joint Institute for the Study of the Atmosphere and Ocean at the University of Washington for the period of 1900 through the current year (http://jisao.washington.edu/pdo/PDO.latest). Figure 2.2 shows a time series plot of the PDO data.

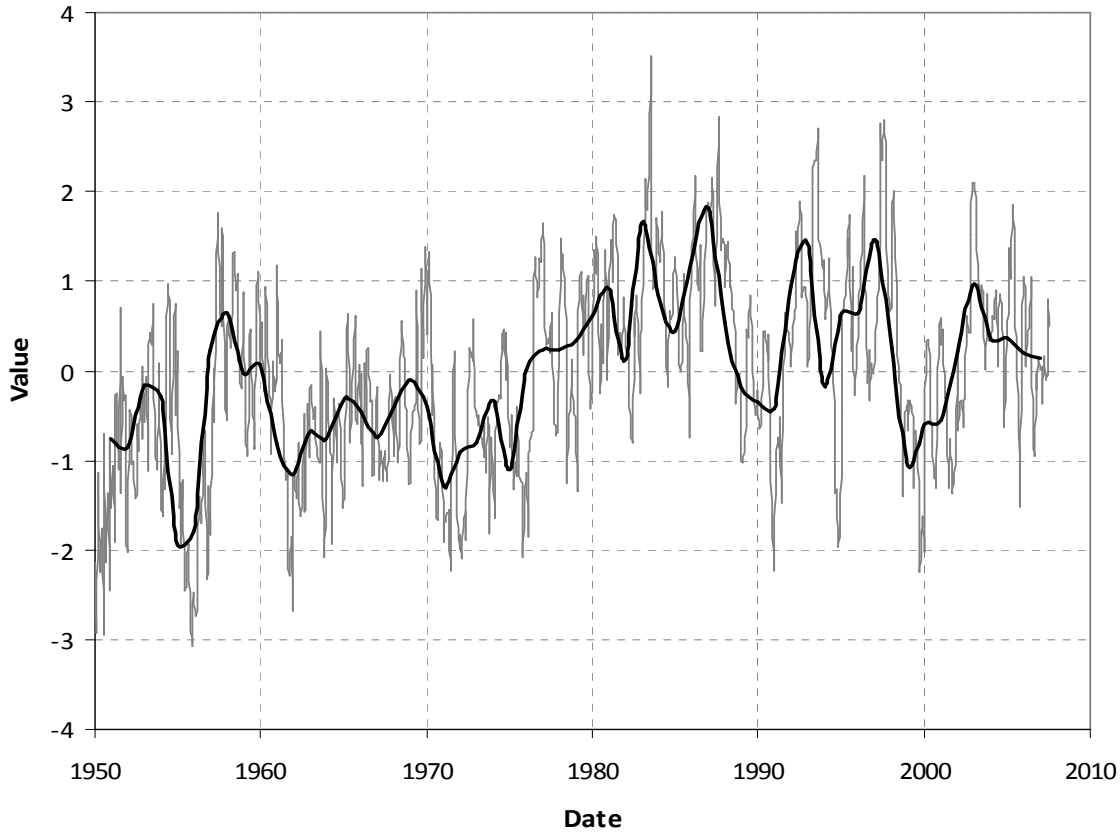

Figure 2.2 Mean PDO values 1950-2007 (monthly-grey / yearly-black)
Data obtained from Earth System Research Laboratory
http://www.esrl.noaa.gov/psd/data/climateindices

Similar to the ENSO, the PDO teleconnection has been identified around the Pacific Ocean basin. Studies showed symmetric atmospheric circulation changes associated with the PDO (Gerreaud and Battisti, 1999; Zhang et al., 1997b). Power et al (1997, 1999a, 1999b) showed how changes in the PDO impact Australian temperatures and rainfall. However, a large number of studies demonstrate the impact the PDO has on marine biology (Mantua and Hare, 2002; Hare et al., 1999; Beamish, 1993; McFarlane and Beamish, 1992; Clark et al., 1999).

The climate impacts of the PDO have been shown to explain hydrologic variability in the western U.S. under several different circumstances including ENSO-

PDO coupling (Minobe, 1997; Gershunov and Barnett, 1998; McCabe and Dettinger, 2002; Hidalgo and Dracup, 2003; Hidalgo, 2004; Beebee and Manga, 2004, Tootle et al., 2005; Timilsena et al., 2009). In general, the PDO signal is often discussed in the context of ENSO, because the PDO signal can either enhance or diminish the ENSO signal, depending on the phase of the PDO (Hamlet and Lettenmaier, 1999). While there are many studies which have discussed the impact of the ENSO, and the PDO, as well as the ENSO-PDO effect on streamflow in the CRB, there is no study which defines the lagged climate-hydrology response of these climate variables on the CRB.

2.4 Atlantic Ocean Climate Indices

The proposed research proposes to use Atlantic Ocean climate data to understand the long-lead impacts associated with the CRB though there is significantly less research connecting the two than with Pacific Ocean data. The two datasets selected for this work include the Northern Atlantic Oscillation (NAO) and the Atlantic Multidecadal Oscillation (AMO). However, Marshall et al (2001) point out that the North Atlantic Ocean temperature and pressure variability can have an effect on weather throughout the northern hemisphere. Because, as Marshall et al. point out, the NAO is a part of the northern hemisphere circulation which is described by the Arctic Oscillation (AO). They go on to demonstrate that the NAO/AO impacts can rival those of the ENSO signal from the Pacific Ocean. Because of this information, there is a good reason to include Atlantic Ocean climate data when considering streamflow responses in the CRB.

2.4.1 Northern Atlantic Oscillation

The NAO is defined as the anomaly differences in sea level pressure between the Azores and Iceland (Hurell, 1995), and has also since been identified as part of northern

annular mode, the Arctic Oscillation (Marshall et al., 2001). Interestingly, teleconnections identifying the NAO were made in the same studies that originally identified the ENSO signal (Walker, 1924; Walker and Bliss, 1932). When in a positive phase, the North Atlantic Jet moves poleward taking with it the storm track (Kushnir, 1994). Barnston and Livezey (1987) describe the NAO contracting northward in summer and expanding southward in winter giving it a variable location which thought to be the result of changes in North Atlantic SSTs (Kushnir et al., 2006). Unlike the ENSO and PDO the NAO index does not remain in one phase for an extended period of time (See Figure 2.3). Its short period of 12-14 days is the result of seasonal-to-interannual (S/I) variability (e.g. affected by volcanic activity or internal dynamics of the climate system) and is therefore nearly impossible to predict (Kushnir et al., 2006).

The NAO index is most famously teleconnected to climate in the northern Atlantic Ocean (Visbeck et al. 2002; Kushnir 1994; Deser and Blackmon 1993; Wallace et al. 1992; Bjerknes 1964). This basic understanding of changes in Atlantic SSTs has led to many studies linking the NAO to hydrologic responses across Europe (Ionita et al., 2009; Karcher et al., 2007; Macklin and Rumsby, 2007; Ukita et al., 2007; Otterson et al., 2000; Frei and Robinson, 1999; Higuchi et al., 1999; Dugam et al., 1997; Nakamura, 1996; Hurell, 1995; Zhifang and Wallace, 1993; Van Loon and Rogers, 1978;). Other studies have shown that this index can also explain variation in surface hydrology across the United States. Morin et al. (2008) demonstrated that the primary mode of total snowfall and number of snow days in the eastern United States is driven by the NAO. Durkee et al. (2008) showed that there is an increase in precipitation across the eastern United States when the NAO is in a positive phase. The use of positive and negative

phases of the NAO were also linked to changes in CRB streamflow by Tootle et al (2005). Because the NAO is a measure of SLP, it is possible to describe the physical connection of the index to changes in storm tracks across Europe. However no explanation is given for the NAO – North American teleconnection.

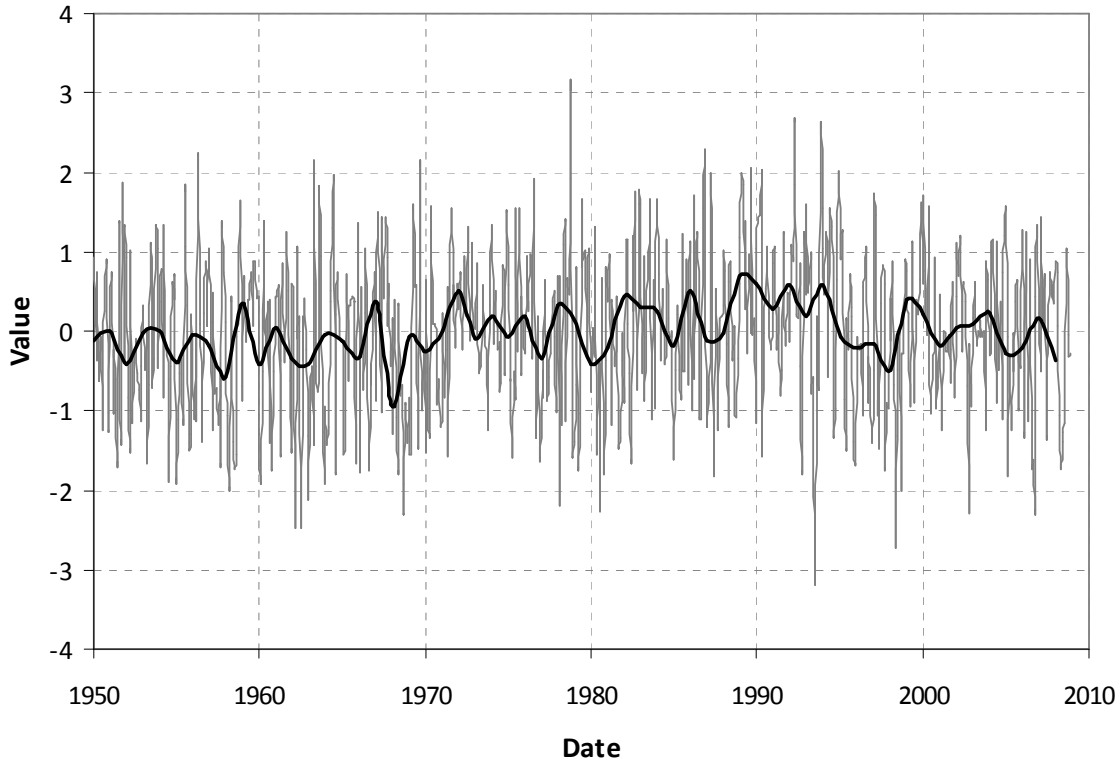

Figure 2.3 Mean NAO values 1950-2009 (monthly-grey / yearly-black)
Data obtained from Earth System Research Laboratory
<http://www.esrl.noaa.gov/psd/data/climateindices>

2.4.2 Atlantic Multi-Decadal Oscillation

The AMO represents a persistent SST pattern observed in the northern Atlantic Ocean between 0 – 70 degrees north bounded by the continents (Gray et al., 2004). In contrast to the other indices discussed, the AMO does not vary drastically, and it is by far the index with the longest cycle period. It is estimated from modeling studies to be 50-70

years, and from tree-ring and arctic ice regression as closer to 80 years (Schlesinger and Ramankutty, 1994; Kerr, 2000). Figure 2.4 shows a time series plot of the AMO from 1950 – 2009. While the initial observation of the index may be attributed to Schlesinger and Ramankutty, the definition of the AMO as an actual oscillation has largely come from work aimed at extending the AMO through analysis of reconstructed SST datasets (Gray et al., 2004; Knight et al., 2005). The increased understanding about the physics of the AMO index (Dijkstra et al., 2006) comes from the studies which defined the teleconnection of AMO and the Thermohaline Circulation (THC) (Sutton and Hodson, 2005; Knight et al., 2005; Dima and Lohman, 2007, Richter and Xie, 2009). Understanding the AMO cycle has also helped understand the trends related to climate change (Hodson, et al., 2009; Keenlyside et al., 2008).

Because the AMO index is also the youngest index there are fewer examples of using this index in teleconnection studies. The AMO appears in research into teleconnections with changes in Asian summer monsoons (Lu et al, 2006), Indian and Sahal summer rainfall (Zhang and Delworth, 2006), northern Pacific Ocean variability (Zhang and Delworth, 2007) and climate in east China (Shuaunglin and Bates, 2003). Some of these teleconnections were also checked in the reconstructed AMO dataset (Knight et al., 2006). Logically it also figures into research related to changes in hurricane activity in the Atlantic Ocean and the resulting changes in precipitation in countries adjacent to the Atlantic basin.

Goldenberg et al. (2001) used the AMO data to help explain the increase in Atlantic Hurricane activity. Because of the longer trends of the AMO data, the study concludes that the increased hurricane activity will persist for many years. Trenbreth and

Shea (2006) used the observed 2005 hurricane season as a backdrop to discuss the observed increases in global temperature as a result of climate change and increases in

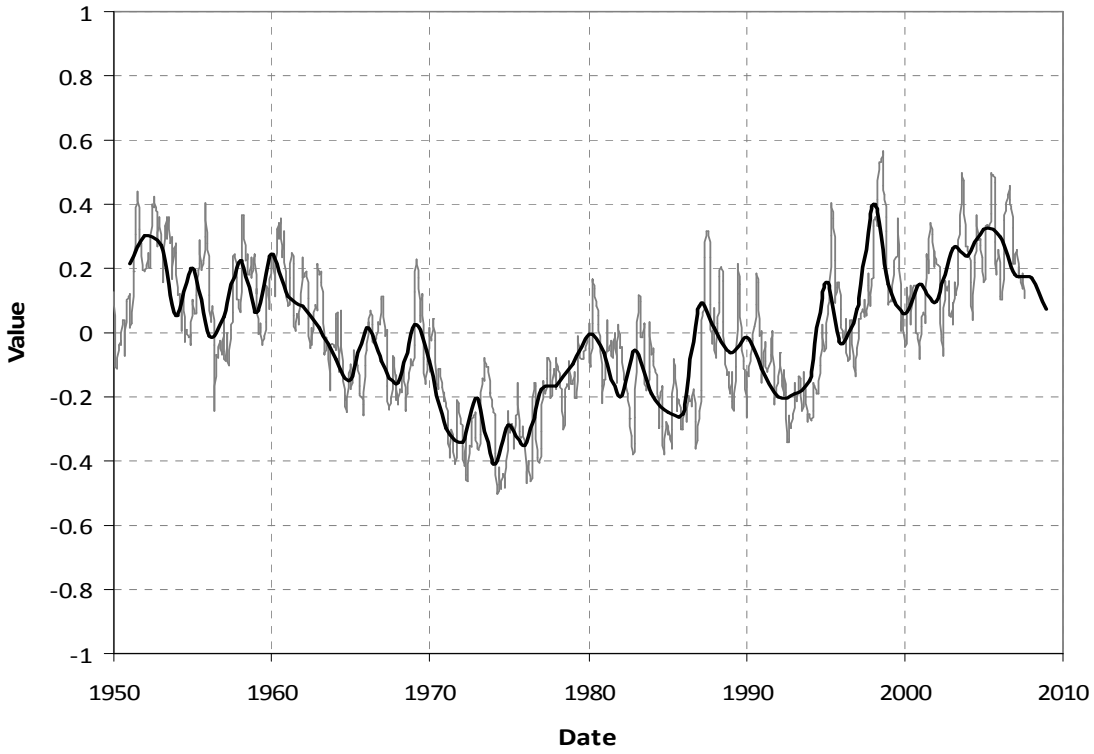

Figure 2.4 Mean AMO values 1950-2009 (monthly-grey / yearly-black)
Data obtained from Earth System Research Laboratory
http://www.esrl.noaa.gov/psd/data/climateindices

the AMO oscillation. Finally, Holland and Webster (2007), defined three regimes of eastern Atlantic SSTs where there are 50% more cyclones and hurricanes in each successive regime.

The connection between AMO and US streamflow has also been introduced in studies showing changes in streamflow across the US, (Enfield et al., 2001), in Florida (Kelley and Gore, 2008) and in gaining an understanding of long-term drought observed in the southwest (Hidalgo, 2004). More pertinent to the current research the AMO-

ENSO coupled effect has appeared in studies looking at the Mississippi Valley streamflow (Rogers and Coleman, 2003) as well as in the CRB (Timilsena et al, 2009, Tootle et al, 2005). The AMO index data from 1948 through the present can be downloaded from the CPC's website (http://www.cdc.noaa.gov/Correlation/amon.us.data).

2.5 Global Gridded Climate Data

In addition to using specific climate indices, the proposed research will use data which is created for the entire globe and represented in a gridded format. These data include Sea Surface Temperatures (SSTs), 500mb Geopotential Height (Z500), and 200mb Zonal wind (U200). The purpose of using the "raw" global data is to be able to identify climate patterns which may not be represented in the defined climate indices already listed

2.5.1 Sea Surface Temperature Data

The SST data used in the proposed research comes from work by Smith and Reynolds (2002) at the National Climate Data Center (NCDC) of the National Oceanic Atmospheric Administration (NOAA). Officially named the Extended Reconstructed Sea Surface Temperature (ERSST) dataset, it comprises of monthly average values at 2-degree grid cells covering the entire globe from 1854 – 1997. The dataset has been improved (Smith and Reynolds 2004; Smith et al, 2008) since the initial reconstruction was performed to reduce bias and modeling error. Figure 2.5 shows the time series for the mean SST values from 60° S – 60° N.

Figure 2.5 60S -60N ERSST Annual Anomaly (1880 – 2009)
Downloaded from NCDC website
(http://www.ncdc.noaa.gov/oa/climate/research/sst/ersstv3.php)

Because this data is available to the public through NOAA's NCDC, it has been used in many applications. A common use of the data has been to use the Empirical Orthogonal Function Analysis (EOF – also known as Principle Component Analysis) to identify Ocean temperature trends in surface responses (Muñoz and Enfield, 2009). An (2004) used the SST data and EOF analysis to identify trends in the ENSO signal, Tootle et al. (2007) used EOF of SST data to run a partial least square regression to create a streamflow forecast model, Garcia et al. (2006) used EOF analysis to indentify ocean teleconnections between Europe and tropical Atlantic and Pacific SSTs, Girardin et al., (2006) used the SST data and EOF to identify a connection between the ocean climate and Canadian drought, and Monahan and Dai, (2004) sought to understand the nonlinear relationships between positive and negative phases of the ENSO signal by using the EOF analysis and Pacific Ocean SST data.

The ERSST data has also been applied to climate questions which are similar to those proposed in this research, namely to use the SST data to define covariance relationships with other observed data (such as streamflow or precipitation). Soukup et

al. (2010) used Singular Value Decomposition (SVD) analysis on streamflow of upper North Platte River Basin (NPRB) and Pacific Ocean SST as well as NPRB streamflow and Pacific Ocean sea level pressure (SLP). This research approach helped identify a region of the Pacific Ocean which was not currently represented by other existing ocean climate indices to explain a majority of the streamflow variance on the upper NPRB. Using the SVD analysis on northern Atlantic Ocean SST and Euro-Atlantic climate, Serrano and Rodriguez (2004) identified that the summer-time SST anomalies have a lagged effect on North Atlantic Ocean zonal wind as well as precipitation anomalies in Europe. Wang and Ting (2000) identified a covariance relationship between Pacific Ocean SST data and winter mean precipitation in the United States. Tootle and Piechota (2006) was also able to identify a region of the Pacific Ocean which demonstrated significant covariance with observed streamflow across the United States. This research is most similar to that proposed here, because Tootle and Piechota used observations of USGS streamflow across the United States and compared them with Pacific and Atlantic Ocean SSTs.

For the proposed research, only the northern Pacific Ocean SSTs will be considered similar to research by Aziz et al (2010). The boundary of the SST data is given as 120º East to 80º West and 70º North to 30º South. This boundary is selected to show the entire northern Pacific basin and enough of the southern Pacific to identify any connection to the ENSO signal. This region is displayed in Figure 2.6.

Geopotential Height is a gravity adjusted elevation about the earth's surface. The adjustment is a function of the change of gravity at a given latitude and elevation in the earth's atmosphere. The geopotential height values are reported at various pressure

levels, and 500mb is simply one of those levels. Therefore the values used for this research are reporting the additional amount of elevation required to "reach" elevation of mean sea level. The geopotential height data are available from the NCEP/NCAR Reanalysis Product (Kalnay et al, 1996), and can be downloaded from the following website http://www.esrl.noaa.gov/psd/data/gridded/data.ncep.reanalysis.html. The 500mb height data will identify circulation patterns in the upper layers of the atmosphere (above land and sea). Therefore some studies use the data to identify teleconnection patterns or atmospheric waves which demonstrate the path of storm tracks in the atmosphere (Mo and White, 1985; Rogers, 1990; Thompson and Wallace, 1998; Yu, 2007).

Figure 2.6 Location Map showing the limits of the SST data.
(120º E – 80º W, 70º N to 30º S)

2.5.2 Geopotential Height

The utility of geopotential height as a climate variable is summarized by Wallace and Gutzler (1981). Wallace and Gutzler used the data to reproduce these patterns and to identify the Pacific/North American (PNA) signal as a teleconnection within the 500mb geopotential height data. It is important to note that it was the sea level pressure data (a subset of the geopotential height data) that Sir Gilbert Walker used initially to identify the SOI as well as the NAO patterns. In general this dataset has been utilized so many times that there is not enough room to list all of them here.

There are a few of the studies which relate to the tasks carried out in this research. For example, work by Goebbert and Leslie (2010) identified a multi-year cycle present in the geopotential height data in the northwest Australian tropical cyclone (TC) area. This analysis showed there is a significant correlation between the wintertime climate variable and the yearly TC frequency and the number of TC days each year. Casola and Wallace (2007) showed the wintertime Z500 data is correlated with the ENSO signal in several regions around the Pacific Basin and North America. Finally, work by Blackmon (1976) helped set the foundation for using power spectrum analysis on the Z500 data to reveal the low frequency signals imbedded in gridded climate data. These three studies show that there is a low frequency cycle to the Z500 data which demonstrates noted teleconnection patterns in the Pacific Basin and these have shown the potential for being correlated with established climate phenomenon such as the ENSO cycle in the Rocky Mountain region.

2.5.3 Zonal Wind Field

The atmospheric water budget is defined by Wang et al., (2010a) as the following.

$$\frac{\partial W}{\partial t} + \nabla \cdot Q = E - P$$

Here, W, P, E, and Q represent respectively, precipitable water, precipitation, evaporation and vertically integrated water vapor flux. Water vapor flux is defined as the integration of specific humidity, q and zonal wind, V from the surface layer to the troposphere.

$$Q = \frac{1}{g}\int_0^{p_s} qVdp$$

This demonstrates that the zonal wind field is a component of quantifying the atmospheric budget. This zonal wind field, as a component in an atmospheric water budget has been used specifically in research to connect the Pacific Ocean climate variability to precipitation in the intermountain west (Wang et al., 2009, 2010a, 2010b). This work uses both components of the water vapor flux as decomposed by Chen (1985), namely the moisture flux streamfunction – a measurement of the amount of moisture carried in the atmosphere – and the moisture flux potential.

The zonal wind field data has been used in studies as a climate variable itself. Because it is also part of the NCEP/NCAR reanalysis product there are myriad research examples using this data. The work by Athanasiadis (2010) used the wintertime 250 mb zonal wind field to identify the location of the wintertime East Asian Jet Stream (EAJS) and its correlation with north American storm tracks. Yang et al (2002) utilized the zonal wind field data to draw between the variations of the EAJS and Asian-Pacific-American winter climate. Zhang et al. (1997a) demonstrated that the presence of high pressures over Siberia, and cold surges from east Asia (travelling on a south-southeast direction from northern china), have a great effect on the winter monsoon season over East Asia. A strong East Asia winter monsoon is characterized by two high-pressure centers: the

first is a warm high pressure center whose mid-point is roughly east of Papua New Guinea while the other center is a cold "dome adjacent to the Siberian region". Between the two high pressure centers is the winter traveling path of the East Asian Jet Stream. These studies demonstrate that the climate of east Asia has an important connection with that of the Pacific Ocean and of North America as well. Therefore the research should identify a connection to the dominant jet stream as well

2.6 Colorado River Basin Streamflow/Forecast Data

The final data used in the proposed research are the observed and forecast data for the CRB. The United States Bureau of Reclamation (USBR) maintains a database of unimpaired, naturalized runoff data for the Colorado River Basin (CRB) and is available for download from the following URL (http://www.usbr.gov/lc/region/g4000/NaturalFlow/current.html). Streamflow gauges are considered naturalized when the effects of human interference (e.g. dams as well as consumptive diversions) have been removed mathematically from the gauge measurements. Unimpaired gauges are those which, for all intents and purposes, measure the natural flowrate of the river where no man-made impacts affect the measurements. Impaired gauges measure streamflow which are affected by upstream storage or diversions. In all, there are 29 streamflow gauges within the upper and lower CRB which report monthly naturalized or unimpaired streamflow volumes from October 1905 thru September 2006. This particular dataset is chosen for this analysis because the USBR uses this data as input into their 24-month study, as well as the fact that it is referenced as the baseline for all forecasts of the CRB. For example, a given CBRFC seasonal forecast is often reported as a percentage of the 30-year average (1971-2000) streamflow volume using this data. However, unlike the

SST data, those who manage this dataset do not publish articles regarding the creation of the data, therefore there is no tracking done on how many other investigations this data has been used. See Figure 2.7 for locations of the 29 streamflow gauges.

Figure 2.7 Location map of 29 USGS streamflow gauges

In addition to this data the NWS also maintains a database of unregulated streamflow observation data to compare with the published forecasts explained in Chapter 1. "Unregulated" streamflow means that the effect of river storage (e.g. dams) has been removed from the river gauge measurements, but the effects of consumptive diversions have not. Therefore, the NWS observations are not the same as those included in the naturalized and unimpaired streamflow data provided by the USBR.

The online database of unregulated forecasts and observations can be downloaded from (http://www.nwrfc.noaa.gov/westernwater/?page=data&id=). The data include the April – July forecasts generated January through July of each year, but not the yearly outlooks generated in August and October. Therefore the "outlook" data will need to be obtained from the CBRFC at a future time, after sufficient progress has been made. Also, CBRFC references gauge identifications which are different from the USGS gauge ID numbers used in the USBR streamflow data. However, from the description of the NWS and USBR gauges a total of 18 gauges were identified to common between the two datasets.

The proposed work will use only the forecast data obtained for these 18 gauge locations to compare the results from the proposed research with the seasonal forecasts generated by the NWS. It should be pointed out that for reasons similar to those with the USBR streamflow data, the number of studies using this data is unknown.

2.7 Summary of Data

In total there are nine (9) data sets used in the proposed work:

- NCEP/NCAR Reanalysis Datasets 1948 through present:
    - 500mb Geopotential Height
    - 200mb Zonal Wind Data
- Southern Oscillation Index (SOI) – 1951 through present
- Pacific Decadal Oscillation (PDO) – 1900 through present
- Northern Atlantic Oscillation (NAO) – 1950 through present
- Atlantic Multidecadal Oscillation (AMO) – 1948 through present
- Extended reconstructed sea surface temperatures (ERSST v.3): 1854 - present

- USBR Naturalized/Unimpaired Streamflow: 1905 – Present for 29 locations

Because of the common length of records of the existing climate indices, the tasks related to the first question will involve data from 1951 – 2004, and compare this with observed yearly streamflow volumes from 1952 – 2005. Extended SVD analysis uses streamflow data from 1952 – 2005 to compare with SST data from 1952 – 2005 (0-year lag), 1952 – 2004 (1-year lag), 1951 – 2003 (2-year lag), and 1950 – 2002 (3-year lag) SST gridded data. The associated correlation analysis in Chapter 4 uses the gridded ocean data for similar lag times. Finally, and because the ESP is calibrated on the period from 1976 – 2005, Chapter 5 will utilize the streamflow data from 1906 – 2005 to complete the three different split sample analyses. This analysis will also require SST data from 1904 – 2005.

CHAPTER 3

A BASIS FOR IMPROVING STREAMFLOW FORECASTING OF THE COLORADO RIVER BASIN

3.1 Introduction

Recent research has provided many tools for the climate scientist to understand the connection between sea surface temperatures (SSTs) and sea level pressure (SLP) with surface climate over the United States (Latif and Barnett 1994; Hidalgo and Dracup 2003; McCabe and Dettinger 1999). Due to the recent drought conditions in the desert southwest, much of this research focuses on ways to describe the streamflow of the Colorado River basin, by observing large-scale climate observations over the Pacific Oceans (Grantz et al. 2005; Kim et al. 2006; Kim et al. 2007). The well known relationships between SST/SLP data and streamflow of the western United States are a result of the El Niño Southern Oscillation (ENSO). However, there are many limitations to what information the ENSO can provide water managers of the Colorado River Basin (CRB) (McCabe and Dettinger 2002).

The first limitation is that the effects of the ENSO are most easily correlated with surface climate of the northwestern and southwestern areas of the United States. There is a large area covering central California, Nevada, Utah, Colorado and Wyoming which does not respond consistently to ENSO variability. The supposition is at times this region is influenced by northerly atmospheric conditions, and at other times southerly conditions influence the region. Another limitation to the ENSO is that its effect on surface hydrology of the western U.S. has a relatively short lead time. For instance, McCabe and Dettinger (2002) found that fall-winter ENSO observations were correlated

with snowpack measurements in the western U.S., and snowpack measurements are well correlated with spring runoff (Clark et al. 2001). Therefore, forecasts generated prior to a given water year, or during a non-ENSO cycle year, have a less successful forecasting ability of CRB streamflow.

Currently the National Weather Service's (NWS) Colorado River Basin River Forecast Center (CBRFC) issues three types of forecasts. These forecasts are then employed by the U.S. Bureau of Reclamation (USBR) offices in Denver and Boulder City to project the amount of water that will be stored or released from the river for the next 24-months. These forecasts include a 3-month forecast of monthly water volumes, a 4-month lump sum water volume for the April – July runoff period, and an "outlook" for the coming water year. The 3-month forecasts are generated each month, the April - July forecast is issued monthly from January 1 to July 1, and the yearly outlook is issued only twice per year - August 1 and October 1. While all of the forecasts are generated using the CBRFC's Ensemble Streamflow prediction Software, there is less confidence in the water year outlooks due to the lack of research supporting 12-month forecasts,. (NWS CBRFC staff, personal communication, 2008).

The 24-month projections use the CBRFC's ESP forecasts as the primary input to their 24-month projections (referred to by USBR staff as the 24-month study) for the first 12-months of their analysis. The second 12-months, or the "out" year, relies upon the 30-year average (1976-2005) streamflow values to continue their release/storage projections (USBR staff, personal communication, 2009).

One limitation of this method for long-term forecasting is the use of the 30-year average monthly data. Using the 30-year average for model calibration assumes a certain

amount of climate stationarity, a concept which lately has been challenged in light of global climate trends (Milly et al. 2008). Another limitation of this method is that the NWS/NRCS forecast, as well as the 24-month study, are deterministic forecasts. From a practical standpoint, this means that the actual probability of each is not reported therefore the quality of the forecast remains unknown. A final limitation is that the forecasts created by the ESP view each of the historical inputs as equally likely in the current forecast.

This Chapter proposes that one improvement to generating long-term forecasts can be found by weighing the historical input data used by the ESP. Currently, after the ESP generates its forecast traces for the forecast period, certain years can be assigned more significance than others based on how similar the forecast year is to the calibrated years. For example, if an El Niño event is taking place during the water year, El Niño years from the historical record can be assigned more weight (e.g., Tootle e al., 2009). While this post-analysis weighting is sometimes performed, this information is not used to generate the official ESP forecast (CBRFC, Personal Communication, 2009). However, developing a forecasting approach where the streamflow traces are weighted post-analysis, provides a greater promise for implementation since the CBRFC are already acquainted with the method. The key to finding an objective weighting measure is to identify a long-lead climate indicator which provides a better indication to changes in streamflow than the 30-year mean. The principle goal of this Chapter is to establish a long-lead teleconnection between existing climate indices, or Pacific Ocean SST's, and CRB streamflow. A physical description of a long-lead teleconnection is the subject of Chapter 4, which will be based on the results from the current chapter.

Much has been discovered about the connection of observed climate indices with the current water year, or two season lag time between the climate and runoff measurements (Grantz et al. 2005). This Chapter builds upon recent studies showing the correlation of large scale climate index phases and streamflow or snowpack measurements in the Colorado River Basin (Tootle et al. 2005; Clark et al. 2001; Werner et al. 2004). Where this study differs from existing work (Timilsena et al, 2007) is that measured data will be used to ascertain the effect of large scale climate on unimpaired/naturalized CRB streamflow data, as opposed to using tree-ring reconstructed streamflow data sets. Another departure from existing research (e.g. Werner et al 2004) is that we will be analyzing the correlation of lead climate indices and the following water year's volume over multiple lag times.

3.2 Data

There are a total of six (6) data sets used in this analysis: naturalized streamflow, observed monthly Southern Oscillation Index (SOI), monthly Pacific Decadal Oscillation (PDO) index, monthly Northern Atlantic Oscillation (NAO) index, monthly Atlantic Multidecadal Oscillation (AMO) index, and Sea Surface Temperatures.

3.2.1 Naturalized Streamflow

The United States Bureau of Reclamation (USBR) maintains a database of naturalized or unimpaired runoff data for the Colorado River Basin (CRB) and is available for download from the following URL (http://www.usbr.gov/lc/region/g4000/NaturalFlow/current.html). Streamflow gauges are considered naturalized when the effects of human interference (e.g. dams and diversions) have been removed (mathematically) from the gauge measurements. For the readers reference, there are two

other kinds of gauges data: Unimpaired and Impaired. Unimpaired gauges are those which, for all intents and purposes, measure the natural flowrate of the river. Impaired gauges measure streamflow which are affected by upstream storage or diversions. In all, there are 29 streamflow gauges within the upper and lower CRB which report naturalized streamflow from 1905 water year (October 1905 – September 1906) thru the 2004 water year. This particular dataset is chosen for this analysis because the USBR uses this data as input into their 24-month study, as well as the fact that it is referenced as the baseline for all forecasts of the CRB. For example, a given CBRFC seasonal forecast is often reported as a percentage of the 30-year average (1971-2000) streamflow volume using this data). Figure 3.1 shows a map of the 29 river gauge locations.

3.2.2 SST and Climate Index Data

Average monthly SST values were obtained from the National Climatic Data Center (http://www.cdc.noaa.gov/cdc/data.noaa.ersst.html). The data is presented in 2º x 2º grid cell for all oceans (Smith and Reynolds, 2003; Smith et al., 2008) and spans the years from 1846 until present. Though the dataset is a reconstruction of SST values for the period, data quality improves from 1950 on as a result of increase coverage ocean monitoring capability. The range of ocean data used in this study covers the area from Longitudes 120º East to 80º West and Latitudes 20º South to 60º North, which is similar to the region studied by Tootle et al. (2006).

Climate index data can be found through the National Oceanic Atmospheric Administration's (NOAA) Climate Prediction Center (CPC) website. These indices have been used previously to demonstrate a correlation between the changes in the index and surface climate changes (Tootle et al. 2005; Shabbar et al. 1997; Rasmussen & Wallace,

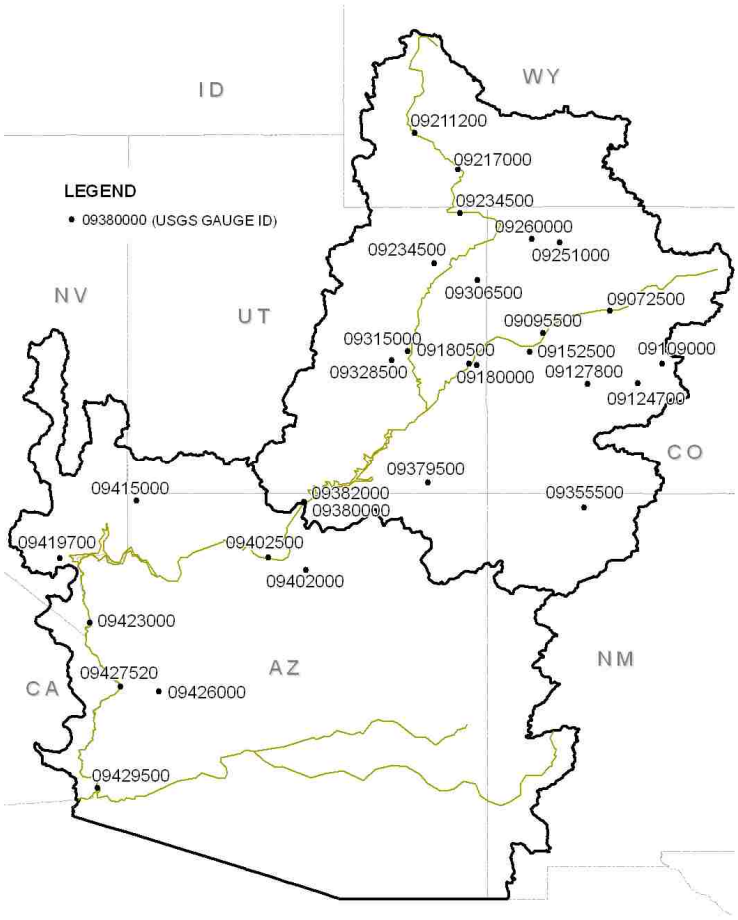

Figure 3.1 Location map of 29 USGS streamflow gauges

1983; McCabe et al. 2007). The availability of continuous data for each index as well as for the streamflow data defines the study period. The SOI data {*http://www.cpc.ncep.noaa.gov/data/indices/soi*} covers monthly standardized values from 1951 thru 2008 (calendar years). PDO index values are available from 1900 through the current year (http://jisao.washington.edu/ pdo/PDO.latest). In addition to these data sets, the available NAO {*http://www.cdc.noaa.gov/Correlation/nao.data*} and AMO {*http://www.cdc.noaa.gov/Correlation/amon.us.data*} index values is available from 1950 and 1948 respectively, until the current year. Based on the data availability, the study period will start in 1951 and end with the 2005 water year.

3.3 Methodology

The correlation between the climate variability and SST with the gauge streamflow was completed using two statistical methods. The first test is the Rank Sum Test. This test is used to compare mean values from two different datasets to determine if they are significantly different. The second test is the Singular Value Decomposition (SVD) method of finding maximum covariance between two fields. SVD was used to compare the SST data with the streamflow data.

3.3.1 Rank Sum Analysis

The rank sum test is an excellent way to test a "before" and "after" scenario without trying to determine if either data set has a defined distribution. Alternatively, it can be used to test for differences between two segmented data sets. Hence, this is a non-parametric test and does not make assumptions about the distributions of either dataset. In the current analysis, we are using the negative and positive phases of the indices to act as our "before" and "after conditions respectively. The mean of the streamflow measured during a negative climate phase is compared with the mean streamflow measured during the positive climate phase. The null hypothesis of this test is that the means from the two sample sets are equal. The results of a rank sum test provide a value of the probability that the two sets are similar. For p-values less than 0.05, the null hypothesis was rejected a theoretical discussion of this test is offered by Alder and Roessler (1977).

In order to determine the effect that the SOI has on CRB streamflow the 3-month and 6-month average SOI values were used to separate the historical streamflow data into "positive" and "negative" groups. Figure 3.2 shows an overview of how the rank sum test uses the historical index values to compare the positive and negative streamflow

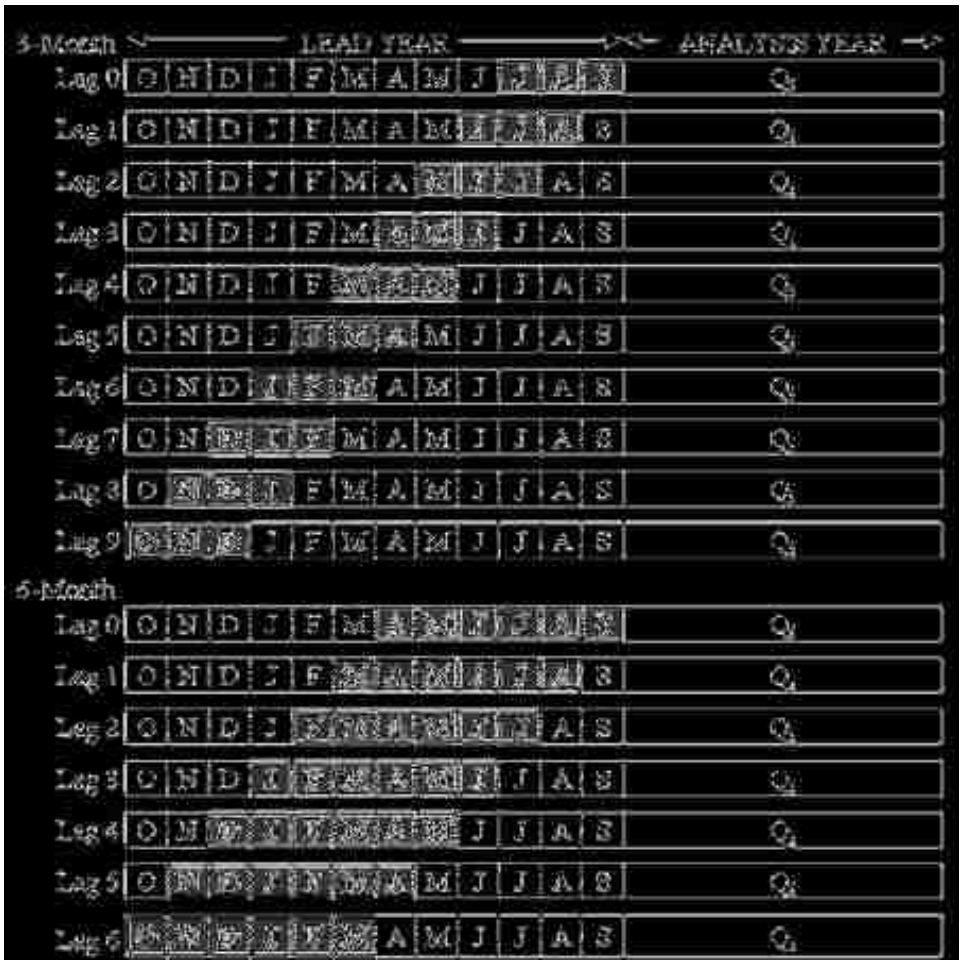

Figure 3.2 Depiction of 3-month and 6-month lag-lead analysis
*(*Qi = yearly total runoff measured at station *i)*

phase groups. Starting with July, August and September average SOI values (lag = 0), the streamflow values from years where this monthly interval is positive were grouped and compared with those streamflow values corresponding to negative SOI values. This test was performed for the measured streamflow values from each station. After each station was compared for the JAS average of SOI values, then the three month SOI interval was lagged back one month (Lag 1 – June, July and August) and the analysis was performed again at all measurement stations. The analysis process was repeated until Lag 9 (average of October, November and December SOI values). We repeated the 3-

month average rank sum test for the PDO (index No. 2), NAO (No. 3), and AMO (No. 4) indices, which provided a total of 1,160 results (29 stations x 10 lags x 4 indices). Similarly we performed the same process for the 6-month average values starting with the April-September interval (AMJJAS; lag = 0) and ending with the October-March interval (ONDJFM; lag = 6) (see Figure 3.2). The 6-month analysis consisted of an additional 812 rank sum tests (29 stations x 7 lags x 4 indices).

3.3.2 Combination of Indices

The next step in the analysis was to compare the combined effect of the indices assuming that the influence from different climatic phenomena can occur at the same time. The process used to determine the effect of an individual climate index was repeated for the combination analysis. This process is shown graphically in Figure 3.3. Using the SOI as a base, the combination analysis compared the PDO-positive and PDO-negative values which also occur under an SOI-*positive* phase (Labeled as analysis No. 5). Likewise, the process was repeated for PDO-positive vs. PDO-negative values under the SOI-*negative* phase (analysis No. 8). The SOI-PDO combination of 3-month and 6-month average values included an additional 986 rank sum tests (29 stations x 10 lags x 2 combination phases + 29 x 7 x 2). In a similar manner, the NAO (analysis No. 6 & 9) and AMO values (analysis No. 7 & 10), were also completed for the 3- month and 6-month values. Therefore the combination analyses yielded a total of 2958 results (986 x 3 indices).

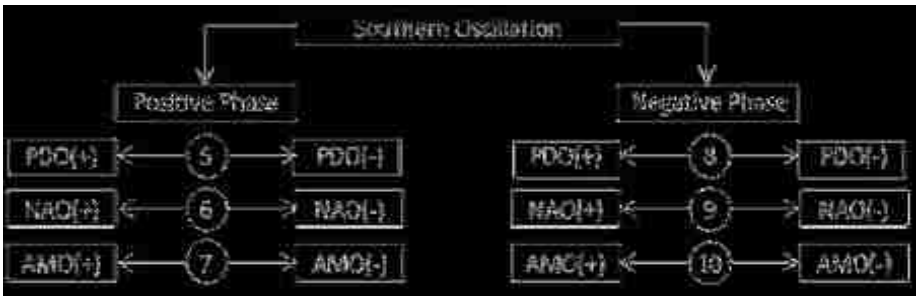

Figure 3.3 Combination rank sum testing using the SOI as a basin

3.3.3 SVD Analysis of Pacific Ocean SSTs

The next step in the analysis process was to determine how Pacific Ocean sea surface temperatures vary with respect to the streamflow measured in the 29 gauges of the CRB. The goal of this analysis was to determine if there is any SST pattern that can be identified, which is not already represented in one of the indices used in the rank sum testing. The process is also known as Maximum Covariance Analysis, because the goal is to identify the dimensions, or modes, which represent the maximum amount of covariance between two temporal fields. Since the spatial component of most climate data is quite large, using the temporal field to compare generally limits the analysis dimension to the number of days, months, or years included in the study period. In this paper our time scale is in years.

The use of SVD to find couple patterns in climate data was explored by Bretherton et al. (1992) who compared five different methods for analyzing climate data. Other research (Wallace and Bretherton 1992; Soukup et al. 2010) has utilized SVD to analyze the covariance of sea level pressure as well as SST with snow water equivalent measurements, precipitation, and, as we do here, with streamflow. The process performed in this analysis is similar to Tootle and Piechota (2006), where SST anomalies

in the Pacific Ocean are coupled with streamflow anomalies across the United States. In this paper we limit the analysis to the CRB streamflow only.

The following description of the SVD process is provided by several sources (Bretherton et al. 1992; Wallace et al. 1992). Before any computations were performed, the raw SST and Streamflow data were standardized based upon each grid location and the values representing land (values of -9999) were deleted from the SST matrix. Next, a covariance matrix using the SST and Streamflow anomalies was determined using the following formula:

$$_{COVAR}TS = (1/n)\ (\boldsymbol{T'S})$$

In this analysis, the number of years in the temporal analysis is, $n = 53$. The SST field *[53 x 3218]* was represented by the letter, ***T***, and ***S*** represents the streamflow data field *[29 x 53]*. The SVD was performed on the $_{COVAR}\boldsymbol{TS}$ matrix *[3218 x 29]* which yielded the following three matrices:

$$SVD(_{COVAR}TS) = \boldsymbol{U\ \Sigma\ V}$$

U *[3218 x k]* and ***V*** *[29 x k]* represent the left and right singular (heterogeneous) matrices respectively, and $\boldsymbol{\Sigma}$ *[53 x 29]* represents the diagonal matrix of singular values from the SVD. The value *k*, represents all modes (columns in the matrix) which contain a squared covariance fraction (SCF) > 10%. SVD (similar to the results from a PCA/EOF analysis) attempts to describe the variance of a given matrix (in this case, the $_{COVAR}$TS matrix) by drawing new axes which are rotated in matrix space to capture as much of the variance (in essence, changes in SST or streamflow) as possible. Each column of the ***U*** and ***V*** represents a new axis and the values in those columns represent the variance captured by that axis. In order to measure the proportion of variance contained within a given

column, Bretherton et al. (1992), used the squared covariance fraction (SCF). The SCF is found by dividing the square of each singular value in the $\boldsymbol{\Sigma}$ matrix by the sum of the squared singular values (sum of squared values from the diagonal) as is shown by the following equation:

$$SCF = \frac{S_{i,i}^2}{\sum_{i=1}^{29} S_{i,i}^2}$$

In this equation S represents the matrix of singular values $\boldsymbol{\Sigma}$ (substituted to avoid confusion with the summation sign in the denominator), and the summation is taken for values of *i* from 1 to 29 because this is the total number of columns of $\boldsymbol{\Sigma}$.

Finally, the left and right temporal expansion series (LTES & RTES) were obtained by projecting ***U*** onto ***T*** and ***V*** onto ***S*** in the following manner:

$$LTES = U' \; T'$$

$$RTES = V' \; S'$$

The LTES *[53 x k]* and RTES *[53 x k]* expansion series are both time series representing the maximum yearly variance of the SST data. The LTES is then standardized to reflect the unit increments of variance. In this format the LTES can now be used in the same way that the climate indices were used to test correlation with the streamflow in the rank sum test. The LTES is run through the lagged correlation testing outlined above, just like the testing approach to the established climate indices.

The final step in the analysis was to determine the significance of the variance observed in the left heterogeneous field (SST) and the right heterogeneous field (streamflow), by calculating the Pearson-r correlation coefficient. The testing for significance was done using a student t-test, which assumes that the correlation

coefficients are normally distributed with a mean value of r = 0. Working backwards, starting with n – 2 degrees of freedom (i.e. 51), we find that $|r| \geq 0.27$ in order to be significant. This value is based on $\alpha = 0.05$.

3.3.4 Forecast Skill Comparison

The final analysis proposed in this chapter is used to compare the forecast skill abilities up to three climate indices at a time. In contrast to the Rank sum analysis, which provides an assessment of significant dissimilarities between streamflow observed under the positive and negative phases of a given index, the forecast skill score will calculate a value which represents the magnitude of contribution that a given index makes to a given forecast model. The comparison between the three indices was completed using a model initially developed by Piechota et al (1998) who were trying to develop long lead-time forecasts of streamflow in Eastern Australia. A detailed explanation of the method is provided in Piechota et al (1998) and in other more recent research (Tootle and Piechota, 2004; Soukup et al, 2010). A brief explanation is provided here.

A probability density function is created using a kernel density estimator and a sorted vector of observed streamflows at a given location. For each observed streamflow a unique probability value is obtained using a given predictor (SOI, PDO, and so forth). The streamflow/probability data pairs are then plotted to create a probability exceedance curve for each predictor. The three exceedance curves are combined to create a composite exceedance curve which is the basis for the forecast model. This new forecast model calculates weights a, b, and c which are applied to the appropriate predictors to optimize the forecast model's linear error in probability space (LEPS) score. The LEPS score was initially developed by Ward and Folland (1991) and subsequently revised by

Potts et al (1996). The revised LEPS score is used here since the formula proposed by Potts et al. gives a higher score to forecasts of extreme values than to forecasts closer to the observe mean.

3.4 Results

There is one limitation to the rank sum test and its significant results. In the current analysis there are a total of 11 climate indices (four climate indices, six combinations of the same, and the LTES) which yielded a total of 5,423 rank sum test results. Of these tests there were a total of 828 significant test results. Based on the chosen α for our analysis, 272 of the significant results (5,423 x 0.05) have a probability of representing Type I errors. In other words, approximately 1/3 of the significant results can come back as false positives. To address this issue, the total number of successful results at each streamflow gauge station was ranked according to the p-value resulting from the Rank Sum test. P-values close to 0.05 have the highest chance of a Type I error, so only the two lowest p-values at each station were reported.

3.4.1 Climate Indices

Figure 3.4 shows the total number of successful results from each climate input. By far, the most successful index input to the rank sum test is the LTES. In fact, the Jan-Feb-Mar LTES rank sum test resulted in significant results at all 29 stations. It is also interesting to point out that the next largest number of successful results came from the NAO and the AMO index tests. As the analysis lag increased so did the number of successful results attributed to the AMO. Table 3.1 shows the top two index inputs at each gauge location. The SST index references in Figure 3.4 is the LTES resulting from the SST-Streamflow SVD analysis for the given interval length and lag number.

USGS Sta. No	Index / Avg Month Interval / Lag	USGS Sta. No.	Index / Avg Month Interval / Lag
09072500	[1] SST / 3 / 8 [2] NAO / 3 / 3	09315000	[1] SST / 3 / 6 [2] SP(p) / 3 / 9
09095500	[1] NAO / 3 / 3 [2] SST / 3 / 8	09328500	[1] SST / 3 / 9 [2] NAO / 3 / 3
09109000	[1] SST / 3 / 8 [2] SN(n) / 3 / 2	09355500	[1] SN(n) / 3 / 2 [2] AMO / 3 / 8
09124700	[1] SN(n) / 3 / 2 [2] NAO / 3 / 3	09379500	[1] SST / 3 / 9 [2] SN(n) / 3 / 2
09127800	[1] SN(n) / 3 / 2 [2] NAO / 3 / 3	09380000	[1] SST / 3 / 6 [2] NAO / 3 / 3
09152500	[1] SST / 3 / 6 [2] AMO / 3 / 8	09382000	[1] SST / 3 / 7 [2] SOI / 6 / 2
09180000	[1] SST / 3 / 9 [2] AMO / 3 / 8	*09402000*	*[1] SST / 3 / 0 [2] AMO / 3 / 9*
09180500	[1] SST / 3 / 6 [2] NAO / 3 / 3	*09402500*	*[1] SST / 3 / 6 [2] NAO / 3 / 3*
09211200	[1] SP(p) / 3 / 9 [2] SOI / 6 / 6	*09415000*	*[1] SST / 3 / 9 [2] SOI / 3 / 5*
09217000	[1] SP(p) / 3 / 9 [2] SST / 3 / 6	*09421500*	*[1] SST / 3 / 6 [2] AMO / 3 / 8*
09234500	[1] SP(p) / 3 / 9 [2] SST / 3 / 6	*09423000*	*[1] SST / 3 / 6 [2] AMO / 3 / 8*
09251000	[1] SST / 3 / 8 [2] NAO / 3 / 3	*09426000*	*[1] SST / 3 / 0 [2] SOI / 3 / 8*
09260000	[1] SST / 3 / 6 [2] SP(p) / 3 / 9	*09427520*	*[1] SST / 3 / 6 [2] AMO / 3 / 8*
09302000	[1] SST / 3 / 6 [2] SN(n) / 3 / 2	*09429490*	*[1] SST / 3 / 6 [2] NAO / 3 / 3*
09306500	[1] NAO / 3 / 3 [2] SST / 3 / 6		

Table 3.1 Top Two Significant Rank Sum Test Results at Each Station.
SP(p) = PDO-pos vs. PDO-neg. under the SOI-neg. phase. SN(n) = NAO-pos vs. NAO-neg. under the SOI-neg. phase. SA(n) = AMO-pos vs. AMO-neg. under the SOI-neg. phase. Italicized cells denote lower CRB gauges.

These simple observations are not enough to draw hard conclusions, but they do identify additional questions: Why are the NAO and AMO out performing the SOI and the PDO? Why are the Pacific Ocean SSTs performing so well when the SOI and the PDO are not?

The answer to the first question is that this research confirms previous research in related areas. Firstly, McCabe et al. (2007) analyzed the effects of the Northern Atlantic,

Northern Pacific, Tropical Pacific, and the Indian Ocean regions on streamflow in the Upper CRB. While our methods to determine a long-term correlation differ, McCabe et al. (2007) was able to show that while all SST input values were teleconnected to streamflow anomalies in the CRB, a PCA analysis showed that the AMO mode represented more of the variance than the PDO or Indian Ocean SST data. Secondly, researchers (McCabe and Dettinger 2002) have identified that SOI, NINO3, PDO and the Pacific/Northern America (PNA) circulations have weak correlations to streamflow in the upper CRB. Those who have observed this suppose that the typical climate of the Upper CRB is not completely similar to either the northwestern or southwestern United States and therefore does not maintain the same consistent correlation signal with the tropical Pacific Ocean data.

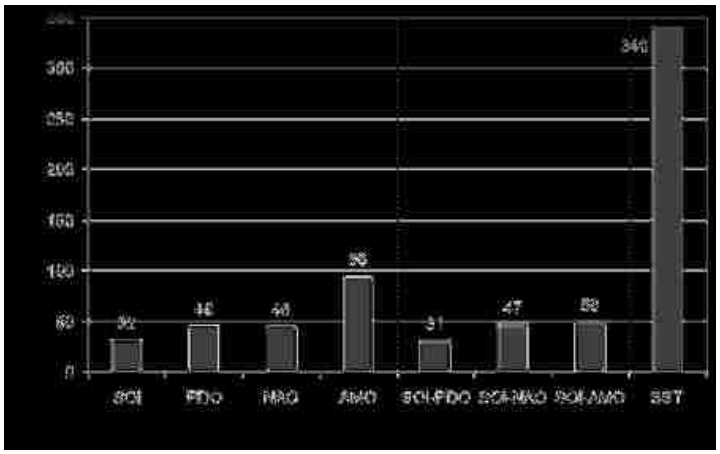

Figure 3.4 Number of significant results of the rank sum test based on climate input recorded across the basin ($\alpha = 0.05$)

As a result of the poor signal response Grantz et al. (2005) developed basin-specific climate indicators as suggested by Yernall and Diaz (1986) . If the established climate indices are not sufficient to determine strong correlation, then it is worth

evaluating whether other regions of the Pacific may serve as predictors. It is along this line of reasoning that the second question was explored: why does the temporal expansion series from the SVD analysis outperform the established climate indices?

3.4.2 Pacific Ocean SSTs

The SVD analysis provides a number of maps which provide a helpful amount of information about what might be a basin-specific climate index (See Figures 3.5 and 3.6). These figures are generated by plotting the significant correlation coefficients of the left (SST) and right (streamflow) heterogeneous matrices. Starting at lag = 0 (Jul-Aug-Sep & Apr-May-Jun-Jul-Aug-Sep) there is a visible signal from the ENSO region of the Pacific which diminishes as the lag number increases. Conversely, as the lag number increases, another area located east and south of Japan begins to grow until reaching its maximum size around lag = 6 for the 3-month average interval, and lag = 4 for the 6-month interval). The difference in sign between the ocean area east of Japan and the streamflow gauges shows that they are negatively correlated: as one is increasing, the other is decreasing.

It is interesting to observe that the region in question is anchored over an area that this paper defines as 150 E to 200 E (160 W) and from 24 N to 34 N. This particular area is south and west of the area which is associated with the northern Pacific signals of the PDO as identified by Mantua and Hare (2002). However, this area is not original to the current research as it has been identified in other research without being specifically

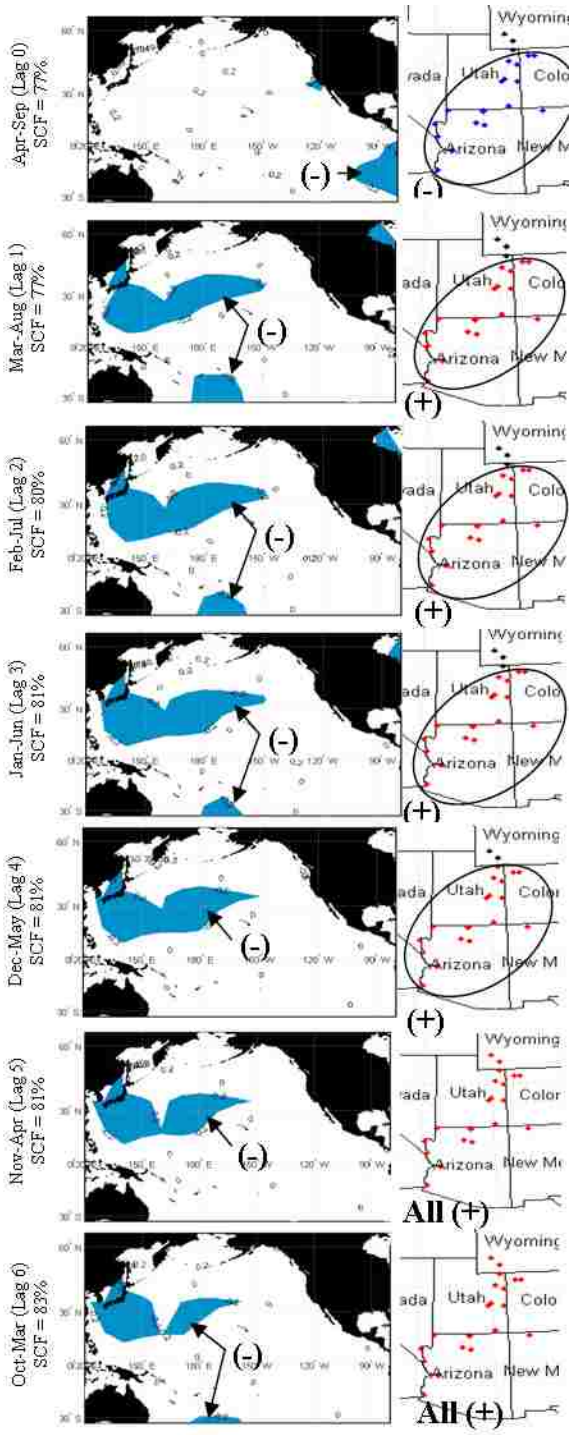

Figure 3.5 6-month left and right heterogeneous correlation maps ($|r| \geq 0.27$) plotted from 6-Month Average SST data, from Lag 0 to Lag 6. SCF values displayed for first mode.

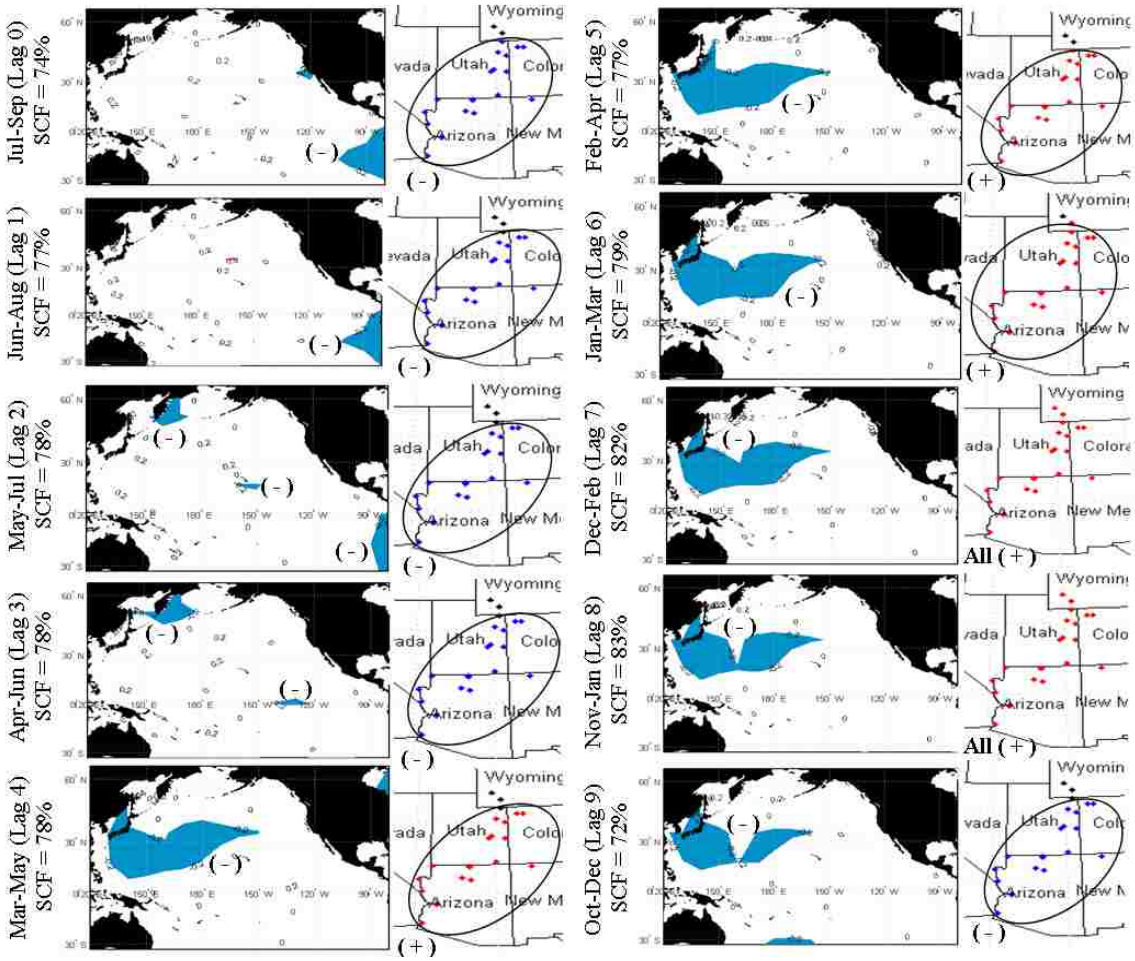

Figure 3.6 3-month left and right heterogeneous correlation maps ($|r| \geq 0.27$) plotted from 3-Month Average SST data, from Lag 0 to Lag 9. SCF values displayed for first mode.

acknowledged or defined Wang and Ting. 2000; Tootle and Piechota 2006; Soukup et al. 2010). Work by Rajagopalan and Lall identified a similar pattern using the Kaplan SST data which is organized at 5° spacing. Because the area is located adjacent to Japan, this paper refers to this area as the Hondo region. *Hondo* is a Japanese word for "main road" or "highway". In Spanish, *hondo* is an adjective meaning "deep", and it is most commonly used when referring to water. Since the word is used in two languages which

are geographically relevant to the research at hand and its meanings are relevant to the research, this region of the ocean lends itself to this designation.

The success of the LTES as an index can be explained through the way in which it is created and how it can be used. Since the LTES is the projection of the SST variance onto the normalized raw SST data, the result is a vector which represents the scaled SST variance within the given 3-month (or 6-month) interval of time selected for the analysis. For all but three of the analysis periods (3-month, lags 0 and 1, as well as 6-month lag 0), the overwhelming majority of the variance could be explained by the first mode, and is therefore captured as part of the LTES. We hypothesize that this is because the influence of other climate indices is stronger during these periods than the rest of the year. The LTES may seem less ideal to use because it is not simply the standardized SST values of the Hondo region (similar to the PDO, or AMO). As already shown the LTES is the product of the SST and Streamflow data. Which creates another question: How do you create a forecast with a model that requires the forecast point in order to be created? We do not propose to answer this question here. However, since the Hondo region is identified by an SVD analysis it is best to continue discussing the SST-streamflow connection in terms of the SVD output (in essence, the left temporal expansion series).

The teleconnection between the SSTs of the western pacific and the streamflow may be explained from the perspective of the East Asian Jet Stream (EAJS). Zhang et al. (1997a) demonstrated that the presence of high pressures over Siberia, and cold surges from east Asia (travelling on a south-southeast direction from northern china), have a great effect on the winter monsoon season over East Asia. A strong East Asia winter monsoon is characterized by two high-pressure centers: the first is a warm high pressure

center whose mid-point is roughly east of Papua New Guinea while the other center is a cold "dome adjacent to the Siberian region". Between the two high pressure centers is the winter traveling path of the East Asian Jet Stream.

Athanasiadis et al (2010), show that the Hondo region is actually the terminus of the EAJS (Asian/Pacific Jet). By completing an EOF (i.e. PCA) of the average wintertime (Dec-Mar) wind field over the northern hemisphere, this study identified the path of the dominant Asian/Pacific jet. Figure 4 of Athanasiadis et al. (2010) is of special note because it displays the dominant wintertime jet (shown in a heavy black line) based on the EOF analysis superimposed upon the teleconnectivity of the 250hPa zonal wind and the 500hPa geopotential height fields (Wallace and Gutzler, 1981, define teleconnectivity as the absolute value of the strongest negative correlation between a grid point and any other grid point). This figure shows that the terminus of the Asian/Pacific Jet is approximately 150 W, and between 30 N and 35 N. This coincides fairly well with the eastern boundary of the Hondo Region. Athanasiadis et al continue to show that while the first mode of the Asian/Pacific jet EOF is closely correlated with the Pacific/North American (PNA) index, the second mode is not identified as being tied to a specific index. However, it is the second mode which determines the location of the Asian/Pacific Jet (and therefore the EAJS) and the storm track that encroaches on the west coast of North America. It is the second mode of the teleconnectivity patterns which approximate the location of the Hondo region the best.

Yang et al. (2002) identified the consistency at which the EAJS crosses the southern Japanese island of Kyūshū and enters the Hondo region. Yang et al. further identified that as the position of the EAJS changes, there are corresponding changes in

SSTs over the eastern Pacific Ocean and western North America. During the strong winter monsoon events, Zhang et al. (1997a) showed that the surface wind patterns show that the EAJS "bifurcates" shortly after exiting the Hondo region. A portion of the flow pattern turns southeast and enters the path of the jet stream. The other portion is diverted north and joins the Aleutian low. Both air streams ultimately cross into the western United States thereafter.

We hypothesize that the EAJS is the vehicle by which strong Monsoonal moisture is carried from East Asia to western North America. Incidentally, Sun and Sun (as cited in Zhang et al. 1997b) propose that a strong winter monsoon usually precedes a drought summer season in East Asia. We hypothesize that operating in such conditions, moisture, which normally would remain in East Asia is carried by the bifurcated wind flow toward North America. The northerly flow path carries some of the moisture to the western United States where it is deposited as snowfall within the CRB (Aziz et al., 2010).

3.4.3 Forecast Skill Comparison Results

After the SVD and Rank Sum testing is complete, a Hondo index is defined as the LTES of the SVD analysis and then compared to the SOI and PDO index. While the use of indices (e.g., SOI, PDO) may result in skillful long lead-time forecasts of streamflow, some streamflow regions may not be teleconnected to established climate signals and, thus, would result in less than skillful forecasts when using such indices. A distinct advantage of applying SVD to SST and streamflow regions is the possible identification of a new SST region that, when used in a forecast model, results in a skillful streamflow forecast.

The Forecast Skill Comparison method described earlier was employed using the SOI, the PDO, and the SST LTES (taken from the JFM SVD analysis) as the third predictor. Figure 3.7 displays the results from this analysis. At this lag time, the analysis shows that the SOI and the PDO result in negative forecast skill values (i.e. their forecasts are less accurate than the observed mean). On the other hand the SST LTES provided an improvement to the forecast skill over the observed mean demonstrating the potential for the new region of the ocean to be used as a forecasting tool.

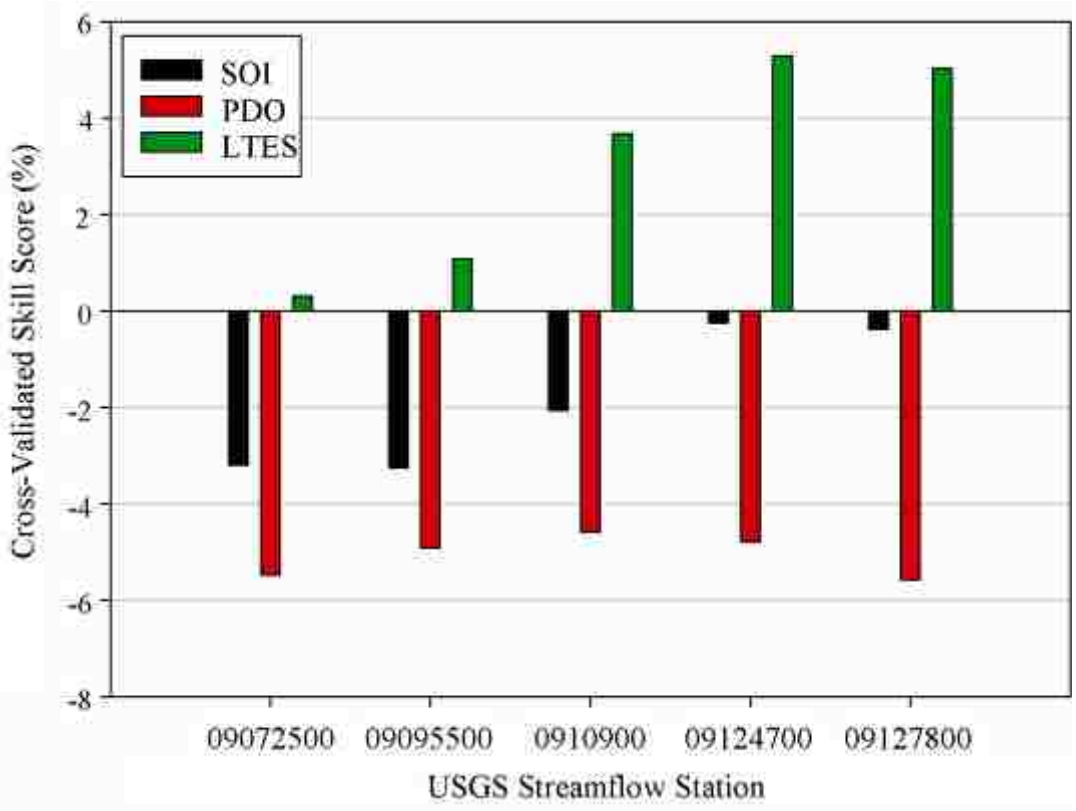

Figure 3.7 Plots showing contribution of index to forecast skill.
Value of '0' is a forecast as good as the mean.

3.5 Conclusion

The goal of this analysis was to find which climate data, combination of climate data, and lead time could be used to increase the skill of forecasting streamflow on the first day of the following water year. The rank sum testing from this research identified at least two different climate inputs for every river gauge in the CRB. For each of the 29 river gauges, there was a significant correlation with an established climate index. However, when comparing the number of successful tests from the different climate inputs, the SST data was more consistent at providing significant results.

Further testing using SVD showed that a long-term correlation exists between the SST anomalies and streamflow anomalies for the Colorado River Basin. SVD testing of 3-month averaged SST data, showed that a region bounded by 150 E to 160 W and 24 N to 34 N, named here as the Hondo region, demonstrates a significant amount of covariance with the streamflow measured over the following water year. As already mentioned, the significance of this region has been demonstrated in other research. The success of the Hondo region lays in the strength and consistency of the Asian winter monsoon, and the effectiveness of the East Asian Jet Stream to transport the moisture across the Pacific Ocean.

The results obtained in this research demonstrate the potential to generate long-lead forecasts of CRB streamflow from SST values observed over the Hondo region in the Pacific Ocean. Therefore, the next steps include identifying a forecast approach which utilizes the climate CRB-streamflow connection observed here. The new work should include a variety of input alternatives to determine the simplest and most effective forecasting model for the entire water year, or simply the seasonal runoff (April – July).

CHAPTER 4

CONNECTING THE PACIFIC OCEAN TO THE COLORADO RIVER BASIN

4.0 Introduction

In recent years there has been increased interest to identify climate-hydrology response relationships using the gridded global data such as sea surface temperature (SST), pressure or zonal wind field data rather than looking to the established climate indices, defined by a subset of the global data, such as the El Niño Southern Oscillation (ENSO) or the Pacific Decadal Oscillation (PDO). The typical application of the global gridded data is to identify covariance relationships between regions of the oceans and surface hydrology such as precipitation, snowpack, and streamflow (Wang and Ting, 2000; Serrano and Rodriguez, 2004; Tootle et al., 2006; Haylock, 2007; Santos et al., 2007; Yuan and Li, 2008; Apipattanavis et al., 2009; Soukup et al., 2010; Wu et al., 2009, Wang et al., 2010a).

The research presented here builds upon Lamb et al (2010) and Aziz et al. (2009) (hereafter referred to as L10 and A10 respectively) which shows there is an area of the Pacific Ocean (150E - 200E, 34N - 24N – hereafter referred to as *Hondo*) which demonstrates a significant correlation with streamflow in the Colorado River Basin (CRB). Both (L10) and (A10) identified this region using a singular value decomposition (SVD) analysis approach. In both cases the Hondo region was identified by isolating the areas whose correlation coefficients exceeded a 95% significance level. Results in (L10) reveal the Hondo region as significant when comparing the winter time SST's from a given water year, with the total yearly streamflow of the following water year. Similarly (A10) identifies the Hondo region when correlating Pacific SSTs with snow water

equivalent (SWE) data from SNOTEL stations located throughout the U.S. Rocky Mountains, also at a year's lag time.

The existing research has left several questions to be answered regarding the Hondo-CRB teleconnection. For example, because the studies L10 & A10 only looked at comparing SST with the streamflow/SWE for the following water year, there is a need to understand how persistent the Hondo effects are noticed in the CRB. In other words, do the Hondo effects appear when climate data are compared with streamflow responses from the *same* water year, as well as at lead times of *more than one* water year? Additionally, since SST's and streamflow are independent variables and are far apart, what is the mechanism connecting the two?

The proposed research has two major tasks: First, the SVD analysis performed in previous papers (L10 & A10) will be extended to include 4 years of SVD analysis: simultaneous response year, and the three years leading up to it. This extended SVD analysis is expected to identify the extent to which the Hondo effects the CRB. Second, the SVD analysis will be applied to atmospheric datasets (such as geopotential height (500mb) and zonal wind (200mb) to delineate dynamical responses to the SST-streamflow relationship identified in the SVD analysis. The hypothesis is that if there is a long-lead physical connection between the Hondo and the CRB streamflow, then the Hondo-CRB teleconnection will appear in the other atmospheric datasets at similar lag times. The goal of this work is to improve the understanding of the climate drivers for the CRB in order to develop an improved long-lead forecasting technique.

4.1 Data

4.1.1 Streamflow Data

The US Bureau of Reclamation (USBR) maintains a spreadsheet of naturalized streamflow data for 29 gauges within the CRB which can be obtained from the following URL (http://www.usbr.gov/lc/region/g4000/NaturalFlow/current.html). Since a given water year actually begins and ends in different calendar years, when this report refers to a given water year (for example, 1996) it is signifies the period October 1, 1995 through September 30, 1996. Therefore when the total yearly streamflow of a given water year is shown, this is referring to the total water volume observed at a given gauge from October 1 through September 30 of the specified water year. In order to maintain some continuity between the previous and current work, this data set is used here because it was used in (L10). The 29 locations are displayed in Figure 4.1.

The SST data comes from work provided by Smith et al (2008) and can be downloaded from the National Oceanic and Atmospheric Administration (NOAA) National Climate Data Center (NCDC) website (http://www.ncdc.noaa.gov/oa/climate/research/sst/ersstv3.php). The SST data are displayed at a 2˚ square grid spacing, and were converted into text files using software, named Ocean Temperature Analysis (OTA), developed at UNLV specifically for this purpose. Apart from the works of Aziz et al., and Lamb et al. this particular SST data has been used in previous works to identify a connection between ocean activity and the response in western U.S. streamflow (Tootle and Piechota, 2006; Tootle et al, 2007; Soukup et al. 2010).

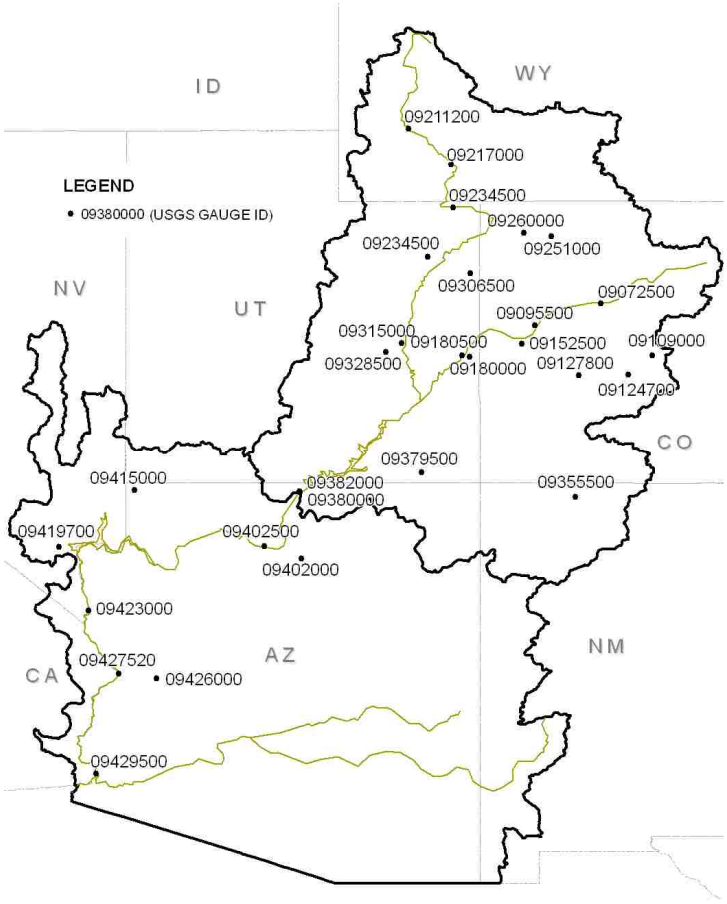

Figure 4.1 Location map of 29 USGS streamflow gauges

4.1.2 Climate Data

The 500mb geopotential height (Z500) and 200mb zonal wind field (U200), are obtained from the NCEP/NCAR reanalysis product (Kalnay et al, 1996) available for download at http://www.esrl.noaa.gov/psd/. The data for the variables listed covers the entire globe at 2.5º square grid spacing. For this analysis, only the northern Pacific Ocean region will be used, (in essence, 120E – 80W and 70 N to the equator (0). Since its inception the reanalysis product has been used in thousands of applications to provide a better understanding of global circulation patterns (Roundy and Gribble-Verhagen 2010; Roundy et al. 2010; Pauluis et al. 2010; Grise et al. 2010), or to improve the

understanding of the connection between global climate and associated responses in hydrologic phenomena (Wang et al., 2010a; Johnstone 2010; Johnstone 2010; Zhao et al. 2009; Patricola and Cook 2009; Fu et al, 2009; Adam et al, 2009) More relevant to the current research, there are some recent examples of how this data is used to improve the understanding of climate impacts on the CRB and closely related areas. Lundquist and Flint (2006) used the data in order to identify reason for the early snowmelt-streamflow runoff season in the Sierra Nevada Mountains observed in 2004. A study by Gochis et al. (2007) looked at the North American Monsoon and its lagged correlation relationship with Pacific and Caribbean Ocean SSTs. Bracken et al (2010) utilized the global dataset to identify potential predictors of streamflow within the CRB. The studies not only demonstrate the applicability of this data, but the utility of using these data as opposed to another dataset.

4.2 Methodology

In (L10), the SVD analysis was performed using 3-month average SST values from July – September and the observed streamflow volume generated during the following water year (October 1 – September 30). This analysis was repeated for June – August average SST values (Lag = 1 Month), for May – July (Lag = 2 Months), and so forth until the average SST values from October – December (Lag = 9 Months) was compared with the water volume from following water year.

In the research presented here the analysis includes comparing SST values and streamflow values with a 0-year lag (simultaneous response year), as well as at 1-, 2- and 3-year lag times, essentially reproducing some of the work provided in Lamb et al (2010), but adding additional lag times. Figure 4.2 demonstrates the progression of the lagged

SVD analysis. However, due to the large number of correlation maps, only the July – September (JAS), April – June (AMJ), January – March (JFM), and October – December (OND) intervals will be displayed here.

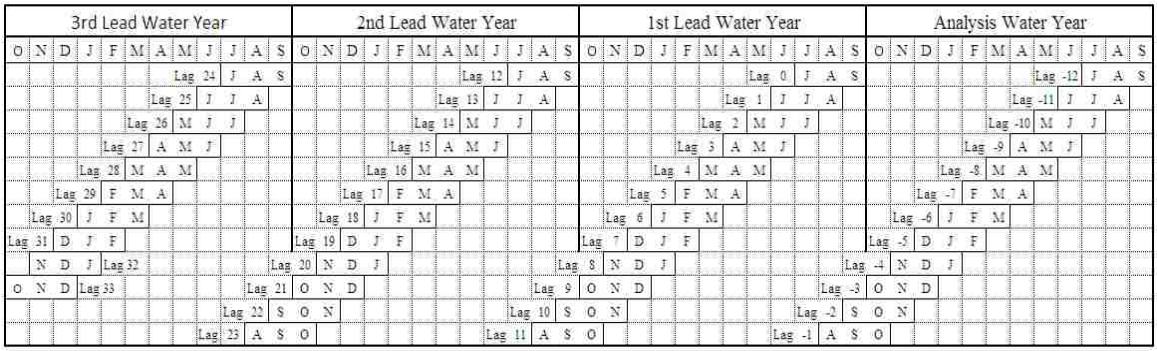

Figure 4.2 Lagged analysis schematic

The SVD analysis itself has been used in many applications when comparing the behavior of two datasets (Prohaska, 1976; Bretherton et al. 1992; Wallace et al. 1992). The method is described in detail in (L10). The purpose of the method is to identify locations in the ocean and streamflow data that are significantly correlated to the principle components identified in the SVD analysis. If the squared covariance fraction (i.e. the percentage of variance explained by a given mode) of the principle component is greater than 10%, then it is used in the correlation analysis. A 95% confidence level is set to determine if the calculated correlation value is occurring by chance. Because the CRB is a relatively small area, it is expected that the vast majority of the variance will be explained by the first mode of the SVD analysis.

The purpose of this analysis is to identify the extent of the impact the Hondo has on the CRB streamflow. It is expected that this analysis will show the Hondo as non-significant in the 0-year lag because of the noise created by extreme ENSO cycles. It is

also expected that the strongest connection will be with the one-year lag, and then a diminishing connection as the lagged analysis increases into the second and third years.

In addition to providing an extended SST-Streamflow SVD analysis (SST-SVD), the current research proposes to utilize the extended SVD results to identify the correlation with Z500 and U200 datasets. These correlation analyses use the streamflow temporal expansion series that is calculated as part of the SVD analysis. While a detailed description of this calculation is provided in L10, a brief explanation of how the temporal expansion series is determined is provided here. The SVD on the SST – Streamflow covariance matrix gives three matrices [SVD(covarTS) = $U \Sigma V$], where V represents the decomposed covariance values closely associated with the streamflow. Therefore, given the decomposed matrix, V, and the original matrix of streamflow anomalies, S, the streamflow temporal expansion series (STES) is determined by the following equation: $STES = V'S'$. The result of this calculation is a series of values, one for each time period in V and S. The STES is then correlated with cell of the Z500 and U200 gridded data so that the correlation responses portray possible circulation anomalies linking SSTs to CRB streamflow.

4.3 Analysis Results

4.3.1 Extended SVD Results

Extended SVD analysis results are displayed in Figures 4.3 and 4.4. Figures 4.3(a) and (b) show the SST-SVD results from the simultaneous response year, and the 1-year lag time respectively. Figures 4.4(a) and (b) show the results from the 2-year and 3-year lag

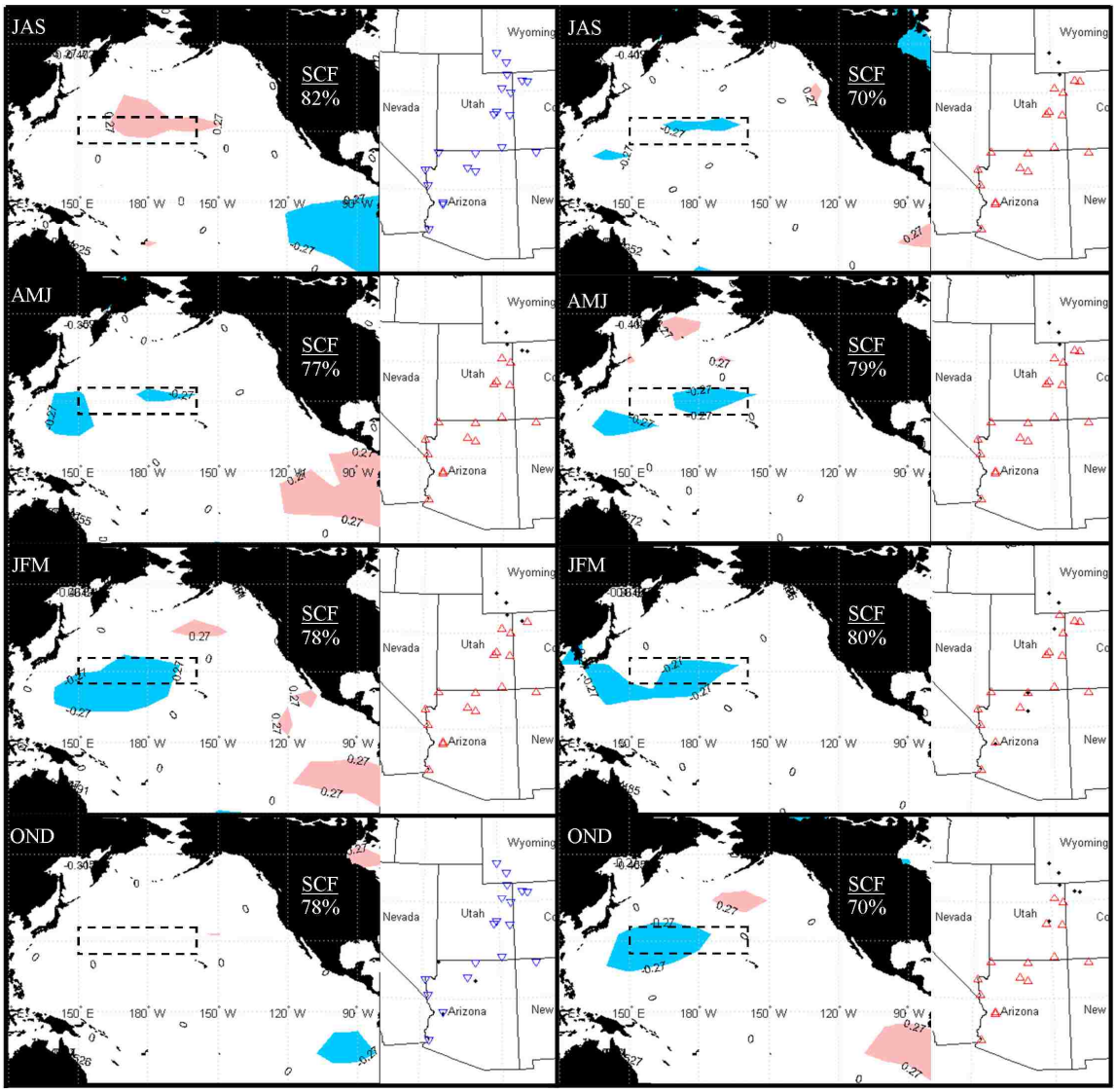

(a) (b)

Figure 4.3 0-year and 1-year lag correlation maps from SVD analysis
Figure (a) shows the correlation maps ($\alpha = 0.05$) for the simultaneous response year and (b) 1-year lag. Red SST regions/Streamflow gauges show increasing temperatures and streamflow, while blue shows decreasing temperatures and streamflow. The Hondo is shown as dashed rectangle.

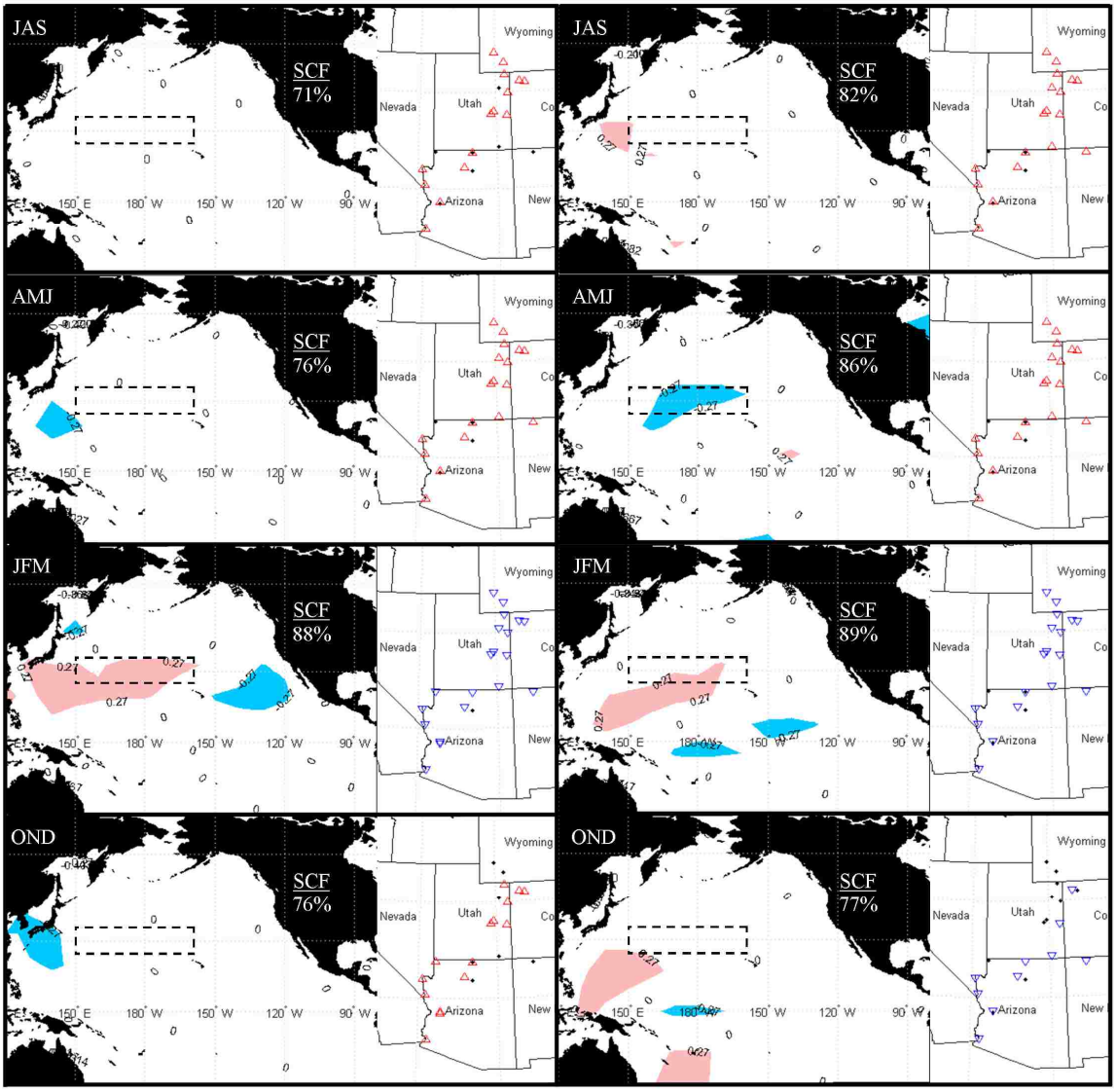

(a) (b)

Figure 4.4 2-year and 3-year lag correlation maps from SVD analysis
Same as Figure 3, but showing the (a) 2-year lag and the (b) 3-year lag times.

times. The "SCF" values labeled on each map represent the squared covariance fraction for the mapped, SVD analysis mode. A black dashed line shows the limits of the Hondo Region as defined by L10 and A10.

These figures display regions of the Pacific Ocean that are linked to streamflow gauges in the CRB. Red/Blue regions of the Pacific Ocean denote increasing/decreasing temperature teleconnections. Similarly, up-oriented red triangles and down-oriented blue triangles represent increasing or decreasing streamflow teleconnections respectively. If the significant region of the ocean and a streamflow gauge have the same color, then this denotes a positive correlation relationship. If the SST and streamflow regions have opposite colors then this displays a negative correlation relationship. If the maps display a region of cool SSTs correlated with increasing streamflow, then we can also say that warm SSTs over the same region will be associated with decreasing streamflow gauges.

During the simultaneous response year analysis, one notices that depending on the time of year, the Hondo or the Eastern Equatorial Pacific Ocean SSTs are more significant. Figure 4.3b, 1st Year Lag analysis, and Figure 4.4a, 2nd Year Lag show how the Hondo is again significant during the winter months, though during the 2nd year, it appears that the impact of the Hondo is diminishing. By the 3rd lag year, the impact of the Hondo is diminished and the central equatorial Pacific Ocean develops into a significant SST region. It is noteworthy that as the lag increases, the Squared Covariance Fraction (SCF) represented in the correlation maps also increases. It is hypothesized that as the lag time increases there is less SST-CRB covariance contained in the data. Therefore it is easier for the first mode to represent more of the data (increasing SCF values) because there is less covariance.

4.3.2 Correlation Analysis Results

Figures 4.5 and 4.6 show the correlation patterns of Z500 correlated with the SST-SVD results. There is a complimentary significant pattern in the geopotential height field. During the simultaneous year winter interval (JFM) a significant cyclonic cell is stationed over the west coast of the U.S. and has a "tail" which extends westward across the Pacific. The cyclonic cell is also viewed as a significant region in the central Pacific Ocean, over the Hondo region, for the 1 and 3-year lag times.

The 2-year lag time shows only the head of the cell that is located over the northwestern U.S., though during OND a train of cyclonic and anticyclonic Z500 cells appear to link the Hondo with the western U.S. These results shows that as the SSTs in the Hondo region cool, there is an associated decrease in atmospheric pressure over the Hondo region, which induces a simultaneous drop in pressure to the west of the CRB through the atmospheric teleconnection. The resulting cyclonic cell near the western U.S. enhances the subtropical jet and, in turn, supplies the CRB with moist air from the subtropical Pacific Ocean.

The U200 correlation analysis, shown in Figures 4.7 – 4.8, also compliments the SST-SVD analysis. Looking at the simultaneous response, a significant region is identified within the Hondo region showing that increasing wind anomalies occur with decreasing SSTs as well as with decreasing atmospheric pressure to the north. This pattern is repeated in the 1st, and 2nd year lags, but is not present during the 3rd year lag. At this time there appears a significant region around the central equatorial Pacific, suggesting a shift in the jet position associated with the geopotential height response (i.e. Figure 4.6, JFM interval).

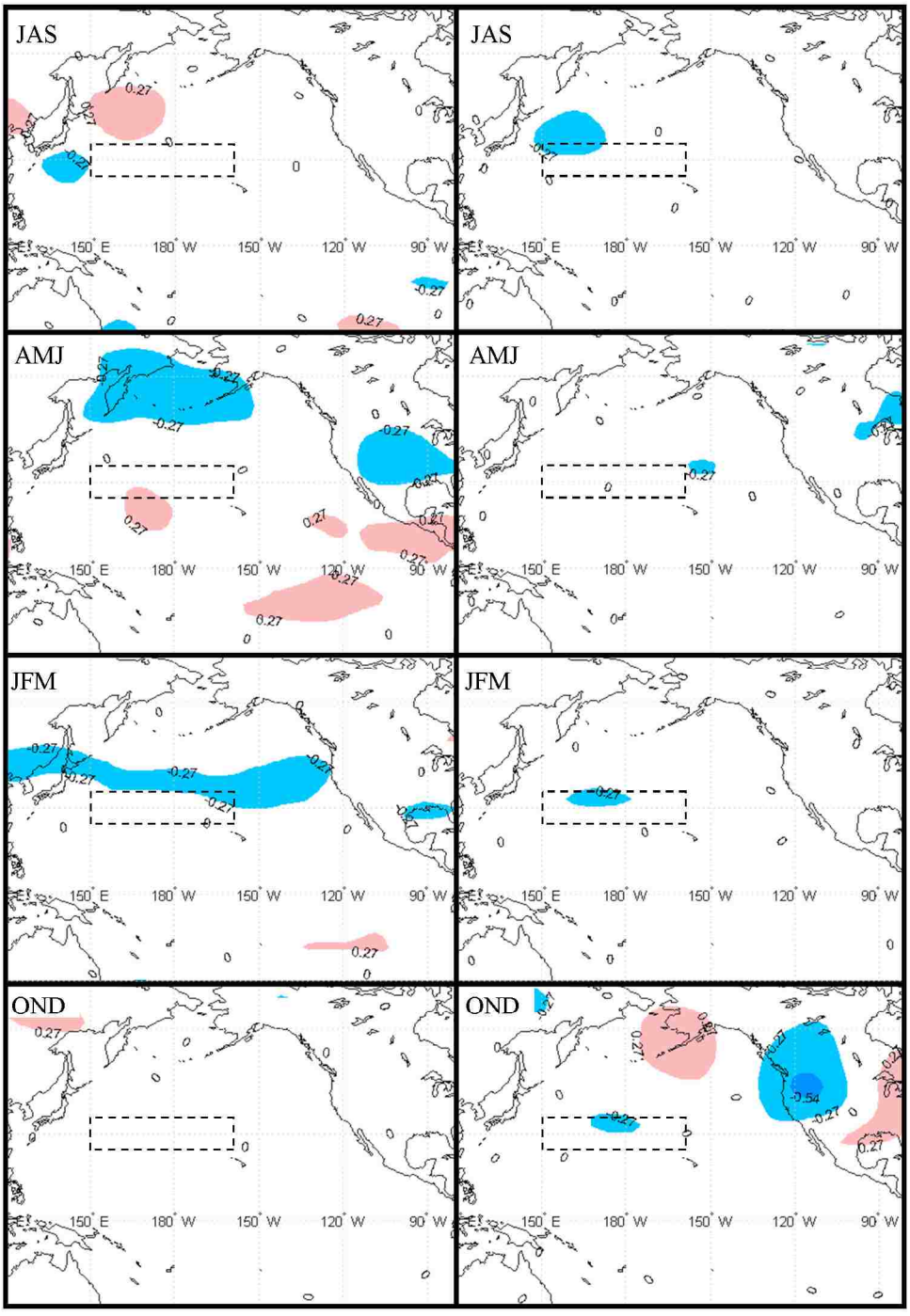

(a) (b)

Figure 4.5 0-year and 1-year Z500 correlation maps
3-month Z500 data correlated with right temporal expansion series from SST-SVD analysis for (a) simultaneous response year and (b) 1-year lag times. Red regions show increasing pressure anomalies while blue show decreasing anomalies. These regions correspond to the streamflow correlation maps shown in Figures 4.3 and 4.4. The Hondo region is shown as dashed rectangle.

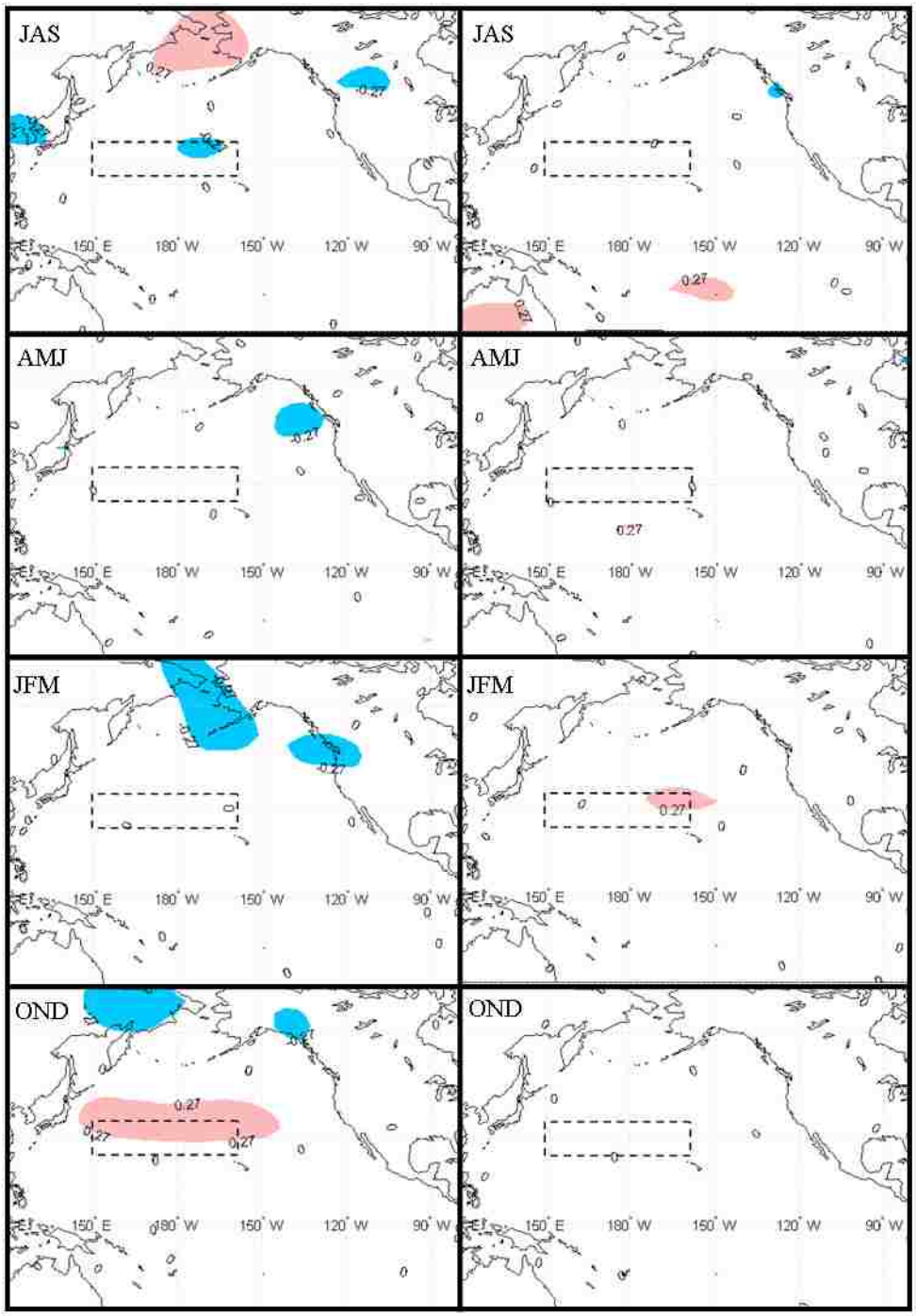

Figure 4.6 2-year and 3-year Z500 correlation maps
Same as Figure 4.5 except showing (a) 2-year and (b) 3-year lag times.

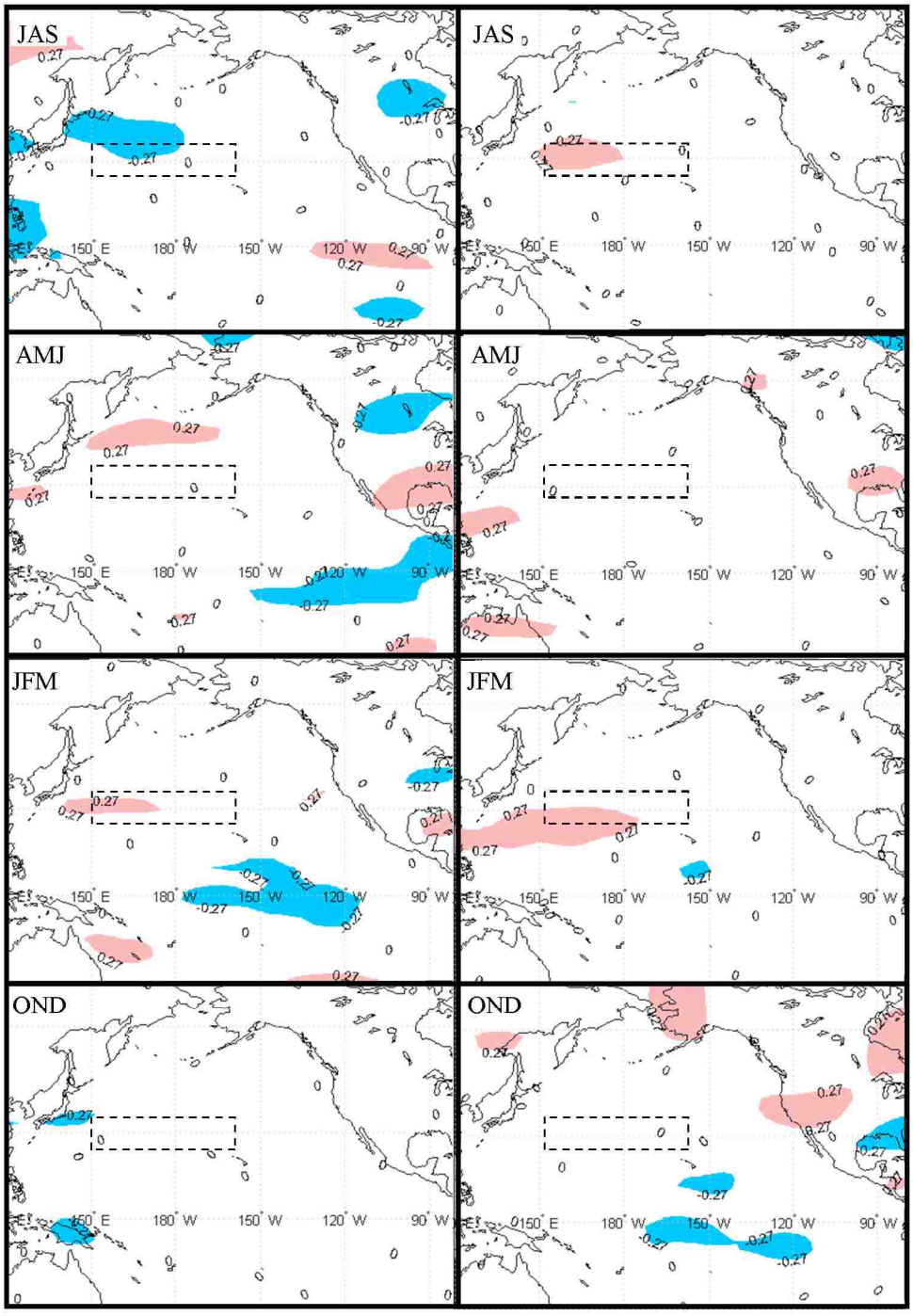

(a) (b)

Figure 4.7 0-year and 1-year U200 correlation maps
Same as Figure 4.5, but for 3-month U200 correlation values showing the (a) simultaneous response and (b) 1-year lag times.

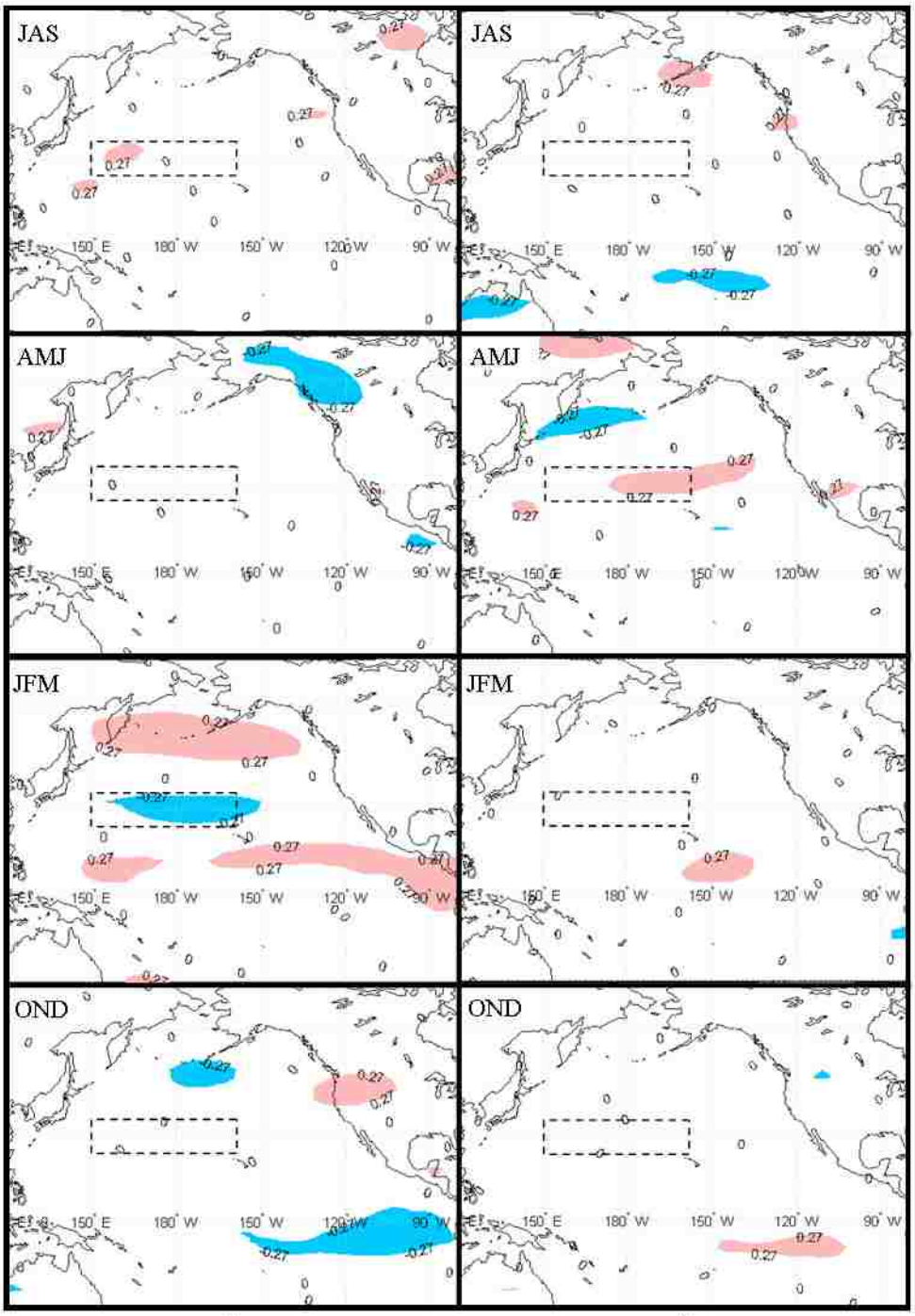

(a) (b)

Figure 4.8 2-year and 3-year U200 correlation maps
Same as Figure 4.7 but for (a) 2-year and (b) 3-year lag times.

Therefore, the Hondo appears to be significant during the JFM interval for the simultaneous year, as well as the 1st, and 2nd lag years. It is also important to point out that the 3rd year shows the Hondo as significant as part of the Z500 correlation analysis, but the SST and U200 analysis show significant regions being in the western tropical Pacific Ocean and central Pacific Ocean respectively. The 'disaggregation' of the significant regions in the 3rd year is explained in the following section.

4.4 Discussion

4.4.1 Climatology

In order to provide a context for a discussion about the results, Figure 4.9 was created to show the mean climatology data (1968 – 1997) of the U200, and SLP data created using the online NCEP/NCAR Reanalysis plotting tool located at http://www.esrl.noaa.gov/psd/cgi-bin/data/composites/printpage.pl. The black and white dashed line on Figure 4.9 depicts the location of the jet core winds greater than 20 m/s.

In general, the U200 climatology maps (Figure 4.9a) shows that the East Asian Jet Stream (EAJS) remains relatively weak (~25 m/s) and somewhat north during the summer months of each year – essentially permitting the North American Jet Stream (NAJS) to transport tropical air into the U.S. During the winter months the EAJS increases in intensity (up to ~65 m/s) and shifts southward until reaching the approximate location of the Hondo region. Though Figure 4.9a shows the U200 jet core (>20 m/s) joining the EAJS and the NAJS, the EAJS splits into a northerly component, which joins the Aleutian low, and a southerly component which joins with the NAJS on its journey across the southern U.S. (hence the southerly dip in the jet core). The fact that the EAJS

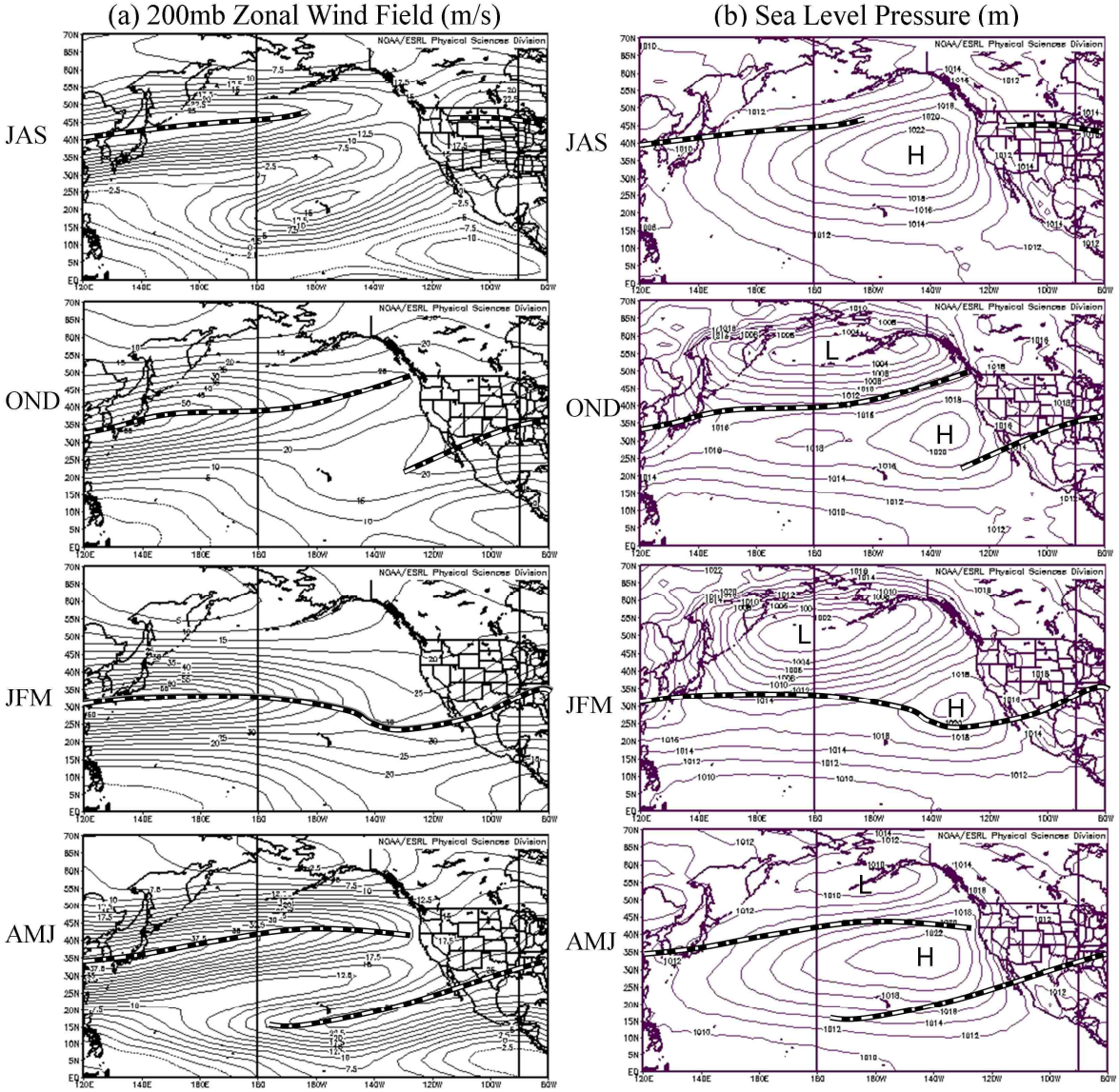

Figure 4.9 Zonal wind field (a) and sea level pressure (b) climatology maps. Climatology mean taken from (1968 – 1977)

is the primary driver of storm tracks toward the U.S. west coast was demonstrated in work by Athanasiadis et al (2010) and many earlier works, and the bifurcation of the EAJS was previously observed and described by Yang et al (2002).

Assisting with this process is the changing subtropical high off the west coast of the U.S. as well as the deepening of the Aleutian low. During the summer months the

weakened EAJS is directed northward by the high pressure dome located off the western coast of the U.S. As summer turns to winter the subtropical high decreases while the Aleutian low becomes deeper and larger. The wintertime circulation patterns observed in Figures 4.3 – 4.8 demonstrate that they are associated with an enhanced EAJS and a decreased subtropical gyre.

Rasmussen and Wallace (1983) helped contrast the climatology with the impacts of the 1983 El Niño event. They showed, for this particular El Niño event, the EAJS extending further into the Pacific Ocean before beginning to disaggregate, thereby carrying more of the storm energy directly toward the central west coast of the U.S. and on to the CRB. Their work helped demonstrate that the concentration and intensity of the EAJS contributed to the most extreme CRB water year of the last century.

Other work (e.g., Tootle et al, 2009) showed how there were some similarities between the ENSO signal predicted for the 2009-2010 Niño 3.4 anomalies, and those observed from past El Niño events – including the 1983 and 2003 events. Interestingly enough the 2009-2010 event was relatively typical as far as its impact on the CRB, the 1982-83 event was the most extreme, and the 2002-03 was the least extreme on record. The contrast between the winter of 1982-83 and 2002-03 can be observed on Figure 4.10. The JFM zonal wind was only slightly greater than climatology, and the west coast pressure dome was only marginally lower than climatology. It appears that these two factors contributed to making the 02-03 El Niño event appear like an average water year. In fact it brought the least amount of rainfall of any El Niño event in the last 60 years, a

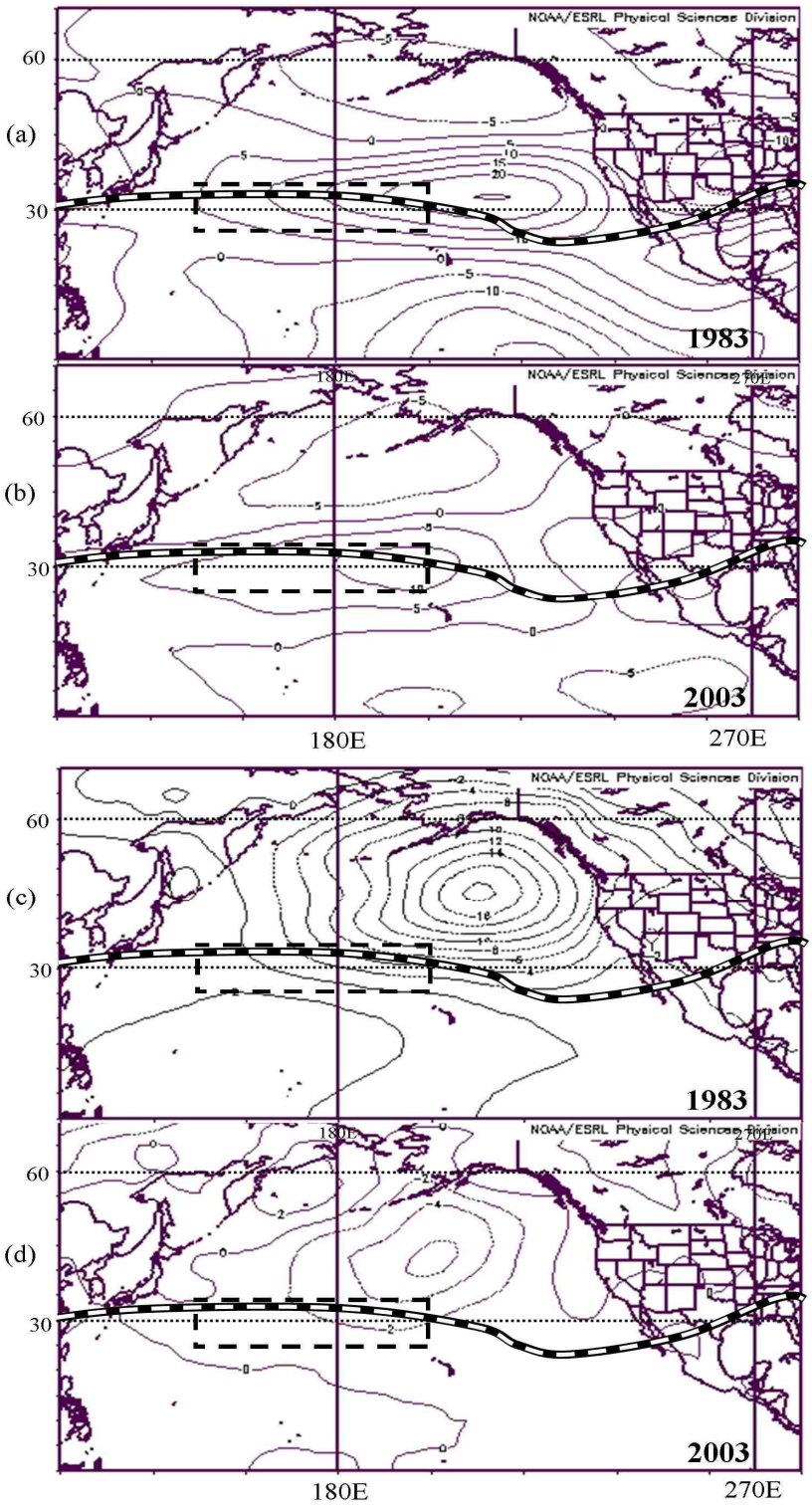

Figure 4.10 Comparison between 1983 and 2003 ENSO Events
Showing (a) mean U200 JFM values from 1983, (b) mean U200 JFM values from 2003, (c) mean SLP JFM values from 1983, and (d) mean SLP JFM values from 2003. Dashed white line represents the dominant location (>20m/s) of the jet stream, and dashed box, the Hondo region.

phenomenon coincident with the quasi-decadal drought cycle as shown in Wang et al. (2009). This information helps demonstrate that the circulation patterns can operate somewhat independently of the ENSO signal, and therefore, need to consider other factors when assessing climate impacts on the CRB.

4.4.2 The Lagged Relationship

Understanding the climatology, it can now be seen that the SVD and correlation results in a proper light. The results from the SST-SVD analysis show a significant covariance region corresponding to the location of the EAJS as well as the associated atmospheric circulation patterns observed in the Z500 analysis and in the SLP climatology maps. In addition to this, there is a noticeable ENSO-like pattern which appears even though the ENSO does not have a significant relationship with the upper CRB (Dettinger et al., 1998; Rajagopalan and Lall, 1998). This ENSO Pattern is not observed in any of the lagged response years, but the Hondo remains identifiable. Therefore one may ask: Are the regions identified in the lagged analysis part of another climate cycle acting on the CRB, of are they simply the results of a statistical analysis?

Research by Wang et al (2009, 2010b, 2010c) (hereafter referred to as W09, W10b, and W10c respectively) helps to answer this question. Examining the observed 10-20 year cycle in precipitation over the intermountain west, W09 demonstrate that within the transition phase of the Pacific Quasi-Decadal Oscillation (PQDO) there is a lagged relationship between pacific SST's and observed precipitation in the intermountain west (It is important to note that the PQDO referred to in this paper is not the same as that defined by Mantua and Hare (2002), but the result of work by Zhang et al. (1997b) which is the first principle component of the Pacific Ocean SST's from 25˚ S

to 60˚ N, which contains the variation from the tropics). Specifically, the analysis in W09 suggests that the PDO cycle leads the intermountain precipitation cycle by 3-4 years.

The research in (W10b) tested the applicability of the 10-20 year climate cycle to a surface water hydrology question, namely: what is the cause behind the prominent coherence between the central tropical Pacific SSTs and the surface elevation of the Great Salt Lake (GSL)? The results of this work reaffirmed the 3-year lagged response between pacific SSTs and precipitation and furthered demonstrated a 3-year lagged response in the GSL elevation following the precipitation. This process leads the GSL to lag the central tropical Pacific SST variations by a half phase (~6 years) of the quasi-decadal cycle of the PQDO. The result of W10b suggests that precipitation fluctuations near the CRB are more strongly influenced by non-extreme ENSO periods rather than by the typical, strong ENSO events.

Comparing the results obtained in W10b with the SST-SVD results from this paper, it becomes apparent that the Hondo region reveals persistent responses in three consecutive lags (0-2) but dissipates in lag 3. Figure 4.4b, while showing a significant region stretching from the western tropical Pacific region into the Hondo, also shows the significance of the central equatorial Pacific Ocean becoming significant (a pattern which is also identified in Figure 4.8b. In other words, it appears that the reason the Hondo SST is no longer significant by the third lag year is that it has past the typical 3 year influence period of the PQDO. The comparison of these two papers appear to show that the significance of the Hondo region, which is also observed during the transition phases of

the PQDO (W10b), can be explained as an intermediate cycle falling in between the inter-annual ENSO events and the slow-varying PQDO cycles.

Additional work in W10c helps solidify this conclusion, by showing that the Hondo may induce an atmospheric wave train which has a direct relationship with the CRB during transition phases. Firstly, the 3-year lag time between the Pacific SSTs and the intermountain precipitation was established by analyzing the water vapor budget over the Great Basin. This examination identified that the water vapor flux convergence (one of the terms in a water vapor budget) is the primary contributor to precipitation over the Great Basin, requiring transient activity (e.g., cyclone waves) to occur in the right place. Therefore an empirical orthogonal function (EOF) analysis was performed using the gridded moisture flux potential data over the Pacific Ocean. The coherence between the Pacific SSTs and the first mode (EOF1) of the moisture flux potential are highly correlated. Likewise the Pacific SSTs are also highly correlated with EOF2, but at a 3-year lag time. In other words the primary modes of the atmospheric moisture budget are associated with Pacific SSTs leading the Great Basin precipitation by about 3 years.

The way that the SVD analysis contained in this research coincides with the physical connection between the Great Basin precipitation and the PQDO identified in W10b and W10c. In particular, the important role of the Hondo SST variability and its associated teleconnection wave train, as were shown in W10c, are both similar to those revealed in the SVD analysis and the circulation patterns throughout lags 0-2 (Figures 4.4-4.8). Along its path the Hondo is visible as a component of this short wave train (see Figure 2b of W10c) which induces anomalous low pressure to the west of the Intermountain region. The location of the starting point of the short-wave train not only

helps to explain Hondo's existence and importance, but it explains why the western tropical Pacific Ocean region shown in Figure 4b (JFM interval) is significant as well. Therefore the Hondo is simply one component on a track of regions responsible for transporting moisture from the tropics to the CRB.

Another insight into the reason for the 1-year lag of the Hondo (and the diminishing 2-year lag as well) is the fact that because the Hondo is part of the wave train during the winter months (JFM) of transition years (non-extreme ENSO years), it should have a stronger signal with the CRB during periods when the ENSO is not impacting climate signals in the Pacific Ocean. Since the ENSO signal is short-lived, the Hondo appears at longer lead times because it is always a part of the mechanism transporting moisture to the CRB. By the 3-year lag time the persistence of the Hondo is superseded by the signal coming from the central equatorial Pacific Ocean (i.e. the QDO). This demonstrates that while ENSO remains a considerable factor affecting the CRB, the Hondo is a "new" factor that has a sustained effect on the CRB streamflow for up to three years. This finding strongly suggests the potential for an extended range of streamflow prediction.

4.5 Summary and Conclusions

The connection between the Hondo and the CRB streamflow is identified through two avenues in this paper. First, the SVD analysis of SST, as well as the correlation analysis with the Z500 and U200 data, showed that the SST-CRB connection identified in Lamb et al (2010) and Aziz et al (2010) exists in the atmospheric data at similar lag times. This analysis demonstrated the connection between the Hondo was not simply a statistical relationship between two independent variables, but a result from the

covariability of the Pacific Ocean and the atmospheric circulation through the so-called teleconnection.

The second way the Hondo-CRB connection was identified was by understanding the physical connection behind the lagged response between the two datasets. The work provided by Wang et al., (2009, 2010a, 2010b) helped identify the quasi-decadal cycle embedded in the Pacific Ocean and the fact that the precipitation in the inter-mountain west region is on a similar cycle, but lags 3-years behind the SST cycle. The physical connection between the Pacific Ocean and the precipitation was outlined by identifying a similar 3-year lag in the first two principle components (EOF1 and EOF2) of the filtered moisture flux stream function. EOF1 was highly correlated with the SST cycle while EOF2 was highly correlated with the precipitation cycle.

The utility of this research is to create the technical confidence needed to use the Hondo as a potential tool for creating long-lead forecasts of the CRB streamflow. The National Weather Service utilizes an Extended Streamflow Prediction (ESP) software tool that employs historic temperature and precipitation time series to generate an ensemble of future streamflow scenarios. Knowledge about the lagged relationship between the Hondo and the CRB can be used to weigh the ESP output, essentially adding a "long-lead cycle" bias to the historical data. The result of this work has the potential to improve the long-lead forecast ability for the CRB.

CHAPTER 5

TESTING A POST-ANALYSIS WEIGHTING TECHNIQUE TO IMPROVE LONG-LEAD FORECASTS OF THE COLORADO RIVER BASIN

5.1 Introduction

The National Weather Service's (NWS) Colorado Basin River Forecast Center (CBRFC) issues regulated water supply forecasts for the Colorado River Basin on a monthly basis. Each month the forecast includes streamflow volumes expected for the following three months. During the winter and spring months, the typical 3-month forecast is accompanied by the season spring runoff forecast, given as a 4-month lump sum volume for the April – July period. In addition to these official forecasts the CBRFC produces a yearly outlook on August 1 and October 1 for a given water year for the following water year. These forecasts represent the best estimate of water resource supply in the Colorado River Basin (CRB), and are created using the Extended Streamflow Prediction (ESP) software.

Water resource managers at the U.S. Bureau of Reclamation (USBR) use the forecasts created by the CBRFC to model the next 24-months of resource storage, releases, and diversions in order to predict future reservoir levels and plan for hydro-power generation supply. Since the CBRFC forecasts run at most for 12 months and the USBR creates a 24-month projection of water usage, the USBR must make estimates of the last 12 months of the 24 month projection. This estimate is partially made by extrapolating information from the CBRFC forecasts and the remainder is filled with the 30-year mean streamflow observed from 1971 – 2000. Therefore an improvement to the

status quo is to identify climate patterns which can increase the accuracy of the long-lead (> 1 year) streamflow forecasts in the CRB.

The utility of long-lead forecasts based on climate has been introduced and assessed in previous research. For example, because of the prominence of the El Niño Southern Oscillation (ENSO) signal on streamflow in the western United States, the related indices explaining the ENSO have appeared in many studies (Piechota and Dracup 1996; Piechota et al. 1997; Hamlet and Lattenmeier, 1999; Clark et al. 2001; McCabe and Dettinger 2002; Werner et al 2004; Grantz et al, 2005). However McCabe and Dettinger (2002) as well as Werner et al (2004) demonstrated that the ENSO has very little impact on CRB streamflow, because of the weak correlation with the upper CRB river gauges. Therefore if the ENSO signal can not enhance the long-lead streamflow forecasts, then which other climate data can be used?

The current paper builds upon recent research (Lamb et al, 2010a; 2010b; Aziz et al, 2009) which shows there is an area of the Pacific Ocean (hereafter referred to as *Hondo*) which demonstrates a significant correlation with streamflow in the Colorado River Basin (CRB). Both Lamb et al. and Aziz et al. identified this region using a singular value decomposition analysis. In both cases the level of significant covariance was determined by finding regions whose covariance exceeded the 95% significance level of the correlation coefficient. Lamb et al (2010a) show the influence of Hondo when comparing the winter time SST's of Hondo from a given water year, with the total yearly streamflow of the following water year. Aziz et al. show a similar Hondo pattern when comparing SST and snow water Equivalent (SWE) data from the Rocky Mountains in the U.S. with a year lag. Finally, Chapter 4 demonstrated that the Hondo is connected

to streamflow in the CRB during the winter months through an enhanced jet stream and decreased subtropical gyre on the west coast of the U.S.

Because the ESP output is an ensemble of possible streamflow scenarios for representing a given forecast period, it is possible to weigh the output and thereby introduce a climate-based bias in order to create a new forecast value. Work by Werner et al (2004) proposed to do this using climate index data based on the ENSO signal, in order to improve the spring runoff forecasts of the CRB based on climate observations from the previous fall or summer.

Because the ENSO signal is weak in the CRB, the existing research has provided the foundation for using the Hondo as a basis for forecasting the streamflow. Therefore, the proposed research aims to determine the 3-month interval, lag time, and weight kernel required to optimize the forecast skill score. The forecast skill scores used are the root mean squared error (RMSE) and the Linear Error in Probability Space (LEPS) score. Both are used since the RMSE is a parametric assessment with a long history of application, while the LEPS score is a non-parametric assessment.

5.2 Data

5.2.1 Streamflow Data

The USBR maintains a spreadsheet of naturalized streamflow data for 29 gauges within the CRB which can be obtained from the following URL (http://www.usbr.gov/lc/region/g4000/NaturalFlow/current.html). Since a given water year actually begins and ends in different calendar years, when this report refers to a given water year (for example, 1996) it is referring to the period October 1, 1995 through September 30, 1996. Therefore when the total yearly streamflow of a given water year is

shown, this is referring to the total water volume observed at a given gauge from October 1 through September 30 of the specified calendar year. In order to maintain some continuity between the previous and current work, this data set is used here because it was used in both papers by Lamb et al (2010a and 2010b). The 29 locations are displayed on Figure 5.1.

5.2.1 Sea Surface Temperature Data

The SST data used in this research is a subset of the gridded data developed by Smith et al (2008). The data is available online at (http://www.ncdc.noaa.gov/oa/climate/research/sst/ersstv3.php) through the National Oceanic Atmospheric Administration (NOAA) National Climate Data Center (NCDC). The SST data are converted into Excel format using software, named Ocean Temperature Analysis (OTA), developed at UNLV specifically for this purpose. The Smith SST dataset is a 2º x 2º monthly mean gridded dataset existing from January 1854 through the present day. The subset of this data is defined to represent the boundary of the Hondo region (i.e. 150 E – 200E, 34N – 24N) as defined by Aziz et al (2010). The mean SST anomaly value for this region is the Hondo index value.

As previously mentioned, the current research showing the Hondo-CRB correlation demonstrates a lag time of more than a year between the changes in temperature and the streamflow. Specifically, the research by Lamb et al (2010a), showed that the 3-month average SST intervals of January-March, and February-April from a given water year, has a significant correlation with streamflow variation for the following water year volume. Other research into the strong winter monsoon from northeast Asia (Zhang et al, 1997a) showed that east Asian jet stream passes over the

Hondo region during the December – February interval. Since this is the case, the current research proposes using three different 3-mononth average predictor intervals, namely December-February (DJF), January-March (JFM), and February-April (FMA).

Figure 5.1 Location map of 29 USGS streamflow gauges

Three split-sample alternative analyses are performed to forecast historic water years. This is done first by applying weights the years 1976-2005 (training sample No.1) in order to forecast the water years from 1906 – 1975 (testing sample No. 1). This particular 30-year period was selected as the weighting period because it is typically used

by the NWS's Colorado Basin River Forecast Center to calibrate their ESP software. The ESP produces output streamflow traces which are based on the temperature and precipitation data from the years 1976-2005. In order to test the sensitivity of the selection of training and testing sample, the second split-sample alternative is performed using 1906 – 1955 as the training sample to forecast the water years of 1956 – 2005. Finally the third alternative uses 1956 – 2005 as the training sample to forecast the water years from 1906 – 1955. The years of data selected for Alternatives 1 and 2 were chosen simply to provide forecasts for the 100 year period stretching from 1906 through 2005.

5.3 Methodology

The forecasts in this work are created using a kernel, to weigh the streamflow at three different lag times: 0-year (simultaneous year), 1-year, and 2-year lags. For example, if a forecast for the 0-year lag is to be created for the 1920 water year the Hondo value from JFM 1920 is compared to the JFM Hondo values from all the years in the training sample. The difference between the 1920 Hondo value and the values of the training set are calculated, sorted in ascending order and then ranked. The difference, or rank, is the primary information used in the weight kernel calculation. Once the kernels are calculated all of the weights for a given year are proportioned so that their sum equals one. Since this process is based on the DJF, JFM and FMA intervals then there are three different sets of weight kernels produced.

Because the differences between all forecast years and all training years are calculated at the start, the lag time for the forecast comes from selecting the appropriate weight vector when the forecast value is generated. For example if the 1920 water year is

forecasted, a 0-year lag time uses the weight vector corresponding to 1920. For a 1-year lag, the 1919 weight vector is used and so forth.

5.3.1 Weighting Kernels

Four different kernels are selected to create forecast values. The kernel which results in the highest improvement in forecast skill is considered the optimal choice. The first weight kernel is taken from research by Rajagopalan and Lall (1999) which is used in a k-Nearest Neighbor (k-NN) technique to downscale climate data from yearly observations to daily data. The kernel is defined as follows:

$$W1_i = \frac{1/R_i}{\sum_{i=1}^{n} 1/R_i}$$

Here R_i, is the rank of a training year i. The kernel is designed to represent directly the probability of resampling as its weights have a possible values of 0 – 1. Since this weight kernel is based on the rank alone, there is some concern that regardless of the difference in Hondo values, there will always be a year which receives a weight of 1.

The second kernel selected is a linearly distributed proportion based on the absolute differences in SST values. W2 is defined as:

$$W2_i = 1 - \frac{|d_i|}{|d_{i,\max}|}$$

The values d_i and $d_{i,max}$ represent the distance between year i and the forecast year, and the maximum distance calculated from all years, respectively. The absolute value is taken because it does not matter if the training year is more or less than the test year. This kernel has two purposes. First, a given year could only have a resampling value of one if and only if the observed SST is the same as the target year SST. Second, each

successive weight is distributed on a roughly linear, but negative, sloping line so that year *i* has only slightly more weight than year *i+1*. However, since the behavior of this kernel is a decreasing linear distribution of weights, then there is a chance that it will give too much weight to years which are not actually "near" to the target year.

The third weight, *W*3 is given as the inverse distance squared weight:

$$W3_i = \frac{1}{d_i^2}$$

Once again, d_i is the difference between the training year and the forecast year. Because the theoretical values of *W3* range from -∞ to ∞, the weights for each forecast year are proportioned so that values range between 0 and 1 and their sum is equal to 1. This weight kernel has a plotted behavior similar to *W*1 except that it gives even less weight to observations with increasing values of d_i. Since this kernel does shift the majority of the weight to the first or second years some relevant information from other years may be ignored.

The final kernel, *W*4 is simply the inverse distance:

$$W4_i = \frac{1}{|d_i|}$$

Both *W*3 and *W*4 are commonly used kernels used in resampling and interpolating applications or as comparisons to other more sophisticated methods. *W*4 does not weigh the closest 1 or 2 as heavily as *W*1 or *W*3, but since it is not linear it also does not distribute the weights to too many of the other, adjacent observations.

Weights are calculated using the raw SST values. A test was run to see if there would be any difference between using raw data and calculating the Hondo anomalies which were used in the SVD analysis (Lamb et al. 2010, Aziz et al,. 2010). The results of

this simple test demonstrated that there was no significant difference between the forecast skill score resulting from these two data sets. Additionally, using proportioned weights were compared to raw (un-proportioned) weights to see if the forecast skill is sensitive to either method. The results of this test demonstrated that there was no significant difference. From these two small tests the use of the raw Hondo data is selected for testing because it is simpler to employ, and the proportioned weights are used because they communicate the idea of resampling probability better than the raw weights.

5.3.2 Forecast Development

Forecasts are created using the weight vector in a weighted bootstrap procedure, where 1000 re-sampled values are taken from the training set. The mean value of each re-sampled set is calculated and then the mean of all these means is calculated to arrive at the forecast value. The weighted bootstrap is a method has been used extensively in a variety of fields (Efron 1979, 1982). Typically the bootstrap method is used to estimate a population parameter from a sample dataset. However, in this application, the goal is to add a bias to the training dataset which reflects the link between known climate conditions and CRB streamflow.

Forecast values are calculated for a given split sample alternative, 3-month period, weight kernel, and lag time. Each combination of alternative-period-kernel-lag represents a single forecast scenario. Since there are three split-sample alternatives, three 3-month periods (DJF, JFM, and FMA); four weight kernels (*W1*, *W2*, *W3* and *W4*); and three lag times (0, 1, or 2 years) there are a total of 108 forecast scenarios (3 x 3 x 4 x 3).

5.3.3 Forecast Skill Scores

Assessing the forecast skill is assessed using the root mean squared error (RMSE) and the linear error in probability space score (LEPS) scores. Relative error (Abramowitz and Stegun, 1972) is also used here as a quick way of assessing the error of a forecast by comparing the forecast error to the observed value using the following equation:

$$RE = \frac{F_{y,l} - O_{y,l}}{O_{y,l}} = \frac{F_{y,l}}{O_{y,l}} - 1$$

Here the forecast, F at streamflow location, l, and year, y, are compared to the observation, O of same location and year. The RE is used here to create a time series plot of the forecasts errors, in order to identify periods of weak forecasting ability. The utility of the RE is not only to provide an indication of how close a given forecast is to the observation value (as a percent fraction of the observed) but also to give an indication of the bias in the forecast method. Since the RE is calculated for each year and location, the mean forecast bias is computed at each location for a given forecast scenario.

The RMSE is widely used to assess forecast errors (Wilks, 2006). A strength of the RMSE is its simplicity in communicating the forecast error in the same units as the forecasts themselves. However, the RMSE assumes that the forecast errors are distributed normally and it is therefore sensitive to forecast error variance. This makes it difficult to interpret the RMSE results as there is no consistent relationship between the RMSE and the average error of forecasts.

The RMSE is not be reported directly. Since the current method of modeling CRB streamflow projection uses the 1976-2005 mean for the long-lead forecasts, then a skill score based on the forecast RMSE and the climatology RMSE (1976-2005) is calculated. The skill score formula is given as

$$SS_{RMSE} = \frac{RMSE_f}{RMSE_c} - 1$$

This equation is used to demonstrate the relative improvement of the forecast method ($RMSE_f$) over the climatology ($RMSE_c$). $RMSE_c$ is calculated by finding the RMSE using the 1976-2005 mean as the forecast value for all years at a given streamflow location.

Also used to asses forecast skill is the Linear Error in Probability Space score (Ward and Folland, 1991; Potts et al, 1996). The LEPS score is used here because it does not assume that the errors have a defined distribution. The LEPS score gives a higher score for forecasts which predict extreme events, as opposed to forecasts of observed values which are closer to the mean. The work by Potts revised the LEPS score by Ward and Folland to remove a "bending back" problem when forecasting a continuous variable, as is the case in this research.

The basic concept of the LEPS score is to compare the forecast point with the observed data inside probability space. To complete this task we generate an empirical cumulative distribution function (eCDF) from the observed data. The eCDF is created from the streamflow data used as the testing set. In other words the first split sample analysis uses observed streamflow from years 1906-1976 create the eCDF (n_1 = 70), the second split sample analysis uses 1956-2005 (n_2 = 50), and the third uses 1906-1955 (n_3 = 50). The eCDF gives a weight of 1/n to each observed value. Since there are 100 observation points at each streamflow gauge, the y-axis of the eCDF is defined by a vector P, where $P = q/101$ as 'q' goes from 1 to 100. P does not include the points '0' or '1' in order to ensure that there can be forecast values interpolated below and above the range of observed streamflow values at a given location.

The LEPS score is calculated from the following formula as developed by Potts et al (1996):

$$LEPS = 3(1 - |P_f - P_o| + P_f^2 - P_f + P_o^2 - P_o) - 1$$

where P_f and P_o represent, respectively, the probabilities of the forecast and observed streamflow values. The values of P_f and P_o are read from the eCDF, (see Figure 2) for a given forecast year *y*, and location *l*. Values of the LEPS score range from -1 to 1.5.

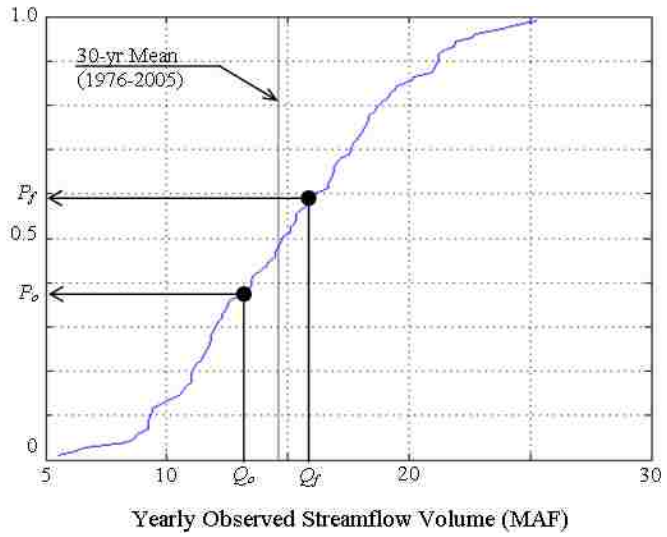

Figure 5.2 Schematic showing how P_f and P_o are obtained from the eCDF

5.3.4 Average Skill Score

The goal of the average skill score is to summarize the LEPS scores obtained at a given location, for all forecast years, and express this skill in terms of a percentage improvement (or decline) with respect to using the mean as the forecast value. The average skill score (Potts et al., 1996) is found by dividing the sum of all LEPS scores at a given location by the sum of the maximum possible, or minimum possible, LEPS scores as determined by the following equation:

$$SK = 100 \cdot \left(\frac{\sum_{y=1}^{n} LEPS}{\sum_{y=1}^{n} LEPS_{\mathrm{m}}} \right)$$

If the numerator is positive, then the denominator is the sum of the maximum possible LEPS scores (when $P_f = P_o$); if the numerator is negative, then the denominator is the sum of the minimum possible LEPS scores. The $LEPS_{min}$ value is obtained when the forecast point is furthest from the observation point. Therefore if $P_f < 0.5$, then the minimum score is found by setting $P_o = 1$. If $P_f > 0.5$, then the minimum score is found by setting $P_o = 0$. Because *SK* is the aggregate of several years of forecasts, a score greater than 10% is considered to be significant.

5.4 Results

5.4.1 Forecast Skill Results Summary

In order to identify the more significant forecasts the average skill score across all gauges is used to identify the most successful forecast scenario for each lag time and for each split-sample forecast alternative. Table 5.1 summarizes these values to provide a quick view of the most successful forecast scenarios. The results are divided to show the difference between the LEPS and RMSE skill scores, the difference between each scenario, and the difference between each split-sample alternative.

It is apparent that the LEPS scores are higher than the relative RMSE scores. Based upon work by Willmott and Matsurra (2005) it is assumed that the RMSE scores are low because this metric assumes the forecast errors are normally distributed. It is also because the RMSE is not constant over a given range of variance in the errors (Willmott and Matsurra, 2005; Shi et al, 2008). Since the LEPS score does not assume a

distribution for the errors its scores are not affected in the same way as the RMSE. However, the LEPS score rewards forecasts of extreme values more than forecasts of values closer to the mean. Therefore the individual LEPS score results must also be examined further.

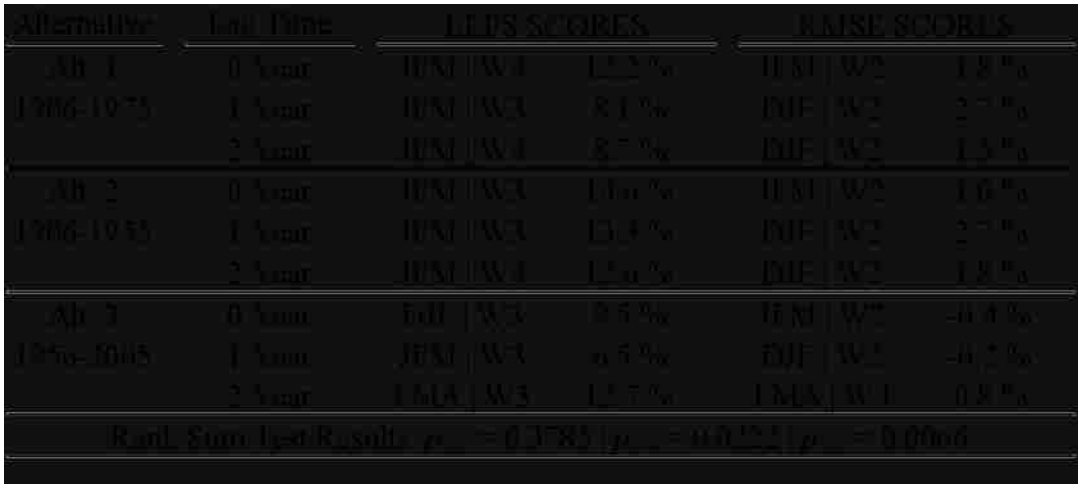

Table 5.1 Summary of successful scenarios based on LEPS and RMSE scores.

It is apparent that the LEPS scores are higher than the relative RMSE scores. Based upon work by Willmott and Matsurra (2005) it is assumed that the RMSE scores are low because this metric assumes the forecast errors are normally distributed. It is also because the RMSE is not constant over a given range of variance in the errors (Willmott and Matsurra, 2005; Shi et al, 2008). Since the LEPS score does not assume a distribution for the errors its scores are not affected in the same way as the RMSE. However, the LEPS score rewards forecasts of extreme values more than forecasts of values closer to the mean. Therefore the individual LEPS score results must also be examined further.

Another quick observation from Table 5.1 is that the JFM average Hondo values and the third weight kernel (JFM | W3) is the most successful scenario at all lag times (based on the LEPS scores). This is helpful because W3 is a simple kernel and, therefore, can be communicated and implemented easier than a more complicated kernel such as W1.

Finally, it appears that the forecast technique is sensitive to the data used in the resampling process. The best results appear when resampling the years of 1956 – 2005 in order to create forecasts for 1906 – 1955. The second best results appear when resampling 1976-2005 to create forecasts for 1906-1975. A rank sum test is performed to compare the relative errors from each alternative in order to determine if the forecast errors from each alternative are significantly different. The test results are shown on the bottom of Table 5.1. There is no significant difference between forecasts of Alternative 1 and 2. However, the probability that either Alternative 1 or 2 is similar to Alternative 3 is sufficiently low to conclude that they are not similar. The latter half of the streamflow data includes some of the wettest (1982-1984) and some of the driest (1999 – 2005) on record. Therefore, it appears that when these years are included in the resampling process (as is the case in Alternatives 1 and 2) the forecast skill improves significantly. It is noteworthy that the CBRFC has identified this benefit as well. Starting with the 2011 water year the CBRFC will begin utilizing the 1981 – 2010 period as the basis for training their ESP software. In a departure from previous forecasting policy, CBRFC will simply add a year to the calibration period (analogous to the resampling period of this study). Therefore by the 2021 water year the ESP software will be using 40 years of

historical inputs (1981 – 2020) to create forecasts (Personal Communication Kevin Werner, CBRFC; May 2010).

5.4.2 Forecast Skill Maps

In order to identify the region of increased or decreased forecast skill, the top forecast scenarios, for each lag time and for all three alternatives, are mapped and displayed on Figure 5.3. This figure displays nine (9) maps showing the average LEPS skill scores at each of the streamflow locations in the basin. The first row of maps on Figure 3 (a – c), representing Alternative 1, show that for the upper reaches of the Green River, the forecast skill does not show a significant improvement. Along the headwaters of the Colorado and Gunnison Rivers there are a few positive results, and in the lower CRB there are only few significant improvements for gauges not along the Colorado River itself. This pattern is generally repeated for each alternative and for each lag year, except for Alternative 3, which generally shows a weak pattern of forecast skill results at 0 and 1-year lag times.

Despite the results of the rank sum test from the previous section, Figure 5.3 shows an observable difference between the forecast skill results of Alternative 1 and 2. For example, Figure 5.3d shows Alternative 2 providing an improved forecast approach in the upper CRB - especially along the headwaters of the basin. It also shows that the skill diminishes as the lag time increases, and that the number of gauges showing successful forecasts also diminishing. It is expected that the forecasts would demonstrate their highest skill scores at the 1 year lag time because of the interference that shorter, more intense climate cycle have upon the basin. Even though the results are not expected

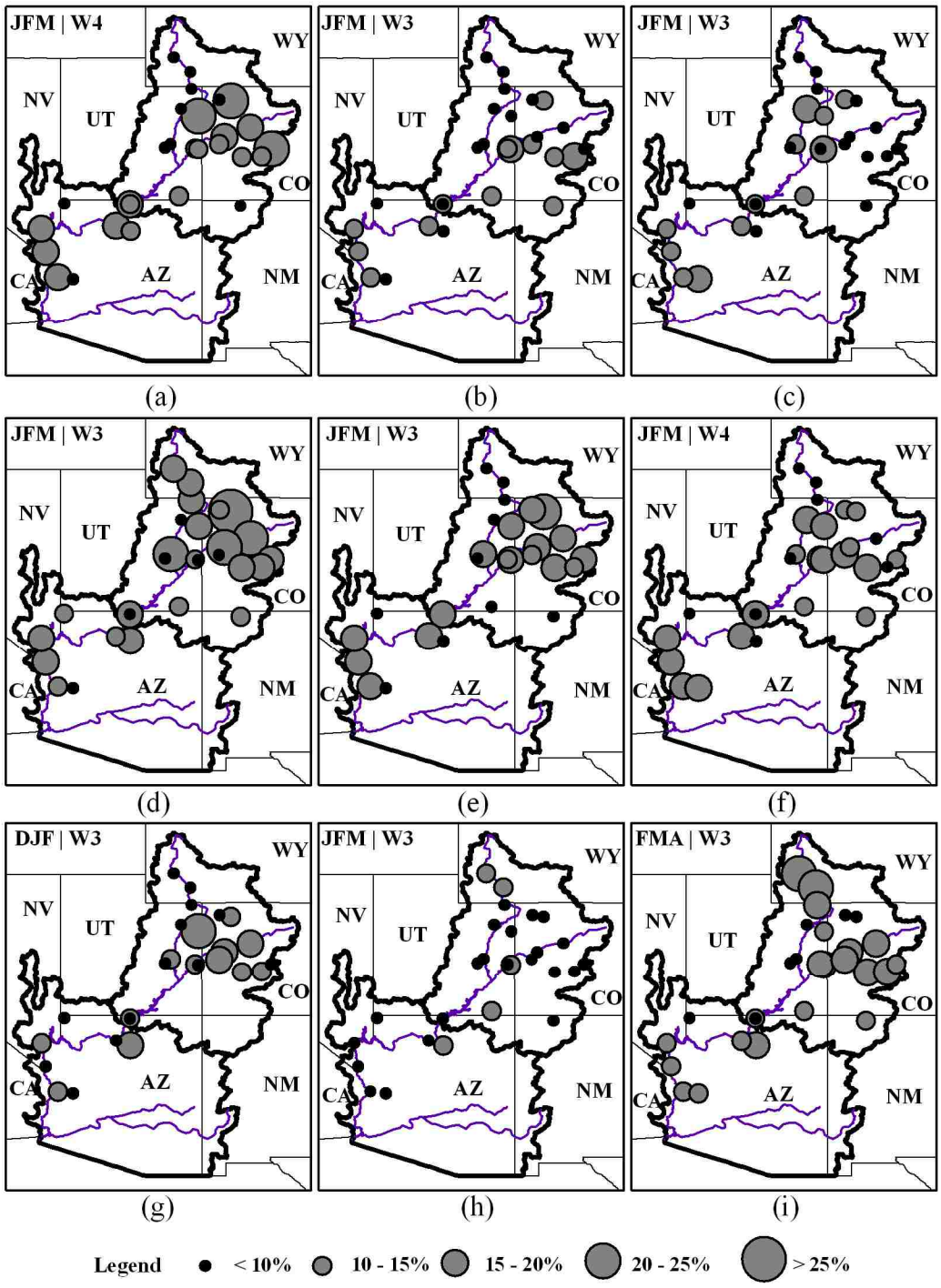

Figure 5.3 Maps showing average skill score results.
Non-significant results (<10%) displayed as black dots. Figures a-c represent the results from the 1st split sample alternative (Alt 1), d - f Alt. 2, and g - i Alt. 3. The first column (Figures a, d, g) are the 0-lag forecasts, the second column (b, e, h) are the 1-year lag forecasts, and the third column (c, f, i) are the 2-year lag forecasts.

they seem to make more sense by showing a decreasing and diminishing ability to use the Hondo as a basis for generating forecasts.

5.4.3 Forecast Time Series

Because the average skill score is a composite of all the forecasts generated at a location, it is necessary to investigate the individual forecast values to determine if the LEPS scores are higher because they give more weight to successful forecasts of extreme values and if there are identifiable patterns in the forecast's successes or failures. Figures 5.4 and 5.5 display scatter plots comparing the forecast and observed values at the 1-year lag time from Alternative 2 and 3 respectively. The correlation value for each scatterplot is displayed in the lower right-hand corner of each plot.

The main observation from Figures 5.4 and 5.5 is that there are few gauges where the correlation between the forecast and observed is significant at the 95% level (i.e. $r > 0.273$) While these figures show an overall performance, they do not explain if there are certain periods of time where the forecasts perform better than others. Figure 5.6 – 5.8 display this observation better by plotting the forecast relative error from alternatives 2 and 3 onto a single time series plot. Figure 5.6 shows the forecast errors at eight gauge locations for the 0-year lag time. Figures 5.7 and 5.8 show the same, except they show the 1-year and 2-year lag times. The highlighted regions shown on these figures identify periods where streamflow was below average at the Lees Ferry gauge (USGS ID 09380000) with less than two consecutive years of above average streamflow in between.

Figure 5.6 shows that, with the exception of (d), (f), and (h) there is a pattern to the skill scores. For example the forecast skill is observed as more erratic for years

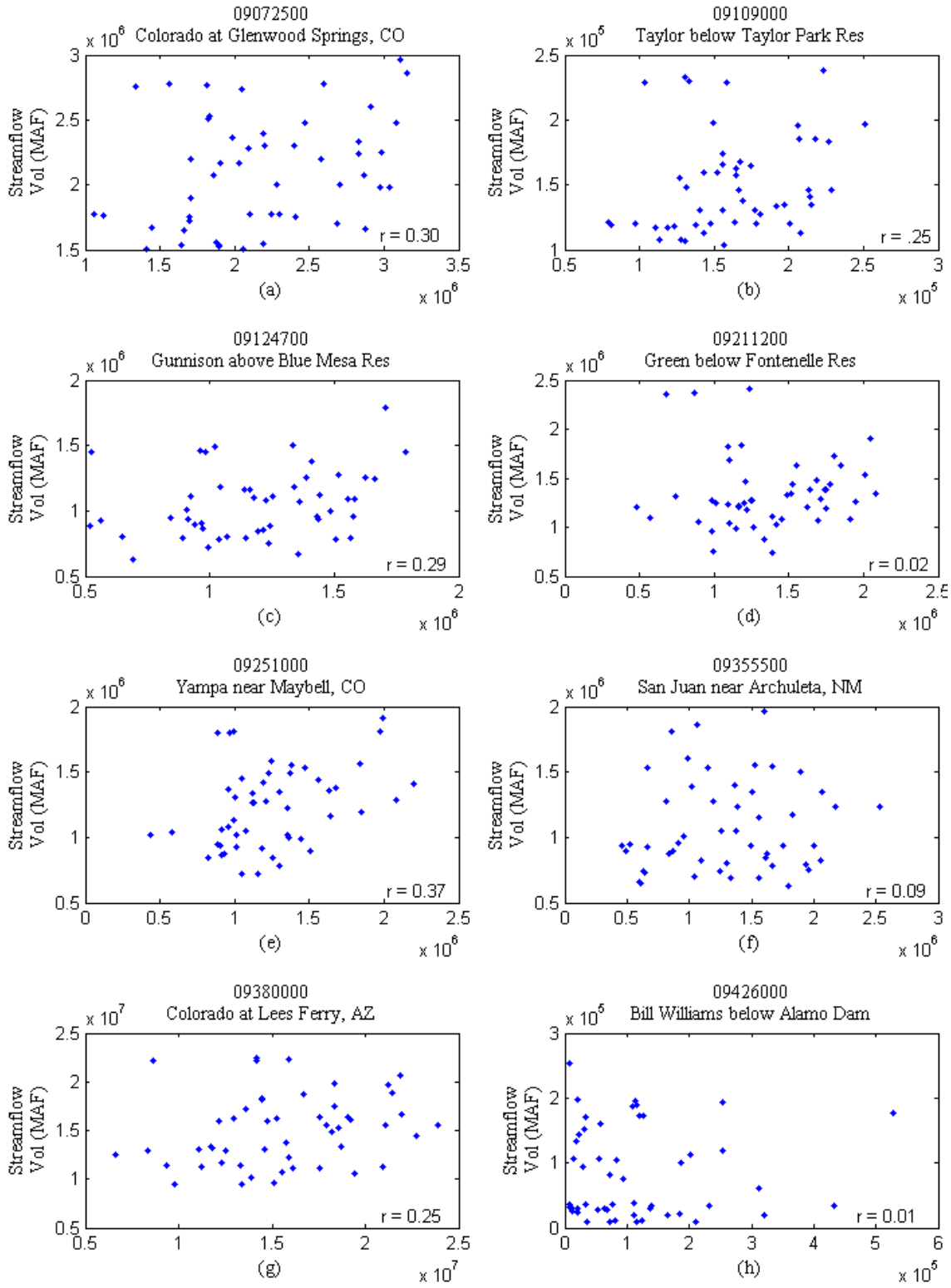

Figure 5.4 Scatterplots from Alternative 2 (Observed vs. Forecast)
Forecasts represented here at 8 sample gauge locations for the 1-year lag time. Pearson-r values are displayed in the lower right-hand corener of each plot.

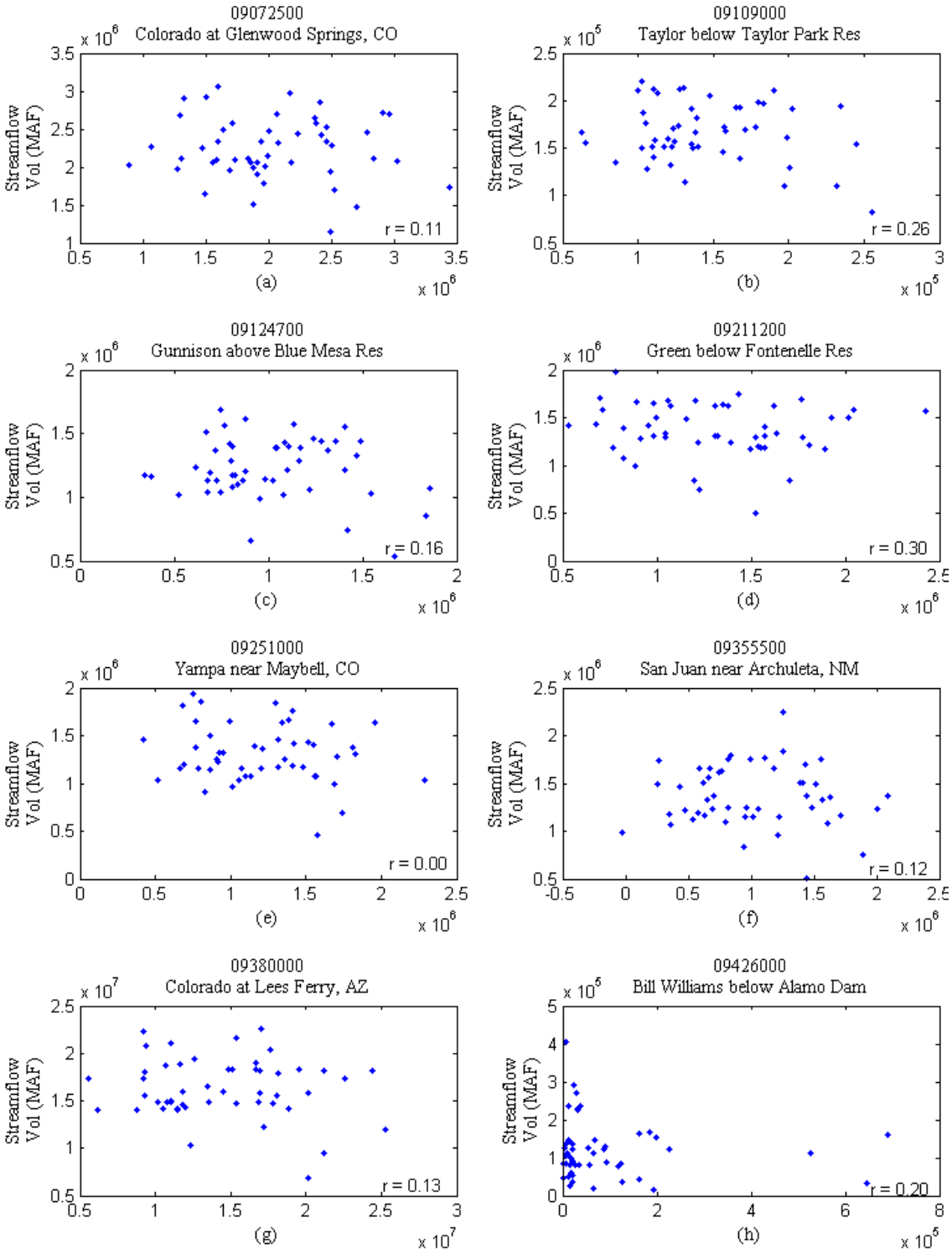

Figure 5.5 Scatterplots from Alternative 3 (Observed vs. Forecast)
Forecasts represented here at 8 sample gauge locations for the 1-year lag time. Pearson-r values are displayed in the lower right-hand corener of each plot.

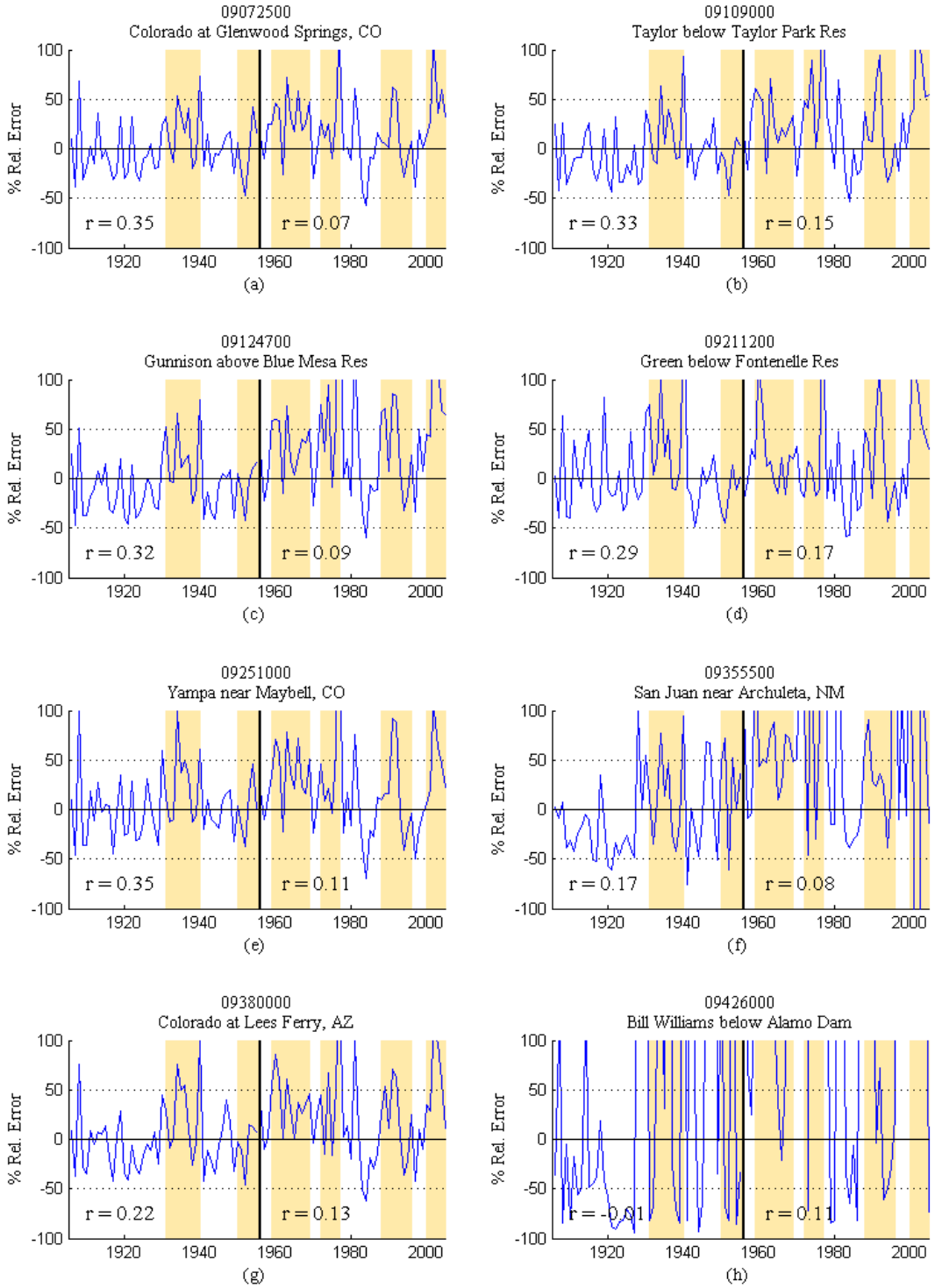

Figure 5.6 0-year lag forecast relative errors for eight gauge locations
Figure displays relative error time series from alternatives 2 & 3 created from 0-year lag time. Shaded areas represent low-flow periods defined as below average streamflow with less than two consecutive years of above average streamflow. Pearson-r values for each alternatives 2 and 3 are displayed in the lowers left and lowere middle of each plot, respectively.

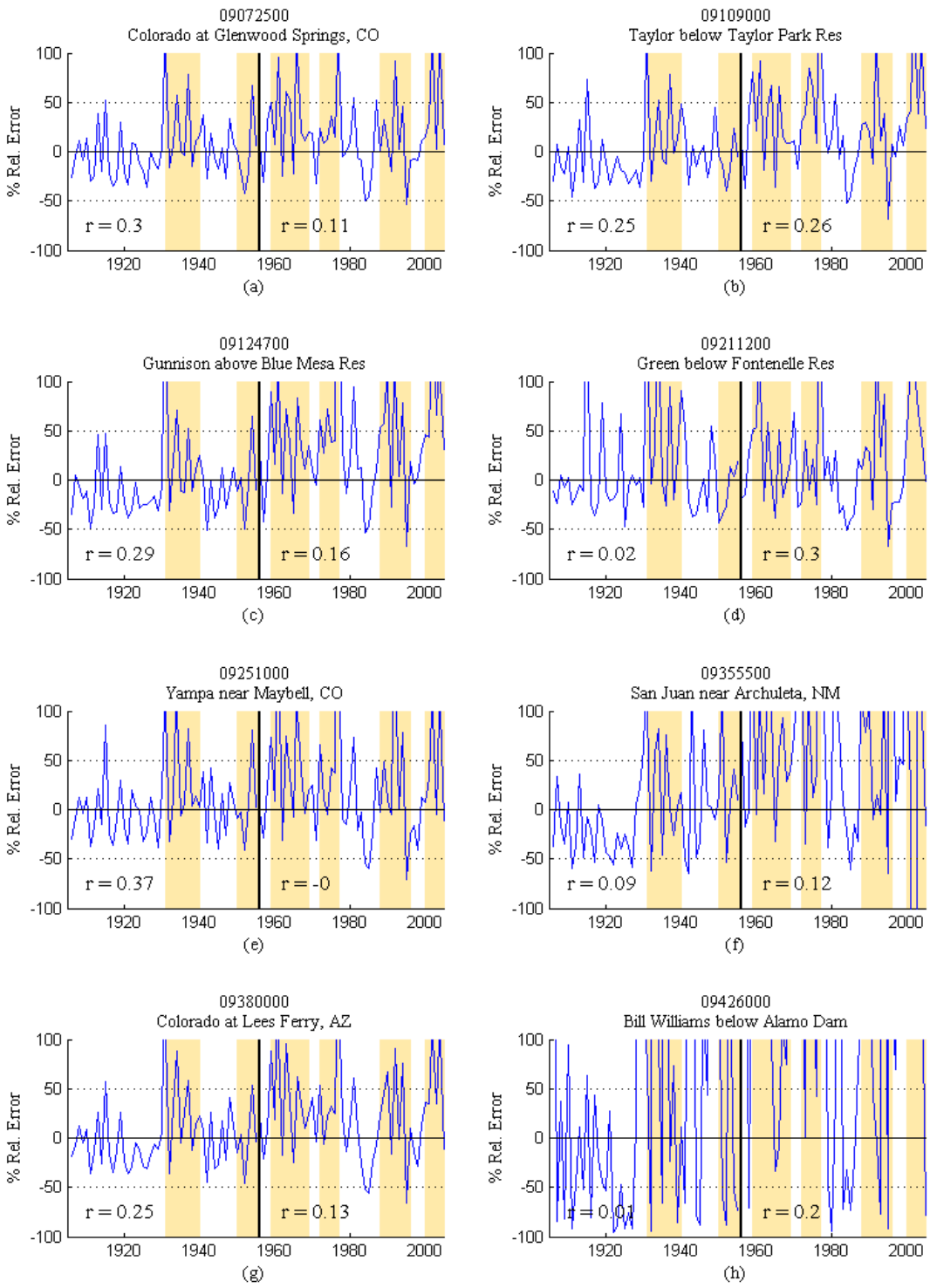

Figure 5.7 1-year lag forecast relative errors for eight gauge locations
Same as Figure 5.6 except showing the 1-year lag time.

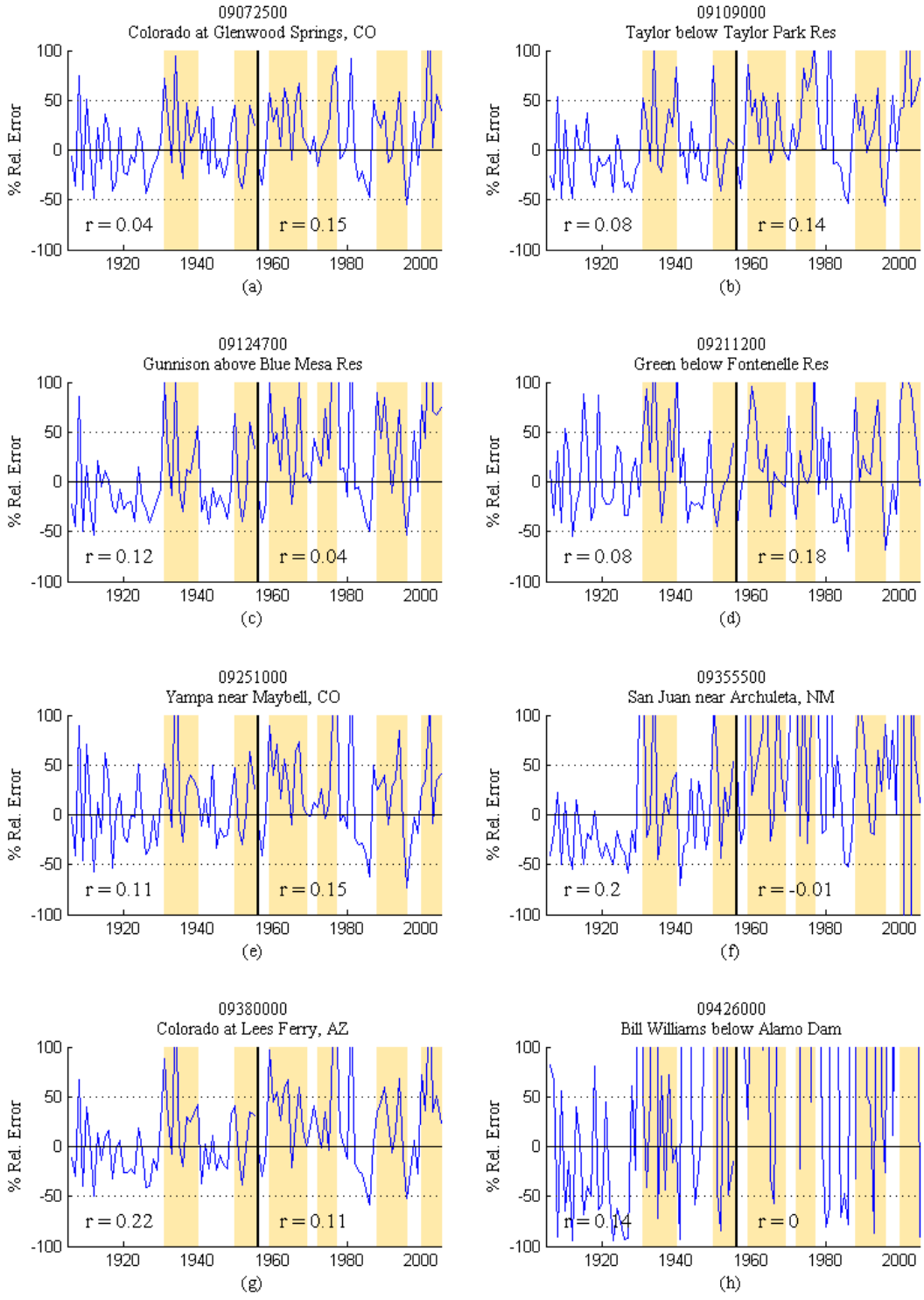

Figure 5.8 2-year lag forecast relative errors for eight gauge locations
Same as Figure 5.6 except showing the 2-year lag time.

highlighted as low flow years. In between these periods the forecast errors are comparatively small and much less erratic (this appears to hold true for all location except for the stations shown on Figure 5.6 – 5.8 (d), (f), and (h)). These periods correspond to several of the driest years of the last century as shown by the highlighted regions. For example (d), appears to show an inconsistent forecast skill until the early 1940's. (f) shows that prior to the late 1920's the forecasts worked well. However, after 1930 the forecast errors are very inconsistent. Finally, Figure (h) shows that the forecast skill of Bill Williams River gauge is not acceptable for any period of time.

The poor forecast skill along the Bill Williams River is not surprising since this location has the highest amount of streamflow variance in the CRB. The skill displayed at the Green River station is also not surprising because the SVD analysis provided by Lamb et al (2010b) showed how the upper reaches of the Green River are not always significantly correlated with the Hondo region. There appears to be a limit to how far north the Hondo can be applied, and perhaps this explains the low skill at the San Juan River station.

Perhaps one reason there may be periods where the forecast skill is extremely poor may be attributed to the change in significance of a particular climate cycle. While climate cycles tend to appear with predictable amplitude and period, they can experience periods of inactivity, where the amplitude of the cycle is noticeably dampened. Wang et al (2010b) identified a quasi-decadal oscillation in Pacific Ocean SSTs which demonstrated a significant correlation with precipitation in the intermountain west region with the SSTs leading precipitation by 3-years. Lamb et al (2010b) identified that the Hondo is part of the short-wave train which transports warm moist air from the tropical

Pacific Ocean toward the intermountain west. From 1900 – 1945 and from 1965 - present the QDO behaves in a predictable manner (see Figure 4 of Wang et al, 2010b) However, during the period from 1945 – 1965 the identified cycle was mostly inactive, showing a diminished correlation with intermountain west precipitation. Therefore, forecasts created from a single climate phenomenon will not always perform the same simply because of climate variability.

5.5 Conclusions and Recommendations

The overall results of this work demonstrated that climate information can be applied to weigh historical data in order to generate improved long-lead forecasts. This approach was tested using streamflow data from the Colorado River Basin (CBR) in an effort to find improved streamflow forecasts at lead times greater than one year. The basis of this approach is rooted in an understanding of the long-lead climate trends impacting the CRB.

Previous studies helped identify a region of the Pacific Ocean, named the Hondo, which represents a portion of the atmospheric short-wave train which transports moist air from the Pacific Ocean Tropics. The weighting technique used the mean, wintertime SST values of the Hondo region to determine how similar a given forecast period is to all of the historical data. Those historic years closest to the forecast period were weighted more in a resampling technique designed to add a climate-bias into the forecasts. Several different weight kernels were tested, and the inverse distance kernel demonstrated the highest skill.

The results of this research show that it is possible to use known climate cycles as a basis for generating forecasts at lead times of 1-year or greater. These results also

identify places for further study. For instance the observation that the periods where forecast errors were unacceptably high also coincided with periods of below average streamflow. It is hypothesize that this is because the current forecast technique does not explicitly consider soil moisture in the formulation of the forecast. Though the soil moisture state is implicit in the SVD analysis of Lamb et al (2010a), one improvement to the current forecast method would be to apply this technique to forecasts produced by the CBRFC's ESP software. Since the ESP utilizes soil moisture as an input into their physical model, weighing the ESP output based on climate relevance would incorporate soil moisture states into this forecasting procedure and potentially increase the forecast skill.

CHAPTER 6

CONTRIBUTIONS AND RECOMMENDATIONS

6.1 Contributions

The research completed in this dissertation presents several contributions to the field of water resource engineering, including an improved understanding of how changes in Pacific Ocean sea surface temperatures impact the Colorado River Basin (CRB), how these changes are connected to the CRB, and how this knowledge can be used to improve long-lead water supply forecasts.

Prior to this work, there was an understanding that the known influences of the El Niño Southern Oscillation did not have a significant impact on the CRB. Therefore any improvement to long-lead CRB water supply forecasts would have to come from an improved understanding of how and where climate impacts CRB streamflow

Answering Question 1 identified a 1-year teleconnection between the Pacific Ocean and the CRB. The region of the ocean with a significant correlation was located from 35N – 25N and from 150E – 200E (160W). The Hondo, as this region was named, had a negative correlation relationship with the CRB streamflow, meaning that decreasing SSTs were correlated with increasing streamflow. This region was identified in other research while studying SST impacts on drought conditions (Rajagopalan and Lall, 2000), precipitation (Wang and Ting, 2000), and North Platte River streamflow (Soukup et al., 2009). Each of these studies used different data, even different SST data, and the Hondo region was identified as significant. A study performed at the same time as Task 1 identified the Hondo when studying the impact of SSTs on snow water equivalent measurements in the Rocky Mountains.

Question No. 2 sought to describe the physical connection between the wintertime SST anomalies (i.e. Hondo anomalies) and the CRB. This analysis demonstrated that the Hondo is correlated with the East Asian Jet Stream (EAJS). During the winter months the EAJS passes across the southern tip of the main island of Japan, and enters the Pacific Ocean over the Hondo, then bifurcates: the northern split joining the Aleutian low, and the southern split dipping southward to join the North American Jet stream. This system is also correlated with a significant low pressure system that develops in conjunction with the intensity of the EAJS and Hondo SSTs in order to impact CRB streamflow. This system was identified to be significant with CRB streamflow at 0, 1 and 2 year lag times. By the third year the Hondo was no longer identified as significant.

Comparing this analysis with the current state of knowledge revealed that the typical water year has a residual impact on the CRB because of the slow response of soil moisture. The quasi-decadal oscillation (QDO) observed in the precipitation data was shown to lead the QDO phase observed in the level of the Great Salt Lake by three years (Wang et al, 2010b). This showed that the total surface hydrology response can have around three years to respond to precipitation. Also, there is a quasi-decadal oscillation in the Pacific Ocean (PQDO) which has a three year lead time correlation with the precipitation QDO. The significant PQDO region is centered over the central tropical Pacific Ocean; basically the existing Niño4 region.

Comparing the results from Task 2 with the current knowledge revealed that the water supply from a given water year is impacted by, on average, the previous two (2) water years. The mechanism creating this connection is explained by the wintertime intensity of the EAJS and observed by the Hondo SST variability. By the third water

year the impact of the Niño4 region and the mechanism transporting moist air from the tropical Pacific Ocean, becomes more significant than the Hondo mechanism. Therefore the research completed by Task 2 identifies that there is a lagged relationship between the Hondo and the CRB which is likely related to basin characteristics. The research also identified that the CRB is also influenced by the PQDO at lag times of around 3 years.

The final task, answering question No. 3, used the Hondo as a basis for forecasting streamflow in the CRB at 0, 1, and 2-year lag times. The results of this task showed that the best forecast skill results appear when using the inverse distance weight kernel, based on the January – March (JFM) Hondo values, to resample the training data set. Tests also showed that forecasts are sensitive to which historical data are selected as the training set to create the forecasts. The analysis results show that the long-lead water supply forecasts are improved by applying the weighted forecast technique.

6.2 Recommendations for Future Work

The research presented here provides a foundation for two separate but related fields in water resource engineering. The first is related to the work presented in Chapters 3 and 4: improving the understanding of climate drivers for a given watershed. The results obtained in these two chapters demonstrate there are atmospheric phenomena linked to, and lagging behind, ocean temperature cycles. In the case of the CRB, the changes in streamflow were also connected to the atmospheric phenomena and, therefore, to changes in the Pacific Ocean. It is highly unlikely that the connection between a large river watershed and the ocean is unique to the CRB. As a result, this analysis approach can be applied to any watershed located around the world in an effort to determine the connection between streamflow and large-scale climate variability.

Focusing solely on the CRB, future work can provide answers as to how the CRB is influenced by other climate cycles. Existing research has identified a connection with the Atlantic Ocean, and yet the mechanism explaining this connection remains unclear. For the time being, the relationship remains solely based in statistics.

The second field related to fusing inter-annual and inter-decadal climate variability to create long-lead water supply forecasts. Much of the existing research has focused on the impact of the El Niño Southern Oscillation (or lack thereof) on the CRB. Chapter 4 demonstrated that the non-extreme years are also correlated and can represent an underlying climate driver apart from the extreme year. Forecasting improvements attempted in Chapter 5 focused on building upon the CBRFC approach, by creating a forecast method capable of weighting the ESP output to create a new forecast method. More work can be done to improve forecasts further if other climate information is included (e.g. Hondo + other climate cycle), and if the approach is attached to a physical hydrologic model such as the ESP. In other watershed basins, there may not be an "official" approach to forecasting. In these regions, research into new forecasting models may need to be done based upon known climate states. Climate based forecast methods, by virtue of being linked to observed climate states, stand a better chance of adapting to non-stationary climate patterns of the future.

APPENDIX 1

DATA AND ANALYSIS CODE

A1.1 Chapter 4 Data

A1.1.1 SST Data Used In Rank Sum Testing

3-mo	JAS	JJA	MJJ	AMJ	MAM	FMA	JFM	DJF	NDJ	OND
1952	-9.16	-15.73	-16.08	-16.66	-15.77	-13.43	3.69	-4.83	-10.86	-10.21
1953	22.04	7.17	1.26	-5.54	-13.93	-13.77	17.18	15.08	14.09	10.05
1954	19.92	-23.24	-21.06	-22.40	-26.56	-24.12	14.24	8.58	7.18	1.24
1955	28.07	-20.57	-21.81	-22.88	-20.24	-19.28	17.42	17.02	14.74	13.49
1956	33.00	-25.41	-27.65	-20.85	-24.07	-33.12	37.34	38.47	28.65	24.18
1957	15.29	-19.75	-15.57	-11.43	-6.50	-10.96	13.40	13.61	4.86	4.81
1958	-22.22	-18.64	-19.00	-14.31	-12.39	0.41	-8.19	-11.97	-10.04	-12.34
1959	0.22	12.35	19.38	20.04	17.55	11.78	-14.27	-19.87	-19.62	-12.63
1960	-0.30	2.11	-1.14	-0.49	-0.12	4.90	-8.19	-6.25	-3.76	0.61
1961	10.73	-10.28	-9.32	-5.33	-7.73	-8.39	5.41	4.50	2.43	1.63
1962	17.75	-12.05	-11.15	-9.82	-10.96	-10.33	9.23	9.13	2.60	3.06
1963	15.99	-39.16	-39.23	-31.89	-21.66	-16.97	13.82	15.80	18.81	17.74
1964	-6.04	-13.98	-8.59	-0.20	8.02	11.32	-10.03	-5.08	-0.85	-6.38
1965	7.11	15.53	6.33	2.77	-3.69	-10.47	9.35	13.63	15.82	13.81
1966	-29.72	-0.21	1.74	9.57	9.77	16.67	-16.06	-17.52	-20.89	-26.00
1967	-12.57	25.72	13.24	4.95	4.41	6.42	-4.65	-1.11	-3.37	-6.10
1968	13.97	11.22	1.56	-2.09	0.72	7.83	-12.63	-6.38	-3.91	-0.09
1969	-19.31	3.90	16.45	19.28	21.59	16.70	-9.91	-0.07	8.37	5.14
1970	-3.47	28.05	25.45	16.66	10.29	10.72	-15.40	-18.48	-9.54	4.50
1971	16.37	7.15	4.62	1.98	-0.21	-5.94	10.96	17.62	19.86	20.11
1972	14.98	-14.49	-18.28	-21.80	-16.50	-25.43	27.76	28.89	17.67	10.88
1973	-27.53	-15.99	-7.88	2.10	11.97	9.71	-9.08	-11.70	-20.12	-17.46
1974	43.08	10.31	8.14	1.83	-5.43	-15.46	21.90	24.88	24.04	26.33
1975	17.68	-32.44	-30.83	-22.79	-13.22	-7.19	9.19	11.24	11.42	3.03
1976	28.37	-20.60	-16.65	-20.34	-19.49	-30.66	35.90	38.68	30.13	22.83

1977	-14.54	-19.51	-17.51	-14.78	-11.20	-13.69	9.39	-8.92	-16.24	-16.83
1978	-24.44	30.88	31.49	20.01	6.66	1.74	-10.29	-26.63	-30.13	-28.03
1979	-22.34	20.14	20.00	27.03	30.28	25.98	-17.14	-15.63	-17.57	-12.83
1980	-32.83	15.38	10.39	7.41	2.29	11.16	-17.97	-25.44	-27.12	-31.26
1981	-12.27	34.75	38.73	34.19	29.30	25.11	-20.68	-24.57	-22.94	-15.98
1982	-17.05	27.06	25.33	20.55	16.38	12.10	-16.37	-28.25	-36.09	-30.54
1983	-63.02	23.23	22.51	18.90	18.29	16.28	-19.80	-23.72	-28.82	-34.24
1984	-17.14	65.25	64.79	65.31	65.15	64.63	-54.90	-49.18	-47.28	-38.34
1985	-22.22	20.46	24.96	19.68	11.07	4.81	-3.60	-5.03	-10.59	-14.71
1986	-9.04	16.36	11.42	0.19	-4.98	-12.30	6.07	-3.56	-9.66	-12.10
1987	-33.44	-4.86	1.21	5.50	9.34	16.25	-17.81	-22.67	-25.82	-27.74
1988	-16.77	16.58	17.79	18.76	20.79	26.31	-26.28	-22.49	-18.44	-13.80
1989	32.54	2.55	-9.19	-12.09	-11.74	-8.61	14.20	22.41	26.48	28.96
1990	8.37	-26.80	-28.47	-27.37	-15.17	-7.93	7.80	7.31	8.42	13.94
1991	6.22	1.55	4.93	1.24	0.92	5.72	-11.15	-7.10	-1.30	-0.45
1992	-23.73	-0.17	9.04	12.60	4.79	-0.67	7.77	7.49	12.16	2.27
1993	-23.80	31.33	31.36	33.32	41.22	54.54	-55.03	-47.37	-35.20	-31.93
1994	-21.25	21.31	23.52	30.84	30.24	32.29	-32.45	-21.25	-11.90	-5.18
1995	-24.40	17.20	12.62	12.19	13.05	15.59	-20.67	-18.91	-20.37	-20.47
1996	17.09	19.07	16.62	24.19	24.71	20.21	-9.54	-10.11	4.82	10.76
1997	-10.77	0.10	11.50	12.74	10.60	17.68	-15.62	-9.91	5.08	2.80
1998	-34.13	8.77	6.93	5.75	7.06	20.10	-35.92	-35.93	-29.91	-28.76
1999	53.00	27.03	25.08	32.07	29.53	15.58	1.81	13.24	21.60	29.81
2000	55.24	-62.67	-61.68	-64.84	-62.89	-69.88	69.87	69.00	63.00	60.10
2001	32.00	-55.50	-54.24	-50.52	-48.03	-48.54	49.64	50.65	44.05	34.38
2002	41.96	-30.99	-27.57	-31.51	-35.96	-41.09	48.51	51.57	51.16	45.49
2003	-3.50	-44.83	-50.89	-53.25	-48.09	-29.71	22.24	20.79	22.40	21.77
2004	6.00	5.34	5.38	1.51	0.55	-4.63	9.53	10.31	12.49	20.69

6-mo	AMJJAS	MAMJJA	FMAMJJ	JFMAMJ	DJFMAM	NDJFMA	ONDJFM
1952	-18.49	-17.32	-17.86	-13.95	-11.04	-3.88	-4.30
1953	4.04	-1.43	-6.22	-11.54	-14.70	-15.79	15.47

1954	-23.58	-27.00	-24.86	-20.83	-18.57	-15.51	7.28
1955	-17.98	-21.03	-22.50	-21.15	-20.21	-19.56	17.74
1956	-21.91	-26.88	-32.26	-33.00	-37.87	-36.35	35.52
1957	-17.55	-16.57	-16.90	-13.66	-12.72	-10.46	11.61
1958	-22.71	-18.41	-11.63	-4.19	1.50	8.07	-12.48
1959	15.37	16.68	19.70	20.82	20.09	17.46	-16.26
1960	-1.59	0.78	1.91	4.32	2.01	4.43	-5.22
1961	-4.72	-7.87	-8.70	-5.44	-5.74	-3.73	1.78
1962	-7.75	-12.29	-13.09	-10.95	-10.30	-6.57	6.55
1963	-34.13	-32.60	-30.39	-25.32	-19.91	-16.63	15.18
1964	-8.68	-2.57	1.08	5.03	7.97	8.97	-10.16
1965	11.45	6.08	-0.90	-3.87	-10.42	-14.65	15.45
1966	1.74	7.05	10.76	14.89	17.21	23.62	-26.49
1967	17.88	14.63	10.82	7.10	1.94	1.12	-1.04
1968	10.41	7.94	6.17	6.88	8.93	9.69	-4.96
1969	14.10	16.13	16.54	14.23	10.90	5.41	-0.29
1970	25.95	21.30	19.12	17.29	17.26	15.26	-11.15
1971	5.91	2.85	-1.13	-5.53	-11.83	-16.29	19.31
1972	-16.98	-16.68	-22.87	-25.76	-23.99	-22.33	22.34
1973	-6.71	-3.13	-0.04	7.46	13.86	17.36	-15.15
1974	2.12	1.04	-2.79	-11.86	-21.00	-26.85	29.32
1975	-31.35	-25.64	-22.72	-18.51	-16.08	-12.80	9.36
1976	-19.69	-21.77	-26.08	-31.05	-32.74	-34.24	32.03
1977	-17.26	-16.24	-15.45	-12.09	-3.65	1.68	-7.76
1978	27.47	20.33	18.36	14.65	17.82	21.12	-27.19
1979	28.70	26.79	26.72	25.41	24.42	22.23	-16.97
1980	13.94	9.28	11.40	13.14	15.58	20.73	-27.99
1981	37.92	37.45	36.50	30.17	32.74	30.62	-27.00
1982	22.55	20.19	21.00	20.21	21.37	24.07	-26.63
1983	24.60	20.61	19.38	20.32	21.51	21.74	-26.88
1984	71.62	70.21	70.22	67.76	65.32	59.86	-50.13
1985	19.18	17.80	16.22	13.17	10.01	9.65	-10.10
1986	11.92	3.01	-1.73	-4.90	-3.94	-4.24	0.58

1987	0.58	4.08	8.35	11.28	18.19	24.38	-28.43
1988	19.54	23.29	25.21	25.61	28.61	26.37	-24.06
1989	0.80	-3.50	-8.87	-14.67	-17.94	-19.92	23.20
1990	-24.17	-21.78	-20.54	-17.70	-9.82	-7.96	10.63
1991	-6.89	1.12	6.42	6.09	5.04	7.02	-6.97
1992	-0.44	3.03	5.71	3.54	-1.43	-7.51	7.37
1993	34.38	38.71	46.35	49.98	51.59	48.78	-45.24
1994	27.61	29.85	31.58	37.34	34.48	29.57	-24.25
1995	17.20	18.20	16.56	16.55	16.62	19.42	-22.19
1996	25.61	22.86	19.99	18.46	16.95	8.51	-0.53
1997	-1.37	5.78	14.87	13.57	10.41	6.09	-5.21
1998	4.65	8.26	13.96	20.62	23.02	28.12	-35.37
1999	25.77	28.35	23.06	18.11	6.65	-6.06	20.83
2000	-72.66	-70.91	-73.96	-73.89	-75.74	-75.26	73.25
2001	-58.19	-56.34	-57.18	-54.90	-55.71	-55.53	50.21
2002	-35.43	-35.67	-37.12	-44.53	-47.93	-50.75	53.08
2003	-55.98	-51.18	-43.56	-40.85	-35.41	-29.24	25.41
2004	3.18	3.14	1.33	-3.85	-3.34	-9.27	16.91

A1.2 Chapter 3 Analysis Code

A1.2.1 Rank Sum Test

```
function [rsum]=SOI3
[alldata,tflow]=xlsread('C:\Matlab\52-ALL.xls');
rsum=zeros(29,10);
for month=1:10
   for station=1:29
      flow_col= alldata(:,station+37);
      soi_col1 = alldata(:,month+1);
      soi_col2 = alldata(:,month+2);
      soi_col3 = alldata(:,month+3);
      soi_col = mean([soi_col1,soi_col2,soi_col3],2);
      pindices=find(soi_col>=0);
      nindices=find(soi_col<0);
      rsum(station, month)=ranksum(flow_col(pindices),flow_col(nindices));
   end
end
```

```
function [rsum]=SOI6
[alldata,tflow]=xlsread('C:\Matlab\52-ALL.xls');
rsum=zeros(29,7);
for month=1:7
   for station=1:29
      flow_col= alldata(:,station+37);
      soi_col1 = alldata(:,month+1);
      soi_col2 = alldata(:,month+2);
      soi_col3 = alldata(:,month+3);
      soi_col4 = alldata(:,month+4);
      soi_col5 = alldata(:,month+5);
      soi_col6 = alldata(:,month+6);
      soi_col = mean([soi_col1,soi_col2,soi_col3,soi_col4,soi_col5,soi_col6],2);
      pindices=find(soi_col>=0);
      nindices=find(soi_col<0);
      rsum(station, month)=ranksum(flow_col(pindices),flow_col(nindices));
   end
end

function [rsum]=PDO3
[alldata,tflow]=xlsread('C:\Matlab\52-ALL.xls');
rsum=zeros(29,10);
for month=1:10
   for station=1:29
      flow_col= alldata(:,station+37);
      pdo_col1 = alldata(:,month+25);
      pdo_col2 = alldata(:,month+26);
      pdo_col3 = alldata(:,month+27);
      pdo_col = mean([pdo_col1,pdo_col2,pdo_col3],2);
      pindices=find(pdo_col>=0);
      nindices=find(pdo_col<0);
      rsum(station, month)=ranksum(flow_col(pindices),flow_col(nindices));
   end
end

function [rsum]=PDO6
[alldata,tflow]=xlsread('C:\Matlab\52-ALL.xls');
rsum=zeros(29,7);
for month=1:7
   for station=1:29
      flow_col= alldata(:,station+37);
      pdo_col1 = alldata(:,month+25);
      pdo_col2 = alldata(:,month+26);
      pdo_col3 = alldata(:,month+27);
      pdo_col4 = alldata(:,month+28);
      pdo_col5 = alldata(:,month+29);
```

```
        pdo_col6 = alldata(:,month+30);
        pdo_col = mean([pdo_col1,pdo_col2,pdo_col3,pdo_col4,pdo_col5,pdo_col6],2);
        pindices=find(pdo_col>=0);
        nindices=find(pdo_col<0);
        rsum(station, month)=ranksum(flow_col(pindices),flow_col(nindices));
    end
end

function [rsum]=NAO3
[alldata,tflow]=xlsread('C:\Matlab\52-ALL.xls');
rsum=zeros(29,10);
for month=1:10
    for station=1:29
        flow_col= alldata(:,station+37);
        nao_col1 = alldata(:,month+13);
        nao_col2 = alldata(:,month+14);
        nao_col3 = alldata(:,month+15);
        nao_col = mean([nao_col1,nao_col2,nao_col3],2);
        pindices=find(nao_col>=0);
        nindices=find(nao_col<0);
        rsum(station, month)=ranksum(flow_col(pindices),flow_col(nindices));
    end
end

function [rsum]=NAO6
[alldata,tflow]=xlsread('C:\Matlab\52-ALL.xls');
rsum=zeros(29,7);
for month=1:7
    for station=1:29
        flow_col= alldata(:,station+37);
        nao_col1 = alldata(:,month+13);
        nao_col2 = alldata(:,month+14);
        nao_col3 = alldata(:,month+15);
        nao_col4 = alldata(:,month+16);
        nao_col5 = alldata(:,month+17);
        nao_col6 = alldata(:,month+18);
        nao_col = mean([nao_col1,nao_col2,nao_col3,nao_col4,nao_col5,nao_col6],2);
        pindices=find(nao_col>=0);
        nindices=find(nao_col<0);
        rsum(station, month)=ranksum(flow_col(pindices),flow_col(nindices));
    end
end

function [rsum]=AMO3
[alldata,tflow]=xlsread('C:\Matlab\52-ALL.xls');
rsum=zeros(29,10);
```

```
for month=1:10
   for station=1:29
      flow_col= alldata(:,station+37);
      amo_col1 = alldata(:,month+66);
      amo_col2 = alldata(:,month+67);
      amo_col3 = alldata(:,month+68);
      amo_col = mean([amo_col1,amo_col2,amo_col3],2);
      pindices=find(amo_col>=0);
      nindices=find(amo_col<0);
      rsum(station, month)=ranksum(flow_col(pindices),flow_col(nindices));
   end
end

function [rsum]=AMO6
[alldata,tflow]=xlsread('C:\Matlab\52-ALL.xls');
rsum=zeros(29,7);
for month=1:7
   for station=1:29
      flow_col= alldata(:,station+37);
      amo_col1 = alldata(:,month+66);
      amo_col2 = alldata(:,month+67);
      amo_col3 = alldata(:,month+68);
      amo_col4 = alldata(:,month+69);
      amo_col5 = alldata(:,month+70);
      amo_col6 = alldata(:,month+71);
      amo_col = mean([amo_col1,amo_col2,amo_col3,amo_col4,amo_col5,amo_col6],2);
      pindices=find(amo_col>=0);
      nindices=find(amo_col<0);
      rsum(station, month)=ranksum(flow_col(pindices),flow_col(nindices));
   end
end

function [rsum]=SPb3
[alldata,tflow]=xlsread('C:\Matlab\52-ALL.xls');
% Calculation of the SOI & PDO pos. versus the SOI pos. & PDO neg.
rsum=zeros(29,10);
for month=1:10
   for station=1:29
      flow_col= alldata(:,station+37);
      soi_col1 = alldata(:,month+1);
      soi_col2 = alldata(:,month+2);
      soi_col3 = alldata(:,month+3);
      pdo_col1 = alldata(:,month+25);
      pdo_col2 = alldata(:,month+26);
      pdo_col3 = alldata(:,month+27);
      soi_col = mean([soi_col1,soi_col2,soi_col3],2);
```

```
      pdo_col = mean([pdo_col1,pdo_col2,pdo_col3],2);
      pindices=find(soi_col>=0 & pdo_col>=0);
      nindices=find(soi_col>=0 & pdo_col<0);
      rsum(station, month)=ranksum(flow_col(pindices),flow_col(nindices));
   end
end

function [rsum]=SPb6
[alldata,tflow]=xlsread('C:\Matlab\52-ALL.xls');
% Calculation of the SOI & PDO pos. versus the SOI pos. & PDO neg.
rsum=zeros(29,7);
for month=1:7
   for station=1:29
      flow_col= alldata(:,station+37);
      soi_col1 = alldata(:,month+1);
      soi_col2 = alldata(:,month+2);
      soi_col3 = alldata(:,month+3);
      soi_col4 = alldata(:,month+4);
      soi_col5 = alldata(:,month+5);
      soi_col6 = alldata(:,month+6);
      pdo_col1 = alldata(:,month+25);
      pdo_col2 = alldata(:,month+26);
      pdo_col3 = alldata(:,month+27);
      pdo_col4 = alldata(:,month+28);
      pdo_col5 = alldata(:,month+29);
      pdo_col6 = alldata(:,month+30);
      soi_col = mean([soi_col1,soi_col2,soi_col3,soi_col4,soi_col5,soi_col6],2);
      pdo_col = mean([pdo_col1,pdo_col2,pdo_col3,pdo_col4,pdo_col5,pdo_col6],2);
      pindices=find(soi_col>=0 & pdo_col>=0);
      nindices=find(soi_col>=0 & pdo_col<0);
      rsum(station, month)=ranksum(flow_col(pindices),flow_col(nindices));
   end
end

function [rsum]=SPd3
[alldata,tflow]=xlsread('C:\Matlab\52-ALL.xls');
% Calculation of the SOI & PDO neg. versus the SOI neg. & PDO pos.
rsum=zeros(29,10);
for month=1:10
   for station=1:29
      flow_col= alldata(:,station+37);
      soi_col1 = alldata(:,month+1);
      soi_col2 = alldata(:,month+2);
      soi_col3 = alldata(:,month+3);
      pdo_col1 = alldata(:,month+25);
      pdo_col2 = alldata(:,month+26);
```

```
      pdo_col3 = alldata(:,month+27);
      soi_col = mean([soi_col1,soi_col2,soi_col3],2);
      pdo_col = mean([pdo_col1,pdo_col2,pdo_col3],2);
      pindices=find(soi_col<0 & pdo_col<0);
      nindices=find(soi_col<0 & pdo_col>=0);
      rsum(station, month)=ranksum(flow_col(pindices),flow_col(nindices));
   end
end

function [rsum]=SPd6
[alldata,tflow]=xlsread('C:\Matlab\52-ALL.xls');
% Calculation of the SOI & PDO neg. versus the SOI neg. & PDO pos.
rsum=zeros(29,7);
for month=1:7
   for station=1:29
      flow_col= alldata(:,station+37);
      soi_col1 = alldata(:,month+1);
      soi_col2 = alldata(:,month+2);
      soi_col3 = alldata(:,month+3);
      soi_col4 = alldata(:,month+4);
      soi_col5 = alldata(:,month+5);
      soi_col6 = alldata(:,month+6);
      pdo_col1 = alldata(:,month+25);
      pdo_col2 = alldata(:,month+26);
      pdo_col3 = alldata(:,month+27);
      pdo_col4 = alldata(:,month+28);
      pdo_col5 = alldata(:,month+29);
      pdo_col6 = alldata(:,month+30);
      soi_col = mean([soi_col1,soi_col2,soi_col3,soi_col4,soi_col5,soi_col6],2);
      pdo_col = mean([pdo_col1,pdo_col2,pdo_col3,pdo_col4,pdo_col5,pdo_col6],2);
      pindices=find(soi_col<0 & pdo_col<0);
      nindices=find(soi_col<0 & pdo_col>=0);
      rsum(station, month)=ranksum(flow_col(pindices),flow_col(nindices));
   end
end

function [rsum]=SNb3
[alldata,tflow]=xlsread('C:\Matlab\52-ALL.xls');
% Calculation of the SOI & NAO pos. versus the SOI pos. & NAO neg.
rsum=zeros(29,10);
for month=1:10
   for station=1:29
      flow_col= alldata(:,station+37);
      soi_col1 = alldata(:,month+1);
      soi_col2 = alldata(:,month+2);
      soi_col3 = alldata(:,month+3);
```

```
      nao_col1 = alldata(:,month+13);
      nao_col2 = alldata(:,month+14);
      nao_col3 = alldata(:,month+15);
      soi_col = mean([soi_col1,soi_col2,soi_col3],2);
      nao_col = mean([nao_col1,nao_col2,nao_col3],2);
      pindices=find(soi_col>=0 & nao_col>=0);
      nindices=find(soi_col>=0 & nao_col<0);
      rsum(station, month)=ranksum(flow_col(pindices),flow_col(nindices));
   end
end

function [rsum]=SNb6
[alldata,tflow]=xlsread('C:\Matlab\52-ALL.xls');
% Calculation of the SOI & NAO pos. versus the SOI pos. & NAO neg.
rsum=zeros(29,7);
for month=1:7
   for station=1:29
      flow_col= alldata(:,station+37);
      soi_col1 = alldata(:,month+1);
      soi_col2 = alldata(:,month+2);
      soi_col3 = alldata(:,month+3);
      soi_col4 = alldata(:,month+4);
      soi_col5 = alldata(:,month+5);
      soi_col6 = alldata(:,month+6);
      nao_col1 = alldata(:,month+13);
      nao_col2 = alldata(:,month+14);
      nao_col3 = alldata(:,month+15);
      nao_col4 = alldata(:,month+16);
      nao_col5 = alldata(:,month+17);
      nao_col6 = alldata(:,month+18);
      soi_col = mean([soi_col1,soi_col2,soi_col3,soi_col4,soi_col5,soi_col6],2);
      nao_col = mean([nao_col1,nao_col2,nao_col3,nao_col4,nao_col5,nao_col6],2);
      pindices=find(soi_col>=0 & nao_col>=0);
      nindices=find(soi_col>=0 & nao_col<0);
      rsum(station, month)=ranksum(flow_col(pindices),flow_col(nindices));
   end
end

function [rsum]=SNd3
[alldata,tflow]=xlsread('C:\Matlab\52-ALL.xls');
% Calculation of the SOI & nao neg. versus the SOI neg. & nao pos.
rsum=zeros(29,10);
for month=1:10
   for station=1:29
      flow_col= alldata(:,station+37);
      soi_col1 = alldata(:,month+1);
```

```
      soi_col2 = alldata(:,month+2);
      soi_col3 = alldata(:,month+3);
      nao_col1 = alldata(:,month+13);
      nao_col2 = alldata(:,month+14);
      nao_col3 = alldata(:,month+15);
      soi_col = mean([soi_col1,soi_col2,soi_col3],2);
      nao_col = mean([nao_col1,nao_col2,nao_col3],2);
      pindices=find(soi_col<0 & nao_col<0);
      nindices=find(soi_col<0 & nao_col>=0);
      rsum(station, month)=ranksum(flow_col(pindices),flow_col(nindices));
   end
end

function [rsum]=SNd6
[alldata,tflow]=xlsread('C:\Matlab\52-ALL.xls');
% Calculation of the SOI & nao neg. versus the SOI neg. & nao pos.
rsum=zeros(29,7);
for month=1:7
   for station=1:29
      flow_col= alldata(:,station+37);
      soi_col1 = alldata(:,month+1);
      soi_col2 = alldata(:,month+2);
      soi_col3 = alldata(:,month+3);
      soi_col4 = alldata(:,month+4);
      soi_col5 = alldata(:,month+5);
      soi_col6 = alldata(:,month+6);
      nao_col1 = alldata(:,month+13);
      nao_col2 = alldata(:,month+14);
      nao_col3 = alldata(:,month+15);
      nao_col4 = alldata(:,month+16);
      nao_col5 = alldata(:,month+17);
      nao_col6 = alldata(:,month+18);
      soi_col = mean([soi_col1,soi_col2,soi_col3,soi_col4,soi_col5,soi_col6],2);
      nao_col = mean([nao_col1,nao_col2,nao_col3,nao_col4,nao_col5,nao_col6],2);
      pindices=find(soi_col<0 & nao_col<0);
      nindices=find(soi_col<0 & nao_col>=0);
      rsum(station, month)=ranksum(flow_col(pindices),flow_col(nindices));
   end
end

function [rsum]=SAb3
[alldata,tflow]=xlsread('C:\Matlab\52-ALL.xls');
% Calculation of the SOI & AMO pos. versus the SOI pos. & AMO neg.
rsum=zeros(29,10);
for month=1:10
   for station=1:29
```

```
      flow_col= alldata(:,station+37);
      soi_col1 = alldata(:,month+1);
      soi_col2 = alldata(:,month+2);
      soi_col3 = alldata(:,month+3);
      amo_col1 = alldata(:,month+66);
      amo_col2 = alldata(:,month+67);
      amo_col3 = alldata(:,month+68);
      soi_col = mean([soi_col1,soi_col2,soi_col3],2);
      amo_col = mean([amo_col1,amo_col2,amo_col3],2);
      pindices=find(soi_col>=0 & amo_col>=0);
      nindices=find(soi_col>=0 & amo_col<0);
      rsum(station, month)=ranksum(flow_col(pindices),flow_col(nindices));
   end
end

function [rsum]=SAb6
[alldata,tflow]=xlsread('C:\Matlab\52-ALL.xls');
% Calculation of the SOI & AMO pos. versus the SOI pos. & AMO neg.
rsum=zeros(29,7);
for month=1:7
   for station=1:29
      flow_col= alldata(:,station+37);
      soi_col1 = alldata(:,month+1);
      soi_col2 = alldata(:,month+2);
      soi_col3 = alldata(:,month+3);
      soi_col4 = alldata(:,month+4);
      soi_col5 = alldata(:,month+5);
      soi_col6 = alldata(:,month+6);
      amo_col1 = alldata(:,month+66);
      amo_col2 = alldata(:,month+67);
      amo_col3 = alldata(:,month+68);
      amo_col4 = alldata(:,month+69);
      amo_col5 = alldata(:,month+70);
      amo_col6 = alldata(:,month+71);
      soi_col = mean([soi_col1,soi_col2,soi_col3,soi_col4,soi_col5,soi_col6],2);
      amo_col = mean([amo_col1,amo_col2,amo_col3,amo_col4,amo_col5,amo_col6],2);
      pindices=find(soi_col>=0 & amo_col>=0);
      nindices=find(soi_col>=0 & amo_col<0);
      rsum(station, month)=ranksum(flow_col(pindices),flow_col(nindices));
   end
end

function [rsum]=SAd3
[alldata,tflow]=xlsread('C:\Matlab\52-ALL.xls');
% Calculation of the SOI & AMO neg. versus the SOI neg. & AMO pos.
rsum=zeros(29,10);
```

```
for month=1:10
   for station=1:29
      flow_col= alldata(:,station+37);
      soi_col1 = alldata(:,month+1);
      soi_col2 = alldata(:,month+2);
      soi_col3 = alldata(:,month+3);
      amo_col1 = alldata(:,month+66);
      amo_col2 = alldata(:,month+67);
      amo_col3 = alldata(:,month+68);
      soi_col = mean([soi_col1,soi_col2,soi_col3],2);
      amo_col = mean([amo_col1,amo_col2,amo_col3],2);
      pindices=find(soi_col<0 & amo_col<0);
      nindices=find(soi_col<0 & amo_col>=0);
      rsum(station, month)=ranksum(flow_col(pindices),flow_col(nindices));
   end
end

function [rsum]=SAd6
[alldata,tflow]=xlsread('C:\Matlab\52-ALL.xls');
% Calculation of the SOI & AMO neg. versus the SOI neg. & AMO pos.
rsum=zeros(29,7);
for month=1:7
   for station=1:29
      flow_col= alldata(:,station+37);
      soi_col1 = alldata(:,month+1);
      soi_col2 = alldata(:,month+2);
      soi_col3 = alldata(:,month+3);
      soi_col4 = alldata(:,month+4);
      soi_col5 = alldata(:,month+5);
      soi_col6 = alldata(:,month+6);
      amo_col1 = alldata(:,month+66);
      amo_col2 = alldata(:,month+67);
      amo_col3 = alldata(:,month+68);
      amo_col4 = alldata(:,month+69);
      amo_col5 = alldata(:,month+70);
      amo_col6 = alldata(:,month+71);
      soi_col = mean([soi_col1,soi_col2,soi_col3,soi_col4,soi_col5,soi_col6],2);
      amo_col = mean([amo_col1,amo_col2,amo_col3,amo_col4,amo_col5,amo_col6],2);
      pindices=find(soi_col<0 & amo_col<0);
      nindices=find(soi_col<0 & amo_col>=0);
      rsum(station, month)=ranksum(flow_col(pindices),flow_col(nindices));
   end
end

function [rsum]=SST3
[alldata]=xlsread('C:\Matlab\52-ALL.xls');
```

```
rsum=zeros(29,10);
for month=1:10
   for station=1:29
      flow_col = alldata(:,station+37);
      sst3_col = alldata(:,month+78);
      pindices=find(sst3_col>=0);
      nindices=find(sst3_col<0);
      rsum(station, month)=ranksum(flow_col(pindices),flow_col(nindices));
   end
end

function [rsum]=SST6
[alldata,tflow]=xlsread('C:\Matlab\52-ALL.xls');
rsum=zeros(29,7);
for month=1:7
   for station=1:29
      flow_col = alldata(:,station+37);
      sst6_col = alldata(:,month+88);
      pindices=find(sst6_col>=0);
      nindices=find(sst6_col<0);
      rsum(station, month)=ranksum(flow_col(pindices),flow_col(nindices));
   end
end
```

A1.2.2 SVD Analysis And Mapping

```
%-------------------------------------------------------------------------------------
%Code reads in SST data and then removes the -9999 values which denote land
temps = xlsread('C:\Matlab\SVD\SST-RAW.xls');
temps = temps(3:end,4:56);

m = 0;

for i = -70:2:70;          % Latitude
   for j = 120:2:280;     % Longitude
     m = m +1;
      b(m,:) = [i j];
   end

end

remv_rows = find(temps(:,1) == -9999);
%all_temps(remv_rows,:) = [];
temps(remv_rows,:) = [];
b(remv_rows,:) = [];
```

```
all_temps = [b temps];

col = size(temps,2);

% Take row average, by adding the ',2' inside the parenthesis.
round1 = mean(temps,2);

%Standardize each row (hence the ',2' term again). The middle term
% (e.g. '0') tells the function to use n-1 when standardizing.
round1st = std(temps,0,2);

for i = 1:col
round2(:,i) = temps(:,i) - round1;  % Substruct each row element to row mean
end
round2mn = mean(round2,2);
round2st = std(round2,0,2);     % Get standard deviation

for j = 1:col
round3(:,j) = (round2(:,j)- round2mn)./round2st;    % Standardize
end
m
round3(isnan(round3))=0;

xlswrite('C:\MATLAB\SVD\SST_lat_long.xls',b);   % Write to excel file
xlswrite('C:\MATLAB\SVD\std_sst.xls',roun3);

%-------------------------------------------------------------------------------------------
% Runs SVD and calculates the correlation values from the SVD results.
% Create a Matlab directory in C
% C:\Matlab
% Or use a different directory. However lines 37 52 53 115-118
% needs to be changed accordingly

% Other parameters that can be changed on lines...
% Lines 12, 13, 146, 147, 219, 220

clc
clear

temp1 = xlsread('C:\matlab\SVD95\SVD-0-JAS\Std_SST.xls');  %import standardized
ssts.
str1 = xlsread('C:\matlab\std-streamflow.xls');   %inport standardized sst
[stations years] = size(str1); %input('Enter the number of years: ');
t = temp1';
s = str1';
```

```
%calculating covariance
covar_ts = (1/years) * t' * s;

% svd calculation
[left, eigs, right] = svd(covar_ts);

% Get the number of modes by calculating
% the square covariance and check for values >10
eigenvalues = diag(eigs);
square_eig = eigenvalues.^2;            %squares of the values
sum_sq_eig = sum(square_eig) ;          %sum of the squares
square_cov = square_eig./sum_sq_eig;    %square covariance
sign_num = find(square_cov >= 0.11);    %find values greater than 10%
sign_num_val = square_cov(sign_num);
num_modes = numel(sign_num);            %How many values greater than 10%

% Export square covariance data to an excel file

xlswrite('C:\matlab\SVD95\SVD-0-JAS\square_covar.xls',square_cov);

% Getting temporal expansion
for i = 1:num_modes; %num_modes;
   a = left(:,i);
   left_exp = t*a;                  %Create a matrix of left
   left_exp_mat(:,i) = left_exp;        %left temporal expansions

   b = right(:,i);
   right_exp = s*b;                   %create a matrix of right
   right_exp_mat(:,i) = right_exp;     %right temporal expansions
end

% Export temporal expansions matrices to excel files

xlswrite('C:\matlab\SVD95\SVD-0-JAS\right_temp_expan.xls',right_exp_mat);
xlswrite('C:\matlab\SVD95\SVD-0-JAS\left_temp_expan.xls',left_exp_mat);

% Getting Left heterogenous correlation

sign_p = input('Significance (in decimal, eg 0.95 for 95%): ');
sign_p = 1 - sign_p;

[rrt cct] = size(t);
[rrs ccs] = size(s);

for n = 1:num_modes;
   rht = right_exp_mat(:,n);
```

```
    for m = 1:cct;

    left_heter = [t(:,m) rht];    % left heterogenous correlations figure

    [r,p] = corrcoef(left_heter); %Compute sample correlation and p-values.
    [k,l] = find(p<sign_p);         % Find significant correlations.
     pp = [k,l];                  % Display their (row,col) indices.
     if isempty(pp)
     rl = 0;
    else
     rl = r(1,2);
     end
    bbb(n,m) = rl;
    r = r(1,2);
    all_left(n,m) = r;
     end

end
    left_corr_values = bbb';
    all_left_correl = all_left';


 %Getting Right heterogeneous correlation

 for u = 1:num_modes;
    lht = left_exp_mat(:,u);

    for v = 1:ccs;

    right_heter = [s(:,v) lht];    % right heterogenous correlations figure

    [rr,pr] = corrcoef(right_heter); %Compute sample correlation and p-values.
    [kr,lr] = find(pr<sign_p);         % Find significant correlations.
     ppr = [kr,lr];                  % Display their (row,col) indices.
     if isempty(ppr)
     rrs = 0;
    else
     rrs = rr(1,2);
     end
    bbbr(u,v) = rrs;
    rr = rr(1,2);
    corr_valz(u,v) = rr;
     end

end
```

```
   right_corr_values = bbbr';
   all_corr_valz = corr_valz';

 %Export significant correlation values to excel files

     xlswrite('C:\matlab\SVD95\SVD-0-JAS\stream_correl.xls',right_corr_values);
     xlswrite('C:\matlab\SVD95\SVD-0-JAS\SST_correl.xls',left_corr_values);
     xlswrite('C:\matlab\SVD95\SVD-0-JAS\all_stream_correl.xls',all_corr_valz);
     xlswrite('C:\matlab\SVD95\SVD-0-JAS\all_sst_correl.xls',all_left_correl);


% Information to display
num_mode_val = 100.* sign_num_val';
mode_total = sum(num_mode_val);
num_m_val = [num_modes mode_total];

fprintf('There are %3.0f modes for this analysis and account for %3.0f percent.
\n',num_m_val)
display(['The square covariance fractions over 10% are ' int2str(num_mode_val) '
percent.'])
disp(' ')

%MAPPING SECTION
%BELOW MAPPING SECTION.
looper = 1;
while looper == 1;          % Loop to view figures of different modes.

% Select what to view, Contour of SST or Streamflow Correlations

graph2view = input('Which view do you want(sst = 1 or runoff = 2)? ');
if graph2view == 2
nm = input('Enter the mode to view: ');
str_latlong = xlsread('C:\matlab\stream_lat_long.xls');%Stream Gauge latitude and
longitude
snlat = str_latlong(:,1);                  %xlsread('LatQ.xls'); %
snlong = str_latlong(:,2);                   %xlsread('LongQ.xls'); %
latlim = [ 25 50];                        % Latitude map limits
lonlim = [-125 -100];                      % longitude map limits
figure
ax = usamap(latlim,lonlim);
axis off
states = shaperead('usastatehi',...
'UseGeoCoords', true, 'BoundingBox', [lonlim', latlim']);
faceColors = makesymbolspec('Polygon',...
{'INDEX', [1 numel(states)], ...
'FaceColor', white(numel(states))}); %polcmap will assign random colors for states
```

```
geoshow(ax, states , 'SymbolSpec',faceColors)
snvalues = right_corr_values;
array1 = [snlat snlong snvalues(:,nm)];
[rows colms]=size(array1);
for i = 1:rows;
   if array1(i,3)>0
      snotlats = array1(i,1);
      snotlongs = array1(i,2);
      plotm(snotlats,snotlongs,'r.')

   elseif array1(i,3)<0
      snotlats = array1(i,1);
      snotlongs = array1(i,2);
      plotm(snotlats,snotlongs,'b.')
   else
      snotlats = array1(i,1);
      snotlongs = array1(i,2);
      plotm(snotlats,snotlongs,'k.')
   end
end

for k = 1:numel(states)
labelPointIsWithinLimits =...
latlim(1) < states(k).LabelLat &&...
latlim(2) > states(k).LabelLat &&...
lonlim(1) < states(k).LabelLon &&...
lonlim(2) > states(k).LabelLon;
if labelPointIsWithinLimits
textm(states(k).LabelLat,...
states(k).LabelLon, states(k).Name, 'HorizontalAlignment', 'center')
end

end

% SSTs contour Mapping

elseif graph2view ==1          %contours

% Load the data and extract the (x,y,z) information:

lat_long = xlsread('C:\Matlab\SVD95\SVD-0-JAS\SST_lat_long.xls'); % SST latitude
and longitude
x = lat_long(:,2); %x = xlsread('Lon.xls'); %
y = lat_long(:,1); %y = xlsread('Lat.xls'); % % %
nn = input('Enter the mode to view: ');
```

```
z = all_left_correl(:,nn);
% Determine the minimum and the maximum x and y values:
xmin = min(x); ymin = min(y);
xmax = max(x); ymax = max(y);
% Define the resolution of the grid:
xres=17;
yres=9;
% Define the range and spacing of the x- and y-coordinates,
% and then fit them into X and Y
xv = linspace(xmin, xmax, xres);
yv = linspace(ymin, ymax, yres);
[Xinterp,Yinterp] = meshgrid(xv,yv);
% Calculate Z in the X-Y interpolation space, which is an
% evenly spaced grid:
[xi,yi,Zinterp] = griddata(x,y,z,Xinterp,Yinterp);

load coast
latlim = [ -33 65];              % SST area map latitude limit
lonlim =[120 -80] ;               % SST area map longitude limit
figure
worldmap(latlim,lonlim);
axis off
patchm(lat,long, 'k') %plotm patchm

[c,h] = contourfm(yi,xi,Zinterp,-0.6:0.2:0.6);
contourcmap(0.3,'jet','colorbar','on','location','horizontal')
load('MyColormaps','sstmap')
set(gcf,'Colormap',sstmap)

h1 = clabelm(c,h);
else
   disp('Not an acceptable choice.')
end
disp(' ')
looper = input('Do you want to print another figure? (yes = 1, no = 0)');
end
disp(' ')
disp('I guess you are done for now...')

%-------------------------------------------------------------
%array used to define the MyColormaps array called in the mapping section
sstmap = [1 1 0; 0 1 1; 0 0 1; 0 0.502 1; 1 1 1; …
   1 1 1; 1 0 0; 0.6588 0 0; 0.5922 0 0.2941; 0.502 0 0.502];
save MyColormaps sstmap
```

A1.3 Chapter 4 Analysis Code

A1.3.1 NetCDF Processing Code in Matlab

```
%Code to read and process the .nc data.
addpath('C:\Program Files (x86)\MATLAB\R2009a
Student\toolbox\matlab\matlab_netCDF_OPeNDAP')
addpath('C:\Program Files (x86)\MATLAB\R2009a Student\toolbox\matlab\mexnc')
addpath('C:\Program Files (x86)\MATLAB\R2009a Student\toolbox\matlab\snctools')

%Step 1. Read in the NetCDF files by grabbing only the correct
%level, Lat, and Lon fields
%NOTE:  NetCDF files are 0-based (e.g first 'column' index is 0 not 1)
%is actually 0, not 1.

%---------------------------------------------------------------------
%Manual input region
east = 280;
west = 120;
north = 70;
south = -30; %use negative numbers to denote lats below the equator
gph_level = 500;
uwnd_level = 200;
mon_int = 3; %This defines how manth months are going to be averaged
%---------------------------------------------------------------------

level = nc_varget('hgt.mon.mean.nc','level');
lat = nc_varget('hgt.mon.mean.nc','lat');
lon = nc_varget('hgt.mon.mean.nc','lon');

glev = find(level(:,1) == gph_level); %Specifies the 500mb level
wlev = find(level(:,1) == uwnd_level); %Specifies the 200mb level

lat_max = find(lat(:,1) == south); %returns northern most lat value
lat_min = find(lat(:,1) == north); %returns southern most lat value

lon_max = find(lon(:,1) == east); %returns eastern most lon value
lon_min = find(lon(:,1) == west); %returns western most lon value

gph = nc_varget('hgt.mon.mean.nc','hgt',[0 glev lat_min lon_min],...
    [-1 1 (lat_max-lat_min+1) (lon_max-lon_min+1)]);

uwnd = nc_varget('uwnd.mon.mean.nc','uwnd',[0 wlev lat_min lon_min],...
    [-1 1 (lat_max-lat_min+1) (lon_max-lon_min+1)]);

slp = nc_varget('slp.mon.mean.nc','slp',[0 lat_min lon_min],...
```

```
   [-1 (lat_max-lat_min+1) (lon_max-lon_min+1)]);

% Reorganize the data to make it so that it is a 2D matrix.
% Such that: Rows = locations, Columns = Time.
p_gph = permute(gph,[2 3 1]); p_uwnd = permute(uwnd,[2 3 1]);
p_slp = permute(slp,[2 3 1]);

sizeg = size(p_gph); sizeu = size(p_uwnd); sizes = size(p_slp);

r_gph = reshape(p_gph,(sizeg(1)*sizeg(2)),sizeg(3));
r_uwnd = reshape(p_uwnd,(sizeu(1)*sizeu(2)),sizeu(3));
r_slp = reshape(p_slp,(sizes(1)*sizes(2)),sizes(3));

a = size(r_gph); b = size(r_uwnd); bb = size(r_slp);

%Standardize the values of the HGT and UWND datasets based upon location
%(i.e. rows of the 2D array).
%formula: std value = (value - mean(row))/std(row);
g500 = zeros(a(1),a(2));
for yr = 1:a(2)
   for loc = 1:a(1)
g500(loc,yr) = (r_gph(loc,yr) - mean(r_gph(loc,:)))/std(r_gph(loc,:));
   end
end

u200 = zeros(b(1),b(2));
for yr = 1:b(2)
   for loc = 1:b(1)
u200(loc,yr) = (r_uwnd(loc,yr) - mean(r_uwnd(loc,:)))/std(r_uwnd(loc,:));
   end
end

slp0 = zeros(bb(1),bb(2));
for yr = 1:bb(2)
   for loc = 1:bb(1)
slp0(loc,yr) = (r_slp(loc,yr) - mean(r_slp(loc,:)))/std(r_slp(loc,:));
   end
end
%-------------------------------------
%Pre-Analysis Calculations
%-------------------------------------

%To create lagged HGT and UWND data, similar to the SST data already used,
%need to create 3-month average values for each year.  The output of this
%step should be a single value for each year in the data record.
```

```
%Create the 3-month average for each year for the HGT data: JFM - OND
agph_m = zeros(length(g500),62,10);
for yr = 1:62
   for mon = 1:10
agph_m(:,yr,mon) = mean(g500(:,12*yr-(12-mon):12*yr-(12-(mon+(mon_int-1)))),2);
   end
end
c = size(agph_m);
ragph_m = reshape(agph_m,(c(1)*c(2)),c(3));

%Create the 3-month average for each year for the HGT data: NDJ - DJF
bgph_m = zeros(length(g500),61,2);
for yr = 1:61
   for month = 1:2
bgph_m(:,yr,month) = mean(g500(:,12*yr-(12-month):12*yr-(12-(month+(mon_int-
1)))),2);
   end
end
d = size(bgph_m);

na_col = NaN(d(1),1,d(3));
bbgph_m = [na_col bgph_m];
dd = size(bbgph_m);
rbgph_m = reshape(bbgph_m,(dd(1)*dd(2)),dd(3));

%Combine two matricies and then resape back into a 3D array such that:
%Rows = locations; Columns = years; z = correspnding 3-month interval.
comb_g = [ragph_m rbgph_m];
%take the DJF, NDJ, OND, SON, ASO inteval and move them to the front of the
%combined matrix so that the final matrix is organized by water year and
%not claendar year.
comb_g2 = [comb_g(:,8:12) comb_g(:,1:7)];
gph_m = reshape(comb_g2,c(1),c(2),12);

save gph_m gph_m
%-------------------------------------------------------------------------
%Repeat process to get 3-month average for each year for the UWND data
%-------------------------------------------------------------------------
awnd_m = zeros(length(u200),62,10);
for yr = 1:62
   for mon = 1:10
awnd_m(:,yr,mon) = mean(u200(:,12*yr-(12-mon):12*yr-(12-(mon+(mon_int-1)))),2);
   end
end
e = size(awnd_m);
rawnd_m = reshape(awnd_m,(e(1)*e(2)),e(3));
```

```
%Create the 3-month average for each year for the HGT data: NDJ - DJF
bwnd_m = zeros(length(u200),61,2);
for yr = 1:61
   for month = 1:2
bwnd_m(:,yr,month) = mean(u200(:,12*yr-(12-month):12*yr-(12-(month+(mon_int-
1)))),2);
   end
end
f = size(bwnd_m);

na_col = NaN(f(1),1,f(3));
bbwnd_m = [na_col bwnd_m];
ff = size(bbwnd_m);
rbwnd_m = reshape(bbwnd_m,(ff(1)*ff(2)),ff(3));

%Combine two matricies and then resape back into a 3D array such that:
%Rows = locations; Columns = years; z = correspnding 3-month interval.

comb_w = [rawnd_m rbwnd_m];
%take the DJF, NDJ, OND, SON, ASO inteval and move them to the front of the
%combined matrix so that the final matrix is organized by water year and
%not claendar year.
comb_w2 = [comb_w(:,8:12) comb_w(:,1:7)];
wnd_m = reshape(comb_w2,e(1),e(2),12);

save wnd_m wnd_m

%-------------------------------------------------------------------------
%Repeat process to get 3-month average for each year for the SLP data
%-------------------------------------------------------------------------
aslp_m = zeros(length(slp0),62,10);
for yr = 1:62
   for mon = 1:10
aslp_m(:,yr,mon) = mean(slp0(:,12*yr-(12-mon):12*yr-(12-(mon+(mon_int-1)))),2);
   end
end
f = size(aslp_m);
raslp_m = reshape(aslp_m,(f(1)*f(2)),f(3));

%Create the 3-month average for each year for the SLP data: NDJ - DJF
bslp_m = zeros(length(slp0),61,2);
for yr = 1:61
   for month = 1:2
bslp_m(:,yr,month) = mean(slp0(:,12*yr-(12-month):12*yr-(12-(month+(mon_int-
1)))),2);
```

```
   end
end
g = size(bslp_m);

na_col = NaN(g(1),1,g(3));
bbslp_m = [na_col bslp_m];
gg = size(bbslp_m);
rbslp_m = reshape(bbslp_m,(gg(1)*gg(2)),gg(3));

%Combine two matricies and then resape back into a 3D array such that:
%Rows = locations; Columns = years; z = correspnding 3-month interval.

comb_s = [raslp_m rbslp_m];
%take the DJF, NDJ, OND, SON, ASO inteval and move them to the front of the
%combined matrix so that the final matrix is organized by water year and
%not claendar year.
comb_s2 = [comb_s(:,8:12) comb_s(:,1:7)];
slp_m = reshape(comb_s2,f(1),f(2),12);

save slp_m slp_m

%---------------------------------------------------------------
%Create the Lat - Lon vector to plot the data in the SVD output
%---------------------------------------------------------------
x = west:2.5:east;
y = south:2.5:north;

for lon = 1:length(x);
   for lat = 1:length(y);
y_all(lon,lat) = y(end+1-lat);
x_all(lon,lat) = x(lon);
   end
end

ry_all = reshape(y_all',numel(y_all),1);
rx_all = reshape(x_all',numel(x_all),1);
lat_lon = [ry_all rx_all];

save lat_lon lat_lon
```

A1.3.2 SVD Analysis And Mapping

```
%import standardized ssts and streamflow.

yr = input('Which lag year do you want to analyze? ');
lag = input('Which 3-month interval do you want to analyze? ');
```

```
load std_sst
temp1 = std_sst(:,13-yr:66-yr,lag+1); %grabs 54 columns
%0 year lag = col13: col66
%JAS interval is std_sst(:, :, 1).
load std_stream
str1 = std_stream; %This is the std streamflow from 1952 - 2005 (N = 54)

[stations years] = size(str1);
t = temp1';
s = str1';

%calculating covariance
covar_ts = (1/years) * t' * s;

% svd calculation
[left, eigs, right] = svd(covar_ts);

% Get the number of modes by calculating
% the square covariance and check for values >10
eigenvalues = diag(eigs);
square_eig = eigenvalues.^2;            %squares of the values
sum_sq_eig = sum(square_eig) ;          %sum of the squares
square_cov = square_eig./sum_sq_eig;    %square covariance
sign_num = find(square_cov >= 0.11);    %find values greater than 10%
sign_num_val = square_cov(sign_num);
num_modes = numel(sign_num);            %How many values greater than 10%

% Export square covariance data to an excel file

xlswrite('L:\Kenneth Data\Matlab\Phase3\SVD\square_covar.xls',square_cov, '4');

% Getting temporal expansion
for i = 1:num_modes; %num_modes;
   a = left(:,i);
   left_exp = t*a;                  %Create a matrix of left
   left_exp_mat(:,i) = left_exp;        %left temporal expansions

   b = right(:,i);
   right_exp = s*b;                   %create a matrix of right
   right_exp_mat(:,i) = right_exp;     %right temporal expansions
end

% Export temporal expansions matrices to excel files

xlswrite('L:\Kenneth Data\matlab\Phase3\SVD\rte.xls',right_exp_mat, '4');
xlswrite('L:\Kenneth Data\matlab\Phase3\SVD\lte.xls',left_exp_mat, '4');
```

```
% Getting Left heterogenous correlation

%sign_p = input('Significance (in decimal, eg 0.95 for 95%): ');
sign_p = 1 - 0.95;
%To reinstate teh use of the input command, simply replace the 0.95 with
%'sign_p', and remove the comment from the previous command.

[rrt cct] = size(t);
[rrs ccs] = size(s);

for n = 1:num_modes;
   rht = right_exp_mat(:,n);

   for m = 1:cct;

   left_heter = [t(:,m) rht];    % left heterogenous correlations figure

   [r,p] = corrcoef(left_heter); %Compute sample correlation and p-values.
   [k,l] = find(p<sign_p);         % Find significant correlations.
    pp = [k,l];                  % Display their (row,col) indices.
    if isempty(pp)
    rl = 0;
   else
    rl = r(1,2);
    end
   bbb(n,m) = rl;
   r = r(1,2);
   all_left(n,m) = r;
    end

end
   left_corr_values = bbb';
   all_left_correl = all_left';


 %Getting Right heterogeneous correlation

 for u = 1:num_modes;
   lht = left_exp_mat(:,u);

   for v = 1:ccs;

   right_heter = [s(:,v) lht];    % right heterogenous correlations figure

   [rr,pr] = corrcoef(right_heter); %Compute sample correlation and p-values.
```

```
    [kr,lr] = find(pr<sign_p);         % Find significant correlations.
     ppr = [kr,lr];                    % Display their (row,col) indices.
     if isempty(ppr)
     rrs = 0;
    else
     rrs = rr(1,2);
     end
    bbbr(u,v) = rrs;
    rr = rr(1,2);
    corr_valz(u,v) = rr;
     end

end
    right_corr_values = bbbr';
    all_corr_valz = corr_valz';

 %Export significant correlation values to excel files

      xlswrite('L:\Kenneth    Data\matlab\Phase3\SVD\stream_correl.xls',right_corr_values,
'4');
      xlswrite('L:\Kenneth Data\matlab\Phase3\SVD\SST_correl.xls',left_corr_values, '4');
      xlswrite('L:\Kenneth     Data\matlab\Phase3\SVD\all_stream_correl.xls',all_corr_valz,
'4');
      xlswrite('L:\Kenneth Data\matlab\Phase3\SVD\all_sst_correl.xls',all_left_correl, '4');


% Information to display
%num_mode_val = 100.* sign_num_val';
%mode_total = sum(num_mode_val);
%num_m_val = [num_modes mode_total];

%fprintf('There are %3.0f modes for this analysis and account for %3.0f percent.
\n',num_m_val)
%display(['The square covariance fractions over 10% are ' int2str(num_mode_val) '
percent.'])
%disp(' ')



%MAPPING SECTION
%BELOW MAPPING SECTION.
looper = 1;
while looper == 1;          % Loop to view figures of different modes.

% Select what to view, Contour of SST or Streamflow Correlations
```

```
graph2view = input('Which view do you want(sst = 1 or runoff = 2)? ');
if graph2view == 2
nm = input('Enter the mode to view: ');
str_latlong = xlsread('L:\Kenneth Data\matlab\PhaseX\stream_lat_long.xls');%Stream
Gauge latitude and longitude
snlat = str_latlong(:,1);
snlong = str_latlong(:,2);
latlim = [ 30 45];                    % Latitude map limits
lonlim = [-120 -105];                   % longitude map limits
figure
ax = usamap(latlim,lonlim);
axis off
states = shaperead('usastatehi',...
'UseGeoCoords', true, 'BoundingBox', [lonlim', latlim']);
faceColors = makesymbolspec('Polygon',...
{'INDEX', [1 numel(states)], ...
'FaceColor', white(numel(states))}); %polcmap will assign random colors for states

geoshow(ax, states , 'SymbolSpec',faceColors)
snvalues = right_corr_values;
array1 = [snlat snlong snvalues(:,nm)];
[rows colms]=size(array1);
for i = 1:rows;
   if array1(i,3)>0
      snotlats = array1(i,1);
      snotlongs = array1(i,2);
      plotm(snotlats,snotlongs,'r^')

   elseif array1(i,3)<0
      snotlats = array1(i,1);
      snotlongs = array1(i,2);
      plotm(snotlats,snotlongs,'bV')
   else
      snotlats = array1(i,1);
      snotlongs = array1(i,2);
      plotm(snotlats,snotlongs,'k.')
   end
end

for k = 1:numel(states)
labelPointIsWithinLimits =...
latlim(1) < states(k).LabelLat &&...
latlim(2) > states(k).LabelLat &&...
lonlim(1) < states(k).LabelLon &&...
lonlim(2) > states(k).LabelLon;
if labelPointIsWithinLimits
```

```
textm(states(k).LabelLat,...
states(k).LabelLon, states(k).Name, 'HorizontalAlignment', 'center')
end

end

% SSTs contour Mapping

elseif graph2view ==1          %contours

% Load the data and extract the (x,y,z) information:
% SST latitude and longitude
lat_long = xlsread('L:\Kenneth Data\Matlab\Phase3\SVD\SST_lat_long.xls');
x = lat_long(:,2);
y = lat_long(:,1);
nn = input('Enter the mode to view: ');
z = all_left_correl(:,nn);
% Determine the minimum and the maximum x and y values:
xmin = min(x); ymin = min(y);
xmax = max(x); ymax = max(y);
% Define the resolution of the grid:
xres=17;
yres=9;
% Define the range and spacing of the x- and y-coordinates,
% and then fit them into X and Y
xv = linspace(xmin, xmax, xres);
yv = linspace(ymin, ymax, yres);
[Xinterp,Yinterp] = meshgrid(xv,yv);
% Calculate Z in the X-Y interpolation space, which is an
% evenly spaced grid:
[xi,yi,Zinterp] = griddata(x,y,z,Xinterp,Yinterp);

load coast
latlim = [ -30 70];              % SST area map latitude limit
lonlim =[120 -80] ;               % SST area map longitude limit
figure
worldmap(latlim,lonlim);
axis off
patchm(lat,long, 'k') %plotm patchm

[c,h] = contourfm(yi,xi,Zinterp,-0.81:0.27:0.81);
contourcmap(0.27,'jet')
load('MyColormaps2','revmap')
set(gcf,'Colormap',revmap)

h1 = clabelm(c,h);
```

```
else
   disp('Not an acceptable choice.')
end
disp(' ')
looper = input('Do you want to print another figure? (yes = 1, no = 0)');
end
disp(' ')
disp('I guess you are done for now...')

%----------------------------
%Define MyColormaps2

revmap =    0 0 1.0000; 0 0.4980 1.0000; 0 0.7490 1.0000; …
   1.0000 1.0000 1.0000; 1.0000 1.0000 1.0000; 1.0000 0.6863 0.6863; …
   1.0000 0.3922 0.3922; 1.0000 0 0];
save MyColormaps2 revmap
```

A1.3.3 Correlation and Mapping

```
looper = 1;
while looper == 1;          % Loop to view figures of different modes.
clear
yr = input('Enter the lag year to correlaate: ');
lag = input('Enter the 3-month interval to correlaate: ');
%lag 0:JAS / lag 1:JJA / lag 2:MJJ / lag 3:AMJ / lag 4:MAM /
%lag 5:FMA / lag 6:JFM / lag 7:DJF / lag 8:NDJ / lag 9:OND /
%lag 10:SON / lag 11:ASO

%yr 0: 1952-2007 (col 5:60) / yr 1: 1951-2006 (col 4:59)
%yr 2: 1950-2005 (col 3:58) / yr 3: 1949-2004 (col 2:57)
%----------------------------------------
% Getting Left heterogenous correlation
%----------------------------------------

%Load the array containing the right temporal expansion series
%rte is organize such that rows = years, columns = month interval
%(increasiing lag moving left to right of the columns), and
%3rd dim = year lag (increasing lag year mving front to back of array)
load rte
rte = rte(:,lag+1,yr+1);

%Read in the climate data
load gph_m
gph = gph_m(:,5-yr:58-yr,12-lag);
t = gph';  % rows = years; columns = locations
```

```
%Define the significance level
sign_p = 0.05;

[t1 t2] = size(t);

rht = rte;

   for m = 1:t2;

   left_heter = [t(:,m) rht];    % left heterogenous correlations figure

   [r,p] = corrcoef(left_heter); %Compute sample correlation and p-values.
   [k,l] = find(p<sign_p);         % Find significant correlations.
    pp = [k,l];                  % Display their (row,col) indices.
%     if isempty(pp)
%     rl = 0;
%    else
%     rl = r(1,2);
%     end
%    bbb(:,m) = rl;
   r = r(1,2);
   all_left(:,m) = r;
    end

%left_corr_values = bbb';
all_left_correl = all_left';

%----------------------------------------
%MAPPING SECTION
%----------------------------------------

% Load the data and extract the (x,y,z) information:
%-----------------------------------------------------------------------
load lat_lon
lat_long = lat_lon; % SST latitude and longitude
%Longitude: 120E - 280E, every 2.5; Latitude = 70N to 70S every 2.5 degrees
x = lat_long(:,2);
y = lat_long(:,1);
nn = 1;

%Create the Map and show continents in background
%----------------------------------------
load coast
latlim = [lat_long(end,1) lat_long(1,1)]; % SST area map latitude limit
lonlim =[lat_long(1,2) lat_long(end,2)] ;  % SST area map longitude limit
```

```
figure
worldmap(latlim, lonlim);
axis off
plotm(lat,long, 'k')

%Read in the correlation values.
%-------------------------------------------------------------------------
z = all_left_correl(:,nn);
%z = left_corr_values(:,nn);

% Determine the minimum and the maximum x and y values:
%-------------------------------------------------------------------------
xmin = min(x); ymin = min(y);
xmax = max(x); ymax = max(y);

% Define the resolution of the grid:
%-------------------------------------------------------------------------
xres=68; %17 was the original value
yres=36; %9 was the original value

% Define the range and spacing of the x- and y-coordinates,
% and then fit them into X and Y
%-------------------------------------------------------------------------
xv = linspace(xmin, xmax, xres);
yv = linspace(ymin, ymax, yres);
[Xinterp,Yinterp] = meshgrid(xv,yv);

% Calculate Z in the X-Y interpolation space, which is an evenly spaced grid:
%-------------------------------------------------------------------------
[xi,yi,Zinterp] = griddata(x,y,z,Xinterp,Yinterp);

%[c,h] = contourfm(yi,xi,Zinterp,-0.6:0.2:0.6);
%contourcmap(0.2,'jet','colorbar','on','location','horizontal')
%load('MyColormaps','sstmap')
%set(gcf,'Colormap',sstmap)

[c,h] = contourfm(yi,xi,Zinterp,[-1.0 -0.354 -0.273 0 0.273 0.354 1.0]);
%contourcmap(0.27,'jet','colorbar','on','location','vertical')
contourcmap(0.27,'jet')
load('MyColormaps2','revmap')
set(gcf,'Colormap',revmap)

h1 = clabelm(c,h);

looper = input('Do you want to print another figure? (yes = 1, no = 0)');
```

```
end
disp(' ')
disp('I guess you are done for now...')
```

A1.4 Chapter 5 Data

A1.4.1 Yearly Mean SST Values for Hondo Region

	DJF	JFM	FMA		DJF	JFM	FMA
1900	2022.815	1949.27	1964.627	***1920***	2068.429	1985.765	1986.894
1901	2056.899	2012.005	2039.143	***1921***	2067.283	2000.262	1999.608
1902	2005.675	1933.828	1927.489	***1922***	2043.847	1960.048	1946.548
1903	2035.812	1934.307	1926.656	***1923***	2077.151	2005.312	1996.18
1904	1992.048	1911.259	1910.868	***1924***	2076.614	2008.937	1998.418
1905	2001.198	1941.69	1963.23	***1925***	2016.159	1935.323	1930.307
1906	2045.942	1954.529	1963.122	***1926***	2071.325	2000.714	1990.741
1907	1989.849	1933.32	1942.307	***1927***	2052.955	1970.712	1947.119
1908	2052.873	1975.553	1973.492	***1928***	2061.862	1989.886	1980.714
1909	2074.878	2005.222	2007.492	***1929***	2013.762	1928.799	1927.923
1910	2064.749	1982.5	1968.093	***1930***	2062.717	1998.778	1984.852
1911	2029.455	1943.116	1941.675	***1931***	2063.405	1975.577	1960.823
1912	2020.46	1935.585	1938.394	***1932***	2095.151	2026.963	2013.5
1913	2012.677	1928.902	1898.979	***1933***	2048.508	1963.791	1935.968
1914	2043.807	1957.04	1936.817	***1934***	2043.447	1972.249	1953.357
1915	2052.688	1949.659	1927.36	***1935***	2011.063	1929.987	1924.944
1916	2066.704	1993.138	1983.206	***1936***	2023.22	1955.071	1977.19

1917	2049.77	1976.937	1976.082	***1937***	2071.915	2002.556	1997.878
1918	2030.571	1977.698	1985.098	***1938***	2123.376	2046.249	2033.709
1919	1984.532	1921.976	1924.22	***1939***	2008.381	1906.86	1877.423
	DJF	JFM	FMA		DJF	JFM	FMA
1940	1991.146	1919.598	1918.323	***1960***	2058.693	1986.333	1976.765
1941	2058.13	1991.045	1990.27	***1961***	2072.267	2005.96	1987.304
1942	2164.354	2076.156	2058.005	***1962***	2083.582	1999.958	1991.487
1943	2115.172	2034.873	2023.27	***1963***	2055.212	1967.788	1949.452
1944	2101.278	2022.698	2009.111	***1964***	2086.942	2020.14	2017.77
1945	2101.278	2022.698	2009.111	***1965***	2027.23	1943.902	1934.209
1946	2115.193	2027.587	2016.627	***1966***	2060.011	1996.46	1978.95
1947	2002.648	1899.728	1889.579	***1967***	2078	2013.347	2004.008
1948	2056.783	1979.442	1969.825	***1968***	2063.37	1951.352	1928.73
1949	2121.063	2047.476	2057.817	***1969***	2040.754	1984.979	2013.19
1950	2101.765	2023.754	2028.101	***1970***	2026.238	1955.307	1969.921
1951	2102.235	2030.913	2016.519	***1971***	2075.556	1995.212	1996.915
1952	2102.019	2020.336	2021.098	***1972***	2056.611	1960.28	1937.794
1953	2106.339	2024.807	2027.212	***1973***	2026.222	1971.233	1989.532
1954	2085.312	1998.011	1977.312	***1974***	2075.423	1985.521	1971.574
1955	2080.09	2007.807	2002.847	***1975***	2096.265	2019.664	2010.733
1956	2063.899	1996.505	1996.897	***1976***	2076.728	1995.921	1994.751
1957	2022.849	1941.767	1942.28	***1977***	2029.807	1951.46	1955.828
1958	2024.865	1939.791	1951.934	***1978***	2008.799	1934.915	1939.325

1959	2025.376	1967.328	1965.392	***1979***	2054.526	1990.474	1977.96
	DJF	JFM	FMA		DJF	JFM	FMA
1980	1966.487	1896.259	1905.571	***2000***	2175.36	2099.556	2084.741
1981	2001.907	1917.37	1928.426	***2001***	2153.397	2085.468	2081.04
1982	2043.955	1941.124	1925.238	***2002***	2146.399	2063.701	2046.508
1983	1993.68	1901.78	1887.46	***2003***	2080.048	1988.72	1988.063
1984	2048.41	1965.214	1974.238	***2004***	2102.019	2013.937	2003.659
1985	2037.328	1960.857	1972.635	***2005***	2059.696	1954.762	1953.495
1986	2021.421	1929.603	1920.201	***2006***	2099.217	2023.487	2026.733
1987	2040.442	1957.68	1943.487	***2007***	2086.664	2011.124	2005.177
1988	2078.698	2013.291	2014.14	***2008***	2158.413	2079.161	2084.825
1989	2127.796	2034.812	2008.376	***2009***	2092.283	2020.627	2033.646
1990	2067.648	1998.177	1982.418				
1991	2038.331	1954.413	1970.59				
1992	2032.19	1959.463	1942.251				
1993	2019.093	1948.365	1945.55				
1994	2032.886	1964.14	1965.04				
1995	2100.968	1980.712	1950.746				
1996	2031.034	1941.413	1945.209				
1997	2004.735	1932.878	1938.563				
1998	2035.299	1948.81	1969.495				
1999	2167.262	2103.463	2113.852				

A1.5 Chapter 5 Analysis Code

A1.5.1 Resampling Weight Calculations

```
% Script that reads the raw Hondo data for DJF, JFM and FMA and finds the
% differences between the test year and all 30 calibration years (1976-05)
load IDX_val
djf = IDX_val(:,1);
djf_test = djf(1:75);
djf30 = djf(76:105);

%Find the difference between each an element in djf_test, and each element in djf30.
djf_diff = zeros(length(djf30),length(djf_test));
for col = 1:length(djf_test)
   for row = 1:length(djf30)
      djf_diff(row,col) = abs(djf_test(col) - djf30(row));
   end
end
xlswrite('L:\Kenneth Data\Matlab\Phase2\Hondo.xls',djf_diff,'k-NN','B34:BX63');

%Create the probability weight from the k-NN weighting kernel
%Weights created in Excel and then read in here

xw1_djf = xlsread('L:\Kenneth Data\Matlab\Phase2\Hondo.xls','k-NN','B2:BX31');
% convert xw1_djf to matrix where each column adds up to 1.0
   w1_djf = zeros(length(djf30),length(djf_test));
      for col = 1:length(djf_test)
         for row = 1:length(djf30)
            w1_djf(row,col) = xw1_djf(row,col)/(sum(xw1_djf(:,col)));
         end
      end

%Create the linear distribution of probability weight
% w2 = 1 - [diff(row,col)/max(dist(:,col))]

w2_djf = zeros(length(djf30),length(djf_test));
xw2_djf = zeros(length(djf30),length(djf_test));
for col = 1:length(djf_test)
   for row = 1:length(djf30)
     xw2_djf(row,col) = 1 - (djf_diff(row,col)/max(djf_diff(:,col)));
   end
end
   % convert w2_djf to matrix where each column adds up to 1.0
   for col = 1:length(djf_test)
      for row = 1:length(djf30)
         w2_djf(row,col) = xw2_djf(row,col)/(sum(xw2_djf(:,col)));
```

```
      end
   end

% Create the inverse difference squared probability weight
% w3 = 1 / diff^2
xw3_djf = zeros(length(djf30),length(djf_test));
w3_djf = zeros(length(djf30),length(djf_test));
for col = 1:length(djf_test)
   for row = 1:length(djf30)
      xw3_djf(row,col) = 1/(djf_diff(row,col)^2);
   end
end
   % convert xw3_djf to matrix where each column adds up to 1.0
   for col = 1:length(djf_test)
      for row = 1:length(djf30)
         w3_djf(row,col) = xw3_djf(row,col)/(sum(xw3_djf(:,col)));
      end
   end

%Create the inverse distance probability weight
% w4 = 1/diff
xw4_djf = zeros(length(djf30),length(djf_test));
w4_djf = zeros(length(djf30),length(djf_test));
for col = 1:length(djf_test)
   for row = 1:length(djf30)
      xw4_djf(row,col) = 1/djf_diff(row,col);
   end
end

% convert xw4_djf to matrix where each column adds up to 1.0
   for col = 1:length(djf_test)
      for row = 1:length(djf30)
         w4_djf(row,col) = xw4_djf(row,col)/(sum(xw4_djf(:,col)));
      end
   end

w_djf = [w1_djf; w2_djf; w3_djf; w4_djf];

%---------------------------------------
%Repeat the Process for the JFM interval
%---------------------------------------

%jfm = xlsread('L:\Kenneth Data\Matlab\Phase2\Hondo.xls','Yearly','D4:D112');
jfm = IDX_val(:,2);
jfm_test = jfm(1:75);
jfm30 = jfm(76:105);
```

```
%Find the difference between each an element in jfm_test, and each element
%in jfm30.

jfm_diff = zeros(30,length(jfm_test));
for col = 1:length(jfm_test)
   for row = 1:length(jfm30)
      jfm_diff(row,col) = abs(jfm_test(col) - jfm30(row));
   end
end

xlswrite('L:\Kenneth Data\Matlab\Phase2\Hondo.xls',jfm_diff,'k-NN','B34:BX63');

%Create the probability weight from the k-NN weighting kernel
%Weights created in Excel and then read in here

xw1_jfm = xlsread('L:\Kenneth Data\Matlab\Phase2\Hondo.xls','k-NN','B2:BX31');
% convert xw1_jfm to matrix where each column adds up to 1.0
   w1_jfm = zeros(length(jfm30),length(jfm_test));
      for col = 1:length(jfm_test)
         for row = 1:length(jfm30)
            w1_jfm(row,col) = xw1_jfm(row,col)/(sum(xw1_jfm(:,col)));
         end
      end

%Create the linear distribution of probability weight
% w2 = 1 - [diff(row,col)/max(dist(:,col))]
w2_jfm = zeros(length(jfm30),length(jfm_test));
xw2_jfm = zeros(length(jfm30),length(jfm_test));
for col = 1:length(djf_test)
   for row = 1:length(jfm30)
     xw2_jfm(row,col) = 1 - (jfm_diff(row,col)/max(jfm_diff(:,col)));
   end
end
   % convert w2_jfm to matrix where each column adds up to 1.0
   for col = 1:length(jfm_test)
      for row = 1:length(jfm30)
         w2_jfm(row,col) = xw2_jfm(row,col)/(sum(xw2_jfm(:,col)));
      end
   end

% Create the inverse difference squared probability weight
% w3 = 1 / diff^2
xw3_jfm = zeros(length(jfm30),length(jfm_test));
w3_jfm = zeros(length(jfm30),length(jfm_test));
for col = 1:length(jfm_test)
```

```
   for row = 1:length(jfm30)
      xw3_jfm(row,col) = 1/(jfm_diff(row,col)^2);
   end
end
   % convert xw3_jfm to matrix where each column adds up to 1.0
   for col = 1:length(jfm_test)
      for row = 1:length(jfm30)
         w3_jfm(row,col) = xw3_jfm(row,col)/(sum(xw3_jfm(:,col)));
      end
   end

%Create the inverse distance probability weight
% w4 = 1/diff
xw4_jfm = zeros(length(jfm30),length(jfm_test));
w4_jfm = zeros(length(jfm30),length(jfm_test));
for col = 1:length(jfm_test)
   for row = 1:length(jfm30)
      xw4_jfm(row,col) = 1/jfm_diff(row,col);
   end
end
    % convert xw4_jfm to matrix where each column adds up to 1.0
   for col = 1:length(jfm_test)
      for row = 1:length(jfm30)
         w4_jfm(row,col) = xw4_jfm(row,col)/(sum(xw4_jfm(:,col)));
      end
   end

w_jfm = [w1_jfm; w2_jfm; w3_jfm; w4_jfm];

%---------------------------------------
%Repeat the Process for the FMA interval
%---------------------------------------

fma = IDX_val(:,3);
fma_test = fma(1:75);
fma30 = fma(76:105);

%Find the difference between each an element in fma_test, and each element
%in fma30.

fma_diff = zeros(30,length(fma_test));
for col = 1:length(fma_test)
   for row = 1:length(fma30)
      fma_diff(row,col) = abs(fma_test(col) - fma30(row));
   end
end
```

```
xlswrite('L:\Kenneth Data\Matlab\Phase2\Hondo.xls',fma_diff,'k-NN','B34:BX63');

%Create the probability weight from the k-NN weighting kernel
%Weights created in Excel and then read in here
xw1_fma = xlsread('L:\Kenneth Data\Matlab\Phase2\Hondo.xls','k-NN','B2:BX31');

% convert xw1_fma to matrix where each column adds up to 1.0
   w1_fma = zeros(length(fma30),length(fma_test));
      for col = 1:length(fma_test)
         for row = 1:length(fma30)
            w1_fma(row,col) = xw1_fma(row,col)/(sum(xw1_fma(:,col)));
         end
      end

%Create the linear distribution of probability weight
% w2 = 1 - [diff(row,col)/max(dist(:,col))]
w2_fma = zeros(length(fma30),length(fma_test));
xw2_fma = zeros(length(fma30),length(fma_test));
for col = 1:length(fma_test)
   for row = 1:length(fma30)
     xw2_fma(row,col) = 1 - (fma_diff(row,col)/max(fma_diff(:,col)));
   end
end
   % convert w2_fma to matrix where each column adds up to 1.0
   for col = 1:length(fma_test)
      for row = 1:length(fma30)
         w2_fma(row,col) = xw2_fma(row,col)/(sum(xw2_fma(:,col)));
      end
   end

% Create the inverse difference squared probability weight
% w3 = 1 / diff^2
xw3_fma = zeros(length(fma30),length(fma_test));
w3_fma = zeros(length(fma30),length(fma_test));
for col = 1:length(fma_test)
   for row = 1:length(fma30)
      xw3_fma(row,col) = 1/(fma_diff(row,col)^2);
   end
end
   % convert xw3_fma to matrix where each column adds up to 1.0
   for col = 1:length(fma_test)
      for row = 1:length(fma30)
         w3_fma(row,col) = xw3_fma(row,col)/(sum(xw3_fma(:,col)));
      end
   end
```

```
%Create the inverse distance probability weight
% w4 = 1/diff
xw4_fma = zeros(length(fma30),length(fma_test));
w4_fma = zeros(length(fma30),length(fma_test));
for col = 1:length(fma_test)
   for row = 1:length(fma30)
      xw4_fma(row,col) = 1/fma_diff(row,col);
   end
end

% convert xw4_fma to matrix where each column adds up to 1.0
   for col = 1:length(fma_test)
      for row = 1:length(fma30)
         w4_fma(row,col) = xw4_fma(row,col)/(sum(xw4_fma(:,col)));
      end
   end

w_fma = [w1_fma; w2_fma; w3_fma; w4_fma];

%----------------------------------------
%Repeat the Process for the Water Year Average interval
%----------------------------------------

yr = IDX_val(:,4);
yr_test = yr(1:75);
yr30 = yr(76:105);

%Find the difference between each an element in yr_test, and each element
%in yr30.
yr_diff = zeros(length(yr30),length(yr_test));
for col = 1:length(yr_test)
   for row = 1:length(yr30)
      yr_diff(row,col) = abs(yr_test(col) - yr30(row));
   end
end

xlswrite('L:\Kenneth Data\Matlab\Phase2\Hondo.xls',yr_diff,'k-NN','B34:BX63');

%Create the probability weight from the k-NN weighting kernel
%Weights created in Excel and then read in here

xw1_yr = xlsread('L:\Kenneth Data\Matlab\Phase2\Hondo.xls','k-NN','B2:BX31');

   % convert w1_yr to matrix where each column adds up to 1.0
   w1_yr = zeros(length(yr30),length(yr_test));
```

```
    for col = 1:length(yr_test)
       for row = 1:length(yr30)
          w1_yr(row,col) = xw1_yr(row,col)/(sum(xw1_yr(:,col)));
       end
    end

%Create the linear distribution of probability weight
% w2 = 1 - [diff(row,col)/max(dist(:,col))]
w2_yr = zeros(length(yr30),length(yr_test));
xw2_yr = zeros(length(yr30),length(yr_test));
for col = 1:length(yr_test)
   for row = 1:length(yr30)
     xw2_yr(row,col) = 1 - (yr_diff(row,col)/max(yr_diff(:,col)));
   end
end
   % convert w2_yr to matrix where each column adds up to 1.0
   for col = 1:length(yr_test)
      for row = 1:length(yr30)
         w2_yr(row,col) = xw2_yr(row,col)/(sum(xw2_yr(:,col)));
      end
   end

% Create the inverse difference squared probability weight
% w3 = 1 / diff^2
xw3_yr = zeros(length(yr30),length(yr_test));
w3_yr = zeros(length(yr30),length(yr_test));
for col = 1:length(yr_test)
   for row = 1:length(yr30)
      xw3_yr(row,col) = 1/(yr_diff(row,col)^2);
   end
end
   % convert xw3_yr to matrix where each column adds up to 1.0
   for col = 1:length(yr_test)
      for row = 1:length(yr30)
         w3_yr(row,col) = xw3_yr(row,col)/(sum(xw3_yr(:,col)));
      end
   end

%Create the inverse distance probability weight
% w4 = 1/diff
xw4_yr = zeros(length(yr30),length(yr_test));
w4_yr = zeros(length(yr30),length(yr_test));
for col = 1:length(yr_test)
   for row = 1:length(yr30)
      xw4_yr(row,col) = 1/yr_diff(row,col);
   end
```

```
end
    % convert xw4_yr to matrix where each column adds up to 1.0
   for col = 1:length(yr_test)
      for row = 1:length(yr30)
         w4_yr(row,col) = xw4_yr(row,col)/(sum(xw4_yr(:,col)));
      end
   end

w_yr = [w1_yr; w2_yr; w3_yr; w4_yr];

aaa = [w_djf w_jfm w_fma w_yr];
[dim1 dim2] = size(aaa);
w_0675 = reshape(aaa,dim1,dim2/4,4);

save w_0675 w_0675
```

A1.5.2 Forecast Creation

```
%THIS CODE CALCUALTES FORECAST VALUES FOR 1906 - 1975 USING THE WEIGHTED
%RESAMPLING (1,000 TIMES) AND THEN FINDS THE MEAN OF EACH RESAMPLE, THEN
%THE MEAN OF ALL RESAMPLING TO OBTAIN THE FORECAST VALUE.
% RUN TIME: 105 minutes

%-------------------------------------
%Read in the weights
%-------------------------------------
load w_0675
djf_wall = w_0675(:,:,1);
jfm_wall = w_0675(:,:,2);
fma_wall = w_0675(:,:,3);

% From this dataset, the lagged relationships can be defined by using the
% following columns from the *_wall matrices created above:
  %0-year lag: 6:75 (1906 - 1975)
  %1-year lag: 5:74 (1905 - 1974)
  %2-year lag: 4:73 (1904 - 1973)
%Total forecasts created at each location = 70

%-------------------------------------
%  Read in the observed data
%-------------------------------------
%qoyr_all = xlsread('L:/Kenneth Data/Matlab/Phase2/Hondo.xls','qobs-y','B2:AD103');
load qoyr_all
```

```
%Create matrices of observed values.  Use the following to know which
%observed values to be used:
%Resampling Data: Rows 71:100 for qoyr_all (1976 - 2005)
%Observation Data: Rows 1:70 (qoaj_all and qoyr_all) 1906 - 1975

%Observed Data Matrix
qo = qoyr_all(1:70,:);

%Resampling Data Matrix
qoy = qoyr_all(71:100,:);

%Create matrix of forecasts using just the 30-yr average
f30 = mean(qoy);

%--------------------------------------
%  Run Analysis on DJF | Lag = 0 Year
%--------------------------------------

djf_0_w1 = djf_wall(1:30,6:75);
djf_0_w2 = djf_wall(31:60,6:75);
djf_0_w3 = djf_wall(61:90,6:75);
djf_0_w4 = djf_wall(91:120,6:75);

%Create matrix of forecast values
djf_0_qfall1 = zeros(29,70,1000);
djf_0_qfall2 = zeros(29,70,1000);
djf_0_qfall3 = zeros(29,70,1000);
djf_0_qfall4 = zeros(29,70,1000);
for loc = 1:29
for yr = 1:70
   for l = 1:1000
      djf_0_qfall1(loc,yr,l) =
mean(randsample(qoy(:,loc),length(djf_0_w1),true,djf_0_w1(:,yr)));
      djf_0_qfall2(loc,yr,l) =
mean(randsample(qoy(:,loc),length(djf_0_w2),true,djf_0_w2(:,yr)));
      djf_0_qfall3(loc,yr,l) =
mean(randsample(qoy(:,loc),length(djf_0_w3),true,djf_0_w3(:,yr)));
      djf_0_qfall4(loc,yr,l) =
mean(randsample(qoy(:,loc),length(djf_0_w4),true,djf_0_w4(:,yr)));
   end
end
end

djf_0_qf1 = transpose(mean(djf_0_qfall1,3));
djf_0_qf2 = transpose(mean(djf_0_qfall2,3));
```

```
djf_0_qf3 = transpose(mean(djf_0_qfall3,3));
djf_0_qf4 = transpose(mean(djf_0_qfall4,3));

%-------------------------------------
%  Run Analysis on DJF | Lag = 1 Year
%-------------------------------------

djf_1_w1 = djf_wall(1:30,5:74);
djf_1_w2 = djf_wall(31:60,5:74);
djf_1_w3 = djf_wall(61:90,5:74);
djf_1_w4 = djf_wall(91:120,5:74);

%Create matrix of forecast values
djf_1_qfall1 = zeros(29,70,1000);
djf_1_qfall2 = zeros(29,70,1000);
djf_1_qfall3 = zeros(29,70,1000);
djf_1_qfall4 = zeros(29,70,1000);
for loc = 1:29
for yr = 1:70
   for l = 1:1000
      djf_1_qfall1(loc,yr,l) =
mean(randsample(qoy(:,loc),length(djf_1_w1),true,djf_1_w1(:,yr)));
      djf_1_qfall2(loc,yr,l) =
mean(randsample(qoy(:,loc),length(djf_1_w2),true,djf_1_w2(:,yr)));
      djf_1_qfall3(loc,yr,l) =
mean(randsample(qoy(:,loc),length(djf_1_w3),true,djf_1_w3(:,yr)));
      djf_1_qfall4(loc,yr,l) =
mean(randsample(qoy(:,loc),length(djf_1_w4),true,djf_1_w4(:,yr)));
   end
end
end

djf_1_qf1 = transpose(mean(djf_1_qfall1,3));
djf_1_qf2 = transpose(mean(djf_1_qfall2,3));
djf_1_qf3 = transpose(mean(djf_1_qfall3,3));
djf_1_qf4 = transpose(mean(djf_1_qfall4,3));


%-------------------------------------
%  Run Analysis on DJF | Lag = 2 Year
%-------------------------------------

djf_2_w1 = djf_wall(1:30,4:73);
djf_2_w2 = djf_wall(31:60,4:73);
djf_2_w3 = djf_wall(61:90,4:73);
djf_2_w4 = djf_wall(91:120,4:73);
```

```
%Create matrix of forecast values
djf_2_qfall1 = zeros(29,70,1000);
djf_2_qfall2 = zeros(29,70,1000);
djf_2_qfall3 = zeros(29,70,1000);
djf_2_qfall4 = zeros(29,70,1000);
for loc = 1:29
for yr = 1:70
   for l = 1:1000
      djf_2_qfall1(loc,yr,l) =
mean(randsample(qoy(:,loc),length(djf_2_w1),true,djf_2_w1(:,yr)));
      djf_2_qfall2(loc,yr,l) =
mean(randsample(qoy(:,loc),length(djf_2_w2),true,djf_2_w2(:,yr)));
      djf_2_qfall3(loc,yr,l) =
mean(randsample(qoy(:,loc),length(djf_2_w3),true,djf_2_w3(:,yr)));
      djf_2_qfall4(loc,yr,l) =
mean(randsample(qoy(:,loc),length(djf_2_w4),true,djf_2_w4(:,yr)));
   end
end
end

djf_2_qf1 = transpose(mean(djf_2_qfall1,3));
djf_2_qf2 = transpose(mean(djf_2_qfall2,3));
djf_2_qf3 = transpose(mean(djf_2_qfall3,3));
djf_2_qf4 = transpose(mean(djf_2_qfall4,3));

%--------------------------------------
%  Run Analysis on JFM | Lag = 0 Year
%--------------------------------------

jfm_0_w1 = jfm_wall(1:30,6:75);
jfm_0_w2 = jfm_wall(31:60,6:75);
jfm_0_w3 = jfm_wall(61:90,6:75);
jfm_0_w4 = jfm_wall(91:120,6:75);

%Create matrix of forecast values
jfm_0_qfall1 = zeros(29,70,1000);
jfm_0_qfall2 = zeros(29,70,1000);
jfm_0_qfall3 = zeros(29,70,1000);
jfm_0_qfall4 = zeros(29,70,1000);
for loc = 1:29
for yr = 1:70
   for l = 1:1000
      jfm_0_qfall1(loc,yr,l) =
mean(randsample(qoy(:,loc),length(jfm_0_w1),true,jfm_0_w1(:,yr)));
```

```
      jfm_0_qfall2(loc,yr,l) =
mean(randsample(qoy(:,loc),length(jfm_0_w2),true,jfm_0_w2(:,yr)));
      jfm_0_qfall3(loc,yr,l) =
mean(randsample(qoy(:,loc),length(jfm_0_w3),true,jfm_0_w3(:,yr)));
      jfm_0_qfall4(loc,yr,l) =
mean(randsample(qoy(:,loc),length(jfm_0_w4),true,jfm_0_w4(:,yr)));
   end
end
end

jfm_0_qf1 = transpose(mean(jfm_0_qfall1,3));
jfm_0_qf2 = transpose(mean(jfm_0_qfall2,3));
jfm_0_qf3 = transpose(mean(jfm_0_qfall3,3));
jfm_0_qf4 = transpose(mean(jfm_0_qfall4,3));

%--------------------------------------
%  Run Analysis on JFM | Lag = 1 Year
%--------------------------------------

jfm_1_w1 = jfm_wall(1:30,5:74);
jfm_1_w2 = jfm_wall(31:60,5:74);
jfm_1_w3 = jfm_wall(61:90,5:74);
jfm_1_w4 = jfm_wall(91:120,5:74);

%Create matrix of forecast values
jfm_1_qfall1 = zeros(29,70,1000);
jfm_1_qfall2 = zeros(29,70,1000);
jfm_1_qfall3 = zeros(29,70,1000);
jfm_1_qfall4 = zeros(29,70,1000);
for loc = 1:29
for yr = 1:70
   for l = 1:1000
      jfm_1_qfall1(loc,yr,l) =
mean(randsample(qoy(:,loc),length(jfm_1_w1),true,jfm_1_w1(:,yr)));
      jfm_1_qfall2(loc,yr,l) =
mean(randsample(qoy(:,loc),length(jfm_1_w2),true,jfm_1_w2(:,yr)));
      jfm_1_qfall3(loc,yr,l) =
mean(randsample(qoy(:,loc),length(jfm_1_w3),true,jfm_1_w3(:,yr)));
      jfm_1_qfall4(loc,yr,l) =
mean(randsample(qoy(:,loc),length(jfm_1_w4),true,jfm_1_w4(:,yr)));
   end
end
end

jfm_1_qf1 = transpose(mean(jfm_1_qfall1,3));
jfm_1_qf2 = transpose(mean(jfm_1_qfall2,3));
```

```
jfm_1_qf3 = transpose(mean(jfm_1_qfall3,3));
jfm_1_qf4 = transpose(mean(jfm_1_qfall4,3));

%-------------------------------------
%  Run Analysis on JFM | Lag = 2 Year
%-------------------------------------

jfm_2_w1 = jfm_wall(1:30,4:73);
jfm_2_w2 = jfm_wall(31:60,4:73);
jfm_2_w3 = jfm_wall(61:90,4:73);
jfm_2_w4 = jfm_wall(91:120,4:73);

%Create matrix of forecast values
jfm_2_qfall1 = zeros(29,70,1000);
jfm_2_qfall2 = zeros(29,70,1000);
jfm_2_qfall3 = zeros(29,70,1000);
jfm_2_qfall4 = zeros(29,70,1000);
for loc = 1:29
for yr = 1:70
   for l = 1:1000
      jfm_2_qfall1(loc,yr,l) =
mean(randsample(qoy(:,loc),length(jfm_2_w1),true,jfm_2_w1(:,yr)));
      jfm_2_qfall2(loc,yr,l) =
mean(randsample(qoy(:,loc),length(jfm_2_w2),true,jfm_2_w2(:,yr)));
      jfm_2_qfall3(loc,yr,l) =
mean(randsample(qoy(:,loc),length(jfm_2_w3),true,jfm_2_w3(:,yr)));
      jfm_2_qfall4(loc,yr,l) =
mean(randsample(qoy(:,loc),length(jfm_2_w4),true,jfm_2_w4(:,yr)));
   end
end
end

jfm_2_qf1 = transpose(mean(jfm_2_qfall1,3));
jfm_2_qf2 = transpose(mean(jfm_2_qfall2,3));
jfm_2_qf3 = transpose(mean(jfm_2_qfall3,3));
jfm_2_qf4 = transpose(mean(jfm_2_qfall4,3));


%-------------------------------------
%  Run Analysis on FMA | Lag = 0 Year
%-------------------------------------

fma_0_w1 = fma_wall(1:30,6:75);
fma_0_w2 = fma_wall(31:60,6:75);
fma_0_w3 = fma_wall(61:90,6:75);
fma_0_w4 = fma_wall(91:120,6:75);
```

```
%Create matrix of forecast values
fma_0_qfall1 = zeros(29,70,1000);
fma_0_qfall2 = zeros(29,70,1000);
fma_0_qfall3 = zeros(29,70,1000);
fma_0_qfall4 = zeros(29,70,1000);
for loc = 1:29
for yr = 1:70
   for l = 1:1000
      fma_0_qfall1(loc,yr,l) =
mean(randsample(qoy(:,loc),length(fma_0_w1),true,fma_0_w1(:,yr)));
      fma_0_qfall2(loc,yr,l) =
mean(randsample(qoy(:,loc),length(fma_0_w2),true,fma_0_w2(:,yr)));
      fma_0_qfall3(loc,yr,l) =
mean(randsample(qoy(:,loc),length(fma_0_w3),true,fma_0_w3(:,yr)));
      fma_0_qfall4(loc,yr,l) =
mean(randsample(qoy(:,loc),length(fma_0_w4),true,fma_0_w4(:,yr)));
   end
end
end

fma_0_qf1 = transpose(mean(fma_0_qfall1,3));
fma_0_qf2 = transpose(mean(fma_0_qfall2,3));
fma_0_qf3 = transpose(mean(fma_0_qfall3,3));
fma_0_qf4 = transpose(mean(fma_0_qfall4,3));

%--------------------------------------
%  Forecasts FMA | Lag = 1 Year
%--------------------------------------

fma_1_w1 = fma_wall(1:30,5:74);
fma_1_w2 = fma_wall(31:60,5:74);
fma_1_w3 = fma_wall(61:90,5:74);
fma_1_w4 = fma_wall(91:120,5:74);

%Create matrix of forecast values
fma_1_qfall1 = zeros(29,70,1000);
fma_1_qfall2 = zeros(29,70,1000);
fma_1_qfall3 = zeros(29,70,1000);
fma_1_qfall4 = zeros(29,70,1000);
for loc = 1:29
for yr = 1:70
   for l = 1:1000
      fma_1_qfall1(loc,yr,l) =
mean(randsample(qoy(:,loc),length(fma_1_w1),true,fma_1_w1(:,yr)));
```

```
      fma_1_qfall2(loc,yr,l) =
mean(randsample(qoy(:,loc),length(fma_1_w2),true,fma_1_w2(:,yr)));
      fma_1_qfall3(loc,yr,l) =
mean(randsample(qoy(:,loc),length(fma_1_w3),true,fma_1_w3(:,yr)));
      fma_1_qfall4(loc,yr,l) =
mean(randsample(qoy(:,loc),length(fma_1_w4),true,fma_1_w4(:,yr)));
   end
end
end

fma_1_qf1 = transpose(mean(fma_1_qfall1,3));
fma_1_qf2 = transpose(mean(fma_1_qfall2,3));
fma_1_qf3 = transpose(mean(fma_1_qfall3,3));
fma_1_qf4 = transpose(mean(fma_1_qfall4,3));

%-------------------------------------
%  Forecasts FMA | Lag = 2 Year
%-------------------------------------

fma_2_w1 = fma_wall(1:30,4:73);
fma_2_w2 = fma_wall(31:60,4:73);
fma_2_w3 = fma_wall(61:90,4:73);
fma_2_w4 = fma_wall(91:120,4:73);

%Create matrix of forecast values
fma_2_qfall1 = zeros(29,70,1000);
fma_2_qfall2 = zeros(29,70,1000);
fma_2_qfall3 = zeros(29,70,1000);
fma_2_qfall4 = zeros(29,70,1000);
for loc = 1:29
for yr = 1:70
   for l = 1:1000
      fma_2_qfall1(loc,yr,l) =
mean(randsample(qoy(:,loc),length(fma_2_w1),true,fma_2_w1(:,yr)));
      fma_2_qfall2(loc,yr,l) =
mean(randsample(qoy(:,loc),length(fma_2_w2),true,fma_2_w2(:,yr)));
      fma_2_qfall3(loc,yr,l) =
mean(randsample(qoy(:,loc),length(fma_2_w3),true,fma_2_w3(:,yr)));
      fma_2_qfall4(loc,yr,l) =
mean(randsample(qoy(:,loc),length(fma_2_w4),true,fma_2_w4(:,yr)));
   end
end
end

fma_2_qf1 = transpose(mean(fma_2_qfall1,3));
fma_2_qf2 = transpose(mean(fma_2_qfall2,3));
```

```
fma_2_qf3 = transpose(mean(fma_2_qfall3,3));
fma_2_qf4 = transpose(mean(fma_2_qfall4,3));

%----------------------------------------
%  Collect forecast values and write to Excel
%----------------------------------------

f_djf_all = [djf_0_qf1 djf_0_qf2 djf_0_qf3 djf_0_qf4 ...
   djf_1_qf1 djf_1_qf2 djf_1_qf3 djf_1_qf4 ...
   djf_2_qf1 djf_2_qf2 djf_2_qf3 djf_2_qf4];
f_jfm_all = [jfm_0_qf1 jfm_0_qf2 jfm_0_qf3 jfm_0_qf4 ...
   jfm_1_qf1 jfm_1_qf2 jfm_1_qf3 jfm_1_qf4 ...
   jfm_2_qf1 jfm_2_qf2 jfm_2_qf3 jfm_2_qf4];
f_fma_all = [fma_0_qf1 fma_0_qf2 fma_0_qf3 fma_0_qf4 ...
   fma_1_qf1 fma_1_qf2 fma_1_qf3 fma_1_qf4 ...
   fma_2_qf1 fma_2_qf2 fma_2_qf3 fma_2_qf4];

%xlswrite('L:/Kenneth Data/Matlab/Phase2/Hondo_f.xls',f_djf_all', 'f_djf','C2');
%xlswrite('L:/Kenneth Data/Matlab/Phase2/Hondo_f.xls',f_jfm_all', 'f_jfm','C2');
%xlswrite('L:/Kenneth Data/Matlab/Phase2/Hondo_f.xls',f_fma_all', 'f_fma','C2');

%aaa = [f_djf_all f_jfm_all f_fma_all];
%[dim1 dim2] = size(aaa);
%f_0675 = reshape(aaa,dim1,dim2/3,3);

%save f_0675 f_0675
```

A1.5.3 LEPS Calculation

```
%Read in the observed data
load qoyr_all
%Create matrices of observed values.  Use the following to know which
%observed values to be used:
%Resampling Data: Rows 71:100 for both qoaj_all and qoyr_all (1976 - 2005)
%Observation Data: Rows 1:70 (qoaj_all and qoyr_all) 1906 - 1975

%Observed Data Matrix
qoyr = qoyr_all(1:70,:);

%Resampling Data Matrix
qoy = qoyr_all(71:100,:);

%Read in Forecast values created with the forecasts.m command
load f_0675
djf_fall = f_0675(:,:,1);
jfm_fall = f_0675(:,:,2);
```

```
fma_fall = f_0675(:,:,3);

%-------------------------------------------
% Calculate for Lag = 0 Year
%-------------------------------------------

%Create zero matrices
yoy = zeros(70,29);
djf_0_yf1 = zeros(70,29);
djf_0_yf2 = zeros(70,29);
djf_0_yf3 = zeros(70,29);
djf_0_yf4 = zeros(70,29);
djf_0_leps1 = zeros(70,29);
djf_0_leps2 = zeros(70,29);
djf_0_leps3 = zeros(70,29);
djf_0_leps4 = zeros(70,29);
djf_0_lepsmax1 = zeros(70,29);
djf_0_lepsmax2 = zeros(70,29);
djf_0_lepsmax3 = zeros(70,29);
djf_0_lepsmax4 = zeros(70,29);
lepsmin = zeros(70,29);
djf_0_sk1 = zeros(29,1);
djf_0_sk2 = zeros(29,1);
djf_0_sk3 = zeros(29,1);
djf_0_sk4 = zeros(29,1);

%Divide out the forecast values into each alternative for this lag time
djf_0_qf1 = djf_fall(:,1:29);
djf_0_qf2 = djf_fall(:,30:58);
djf_0_qf3 = djf_fall(:,59:87);
djf_0_qf4 = djf_fall(:,88:116);

%Find the Probabilities to define the y-axis of the eCDF.  Create seperate
%eCDF function for the Apr-Jul observations and the Yearly observations.
P = transpose((1:size(qoyr,1))/(size(qoyr,1)+1));

%Find the probabilities of the observed (yo) and forecasted (yf) values
%on the PDF by interpolating along the qopdf data.
for loc = 1:29
for yr = 1:70
   yoy(yr,loc) = interp1(sort(qoyr(:,loc)),P,qoyr(yr,loc),'linear','extrap' );

   djf_0_yf1(yr,loc) = interp1(sort(qoyr(:,loc)),P,djf_0_qf1(yr,loc),'linear','extrap' );
   djf_0_yf2(yr,loc) = interp1(sort(qoyr(:,loc)),P,djf_0_qf2(yr,loc),'linear','extrap' );
   djf_0_yf3(yr,loc) = interp1(sort(qoyr(:,loc)),P,djf_0_qf3(yr,loc),'linear','extrap' );
   djf_0_yf4(yr,loc) = interp1(sort(qoyr(:,loc)),P,djf_0_qf4(yr,loc),'linear','extrap' );
```

```
end
end

% Calculate the min LEPS Scores possible from the April-July and Yearly
% volumes
for loc = 1:29
for yr = 1:70
   if yoy(yr,loc)>=0.5
   lepsmin(yr,loc) = (3*(1-abs(0 - yoy(yr,loc)) + yoy(yr,loc)^2 - yoy(yr,loc)) - 1);
   else
   lepsmin(yr,loc) = (3*(1-abs(1 - yoy(yr,loc)) + yoy(yr,loc)^2 - yoy(yr,loc)) - 1);
   end
end
end

%Calculate the max possible LEPS scores
for loc = 1:29
for yr = 1:70
   djf_0_lepsmax1(yr,loc) = (3*(1-abs(djf_0_yf1(yr,loc) - djf_0_yf1(yr,loc))...
      + djf_0_yf1(yr,loc)^2 - djf_0_yf1(yr,loc) + djf_0_yf1(yr,loc)^2 - djf_0_yf1(yr,loc))
- 1);
   djf_0_lepsmax2(yr,loc) = (3*(1-abs(djf_0_yf2(yr,loc) - djf_0_yf2(yr,loc))...
      + djf_0_yf2(yr,loc)^2 - djf_0_yf2(yr,loc) + djf_0_yf2(yr,loc)^2 - djf_0_yf2(yr,loc))
- 1);
   djf_0_lepsmax3(yr,loc) = (3*(1-abs(djf_0_yf3(yr,loc) - djf_0_yf3(yr,loc))...
      + djf_0_yf3(yr,loc)^2 - djf_0_yf3(yr,loc) + djf_0_yf3(yr,loc)^2 - djf_0_yf3(yr,loc))
- 1);
   djf_0_lepsmax4(yr,loc) = (3*(1-abs(djf_0_yf4(yr,loc) - djf_0_yf4(yr,loc))...
      + djf_0_yf4(yr,loc)^2 - djf_0_yf4(yr,loc) + djf_0_yf4(yr,loc)^2 - djf_0_yf4(yr,loc))
- 1);
end
end

%Calculate the LEPS scores from the yfx and the yo matrices
for loc = 1:29
for yr = 1:70
   djf_0_leps1(yr,loc) = (3*(1-abs(djf_0_yf1(yr,loc) - yoy(yr,loc))...
      + djf_0_yf1(yr,loc)^2 - djf_0_yf1(yr,loc) + yoy(yr,loc)^2 - yoy(yr,loc)) - 1);
   djf_0_leps2(yr,loc) = (3*(1-abs(djf_0_yf2(yr,loc) - yoy(yr,loc))...
      + djf_0_yf2(yr,loc)^2 - djf_0_yf2(yr,loc) + yoy(yr,loc)^2 - yoy(yr,loc)) - 1);
   djf_0_leps3(yr,loc) = (3*(1-abs(djf_0_yf3(yr,loc) - yoy(yr,loc))...
      + djf_0_yf3(yr,loc)^2 - djf_0_yf3(yr,loc) + yoy(yr,loc)^2 - yoy(yr,loc)) - 1);
   djf_0_leps4(yr,loc) = (3*(1-abs(djf_0_yf4(yr,loc) - yoy(yr,loc))...
      + djf_0_yf4(yr,loc)^2 - djf_0_yf4(yr,loc) + yoy(yr,loc)^2 - yoy(yr,loc)) - 1);
end
end
```

```
%Calculate the Average Skill score at each location
for loc = 1:29
   if sum(djf_0_leps1(:,loc))>=0
      djf_0_sk1(loc) = sum(djf_0_leps1(:,loc))/sum(djf_0_lepsmax1(:,loc));
   else
      djf_0_sk1(loc) = sum(djf_0_leps1(:,loc))/sum(lepsmin(:,loc));
   end
   if sum(djf_0_leps2(:,loc))>=0
      djf_0_sk2(loc) = sum(djf_0_leps2(:,loc))/sum(djf_0_lepsmax2(:,loc));
   else
      djf_0_sk2(loc) = sum(djf_0_leps2(:,loc))/sum(lepsmin(:,loc));
   end
   if sum(djf_0_leps3(:,loc))>=0
      djf_0_sk3(loc) = sum(djf_0_leps3(:,loc))/sum(djf_0_lepsmax3(:,loc));
   else
      djf_0_sk3(loc) = sum(djf_0_leps3(:,loc))/sum(lepsmin(:,loc));
   end
   if sum(djf_0_leps4(:,loc))>=0
      djf_0_sk4(loc) = sum(djf_0_leps4(:,loc))/sum(djf_0_lepsmax4(:,loc));
   else
      djf_0_sk4(loc) = sum(djf_0_leps4(:,loc))/sum(lepsmin(:,loc));
   end
end

djf_0_sk = 100*[djf_0_sk1 djf_0_sk2 djf_0_sk3 djf_0_sk4];

%-------------------------------------------
% Recalculate for Lag = 1Year
%-------------------------------------------

%Divide weight data into each weight for the lag 1 alternative
djf_1_yf1 = zeros(70,29);
djf_1_yf2 = zeros(70,29);
djf_1_yf3 = zeros(70,29);
djf_1_yf4 = zeros(70,29);
djf_1_leps1 = zeros(70,29);
djf_1_leps2 = zeros(70,29);
djf_1_leps3 = zeros(70,29);
djf_1_leps4 = zeros(70,29);
djf_1_lepsmax1 = zeros(70,29);
djf_1_lepsmax2 = zeros(70,29);
djf_1_lepsmax3 = zeros(70,29);
djf_1_lepsmax4 = zeros(70,29);
djf_1_sk1 = zeros(29,1);
djf_1_sk2 = zeros(29,1);
```

```
djf_1_sk3 = zeros(29,1);
djf_1_sk4 = zeros(29,1);

%Divide out the forecast values into each alternative for this lag time
djf_1_qf1 = djf_fall(:,117:145);
djf_1_qf2 = djf_fall(:,146:174);
djf_1_qf3 = djf_fall(:,175:203);
djf_1_qf4 = djf_fall(:,204:232);

%Find the Probabilities to define the y-axis of the eCDF.  Create seperate
%eCDF function for the Apr-Jul observations and the Yearly observations.
P = transpose((1:size(qoyr,1))/(size(qoyr,1)+1));

%Find the probabilities of the observed (yo) and forecasted (yf) values
%on the PDF by interpolating along the qopdf data.
for loc = 1:29
for yr = 1:70
   yoy(yr,loc) = interp1(sort(qoyr(:,loc)),P,qoyr(yr,loc),'linear','extrap' );

   djf_1_yf1(yr,loc) = interp1(sort(qoyr(:,loc)),P,djf_1_qf1(yr,loc),'linear','extrap' );
   djf_1_yf2(yr,loc) = interp1(sort(qoyr(:,loc)),P,djf_1_qf2(yr,loc),'linear','extrap' );
   djf_1_yf3(yr,loc) = interp1(sort(qoyr(:,loc)),P,djf_1_qf3(yr,loc),'linear','extrap' );
   djf_1_yf4(yr,loc) = interp1(sort(qoyr(:,loc)),P,djf_1_qf4(yr,loc),'linear','extrap' );
end
end

%Calculate the max possible LEPS scores
for loc = 1:29
for yr = 1:70
   djf_1_lepsmax1(yr,loc) = (3*(1-abs(djf_1_yf1(yr,loc) - djf_1_yf1(yr,loc))...
      + djf_1_yf1(yr,loc)^2 - djf_1_yf1(yr,loc) + djf_1_yf1(yr,loc)^2 - djf_1_yf1(yr,loc))
- 1);
   djf_1_lepsmax2(yr,loc) = (3*(1-abs(djf_1_yf2(yr,loc) - djf_1_yf2(yr,loc))...
      + djf_1_yf2(yr,loc)^2 - djf_1_yf2(yr,loc) + djf_1_yf2(yr,loc)^2 - djf_1_yf2(yr,loc))
- 1);
   djf_1_lepsmax3(yr,loc) = (3*(1-abs(djf_1_yf3(yr,loc) - djf_1_yf3(yr,loc))...
      + djf_1_yf3(yr,loc)^2 - djf_1_yf3(yr,loc) + djf_1_yf3(yr,loc)^2 - djf_1_yf3(yr,loc))
- 1);
   djf_1_lepsmax4(yr,loc) = (3*(1-abs(djf_1_yf4(yr,loc) - djf_1_yf4(yr,loc))...
      + djf_1_yf4(yr,loc)^2 - djf_1_yf4(yr,loc) + djf_1_yf4(yr,loc)^2 - djf_1_yf4(yr,loc))
- 1);
end
end

%Calculate the LEPS scores from the yfx and the yo matrices
for loc = 1:29
```

```
for yr = 1:70
   djf_1_leps1(yr,loc) = (3*(1-abs(djf_1_yf1(yr,loc) - yoy(yr,loc))...
      + djf_1_yf1(yr,loc)^2 - djf_1_yf1(yr,loc) + yoy(yr,loc)^2 - yoy(yr,loc)) - 1);
   djf_1_leps2(yr,loc) = (3*(1-abs(djf_1_yf2(yr,loc) - yoy(yr,loc))...
      + djf_1_yf2(yr,loc)^2 - djf_1_yf2(yr,loc) + yoy(yr,loc)^2 - yoy(yr,loc)) - 1);
   djf_1_leps3(yr,loc) = (3*(1-abs(djf_1_yf3(yr,loc) - yoy(yr,loc))...
      + djf_1_yf3(yr,loc)^2 - djf_1_yf3(yr,loc) + yoy(yr,loc)^2 - yoy(yr,loc)) - 1);
   djf_1_leps4(yr,loc) = (3*(1-abs(djf_1_yf4(yr,loc) - yoy(yr,loc))...
      + djf_1_yf4(yr,loc)^2 - djf_1_yf4(yr,loc) + yoy(yr,loc)^2 - yoy(yr,loc)) - 1);
end
end

%Calculate the Average Skill score at each location
for loc = 1:29
   if sum(djf_1_leps1(:,loc))>=0
      djf_1_sk1(loc) = sum(djf_1_leps1(:,loc))/sum(djf_1_lepsmax1(:,loc));
   else
      djf_1_sk1(loc) = sum(djf_1_leps1(:,loc))/sum(lepsmin(:,loc));
   end
   if sum(djf_1_leps2(:,loc))>=0
      djf_1_sk2(loc) = sum(djf_1_leps2(:,loc))/sum(djf_1_lepsmax2(:,loc));
   else
      djf_1_sk2(loc) = sum(djf_1_leps2(:,loc))/sum(lepsmin(:,loc));
   end
   if sum(djf_1_leps3(:,loc))>=0
      djf_1_sk3(loc) = sum(djf_1_leps3(:,loc))/sum(djf_1_lepsmax3(:,loc));
   else
      djf_1_sk3(loc) = sum(djf_1_leps3(:,loc))/sum(lepsmin(:,loc));
   end
   if sum(djf_1_leps4(:,loc))>=0
      djf_1_sk4(loc) = sum(djf_1_leps4(:,loc))/sum(djf_1_lepsmax4(:,loc));
   else
      djf_1_sk4(loc) = sum(djf_1_leps4(:,loc))/sum(lepsmin(:,loc));
   end
end

djf_1_sk = 100*[djf_1_sk1 djf_1_sk2 djf_1_sk3 djf_1_sk4];

%-------------------------------------------
% Recalculate for Lag = 2 Years
%-------------------------------------------

djf_2_yf1 = zeros(70,29);
djf_2_yf2 = zeros(70,29);
djf_2_yf3 = zeros(70,29);
djf_2_yf4 = zeros(70,29);
```

```
djf_2_leps1 = zeros(70,29);
djf_2_leps2 = zeros(70,29);
djf_2_leps3 = zeros(70,29);
djf_2_leps4 = zeros(70,29);
djf_2_lepsmax1 = zeros(70,29);
djf_2_lepsmax2 = zeros(70,29);
djf_2_lepsmax3 = zeros(70,29);
djf_2_lepsmax4 = zeros(70,29);
djf_2_sk1 = zeros(29,1);
djf_2_sk2 = zeros(29,1);
djf_2_sk3 = zeros(29,1);
djf_2_sk4 = zeros(29,1);

%Divide out the forecast values into each alternative for this lag time
djf_2_qf1 = djf_fall(:,233:261);
djf_2_qf2 = djf_fall(:,262:290);
djf_2_qf3 = djf_fall(:,291:319);
djf_2_qf4 = djf_fall(:,320:348);

%Find the Probabilities to define the y-axis of the eCDF.  Create seperate
%eCDF function for the Apr-Jul observations and the Yearly observations.
P = transpose((1:size(qoyr,1))/(size(qoyr,1)+1));

%Find the probabilities of the observed (yo) and forecasted (yf) values
%on the PDF by interpolating along the qopdf data.
for loc = 1:29
for yr = 1:70
   yoy(yr,loc) = interp1(sort(qoyr(:,loc)),P,qoyr(yr,loc),'linear','extrap' );

   djf_2_yf1(yr,loc) = interp1(sort(qoyr(:,loc)),P,djf_2_qf1(yr,loc),'linear','extrap' );
   djf_2_yf2(yr,loc) = interp1(sort(qoyr(:,loc)),P,djf_2_qf2(yr,loc),'linear','extrap' );
   djf_2_yf3(yr,loc) = interp1(sort(qoyr(:,loc)),P,djf_2_qf3(yr,loc),'linear','extrap' );
   djf_2_yf4(yr,loc) = interp1(sort(qoyr(:,loc)),P,djf_2_qf4(yr,loc),'linear','extrap' );
end
end

%Calculate the max possible LEPS scores
for loc = 1:29
for yr = 1:70
   djf_2_lepsmax1(yr,loc) = (3*(1-abs(djf_2_yf1(yr,loc) - djf_2_yf1(yr,loc))...
      + djf_2_yf1(yr,loc)^2 - djf_2_yf1(yr,loc) + djf_2_yf1(yr,loc)^2 - djf_2_yf1(yr,loc))
- 1);
   djf_2_lepsmax2(yr,loc) = (3*(1-abs(djf_2_yf2(yr,loc) - djf_2_yf2(yr,loc))...
      + djf_2_yf2(yr,loc)^2 - djf_2_yf2(yr,loc) + djf_2_yf2(yr,loc)^2 - djf_2_yf2(yr,loc))
- 1);
   djf_2_lepsmax3(yr,loc) = (3*(1-abs(djf_2_yf3(yr,loc) - djf_2_yf3(yr,loc))...
```

```
      + djf_2_yf3(yr,loc)^2 - djf_2_yf3(yr,loc) + djf_2_yf3(yr,loc)^2 - djf_2_yf3(yr,loc))
- 1);
   djf_2_lepsmax4(yr,loc) = (3*(1-abs(djf_2_yf4(yr,loc) - djf_2_yf4(yr,loc))...
      + djf_2_yf4(yr,loc)^2 - djf_2_yf4(yr,loc) + djf_2_yf4(yr,loc)^2 - djf_2_yf4(yr,loc))
- 1);
end
end

%Calculate the LEPS scores from the yfx and the yo matrices
for loc = 1:29
for yr = 1:70
   djf_2_leps1(yr,loc) = (3*(1-abs(djf_2_yf1(yr,loc) - yoy(yr,loc))...
      + djf_2_yf1(yr,loc)^2 - djf_2_yf1(yr,loc) + yoy(yr,loc)^2 - yoy(yr,loc)) - 1);
   djf_2_leps2(yr,loc) = (3*(1-abs(djf_2_yf2(yr,loc) - yoy(yr,loc))...
      + djf_2_yf2(yr,loc)^2 - djf_2_yf2(yr,loc) + yoy(yr,loc)^2 - yoy(yr,loc)) - 1);
   djf_2_leps3(yr,loc) = (3*(1-abs(djf_2_yf3(yr,loc) - yoy(yr,loc))...
      + djf_2_yf3(yr,loc)^2 - djf_2_yf3(yr,loc) + yoy(yr,loc)^2 - yoy(yr,loc)) - 1);
   djf_2_leps4(yr,loc) = (3*(1-abs(djf_2_yf4(yr,loc) - yoy(yr,loc))...
      + djf_2_yf4(yr,loc)^2 - djf_2_yf4(yr,loc) + yoy(yr,loc)^2 - yoy(yr,loc)) - 1);
end
end

%Calculate the Average Skill score at each location
for loc = 1:29
   if sum(djf_2_leps1(:,loc))>=0
      djf_2_sk1(loc) = sum(djf_2_leps1(:,loc))/sum(djf_2_lepsmax1(:,loc));
   else
      djf_2_sk1(loc) = sum(djf_2_leps1(:,loc))/sum(lepsmin(:,loc));
   end
   if sum(djf_2_leps2(:,loc))>=0
      djf_2_sk2(loc) = sum(djf_2_leps2(:,loc))/sum(djf_2_lepsmax2(:,loc));
   else
      djf_2_sk2(loc) = sum(djf_2_leps2(:,loc))/sum(lepsmin(:,loc));
   end
   if sum(djf_2_leps3(:,loc))>=0
      djf_2_sk3(loc) = sum(djf_2_leps3(:,loc))/sum(djf_2_lepsmax3(:,loc));
   else
      djf_2_sk3(loc) = sum(djf_2_leps3(:,loc))/sum(lepsmin(:,loc));
   end
   if sum(djf_2_leps4(:,loc))>=0
      djf_2_sk4(loc) = sum(djf_2_leps4(:,loc))/sum(djf_2_lepsmax4(:,loc));
   else
      djf_2_sk4(loc) = sum(djf_2_leps4(:,loc))/sum(lepsmin(:,loc));
   end
end
```

```
djf_2_sk = 100*[djf_2_sk1 djf_2_sk2 djf_2_sk3 djf_2_sk4];
toc
%------------------------------
%Recalc for JFM | lag = 0
%------------------------------

jfm_0_yf1 = zeros(70,29);
jfm_0_yf2 = zeros(70,29);
jfm_0_yf3 = zeros(70,29);
jfm_0_yf4 = zeros(70,29);
jfm_0_leps1 = zeros(70,29);
jfm_0_leps2 = zeros(70,29);
jfm_0_leps3 = zeros(70,29);
jfm_0_leps4 = zeros(70,29);
jfm_0_lepsmax1 = zeros(70,29);
jfm_0_lepsmax2 = zeros(70,29);
jfm_0_lepsmax3 = zeros(70,29);
jfm_0_lepsmax4 = zeros(70,29);
jfm_0_sk1 = zeros(29,1);
jfm_0_sk2 = zeros(29,1);
jfm_0_sk3 = zeros(29,1);
jfm_0_sk4 = zeros(29,1);

%Divide out the forecast values into each alternative for this lag time
jfm_0_qf1 = jfm_fall(:,1:29);
jfm_0_qf2 = jfm_fall(:,30:58);
jfm_0_qf3 = jfm_fall(:,59:87);
jfm_0_qf4 = jfm_fall(:,88:116);

%Find the Probabilities to define the y-axis of the eCDF.  Create seperate
%eCDF function for the Apr-Jul observations and the Yearly observations.
P = transpose((1:size(qoyr,1))/(size(qoyr,1)+1));

%Find the probabilities of the observed (yo) and forecasted (yf) values
%on the PDF by interpolating along the qopdf data.
for loc = 1:29
for yr = 1:70
   yoy(yr,loc) = interp1(sort(qoyr(:,loc)),P,qoyr(yr,loc),'linear','extrap' );

   jfm_0_yf1(yr,loc) = interp1(sort(qoyr(:,loc)),P,jfm_0_qf1(yr,loc),'linear','extrap' );
   jfm_0_yf2(yr,loc) = interp1(sort(qoyr(:,loc)),P,jfm_0_qf2(yr,loc),'linear','extrap' );
   jfm_0_yf3(yr,loc) = interp1(sort(qoyr(:,loc)),P,jfm_0_qf3(yr,loc),'linear','extrap' );
   jfm_0_yf4(yr,loc) = interp1(sort(qoyr(:,loc)),P,jfm_0_qf4(yr,loc),'linear','extrap' );
end
end
```

```
% Calculate the min LEPS Scores possible from the April-July and Yearly
% volumes
for loc = 1:29
for yr = 1:70
if yoy(yr,loc)>=0.5
   lepsmin(yr,loc) = (3*(1-abs(0 - yoy(yr,loc)) + yoy(yr,loc)^2 - yoy(yr,loc)) - 1);
else
   lepsmin(yr,loc) = (3*(1-abs(1 - yoy(yr,loc)) + yoy(yr,loc)^2 - yoy(yr,loc)) - 1);
end
end
end

%Calculate the max possible LEPS scores
for loc = 1:29
for yr = 1:70
   jfm_0_lepsmax1(yr,loc) = (3*(1-abs(jfm_0_yf1(yr,loc) - jfm_0_yf1(yr,loc))...
      +    jfm_0_yf1(yr,loc)^2    -    jfm_0_yf1(yr,loc)    +    jfm_0_yf1(yr,loc)^2    -
jfm_0_yf1(yr,loc)) - 1);
   jfm_0_lepsmax2(yr,loc) = (3*(1-abs(jfm_0_yf2(yr,loc) - jfm_0_yf2(yr,loc))...
      +    jfm_0_yf2(yr,loc)^2    -    jfm_0_yf2(yr,loc)    +    jfm_0_yf2(yr,loc)^2    -
jfm_0_yf2(yr,loc)) - 1);
   jfm_0_lepsmax3(yr,loc) = (3*(1-abs(jfm_0_yf3(yr,loc) - jfm_0_yf3(yr,loc))...
      +    jfm_0_yf3(yr,loc)^2    -    jfm_0_yf3(yr,loc)    +    jfm_0_yf3(yr,loc)^2    -
jfm_0_yf3(yr,loc)) - 1);
   jfm_0_lepsmax4(yr,loc) = (3*(1-abs(jfm_0_yf4(yr,loc) - jfm_0_yf4(yr,loc))...
      +    jfm_0_yf4(yr,loc)^2    -    jfm_0_yf4(yr,loc)    +    jfm_0_yf4(yr,loc)^2    -
jfm_0_yf4(yr,loc)) - 1);
end
end

%Calculate the LEPS scores from the yfx and the yo matrices
for loc = 1:29
for yr = 1:70
   jfm_0_leps1(yr,loc) = (3*(1-abs(jfm_0_yf1(yr,loc) - yoy(yr,loc))...
      + jfm_0_yf1(yr,loc)^2 - jfm_0_yf1(yr,loc) + yoy(yr,loc)^2 - yoy(yr,loc)) - 1);
   jfm_0_leps2(yr,loc) = (3*(1-abs(jfm_0_yf2(yr,loc) - yoy(yr,loc))...
      + jfm_0_yf2(yr,loc)^2 - jfm_0_yf2(yr,loc) + yoy(yr,loc)^2 - yoy(yr,loc)) - 1);
   jfm_0_leps3(yr,loc) = (3*(1-abs(jfm_0_yf3(yr,loc) - yoy(yr,loc))...
      + jfm_0_yf3(yr,loc)^2 - jfm_0_yf3(yr,loc) + yoy(yr,loc)^2 - yoy(yr,loc)) - 1);
   jfm_0_leps4(yr,loc) = (3*(1-abs(jfm_0_yf4(yr,loc) - yoy(yr,loc))...
      + jfm_0_yf4(yr,loc)^2 - jfm_0_yf4(yr,loc) + yoy(yr,loc)^2 - yoy(yr,loc)) - 1);
end
end

%Calculate the Average Skill score at each location
for loc = 1:29
```

```
    if sum(jfm_0_leps1(:,loc))>=0
       jfm_0_sk1(loc) = sum(jfm_0_leps1(:,loc))/sum(jfm_0_lepsmax1(:,loc));
    else
       jfm_0_sk1(loc) = sum(jfm_0_leps1(:,loc))/sum(lepsmin(:,loc));
    end
    if sum(jfm_0_leps2(:,loc))>=0
       jfm_0_sk2(loc) = sum(jfm_0_leps2(:,loc))/sum(jfm_0_lepsmax2(:,loc));
    else
       jfm_0_sk2(loc) = sum(jfm_0_leps2(:,loc))/sum(lepsmin(:,loc));
    end
    if sum(jfm_0_leps3(:,loc))>=0
       jfm_0_sk3(loc) = sum(jfm_0_leps3(:,loc))/sum(jfm_0_lepsmax3(:,loc));
    else
       jfm_0_sk3(loc) = sum(jfm_0_leps3(:,loc))/sum(lepsmin(:,loc));
    end
    if sum(jfm_0_leps4(:,loc))>=0
       jfm_0_sk4(loc) = sum(jfm_0_leps4(:,loc))/sum(jfm_0_lepsmax4(:,loc));
    else
       jfm_0_sk4(loc) = sum(jfm_0_leps4(:,loc))/sum(lepsmin(:,loc));
    end
end

jfm_0_sk = 100*[jfm_0_sk1 jfm_0_sk2 jfm_0_sk3 jfm_0_sk4];

%-------------------------------------------
% Recalculate for JFM | Lag = 1Year
%-------------------------------------------
jfm_1_yf1 = zeros(70,29);
jfm_1_yf2 = zeros(70,29);
jfm_1_yf3 = zeros(70,29);
jfm_1_yf4 = zeros(70,29);
jfm_1_leps1 = zeros(70,29);
jfm_1_leps2 = zeros(70,29);
jfm_1_leps3 = zeros(70,29);
jfm_1_leps4 = zeros(70,29);
jfm_1_lepsmax1 = zeros(70,29);
jfm_1_lepsmax2 = zeros(70,29);
jfm_1_lepsmax3 = zeros(70,29);
jfm_1_lepsmax4 = zeros(70,29);
jfm_1_sk1 = zeros(29,1);
jfm_1_sk2 = zeros(29,1);
jfm_1_sk3 = zeros(29,1);
jfm_1_sk4 = zeros(29,1);

%Divide out the forecast values into each alternative for this lag time
jfm_1_qf1 = jfm_fall(:,117:145);
```

```
jfm_1_qf2 = jfm_fall(:,146:174);
jfm_1_qf3 = jfm_fall(:,175:203);
jfm_1_qf4 = jfm_fall(:,204:232);

%Find the Probabilities to define the y-axis of the eCDF.  Create seperate
%eCDF function for the Apr-Jul observations and the Yearly observations.
P = transpose((1:size(qoyr,1))/(size(qoyr,1)+1));

%Find the probabilities of the observed (yo) and forecasted (yf) values
%on the PDF by interpolating along the qopdf data.
for loc = 1:29
for yr = 1:70
   yoy(yr,loc) = interp1(sort(qoyr(:,loc)),P,qoyr(yr,loc),'linear','extrap' );

   jfm_1_yf1(yr,loc) = interp1(sort(qoyr(:,loc)),P,jfm_1_qf1(yr,loc),'linear','extrap' );
   jfm_1_yf2(yr,loc) = interp1(sort(qoyr(:,loc)),P,jfm_1_qf2(yr,loc),'linear','extrap' );
   jfm_1_yf3(yr,loc) = interp1(sort(qoyr(:,loc)),P,jfm_1_qf3(yr,loc),'linear','extrap' );
   jfm_1_yf4(yr,loc) = interp1(sort(qoyr(:,loc)),P,jfm_1_qf4(yr,loc),'linear','extrap' );
end
end

%Calculate the max possible LEPS scores
for loc = 1:29
for yr = 1:70
   jfm_1_lepsmax1(yr,loc) = (3*(1-abs(jfm_1_yf1(yr,loc) - jfm_1_yf1(yr,loc))...
      +    jfm_1_yf1(yr,loc)^2    -    jfm_1_yf1(yr,loc)    +    jfm_1_yf1(yr,loc)^2    -
jfm_1_yf1(yr,loc)) - 1);
   jfm_1_lepsmax2(yr,loc) = (3*(1-abs(jfm_1_yf2(yr,loc) - jfm_1_yf2(yr,loc))...
      +    jfm_1_yf2(yr,loc)^2    -    jfm_1_yf2(yr,loc)    +    jfm_1_yf2(yr,loc)^2    -
jfm_1_yf2(yr,loc)) - 1);
   jfm_1_lepsmax3(yr,loc) = (3*(1-abs(jfm_1_yf3(yr,loc) - jfm_1_yf3(yr,loc))...
      +    jfm_1_yf3(yr,loc)^2    -    jfm_1_yf3(yr,loc)    +    jfm_1_yf3(yr,loc)^2    -
jfm_1_yf3(yr,loc)) - 1);
   jfm_1_lepsmax4(yr,loc) = (3*(1-abs(jfm_1_yf4(yr,loc) - jfm_1_yf4(yr,loc))...
      +    jfm_1_yf4(yr,loc)^2    -    jfm_1_yf4(yr,loc)    +    jfm_1_yf4(yr,loc)^2    -
jfm_1_yf4(yr,loc)) - 1);
end
end

%Calculate the LEPS scores from the yfx and the yo matrices
for loc = 1:29
for yr = 1:70
   jfm_1_leps1(yr,loc) = (3*(1-abs(jfm_1_yf1(yr,loc) - yoy(yr,loc))...
      + jfm_1_yf1(yr,loc)^2 - jfm_1_yf1(yr,loc) + yoy(yr,loc)^2 - yoy(yr,loc)) - 1);
   jfm_1_leps2(yr,loc) = (3*(1-abs(jfm_1_yf2(yr,loc) - yoy(yr,loc))...
      + jfm_1_yf2(yr,loc)^2 - jfm_1_yf2(yr,loc) + yoy(yr,loc)^2 - yoy(yr,loc)) - 1);
```

```
    jfm_1_leps3(yr,loc) = (3*(1-abs(jfm_1_yf3(yr,loc) - yoy(yr,loc))...
        + jfm_1_yf3(yr,loc)^2 - jfm_1_yf3(yr,loc) + yoy(yr,loc)^2 - yoy(yr,loc)) - 1);
    jfm_1_leps4(yr,loc) = (3*(1-abs(jfm_1_yf4(yr,loc) - yoy(yr,loc))...
        + jfm_1_yf4(yr,loc)^2 - jfm_1_yf4(yr,loc) + yoy(yr,loc)^2 - yoy(yr,loc)) - 1);
end
end

%Calculate the Average Skill score at each location
for loc = 1:29
    if sum(jfm_1_leps1(:,loc))>=0
        jfm_1_sk1(loc) = sum(jfm_1_leps1(:,loc))/sum(jfm_1_lepsmax1(:,loc));
    else
        jfm_1_sk1(loc) = sum(jfm_1_leps1(:,loc))/sum(lepsmin(:,loc));
    end
    if sum(jfm_1_leps2(:,loc))>=0
        jfm_1_sk2(loc) = sum(jfm_1_leps2(:,loc))/sum(jfm_1_lepsmax2(:,loc));
    else
        jfm_1_sk2(loc) = sum(jfm_1_leps2(:,loc))/sum(lepsmin(:,loc));
    end
    if sum(jfm_1_leps3(:,loc))>=0
        jfm_1_sk3(loc) = sum(jfm_1_leps3(:,loc))/sum(jfm_1_lepsmax3(:,loc));
    else
        jfm_1_sk3(loc) = sum(jfm_1_leps3(:,loc))/sum(lepsmin(:,loc));
    end
    if sum(jfm_1_leps4(:,loc))>=0
        jfm_1_sk4(loc) = sum(jfm_1_leps4(:,loc))/sum(jfm_1_lepsmax4(:,loc));
    else
        jfm_1_sk4(loc) = sum(jfm_1_leps4(:,loc))/sum(lepsmin(:,loc));
    end
end

jfm_1_sk = 100*[jfm_1_sk1 jfm_1_sk2 jfm_1_sk3 jfm_1_sk4];

%---------------------------------------------
% Recalculate for JFM | Lag = 2 Years
%---------------------------------------------
jfm_2_yf1 = zeros(70,29);
jfm_2_yf2 = zeros(70,29);
jfm_2_yf3 = zeros(70,29);
jfm_2_yf4 = zeros(70,29);
jfm_2_leps1 = zeros(70,29);
jfm_2_leps2 = zeros(70,29);
jfm_2_leps3 = zeros(70,29);
jfm_2_leps4 = zeros(70,29);
jfm_2_lepsmax1 = zeros(70,29);
jfm_2_lepsmax2 = zeros(70,29);
```

```
jfm_2_lepsmax3 = zeros(70,29);
jfm_2_lepsmax4 = zeros(70,29);
jfm_2_sk1 = zeros(29,1);
jfm_2_sk2 = zeros(29,1);
jfm_2_sk3 = zeros(29,1);
jfm_2_sk4 = zeros(29,1);

%Divide out the forecast values into each alternative for this lag time
jfm_2_qf1 = jfm_fall(:,233:261);
jfm_2_qf2 = jfm_fall(:,262:290);
jfm_2_qf3 = jfm_fall(:,291:319);
jfm_2_qf4 = jfm_fall(:,320:348);

%Find the Probabilities to define the y-axis of the eCDF.  Create seperate
%eCDF function for the Apr-Jul observations and the Yearly observations.
P = transpose((1:size(qoyr,1))/(size(qoyr,1)+1));

%Find the probabilities of the observed (yo) and forecasted (yf) values
%on the PDF by interpolating along the qopdf data.
for loc = 1:29
for yr = 1:70
   yoy(yr,loc) = interp1(sort(qoyr(:,loc)),P,qoyr(yr,loc),'linear','extrap' );

   jfm_2_yf1(yr,loc) = interp1(sort(qoyr(:,loc)),P,jfm_2_qf1(yr,loc),'linear','extrap' );
   jfm_2_yf2(yr,loc) = interp1(sort(qoyr(:,loc)),P,jfm_2_qf2(yr,loc),'linear','extrap' );
   jfm_2_yf3(yr,loc) = interp1(sort(qoyr(:,loc)),P,jfm_2_qf3(yr,loc),'linear','extrap' );
   jfm_2_yf4(yr,loc) = interp1(sort(qoyr(:,loc)),P,jfm_2_qf4(yr,loc),'linear','extrap' );
end
end

%Calculate the max possible LEPS scores
for loc = 1:29
for yr = 1:70
   jfm_2_lepsmax1(yr,loc) = (3*(1-abs(jfm_2_yf1(yr,loc) - jfm_2_yf1(yr,loc))...
      +    jfm_2_yf1(yr,loc)^2    -    jfm_2_yf1(yr,loc)    +    jfm_2_yf1(yr,loc)^2    -
jfm_2_yf1(yr,loc)) - 1);
   jfm_2_lepsmax2(yr,loc) = (3*(1-abs(jfm_2_yf2(yr,loc) - jfm_2_yf2(yr,loc))...
      +    jfm_2_yf2(yr,loc)^2    -    jfm_2_yf2(yr,loc)    +    jfm_2_yf2(yr,loc)^2    -
jfm_2_yf2(yr,loc)) - 1);
   jfm_2_lepsmax3(yr,loc) = (3*(1-abs(jfm_2_yf3(yr,loc) - jfm_2_yf3(yr,loc))...
      +    jfm_2_yf3(yr,loc)^2    -    jfm_2_yf3(yr,loc)    +    jfm_2_yf3(yr,loc)^2    -
jfm_2_yf3(yr,loc)) - 1);
   jfm_2_lepsmax4(yr,loc) = (3*(1-abs(jfm_2_yf4(yr,loc) - jfm_2_yf4(yr,loc))...
      +    jfm_2_yf4(yr,loc)^2    -    jfm_2_yf4(yr,loc)    +    jfm_2_yf4(yr,loc)^2    -
jfm_2_yf4(yr,loc)) - 1);
end
```

```
end

%Calculate the LEPS scores from the yfx and the yo matrices
for loc = 1:29
for yr = 1:70
   jfm_2_leps1(yr,loc) = (3*(1-abs(jfm_2_yf1(yr,loc) - yoy(yr,loc))...
      + jfm_2_yf1(yr,loc)^2 - jfm_2_yf1(yr,loc) + yoy(yr,loc)^2 - yoy(yr,loc)) - 1);
   jfm_2_leps2(yr,loc) = (3*(1-abs(jfm_2_yf2(yr,loc) - yoy(yr,loc))...
      + jfm_2_yf2(yr,loc)^2 - jfm_2_yf2(yr,loc) + yoy(yr,loc)^2 - yoy(yr,loc)) - 1);
   jfm_2_leps3(yr,loc) = (3*(1-abs(jfm_2_yf3(yr,loc) - yoy(yr,loc))...
      + jfm_2_yf3(yr,loc)^2 - jfm_2_yf3(yr,loc) + yoy(yr,loc)^2 - yoy(yr,loc)) - 1);
   jfm_2_leps4(yr,loc) = (3*(1-abs(jfm_2_yf4(yr,loc) - yoy(yr,loc))...
      + jfm_2_yf4(yr,loc)^2 - jfm_2_yf4(yr,loc) + yoy(yr,loc)^2 - yoy(yr,loc)) - 1);
end
end

%Calculate the Average Skill score at each location
for loc = 1:29
   if sum(jfm_2_leps1(:,loc))>=0
      jfm_2_sk1(loc) = sum(jfm_2_leps1(:,loc))/sum(jfm_2_lepsmax1(:,loc));
   else
      jfm_2_sk1(loc) = sum(jfm_2_leps1(:,loc))/sum(lepsmin(:,loc));
   end
   if sum(jfm_2_leps2(:,loc))>=0
      jfm_2_sk2(loc) = sum(jfm_2_leps2(:,loc))/sum(jfm_2_lepsmax2(:,loc));
   else
      jfm_2_sk2(loc) = sum(jfm_2_leps2(:,loc))/sum(lepsmin(:,loc));
   end
   if sum(jfm_2_leps3(:,loc))>=0
      jfm_2_sk3(loc) = sum(jfm_2_leps3(:,loc))/sum(jfm_2_lepsmax3(:,loc));
   else
      jfm_2_sk3(loc) = sum(jfm_2_leps3(:,loc))/sum(lepsmin(:,loc));
   end
   if sum(jfm_2_leps4(:,loc))>=0
      jfm_2_sk4(loc) = sum(jfm_2_leps4(:,loc))/sum(jfm_2_lepsmax4(:,loc));
   else
      jfm_2_sk4(loc) = sum(jfm_2_leps4(:,loc))/sum(lepsmin(:,loc));
   end
end

jfm_2_sk = 100*[jfm_2_sk1 jfm_2_sk2 jfm_2_sk3 jfm_2_sk4];

%-------------------------------
%Recalc for FMA | lag = 0
%-------------------------------
fma_0_yf1 = zeros(70,29);
```

```
fma_0_yf2 = zeros(70,29);
fma_0_yf3 = zeros(70,29);
fma_0_yf4 = zeros(70,29);
fma_0_leps1 = zeros(70,29);
fma_0_leps2 = zeros(70,29);
fma_0_leps3 = zeros(70,29);
fma_0_leps4 = zeros(70,29);
fma_0_lepsmax1 = zeros(70,29);
fma_0_lepsmax2 = zeros(70,29);
fma_0_lepsmax3 = zeros(70,29);
fma_0_lepsmax4 = zeros(70,29);
fma_0_sk1 = zeros(29,1);
fma_0_sk2 = zeros(29,1);
fma_0_sk3 = zeros(29,1);
fma_0_sk4 = zeros(29,1);

%Divide out the forecast values into each alternative for this lag time
fma_0_qf1 = fma_fall(:,1:29);
fma_0_qf2 = fma_fall(:,30:58);
fma_0_qf3 = fma_fall(:,59:87);
fma_0_qf4 = fma_fall(:,88:116);

%Find the Probabilities to define the y-axis of the eCDF.  Create seperate
%eCDF function for the Apr-Jul observations and the Yearly observations.
P = transpose((1:size(qoyr,1))/(size(qoyr,1)+1));

%Find the probabilities of the observed (yo) and forecasted (yf) values
%on the PDF by interpolating along the qopdf data.
for loc = 1:29
for yr = 1:70
   yoy(yr,loc) = interp1(sort(qoyr(:,loc)),P,qoyr(yr,loc),'linear','extrap' );

   fma_0_yf1(yr,loc) = interp1(sort(qoyr(:,loc)),P,fma_0_qf1(yr,loc),'linear','extrap' );
   fma_0_yf2(yr,loc) = interp1(sort(qoyr(:,loc)),P,fma_0_qf2(yr,loc),'linear','extrap' );
   fma_0_yf3(yr,loc) = interp1(sort(qoyr(:,loc)),P,fma_0_qf3(yr,loc),'linear','extrap' );
   fma_0_yf4(yr,loc) = interp1(sort(qoyr(:,loc)),P,fma_0_qf4(yr,loc),'linear','extrap' );
end
end

% Calculate the min LEPS Scores possible from the April-July and Yearly
% volumes
for loc = 1:29
for yr = 1:70
if yoy(yr,loc)>=0.5
   lepsmin(yr,loc) = (3*(1-abs(0 - yoy(yr,loc)) + yoy(yr,loc)^2 - yoy(yr,loc)) - 1);
else
```

```
   lepsmin(yr,loc) = (3*(1-abs(1 - yoy(yr,loc)) + yoy(yr,loc)^2 - yoy(yr,loc)) - 1);
end
end
end

%Calculate the max possible LEPS scores
for loc = 1:29
for yr = 1:70
   fma_0_lepsmax1(yr,loc) = (3*(1-abs(fma_0_yf1(yr,loc) - fma_0_yf1(yr,loc))...
      +  fma_0_yf1(yr,loc)^2  -  fma_0_yf1(yr,loc)  +  fma_0_yf1(yr,loc)^2  -
fma_0_yf1(yr,loc)) - 1);
   fma_0_lepsmax2(yr,loc) = (3*(1-abs(fma_0_yf2(yr,loc) - fma_0_yf2(yr,loc))...
      +  fma_0_yf2(yr,loc)^2  -  fma_0_yf2(yr,loc)  +  fma_0_yf2(yr,loc)^2  -
fma_0_yf2(yr,loc)) - 1);
   fma_0_lepsmax3(yr,loc) = (3*(1-abs(fma_0_yf3(yr,loc) - fma_0_yf3(yr,loc))...
      +  fma_0_yf3(yr,loc)^2  -  fma_0_yf3(yr,loc)  +  fma_0_yf3(yr,loc)^2  -
fma_0_yf3(yr,loc)) - 1);
   fma_0_lepsmax4(yr,loc) = (3*(1-abs(fma_0_yf4(yr,loc) - fma_0_yf4(yr,loc))...
      +  fma_0_yf4(yr,loc)^2  -  fma_0_yf4(yr,loc)  +  fma_0_yf4(yr,loc)^2  -
fma_0_yf4(yr,loc)) - 1);
end
end

%Calculate the LEPS scores from the yfx and the yo matrices
for loc = 1:29
for yr = 1:70
   fma_0_leps1(yr,loc) = (3*(1-abs(fma_0_yf1(yr,loc) - yoy(yr,loc))...
      + fma_0_yf1(yr,loc)^2 - fma_0_yf1(yr,loc) + yoy(yr,loc)^2 - yoy(yr,loc)) - 1);
   fma_0_leps2(yr,loc) = (3*(1-abs(fma_0_yf2(yr,loc) - yoy(yr,loc))...
      + fma_0_yf2(yr,loc)^2 - fma_0_yf2(yr,loc) + yoy(yr,loc)^2 - yoy(yr,loc)) - 1);
   fma_0_leps3(yr,loc) = (3*(1-abs(fma_0_yf3(yr,loc) - yoy(yr,loc))...
      + fma_0_yf3(yr,loc)^2 - fma_0_yf3(yr,loc) + yoy(yr,loc)^2 - yoy(yr,loc)) - 1);
   fma_0_leps4(yr,loc) = (3*(1-abs(fma_0_yf4(yr,loc) - yoy(yr,loc))...
      + fma_0_yf4(yr,loc)^2 - fma_0_yf4(yr,loc) + yoy(yr,loc)^2 - yoy(yr,loc)) - 1);
end
end

%Calculate the Average Skill score at each location
for loc = 1:29
   if sum(fma_0_leps1(:,loc))>=0
      fma_0_sk1(loc) = sum(fma_0_leps1(:,loc))/sum(fma_0_lepsmax1(:,loc));
   else
      fma_0_sk1(loc) = sum(fma_0_leps1(:,loc))/sum(lepsmin(:,loc));
   end
   if sum(fma_0_leps2(:,loc))>=0
      fma_0_sk2(loc) = sum(fma_0_leps2(:,loc))/sum(fma_0_lepsmax2(:,loc));
```

```
    else
        fma_0_sk2(loc) = sum(fma_0_leps2(:,loc))/sum(lepsmin(:,loc));
    end
    if sum(fma_0_leps3(:,loc))>=0
        fma_0_sk3(loc) = sum(fma_0_leps3(:,loc))/sum(fma_0_lepsmax3(:,loc));
    else
        fma_0_sk3(loc) = sum(fma_0_leps3(:,loc))/sum(lepsmin(:,loc));
    end
    if sum(fma_0_leps4(:,loc))>=0
        fma_0_sk4(loc) = sum(fma_0_leps4(:,loc))/sum(fma_0_lepsmax4(:,loc));
    else
        fma_0_sk4(loc) = sum(fma_0_leps4(:,loc))/sum(lepsmin(:,loc));
    end
end

fma_0_sk = 100*[fma_0_sk1 fma_0_sk2 fma_0_sk3 fma_0_sk4];

%-------------------------------------------
% Recalculate for FMA | Lag = 1Year
%-------------------------------------------
fma_1_yf1 = zeros(70,29);
fma_1_yf2 = zeros(70,29);
fma_1_yf3 = zeros(70,29);
fma_1_yf4 = zeros(70,29);
fma_1_leps1 = zeros(70,29);
fma_1_leps2 = zeros(70,29);
fma_1_leps3 = zeros(70,29);
fma_1_leps4 = zeros(70,29);
fma_1_lepsmax1 = zeros(70,29);
fma_1_lepsmax2 = zeros(70,29);
fma_1_lepsmax3 = zeros(70,29);
fma_1_lepsmax4 = zeros(70,29);
fma_1_sk1 = zeros(29,1);
fma_1_sk2 = zeros(29,1);
fma_1_sk3 = zeros(29,1);
fma_1_sk4 = zeros(29,1);

%Divide out the forecast values into each alternative for this lag time
fma_1_qf1 = fma_fall(:,117:145);
fma_1_qf2 = fma_fall(:,146:174);
fma_1_qf3 = fma_fall(:,175:203);
fma_1_qf4 = fma_fall(:,204:232);

%Find the Probabilities to define the y-axis of the eCDF.  Create seperate
%eCDF function for the Apr-Jul observations and the Yearly observations.
P = transpose((1:size(qoyr,1))/(size(qoyr,1)+1));
```

```
%Find the probabilities of the observed (yo) and forecasted (yf) values
%on the PDF by interpolating along the qopdf data.
for loc = 1:29
for yr = 1:70
   yoy(yr,loc) = interp1(sort(qoyr(:,loc)),P,qoyr(yr,loc),'linear','extrap' );

   fma_1_yf1(yr,loc) = interp1(sort(qoyr(:,loc)),P,fma_1_qf1(yr,loc),'linear','extrap' );
   fma_1_yf2(yr,loc) = interp1(sort(qoyr(:,loc)),P,fma_1_qf2(yr,loc),'linear','extrap' );
   fma_1_yf3(yr,loc) = interp1(sort(qoyr(:,loc)),P,fma_1_qf3(yr,loc),'linear','extrap' );
   fma_1_yf4(yr,loc) = interp1(sort(qoyr(:,loc)),P,fma_1_qf4(yr,loc),'linear','extrap' );
end
end

%Calculate the max possible LEPS scores
for loc = 1:29
for yr = 1:70
   fma_1_lepsmax1(yr,loc) = (3*(1-abs(fma_1_yf1(yr,loc) - fma_1_yf1(yr,loc))...
      + fma_1_yf1(yr,loc)^2 - fma_1_yf1(yr,loc) + fma_1_yf1(yr,loc)^2 -
fma_1_yf1(yr,loc)) - 1);
   fma_1_lepsmax2(yr,loc) = (3*(1-abs(fma_1_yf2(yr,loc) - fma_1_yf2(yr,loc))...
      + fma_1_yf2(yr,loc)^2 - fma_1_yf2(yr,loc) + fma_1_yf2(yr,loc)^2 -
fma_1_yf2(yr,loc)) - 1);
   fma_1_lepsmax3(yr,loc) = (3*(1-abs(fma_1_yf3(yr,loc) - fma_1_yf3(yr,loc))...
      + fma_1_yf3(yr,loc)^2 - fma_1_yf3(yr,loc) + fma_1_yf3(yr,loc)^2 -
fma_1_yf3(yr,loc)) - 1);
   fma_1_lepsmax4(yr,loc) = (3*(1-abs(fma_1_yf4(yr,loc) - fma_1_yf4(yr,loc))...
      + fma_1_yf4(yr,loc)^2 - fma_1_yf4(yr,loc) + fma_1_yf4(yr,loc)^2 -
fma_1_yf4(yr,loc)) - 1);
end
end

%Calculate the LEPS scores from the yfx and the yo matrices
for loc = 1:29
for yr = 1:70
   fma_1_leps1(yr,loc) = (3*(1-abs(fma_1_yf1(yr,loc) - yoy(yr,loc))...
      + fma_1_yf1(yr,loc)^2 - fma_1_yf1(yr,loc) + yoy(yr,loc)^2 - yoy(yr,loc)) - 1);
   fma_1_leps2(yr,loc) = (3*(1-abs(fma_1_yf2(yr,loc) - yoy(yr,loc))...
      + fma_1_yf2(yr,loc)^2 - fma_1_yf2(yr,loc) + yoy(yr,loc)^2 - yoy(yr,loc)) - 1);
   fma_1_leps3(yr,loc) = (3*(1-abs(fma_1_yf3(yr,loc) - yoy(yr,loc))...
      + fma_1_yf3(yr,loc)^2 - fma_1_yf3(yr,loc) + yoy(yr,loc)^2 - yoy(yr,loc)) - 1);
   fma_1_leps4(yr,loc) = (3*(1-abs(fma_1_yf4(yr,loc) - yoy(yr,loc))...
      + fma_1_yf4(yr,loc)^2 - fma_1_yf4(yr,loc) + yoy(yr,loc)^2 - yoy(yr,loc)) - 1);
end
end
```

```
%Calculate the Average Skill score at each location
for loc = 1:29
   if sum(fma_1_leps1(:,loc))>=0
      fma_1_sk1(loc) = sum(fma_1_leps1(:,loc))/sum(fma_1_lepsmax1(:,loc));
   else
      fma_1_sk1(loc) = sum(fma_1_leps1(:,loc))/sum(lepsmin(:,loc));
   end
   if sum(fma_1_leps2(:,loc))>=0
      fma_1_sk2(loc) = sum(fma_1_leps2(:,loc))/sum(fma_1_lepsmax2(:,loc));
   else
      fma_1_sk2(loc) = sum(fma_1_leps2(:,loc))/sum(lepsmin(:,loc));
   end
   if sum(fma_1_leps3(:,loc))>=0
      fma_1_sk3(loc) = sum(fma_1_leps3(:,loc))/sum(fma_1_lepsmax3(:,loc));
   else
      fma_1_sk3(loc) = sum(fma_1_leps3(:,loc))/sum(lepsmin(:,loc));
   end
   if sum(fma_1_leps4(:,loc))>=0
      fma_1_sk4(loc) = sum(fma_1_leps4(:,loc))/sum(fma_1_lepsmax4(:,loc));
   else
      fma_1_sk4(loc) = sum(fma_1_leps4(:,loc))/sum(lepsmin(:,loc));
   end
end

fma_1_sk = 100*[fma_1_sk1 fma_1_sk2 fma_1_sk3 fma_1_sk4];

%-------------------------------------------
% Recalculate for FMA | Lag = 2 Years
%-------------------------------------------
fma_2_yf1 = zeros(70,29);
fma_2_yf2 = zeros(70,29);
fma_2_yf3 = zeros(70,29);
fma_2_yf4 = zeros(70,29);
fma_2_leps1 = zeros(70,29);
fma_2_leps2 = zeros(70,29);
fma_2_leps3 = zeros(70,29);
fma_2_leps4 = zeros(70,29);
fma_2_lepsmax1 = zeros(70,29);
fma_2_lepsmax2 = zeros(70,29);
fma_2_lepsmax3 = zeros(70,29);
fma_2_lepsmax4 = zeros(70,29);
fma_2_sk1 = zeros(29,1);
fma_2_sk2 = zeros(29,1);
fma_2_sk3 = zeros(29,1);
fma_2_sk4 = zeros(29,1);
```

```
%Divide out the forecast values into each alternative for this lag time
fma_2_qf1 = fma_fall(:,233:261);
fma_2_qf2 = fma_fall(:,262:290);
fma_2_qf3 = fma_fall(:,291:319);
fma_2_qf4 = fma_fall(:,320:348);

%Find the Probabilities to define the y-axis of the eCDF.  Create seperate
%eCDF function for the Apr-Jul observations and the Yearly observations.
P = transpose((1:size(qoyr,1))/(size(qoyr,1)+1));

%Find the probabilities of the observed (yo) and forecasted (yf) values
%on the PDF by interpolating along the qopdf data.
for loc = 1:29
for yr = 1:70
   yoy(yr,loc) = interp1(sort(qoyr(:,loc)),P,qoyr(yr,loc),'linear','extrap' );

   fma_2_yf1(yr,loc) = interp1(sort(qoyr(:,loc)),P,fma_2_qf1(yr,loc),'linear','extrap' );
   fma_2_yf2(yr,loc) = interp1(sort(qoyr(:,loc)),P,fma_2_qf2(yr,loc),'linear','extrap' );
   fma_2_yf3(yr,loc) = interp1(sort(qoyr(:,loc)),P,fma_2_qf3(yr,loc),'linear','extrap' );
   fma_2_yf4(yr,loc) = interp1(sort(qoyr(:,loc)),P,fma_2_qf4(yr,loc),'linear','extrap' );
end
end

%Calculate the max possible LEPS scores
for loc = 1:29
for yr = 1:70
   fma_2_lepsmax1(yr,loc) = (3*(1-abs(fma_2_yf1(yr,loc) - fma_2_yf1(yr,loc))...
      + fma_2_yf1(yr,loc)^2 - fma_2_yf1(yr,loc) + fma_2_yf1(yr,loc)^2 -
fma_2_yf1(yr,loc)) - 1);
   fma_2_lepsmax2(yr,loc) = (3*(1-abs(fma_2_yf2(yr,loc) - fma_2_yf2(yr,loc))...
      + fma_2_yf2(yr,loc)^2 - fma_2_yf2(yr,loc) + fma_2_yf2(yr,loc)^2 -
fma_2_yf2(yr,loc)) - 1);
   fma_2_lepsmax3(yr,loc) = (3*(1-abs(fma_2_yf3(yr,loc) - fma_2_yf3(yr,loc))...
      + fma_2_yf3(yr,loc)^2 - fma_2_yf3(yr,loc) + fma_2_yf3(yr,loc)^2 -
fma_2_yf3(yr,loc)) - 1);
   fma_2_lepsmax4(yr,loc) = (3*(1-abs(fma_2_yf4(yr,loc) - fma_2_yf4(yr,loc))...
      + fma_2_yf4(yr,loc)^2 - fma_2_yf4(yr,loc) + fma_2_yf4(yr,loc)^2 -
fma_2_yf4(yr,loc)) - 1);
end
end

%Calculate the LEPS scores from the yfx and the yo matrices
for loc = 1:29
for yr = 1:70
   fma_2_leps1(yr,loc) = (3*(1-abs(fma_2_yf1(yr,loc) - yoy(yr,loc))...
      + fma_2_yf1(yr,loc)^2 - fma_2_yf1(yr,loc) + yoy(yr,loc)^2 - yoy(yr,loc)) - 1);
```

```
   fma_2_leps2(yr,loc) = (3*(1-abs(fma_2_yf2(yr,loc) - yoy(yr,loc))...
      + fma_2_yf2(yr,loc)^2 - fma_2_yf2(yr,loc) + yoy(yr,loc)^2 - yoy(yr,loc)) - 1);
   fma_2_leps3(yr,loc) = (3*(1-abs(fma_2_yf3(yr,loc) - yoy(yr,loc))...
      + fma_2_yf3(yr,loc)^2 - fma_2_yf3(yr,loc) + yoy(yr,loc)^2 - yoy(yr,loc)) - 1);
   fma_2_leps4(yr,loc) = (3*(1-abs(fma_2_yf4(yr,loc) - yoy(yr,loc))...
      + fma_2_yf4(yr,loc)^2 - fma_2_yf4(yr,loc) + yoy(yr,loc)^2 - yoy(yr,loc)) - 1);
end
end

%Calculate the Average Skill score at each location
for loc = 1:29
   if sum(fma_2_leps1(:,loc))>=0
      fma_2_sk1(loc) = sum(fma_2_leps1(:,loc))/sum(fma_2_lepsmax1(:,loc));
   else
      fma_2_sk1(loc) = sum(fma_2_leps1(:,loc))/sum(lepsmin(:,loc));
   end
   if sum(fma_2_leps2(:,loc))>=0
      fma_2_sk2(loc) = sum(fma_2_leps2(:,loc))/sum(fma_2_lepsmax2(:,loc));
   else
      fma_2_sk2(loc) = sum(fma_2_leps2(:,loc))/sum(lepsmin(:,loc));
   end
   if sum(fma_2_leps3(:,loc))>=0
      fma_2_sk3(loc) = sum(fma_2_leps3(:,loc))/sum(fma_2_lepsmax3(:,loc));
   else
      fma_2_sk3(loc) = sum(fma_2_leps3(:,loc))/sum(lepsmin(:,loc));
   end
   if sum(fma_2_leps4(:,loc))>=0
      fma_2_sk4(loc) = sum(fma_2_leps4(:,loc))/sum(fma_2_lepsmax4(:,loc));
   else
      fma_2_sk4(loc) = sum(fma_2_leps4(:,loc))/sum(lepsmin(:,loc));
   end
end

fma_2_sk = 100*[fma_2_sk1 fma_2_sk2 fma_2_sk3 fma_2_sk4];

%-------------------------
%EXPORT RESULTS TO EXCEL
sk_0675 = [djf_0_sk jfm_0_sk fma_0_sk djf_1_sk jfm_1_sk fma_1_sk djf_2_sk
jfm_2_sk fma_2_sk];
xlswrite('L:/Kenneth Data/Matlab/Phase2/Hondo.xls',sk_0675, 'LEPS','C2');
save sk_0675 sk_0675
```

A1.5.4 Relative Error Calculation

```
%-------------------------------------
%  Read in Input Data
```

```
%--------------------------------------
%Create matrices of observed values.  Use the following to know which
%observed values to be used:
%Resampling Data: Rows 71:100 for both qoaj_all and qoyr_all (1976 - 2005)
%Observation Data: Rows 1:70 (qoaj_all and qoyr_all) 1906 - 1975

%Read in observed values stored in the spreadsheet
load qoyr_all

%Observed Data Matrix
qo = qoyr_all(1:70,:);

%Resampling Data Matrix
qoy = qoyr_all(71:100,:);

%Create matrix of forecasts using just the 30-yr average
f30 = mean(qoy);

%Find the realtive error matrix between the mean forecasts and the observed streamflow
re30 = zeros(70,29);
for loc = 1:29
   for yr = 1:70
      re30(yr,loc) = (f30(loc)/qo(yr,loc))-1;
   end
end

%Find the mean of the relative errors at each location
mre30 = mean(re30);

%Find the mean of the relative errors at all locations for each year
yre30 = 100*mean(re30,2);

%Read in Forecast values created with the forecasts.m command
load f_0675
djf_fall = f_0675(:,:,1)';
jfm_fall = f_0675(:,:,2)';
fma_fall = f_0675(:,:,3)';

%--------------------------------------
%  Run Analysis on DJF | Lag = 0 Year
%--------------------------------------

%Divide out the forecast values into each alternative for this lag time
djf_0_qf1 = djf_fall(1:29,:)';
djf_0_qf2 = djf_fall(30:58,:)';
djf_0_qf3 = djf_fall(59:87,:)';
```

```
djf_0_qf4 = djf_fall(88:116,:)';

% Find the relative error between forecast values and observed values at
% each station (the error matrix).
djf_0_re1 = zeros(70,29);
djf_0_re2 = zeros(70,29);
djf_0_re3 = zeros(70,29);
djf_0_re4 = zeros(70,29);
for loc = 1:29
   for yr = 1:70
djf_0_re1(yr,loc) = (djf_0_qf1(yr,loc)/qo(yr,loc))-1;
djf_0_re2(yr,loc) = (djf_0_qf2(yr,loc)/qo(yr,loc))-1;
djf_0_re3(yr,loc) = (djf_0_qf3(yr,loc)/qo(yr,loc))-1;
djf_0_re4(yr,loc) = (djf_0_qf4(yr,loc)/qo(yr,loc))-1;
   end
end

%Find the mean of the realtive errors at each qauge location
djf_0_mre1 = mean(djf_0_re1);
djf_0_mre2 = mean(djf_0_re2);
djf_0_mre3 = mean(djf_0_re3);
djf_0_mre4 = mean(djf_0_re4);

djf_0_sk = 100*[djf_0_mre1' djf_0_mre2' djf_0_mre3' djf_0_mre4'];

%Find the mean relative error at all stations for each year
djf_0_yre1 = mean(djf_0_re1,2);
djf_0_yre2 = mean(djf_0_re2,2);
djf_0_yre3 = mean(djf_0_re3,2);
djf_0_yre4 = mean(djf_0_re4,2);

djf_0_y = 100*[djf_0_yre1 djf_0_yre2 djf_0_yre3 djf_0_yre4];

%--------------------------------------
%  Run Analysis on DJF | Lag = 1 Year
%--------------------------------------

%Divide out the forecast values into each alternative for this lag time
djf_1_qf1 = djf_fall(117:145,:)';
djf_1_qf2 = djf_fall(146:174,:)';
djf_1_qf3 = djf_fall(175:203,:)';
djf_1_qf4 = djf_fall(204:232,:)';

% Find the relative error between forecast values and observed values at
% each station (the error matrix).
djf_1_re1 = zeros(70,29);
```

```
djf_1_re2 = zeros(70,29);
djf_1_re3 = zeros(70,29);
djf_1_re4 = zeros(70,29);
for loc = 1:29
   for yr = 1:70
      djf_1_re1(yr,loc) = (djf_1_qf1(yr,loc)/qo(yr,loc))-1;
      djf_1_re2(yr,loc) = (djf_1_qf2(yr,loc)/qo(yr,loc))-1;
      djf_1_re3(yr,loc) = (djf_1_qf3(yr,loc)/qo(yr,loc))-1;
      djf_1_re4(yr,loc) = (djf_1_qf4(yr,loc)/qo(yr,loc))-1;
   end
end

%Find the mean of the realtive errors at each qauge location
djf_1_mre1 = mean(djf_1_re1);
djf_1_mre2 = mean(djf_1_re2);
djf_1_mre3 = mean(djf_1_re3);
djf_1_mre4 = mean(djf_1_re4);

djf_1_sk = 100*[djf_1_mre1' djf_1_mre2' djf_1_mre3' djf_1_mre4'];

%Find the mean relative error at all stations for each year
djf_1_yre1 = mean(djf_1_re1,2);
djf_1_yre2 = mean(djf_1_re2,2);
djf_1_yre3 = mean(djf_1_re3,2);
djf_1_yre4 = mean(djf_1_re4,2);

djf_1_y = 100*[djf_1_yre1 djf_1_yre2 djf_1_yre3 djf_1_yre4];

%--------------------------------------
%  Run Analysis on DJF | Lag = 2 Year
%--------------------------------------

%Divide out the forecast values into each alternative for this lag time
djf_2_qf1 = djf_fall(233:261,:)';
djf_2_qf2 = djf_fall(262:290,:)';
djf_2_qf3 = djf_fall(291:319,:)';
djf_2_qf4 = djf_fall(320:348,:)';

% Find the relative error between forecast values and observed values at
% each station (the error matrix).
djf_2_re1 = zeros(70,29);
djf_2_re2 = zeros(70,29);
djf_2_re3 = zeros(70,29);
djf_2_re4 = zeros(70,29);
for loc = 1:29
   for yr = 1:70
```

```
      djf_2_re1(yr,loc) = (djf_2_qf1(yr,loc)/qo(yr,loc))-1;
      djf_2_re2(yr,loc) = (djf_2_qf2(yr,loc)/qo(yr,loc))-1;
      djf_2_re3(yr,loc) = (djf_2_qf3(yr,loc)/qo(yr,loc))-1;
      djf_2_re4(yr,loc) = (djf_2_qf4(yr,loc)/qo(yr,loc))-1;
   end
end

%Find the mean of the realtive errors at each qauge location
djf_2_mre1 = mean(djf_2_re1);
djf_2_mre2 = mean(djf_2_re2);
djf_2_mre3 = mean(djf_2_re3);
djf_2_mre4 = mean(djf_2_re4);

djf_2_sk = 100*[djf_2_mre1' djf_2_mre2' djf_2_mre3' djf_2_mre4'];

%Find the mean relative error at all stations for each year
djf_2_yre1 = mean(djf_2_re1,2);
djf_2_yre2 = mean(djf_2_re2,2);
djf_2_yre3 = mean(djf_2_re3,2);
djf_2_yre4 = mean(djf_2_re4,2);

djf_2_y = 100*[djf_2_yre1 djf_2_yre2 djf_2_yre3 djf_2_yre4];

%--------------------------------------
%  Run Analysis on JFM | Lag = 0 Year
%--------------------------------------

%Divide out the forecast values into each alternative for this lag time
jfm_0_qf1 = jfm_fall(1:29,:)';
jfm_0_qf2 = jfm_fall(30:58,:)';
jfm_0_qf3 = jfm_fall(59:87,:)';
jfm_0_qf4 = jfm_fall(88:116,:)';

% Find the relative error between forecast values and observed values at
% each station (the error matrix).
jfm_0_re1 = zeros(70,29);
jfm_0_re2 = zeros(70,29);
jfm_0_re3 = zeros(70,29);
jfm_0_re4 = zeros(70,29);
for loc = 1:29
   for yr = 1:70
      jfm_0_re1(yr,loc) = (jfm_0_qf1(yr,loc)/qo(yr,loc))-1;
      jfm_0_re2(yr,loc) = (jfm_0_qf2(yr,loc)/qo(yr,loc))-1;
      jfm_0_re3(yr,loc) = (jfm_0_qf3(yr,loc)/qo(yr,loc))-1;
      jfm_0_re4(yr,loc) = (jfm_0_qf4(yr,loc)/qo(yr,loc))-1;
   end
```

```
end

%Find the mean of the realtive errors at each qauge location
jfm_0_mre1 = mean(jfm_0_re1);
jfm_0_mre2 = mean(jfm_0_re2);
jfm_0_mre3 = mean(jfm_0_re3);
jfm_0_mre4 = mean(jfm_0_re4);

jfm_0_sk = 100*[jfm_0_mre1' jfm_0_mre2' jfm_0_mre3' jfm_0_mre4'];

%Find the mean relative error at all stations for each year
jfm_0_yre1 = mean(jfm_0_re1,2);
jfm_0_yre2 = mean(jfm_0_re2,2);
jfm_0_yre3 = mean(jfm_0_re3,2);
jfm_0_yre4 = mean(jfm_0_re4,2);

jfm_0_y = 100*[jfm_0_yre1 jfm_0_yre2 jfm_0_yre3 jfm_0_yre4];

%--------------------------------------
%  Run Analysis on JFM | Lag = 1 Year
%--------------------------------------

%Divide out the forecast values into each alternative for this lag time
jfm_1_qf1 = jfm_fall(117:145,:)';
jfm_1_qf2 = jfm_fall(146:174,:)';
jfm_1_qf3 = jfm_fall(175:203,:)';
jfm_1_qf4 = jfm_fall(204:232,:)';

% Find the relative error between forecast values and observed values at
% each station (the error matrix).
jfm_1_re1 = zeros(70,29);
jfm_1_re2 = zeros(70,29);
jfm_1_re3 = zeros(70,29);
jfm_1_re4 = zeros(70,29);
for loc = 1:29
   for yr = 1:70
      jfm_1_re1(yr,loc) = (jfm_1_qf1(yr,loc)/qo(yr,loc))-1;
      jfm_1_re2(yr,loc) = (jfm_1_qf2(yr,loc)/qo(yr,loc))-1;
      jfm_1_re3(yr,loc) = (jfm_1_qf3(yr,loc)/qo(yr,loc))-1;
      jfm_1_re4(yr,loc) = (jfm_1_qf4(yr,loc)/qo(yr,loc))-1;
   end
end

%Find the mean of the realtive errors at each qauge location
jfm_1_mre1 = mean(jfm_1_re1);
jfm_1_mre2 = mean(jfm_1_re2);
```

```
jfm_1_mre3 = mean(jfm_1_re3);
jfm_1_mre4 = mean(jfm_1_re4);

jfm_1_sk = 100*[jfm_1_mre1' jfm_1_mre2' jfm_1_mre3' jfm_1_mre4'];

%Find the mean relative error at all stations for each year
jfm_1_yre1 = mean(jfm_1_re1,2);
jfm_1_yre2 = mean(jfm_1_re2,2);
jfm_1_yre3 = mean(jfm_1_re3,2);
jfm_1_yre4 = mean(jfm_1_re4,2);

jfm_1_y = 100*[jfm_1_yre1 jfm_1_yre2 jfm_1_yre3 jfm_1_yre4];

%--------------------------------------
%  Run Analysis on JFM | Lag = 2 Year
%--------------------------------------

%Divide out the forecast values into each alternative for this lag time
jfm_2_qf1 = jfm_fall(233:261,:)';
jfm_2_qf2 = jfm_fall(262:290,:)';
jfm_2_qf3 = jfm_fall(291:319,:)';
jfm_2_qf4 = jfm_fall(320:348,:)';

% Find the relative error between forecast values and observed values at
% each station (the error matrix).
jfm_2_re1 = zeros(70,29);
jfm_2_re2 = zeros(70,29);
jfm_2_re3 = zeros(70,29);
jfm_2_re4 = zeros(70,29);
for loc = 1:29
   for yr = 1:70
      jfm_2_re1(yr,loc) = (jfm_2_qf1(yr,loc)/qo(yr,loc))-1;
      jfm_2_re2(yr,loc) = (jfm_2_qf2(yr,loc)/qo(yr,loc))-1;
      jfm_2_re3(yr,loc) = (jfm_2_qf3(yr,loc)/qo(yr,loc))-1;
      jfm_2_re4(yr,loc) = (jfm_2_qf4(yr,loc)/qo(yr,loc))-1;
   end
end

%Find the mean of the realtive errors at each qauge location
jfm_2_mre1 = mean(jfm_2_re1);
jfm_2_mre2 = mean(jfm_2_re2);
jfm_2_mre3 = mean(jfm_2_re3);
jfm_2_mre4 = mean(jfm_2_re4);

jfm_2_sk = 100*[jfm_2_mre1' jfm_2_mre2' jfm_2_mre3' jfm_2_mre4'];
```

```
%Find the mean relative error at all stations for each year
jfm_2_yre1 = mean(jfm_2_re1,2);
jfm_2_yre2 = mean(jfm_2_re2,2);
jfm_2_yre3 = mean(jfm_2_re3,2);
jfm_2_yre4 = mean(jfm_2_re4,2);

jfm_2_y = 100*[jfm_2_yre1 jfm_2_yre2 jfm_2_yre3 jfm_2_yre4];

%--------------------------------------
%  Run Analysis on FMA | Lag = 0 Year
%--------------------------------------

%Divide out the forecast values into each alternative for this lag time
fma_0_qf1 = fma_fall(1:29,:)';
fma_0_qf2 = fma_fall(30:58,:)';
fma_0_qf3 = fma_fall(59:87,:)';
fma_0_qf4 = fma_fall(88:116,:)';

% Find the relative error between forecast values and observed values at
% each station (the error matrix).
fma_0_re1 = zeros(70,29);
fma_0_re2 = zeros(70,29);
fma_0_re3 = zeros(70,29);
fma_0_re4 = zeros(70,29);
for loc = 1:29
   for yr = 1:70
      fma_0_re1(yr,loc) = (fma_0_qf1(yr,loc)/qo(yr,loc))-1;
      fma_0_re2(yr,loc) = (fma_0_qf2(yr,loc)/qo(yr,loc))-1;
      fma_0_re3(yr,loc) = (fma_0_qf3(yr,loc)/qo(yr,loc))-1;
      fma_0_re4(yr,loc) = (fma_0_qf4(yr,loc)/qo(yr,loc))-1;
   end
end

%Find the mean of the realtive errors at each qauge location
fma_0_mre1 = mean(fma_0_re1);
fma_0_mre2 = mean(fma_0_re2);
fma_0_mre3 = mean(fma_0_re3);
fma_0_mre4 = mean(fma_0_re4);

fma_0_sk = 100*[fma_0_mre1' fma_0_mre2' fma_0_mre3' fma_0_mre4'];

%Find the mean relative error at all stations for each year
fma_0_yre1 = mean(fma_0_re1,2);
fma_0_yre2 = mean(fma_0_re2,2);
fma_0_yre3 = mean(fma_0_re3,2);
fma_0_yre4 = mean(fma_0_re4,2);
```

```
fma_0_y = 100*[fma_0_yre1 fma_0_yre2 fma_0_yre3 fma_0_yre4];

%-------------------------------------
%  Run Analysis on FMA | Lag = 1 Year
%-------------------------------------

%Divide out the forecast values into each alternative for this lag time
fma_1_qf1 = fma_fall(117:145,:)';
fma_1_qf2 = fma_fall(146:174,:)';
fma_1_qf3 = fma_fall(175:203,:)';
fma_1_qf4 = fma_fall(204:232,:)';

% Find the relative error between forecast values and observed values at
% each station (the error matrix).
fma_1_re1 = zeros(70,29);
fma_1_re2 = zeros(70,29);
fma_1_re3 = zeros(70,29);
fma_1_re4 = zeros(70,29);
for loc = 1:29
   for yr = 1:70
      fma_1_re1(yr,loc) = (fma_1_qf1(yr,loc)/qo(yr,loc))-1;
      fma_1_re2(yr,loc) = (fma_1_qf2(yr,loc)/qo(yr,loc))-1;
      fma_1_re3(yr,loc) = (fma_1_qf3(yr,loc)/qo(yr,loc))-1;
      fma_1_re4(yr,loc) = (fma_1_qf4(yr,loc)/qo(yr,loc))-1;
   end
end

%Find the mean of the realtive errors at each qauge location
fma_1_mre1 = mean(fma_1_re1);
fma_1_mre2 = mean(fma_1_re2);
fma_1_mre3 = mean(fma_1_re3);
fma_1_mre4 = mean(fma_1_re4);

fma_1_sk = 100*[fma_1_mre1' fma_1_mre2' fma_1_mre3' fma_1_mre4'];

%Find the mean relative error at all stations for each year
fma_1_yre1 = mean(fma_1_re1,2);
fma_1_yre2 = mean(fma_1_re2,2);
fma_1_yre3 = mean(fma_1_re3,2);
fma_1_yre4 = mean(fma_1_re4,2);

fma_1_y = 100*[fma_1_yre1 fma_1_yre2 fma_1_yre3 fma_1_yre4];

%-------------------------------------
%  Run Analysis on FMA | Lag = 2 Year
```

```
%-------------------------------------

%Divide out the forecast values into each alternative for this lag time
fma_2_qf1 = fma_fall(233:261,:)';
fma_2_qf2 = fma_fall(262:290,:)';
fma_2_qf3 = fma_fall(291:319,:)';
fma_2_qf4 = fma_fall(320:348,:)';

% Find the relative error between forecast values and observed values at
% each station (the error matrix).
fma_2_re1 = zeros(70,29);
fma_2_re2 = zeros(70,29);
fma_2_re3 = zeros(70,29);
fma_2_re4 = zeros(70,29);
for loc = 1:29
   for yr = 1:70
      fma_2_re1(yr,loc) = (fma_2_qf1(yr,loc)/qo(yr,loc))-1;
      fma_2_re2(yr,loc) = (fma_2_qf2(yr,loc)/qo(yr,loc))-1;
      fma_2_re3(yr,loc) = (fma_2_qf3(yr,loc)/qo(yr,loc))-1;
      fma_2_re4(yr,loc) = (fma_2_qf4(yr,loc)/qo(yr,loc))-1;
   end
end

%Find the mean of the realtive errors at each qauge location
fma_2_mre1 = mean(fma_2_re1);
fma_2_mre2 = mean(fma_2_re2);
fma_2_mre3 = mean(fma_2_re3);
fma_2_mre4 = mean(fma_2_re4);

fma_2_sk = 100*[fma_2_mre1' fma_2_mre2' fma_2_mre3' fma_2_mre4'];

%Find the mean relative error at all stations for each year
fma_2_yre1 = mean(fma_2_re1,2);
fma_2_yre2 = mean(fma_2_re2,2);
fma_2_yre3 = mean(fma_2_re3,2);
fma_2_yre4 = mean(fma_2_re4,2);

fma_2_y = 100*[fma_2_yre1 fma_2_yre2 fma_2_yre3 fma_2_yre4];

re_0675 = [djf_0_sk jfm_0_sk fma_0_sk djf_1_sk jfm_1_sk fma_1_sk djf_2_sk
jfm_2_sk fma_2_sk];
xlswrite('L:/Kenneth Data/Matlab/Phase2/Hondo.xls',re_0675, 'RE','B2');
save re_0675 re_0675

%Export error of forecasts to the hondo.xls spreadsheet
e_djf_all = [djf_0_re1 djf_0_re2 djf_0_re3 djf_0_re4 ...
```

```
   djf_1_re1 djf_1_re2 djf_1_re3 djf_1_re4 ...
   djf_2_re1 djf_2_re2 djf_2_re3 djf_2_re4];
e_jfm_all = [jfm_0_re1 jfm_0_re2 jfm_0_re3 jfm_0_re4 ...
   jfm_1_re1 jfm_1_re2 jfm_1_re3 jfm_1_re4 ...
   jfm_2_re1 jfm_2_re2 jfm_2_re3 jfm_2_re4];
e_fma_all = [fma_0_re1 fma_0_re2 fma_0_re3 fma_0_re4 ...
   fma_1_re1 fma_1_re2 fma_1_re3 fma_1_re4 ...
   fma_2_re1 fma_2_re2 fma_2_re3 fma_2_re4];
aaa = [e_djf_all e_jfm_all e_fma_all];
[dim1 dim2] = size(aaa);
re_0675_all = reshape(aaa,dim1,dim2/3,3);
save re_0675_all re_0675_all
```

A1.5.5 Root Mean Squared Error Calculation

```
%Read in observed data and analyze
load qoyr_all

%Create matrices of observed values.  Use the following to know which
%observed values to be used:
%Resampling Data: Rows 71:100 for both qoaj_all and qoyr_all (1976 - 2005)
%Observation Data: Rows 1:70 (qoaj_all and qoyr_all) 1906 - 1975

%Observed Data Matrix
qo = qoyr_all(1:70,:);

%Resampling Data Matrix
qoy = qoyr_all(71:100,:);

%Create matrix of forecasts using just the 30-yr average
f30 = mean(qoy);

%Find the error matrix between the mean forecasts and the observed streamflow
e30 = zeros(70,29);
for loc = 1:29
   for yr = 1:70
      e30(yr,loc) = qo(yr,loc) - f30(loc);
   end
end

%Square each element of the error matrix
se30 = zeros(70,29);
for loc = 1:29
   for yr = 1:70
      se30(yr,loc) = e30(yr,loc)^2;
```

```
   end
end

%Find the mean of the square of the errors at each location
mse30 = mean(se30);

%Find the root of the mean sum of squares
rmse30 = sqrt(mse30);

%--------------------------------------
%  Run Analysis on DJF | Lag = 0 Year
%--------------------------------------

%Read in Forecast values created with the forecasts.m command
load f_0675
djf_fall = f_0675(:,:,1)';
jfm_fall = f_0675(:,:,2)';
fma_fall = f_0675(:,:,3)';

%djf_fall = xlsread('L:/Kenneth Data/Matlab/Phase2/Hondo_f.xls','f_djf','C2:BT349');
%jfm_fall = xlsread('L:/Kenneth Data/Matlab/Phase2/Hondo_f.xls','f_jfm','C2:BT349');
%fma_fall = xlsread('L:/Kenneth Data/Matlab/Phase2/Hondo_f.xls','f_fma','C2:BT349');

%Divide out the forecast values into each alternative for this lag time
djf_0_qf1 = djf_fall(1:29,:)';
djf_0_qf2 = djf_fall(30:58,:)';
djf_0_qf3 = djf_fall(59:87,:)';
djf_0_qf4 = djf_fall(88:116,:)';

% Find difference between forecast values and observed values at
% each station (the error matrix).
djf_0_e1 = qo - djf_0_qf1;
djf_0_e2 = qo - djf_0_qf2;
djf_0_e3 = qo - djf_0_qf3;
djf_0_e4 = qo - djf_0_qf4;

%Find the square of each element in the error matrix
djf_0_se1 = zeros(70,29);
djf_0_se2 = zeros(70,29);
djf_0_se3 = zeros(70,29);
djf_0_se4 = zeros(70,29);
for loc = 1:29
   for yr = 1:70
      djf_0_se1(yr,loc) = djf_0_e1(yr,loc)^2;
      djf_0_se2(yr,loc) = djf_0_e2(yr,loc)^2;
      djf_0_se3(yr,loc) = djf_0_e3(yr,loc)^2;
```

```
      djf_0_se4(yr,loc) = djf_0_e4(yr,loc)^2;
   end
end

%Find the mean of the squared errors at each qauge location
djf_0_mse1 = mean(djf_0_se1,1);
djf_0_mse2 = mean(djf_0_se2,1);
djf_0_mse3 = mean(djf_0_se3,1);
djf_0_mse4 = mean(djf_0_se4,1);

%Find the root of the mean squared error at each location
djf_0_rmse1 = sqrt(djf_0_mse1);
djf_0_rmse2 = sqrt(djf_0_mse2);
djf_0_rmse3 = sqrt(djf_0_mse3);
djf_0_rmse4 = sqrt(djf_0_mse4);

%Compare the results here with the rmse30 vector to assess
%the improvement in the forecast skill compared to the 30-mean
djf_0_comp1 = zeros(1,29);
djf_0_comp2 = zeros(1,29);
djf_0_comp3 = zeros(1,29);
djf_0_comp4 = zeros(1,29);
for loc = 1:29;
   djf_0_comp1(loc) = (rmse30(loc) - djf_0_rmse1(loc)) / rmse30(loc);
   djf_0_comp2(loc) = (rmse30(loc) - djf_0_rmse2(loc)) / rmse30(loc);
   djf_0_comp3(loc) = (rmse30(loc) - djf_0_rmse3(loc)) / rmse30(loc);
   djf_0_comp4(loc) = (rmse30(loc) - djf_0_rmse4(loc)) / rmse30(loc);
end

djf_0_sk = 100*[djf_0_comp1' djf_0_comp2' djf_0_comp3' djf_0_comp4'];

%--------------------------------------
%  Run Analysis on DJF | Lag = 1 Year
%--------------------------------------
%Divide out the forecast values into each alternative for this lag time
djf_1_qf1 = djf_fall(117:145,:)';
djf_1_qf2 = djf_fall(146:174,:)';
djf_1_qf3 = djf_fall(175:203,:)';
djf_1_qf4 = djf_fall(204:232,:)';

% Find difference between forecast values and observed values at
% each station (the error matrix).
djf_1_e1 = qo - djf_1_qf1;
djf_1_e2 = qo - djf_1_qf2;
djf_1_e3 = qo - djf_1_qf3;
djf_1_e4 = qo - djf_1_qf4;
```

```
%Find the square of each element in the error matrix
djf_1_se1 = zeros(70,29);
djf_1_se2 = zeros(70,29);
djf_1_se3 = zeros(70,29);
djf_1_se4 = zeros(70,29);
for loc = 1:29
   for yr = 1:70
      djf_1_se1(yr,loc) = djf_1_e1(yr,loc)^2;
      djf_1_se2(yr,loc) = djf_1_e2(yr,loc)^2;
      djf_1_se3(yr,loc) = djf_1_e3(yr,loc)^2;
      djf_1_se4(yr,loc) = djf_1_e4(yr,loc)^2;
   end
end

%Find the mean of the squared errors at each qauge location
djf_1_mse1 = mean(djf_1_se1,1);
djf_1_mse2 = mean(djf_1_se2,1);
djf_1_mse3 = mean(djf_1_se3,1);
djf_1_mse4 = mean(djf_1_se4,1);

%Find the root of the mean squared error at each location
djf_1_rmse1 = sqrt(djf_1_mse1);
djf_1_rmse2 = sqrt(djf_1_mse2);
djf_1_rmse3 = sqrt(djf_1_mse3);
djf_1_rmse4 = sqrt(djf_1_mse4);

%Compare the results here with the rmse30 vector to assess
%the improvement in the forecast skill compared to the 30-mean
djf_1_comp1 = zeros(1,29);
djf_1_comp2 = zeros(1,29);
djf_1_comp3 = zeros(1,29);
djf_1_comp4 = zeros(1,29);
for loc = 1:29;
   djf_1_comp1(loc) = (rmse30(loc) - djf_1_rmse1(loc)) / rmse30(loc);
   djf_1_comp2(loc) = (rmse30(loc) - djf_1_rmse2(loc)) / rmse30(loc);
   djf_1_comp3(loc) = (rmse30(loc) - djf_1_rmse3(loc)) / rmse30(loc);
   djf_1_comp4(loc) = (rmse30(loc) - djf_1_rmse4(loc)) / rmse30(loc);
end

djf_1_sk = 100*[djf_1_comp1' djf_1_comp2' djf_1_comp3' djf_1_comp4'];

%--------------------------------------
%  Run Analysis on DJF | Lag = 2 Year
%--------------------------------------
%Divide out the forecast values into each alternative for this lag time
```

```
djf_2_qf1 = djf_fall(233:261,:)';
djf_2_qf2 = djf_fall(262:290,:)';
djf_2_qf3 = djf_fall(291:319,:)';
djf_2_qf4 = djf_fall(320:348,:)';

% Find difference between forecast values and observed values at
% each station (the error matrix).
djf_2_e1 = qo - djf_2_qf1;
djf_2_e2 = qo - djf_2_qf2;
djf_2_e3 = qo - djf_2_qf3;
djf_2_e4 = qo - djf_2_qf4;

%Find the square of each element in the error matrix
djf_2_se1 = zeros(70,29);
djf_2_se2 = zeros(70,29);
djf_2_se3 = zeros(70,29);
djf_2_se4 = zeros(70,29);
for loc = 1:29
   for yr = 1:70
      djf_2_se1(yr,loc) = djf_2_e1(yr,loc)^2;
      djf_2_se2(yr,loc) = djf_2_e2(yr,loc)^2;
      djf_2_se3(yr,loc) = djf_2_e3(yr,loc)^2;
      djf_2_se4(yr,loc) = djf_2_e4(yr,loc)^2;
   end
end

%Find the mean of the squared errors at each qauge location
djf_2_mse1 = mean(djf_2_se1,1);
djf_2_mse2 = mean(djf_2_se2,1);
djf_2_mse3 = mean(djf_2_se3,1);
djf_2_mse4 = mean(djf_2_se4,1);

%Find the root of the mean squared error at each location
djf_2_rmse1 = sqrt(djf_2_mse1);
djf_2_rmse2 = sqrt(djf_2_mse2);
djf_2_rmse3 = sqrt(djf_2_mse3);
djf_2_rmse4 = sqrt(djf_2_mse4);

%Compare the results here with the rmse30 vector to assess
%the improvement in the forecast skill compared to the 30-mean
djf_2_comp1 = zeros(1,29);
djf_2_comp2 = zeros(1,29);
djf_2_comp3 = zeros(1,29);
djf_2_comp4 = zeros(1,29);
for loc = 1:29;
   djf_2_comp1(loc) = (rmse30(loc) - djf_2_rmse1(loc)) / rmse30(loc);
```

```
   djf_2_comp2(loc) = (rmse30(loc) - djf_2_rmse2(loc)) / rmse30(loc);
   djf_2_comp3(loc) = (rmse30(loc) - djf_2_rmse3(loc)) / rmse30(loc);
   djf_2_comp4(loc) = (rmse30(loc) - djf_2_rmse4(loc)) / rmse30(loc);
end

djf_2_sk = 100*[djf_2_comp1' djf_2_comp2' djf_2_comp3' djf_2_comp4'];

%---------------------------------------------
% Recalculate for JFM | Lag = 0 Year
%---------------------------------------------
%Divide out the forecast values into each alternative for this lag time
jfm_0_qf1 = jfm_fall(1:29,:)';
jfm_0_qf2 = jfm_fall(30:58,:)';
jfm_0_qf3 = jfm_fall(59:87,:)';
jfm_0_qf4 = jfm_fall(88:116,:)';

% Find difference between forecast values and observed values at
% each station (the error matrix).
jfm_0_e1 = qo - jfm_0_qf1;
jfm_0_e2 = qo - jfm_0_qf2;
jfm_0_e3 = qo - jfm_0_qf3;
jfm_0_e4 = qo - jfm_0_qf4;

%Find the square of each element in the error matrix
jfm_0_se1 = zeros(70,29);
jfm_0_se2 = zeros(70,29);
jfm_0_se3 = zeros(70,29);
jfm_0_se4 = zeros(70,29);
for loc = 1:29
   for yr = 1:70
      jfm_0_se1(yr,loc) = jfm_0_e1(yr,loc)^2;
      jfm_0_se2(yr,loc) = jfm_0_e2(yr,loc)^2;
      jfm_0_se3(yr,loc) = jfm_0_e3(yr,loc)^2;
      jfm_0_se4(yr,loc) = jfm_0_e4(yr,loc)^2;
   end
end

%Find the mean of the squared errors at each qauge location
jfm_0_mse1 = mean(jfm_0_se1,1);
jfm_0_mse2 = mean(jfm_0_se2,1);
jfm_0_mse3 = mean(jfm_0_se3,1);
jfm_0_mse4 = mean(jfm_0_se4,1);

%Find the root of the mean squared error at each location
jfm_0_rmse1 = sqrt(jfm_0_mse1);
jfm_0_rmse2 = sqrt(jfm_0_mse2);
```

```
jfm_0_rmse3 = sqrt(jfm_0_mse3);
jfm_0_rmse4 = sqrt(jfm_0_mse4);

%Compare the results here with the rmse30 vector to assess
%the improvement in the forecast skill compared to the 30-mean
jfm_0_comp1 = zeros(1,29);
jfm_0_comp2 = zeros(1,29);
jfm_0_comp3 = zeros(1,29);
jfm_0_comp4 = zeros(1,29);
for loc = 1:29;
   jfm_0_comp1(loc) = (rmse30(loc) - jfm_0_rmse1(loc)) / rmse30(loc);
   jfm_0_comp2(loc) = (rmse30(loc) - jfm_0_rmse2(loc)) / rmse30(loc);
   jfm_0_comp3(loc) = (rmse30(loc) - jfm_0_rmse3(loc)) / rmse30(loc);
   jfm_0_comp4(loc) = (rmse30(loc) - jfm_0_rmse4(loc)) / rmse30(loc);
end

jfm_0_sk = 100*[jfm_0_comp1' jfm_0_comp2' jfm_0_comp3' jfm_0_comp4'];

%-------------------------------------------
% Recalculate for JFM | Lag = 1 Year
%-------------------------------------------
%Divide out the forecast values into each alternative for this lag time
jfm_1_qf1 = jfm_fall(117:145,:)';
jfm_1_qf2 = jfm_fall(146:174,:)';
jfm_1_qf3 = jfm_fall(175:203,:)';
jfm_1_qf4 = jfm_fall(204:232,:)';

% Find difference between forecast values and observed values at
% each station (the error matrix).
jfm_1_e1 = qo - jfm_1_qf1;
jfm_1_e2 = qo - jfm_1_qf2;
jfm_1_e3 = qo - jfm_1_qf3;
jfm_1_e4 = qo - jfm_1_qf4;

%Find the square of each element in the error matrix
jfm_1_se1 = zeros(70,29);
jfm_1_se2 = zeros(70,29);
jfm_1_se3 = zeros(70,29);
jfm_1_se4 = zeros(70,29);
for loc = 1:29
   for yr = 1:70
      jfm_1_se1(yr,loc) = jfm_1_e1(yr,loc)^2;
      jfm_1_se2(yr,loc) = jfm_1_e2(yr,loc)^2;
      jfm_1_se3(yr,loc) = jfm_1_e3(yr,loc)^2;
      jfm_1_se4(yr,loc) = jfm_1_e4(yr,loc)^2;
   end
```

```
end

%Find the mean of the squared errors at each qauge location
jfm_1_mse1 = mean(jfm_1_se1,1);
jfm_1_mse2 = mean(jfm_1_se2,1);
jfm_1_mse3 = mean(jfm_1_se3,1);
jfm_1_mse4 = mean(jfm_1_se4,1);

%Find the root of the mean squared error at each location
jfm_1_rmse1 = sqrt(jfm_1_mse1);
jfm_1_rmse2 = sqrt(jfm_1_mse2);
jfm_1_rmse3 = sqrt(jfm_1_mse3);
jfm_1_rmse4 = sqrt(jfm_1_mse4);

%Compare the results here with the rmse30 vector to assess
%the improvement in the forecast skill compared to the 30-mean
jfm_1_comp1 = zeros(1,29);
jfm_1_comp2 = zeros(1,29);
jfm_1_comp3 = zeros(1,29);
jfm_1_comp4 = zeros(1,29);
for loc = 1:29;
   jfm_1_comp1(loc) = (rmse30(loc) - jfm_1_rmse1(loc)) / rmse30(loc);
   jfm_1_comp2(loc) = (rmse30(loc) - jfm_1_rmse2(loc)) / rmse30(loc);
   jfm_1_comp3(loc) = (rmse30(loc) - jfm_1_rmse3(loc)) / rmse30(loc);
   jfm_1_comp4(loc) = (rmse30(loc) - jfm_1_rmse4(loc)) / rmse30(loc);
end

jfm_1_sk = 100*[jfm_1_comp1' jfm_1_comp2' jfm_1_comp3' jfm_1_comp4'];

%-------------------------------------------
% Recalculate for JFM | Lag = 2 Year
%-------------------------------------------
%Divide out the forecast values into each alternative for this lag time
jfm_2_qf1 = jfm_fall(233:261,:)';
jfm_2_qf2 = jfm_fall(262:290,:)';
jfm_2_qf3 = jfm_fall(291:319,:)';
jfm_2_qf4 = jfm_fall(320:348,:)';

% Find difference between forecast values and observed values at
% each station (the error matrix).
jfm_2_e1 = qo - jfm_2_qf1;
jfm_2_e2 = qo - jfm_2_qf2;
jfm_2_e3 = qo - jfm_2_qf3;
jfm_2_e4 = qo - jfm_2_qf4;

%Find the square of each element in the error matrix
```

```
jfm_2_se1 = zeros(70,29);
jfm_2_se2 = zeros(70,29);
jfm_2_se3 = zeros(70,29);
jfm_2_se4 = zeros(70,29);
for loc = 1:29
   for yr = 1:70
      jfm_2_se1(yr,loc) = jfm_2_e1(yr,loc)^2;
      jfm_2_se2(yr,loc) = jfm_2_e2(yr,loc)^2;
      jfm_2_se3(yr,loc) = jfm_2_e3(yr,loc)^2;
      jfm_2_se4(yr,loc) = jfm_2_e4(yr,loc)^2;
   end
end

%Find the mean of the squared errors at each qauge location
jfm_2_mse1 = mean(jfm_2_se1,1);
jfm_2_mse2 = mean(jfm_2_se2,1);
jfm_2_mse3 = mean(jfm_2_se3,1);
jfm_2_mse4 = mean(jfm_2_se4,1);

%Find the root of the mean squared error at each location
jfm_2_rmse1 = sqrt(jfm_2_mse1);
jfm_2_rmse2 = sqrt(jfm_2_mse2);
jfm_2_rmse3 = sqrt(jfm_2_mse3);
jfm_2_rmse4 = sqrt(jfm_2_mse4);

%Compare the results here with the rmse30 vector to assess
%the improvement in the forecast skill compared to the 30-mean
jfm_2_comp1 = zeros(1,29);
jfm_2_comp2 = zeros(1,29);
jfm_2_comp3 = zeros(1,29);
jfm_2_comp4 = zeros(1,29);
for loc = 1:29;
   jfm_2_comp1(loc) = (rmse30(loc) - jfm_2_rmse1(loc)) / rmse30(loc);
   jfm_2_comp2(loc) = (rmse30(loc) - jfm_2_rmse2(loc)) / rmse30(loc);
   jfm_2_comp3(loc) = (rmse30(loc) - jfm_2_rmse3(loc)) / rmse30(loc);
   jfm_2_comp4(loc) = (rmse30(loc) - jfm_2_rmse4(loc)) / rmse30(loc);
end

jfm_2_sk = 100*[jfm_2_comp1' jfm_2_comp2' jfm_2_comp3' jfm_2_comp4'];

%-------------------------------------------
% Recalculate for FMA | Lag = 0 Year
%-------------------------------------------

%Divide out the forecast values into each alternative for this lag time
fma_0_qf1 = fma_fall(1:29,:)';
```

```
fma_0_qf2 = fma_fall(30:58,:)';
fma_0_qf3 = fma_fall(59:87,:)';
fma_0_qf4 = fma_fall(88:116,:)';

% Find difference between forecast values and observed values at
% each station (the error matrix).
fma_0_e1 = qo - fma_0_qf1;
fma_0_e2 = qo - fma_0_qf2;
fma_0_e3 = qo - fma_0_qf3;
fma_0_e4 = qo - fma_0_qf4;

%Find the square of each element in the error matrix
fma_0_se1 = zeros(70,29);
fma_0_se2 = zeros(70,29);
fma_0_se3 = zeros(70,29);
fma_0_se4 = zeros(70,29);
for loc = 1:29
   for yr = 1:70
      fma_0_se1(yr,loc) = fma_0_e1(yr,loc)^2;
      fma_0_se2(yr,loc) = fma_0_e2(yr,loc)^2;
      fma_0_se3(yr,loc) = fma_0_e3(yr,loc)^2;
      fma_0_se4(yr,loc) = fma_0_e4(yr,loc)^2;
   end
end

%Find the mean of the squared errors at each qauge location
fma_0_mse1 = mean(fma_0_se1,1);
fma_0_mse2 = mean(fma_0_se2,1);
fma_0_mse3 = mean(fma_0_se3,1);
fma_0_mse4 = mean(fma_0_se4,1);

%Find the root of the mean squared error at each location
fma_0_rmse1 = sqrt(fma_0_mse1);
fma_0_rmse2 = sqrt(fma_0_mse2);
fma_0_rmse3 = sqrt(fma_0_mse3);
fma_0_rmse4 = sqrt(fma_0_mse4);

%Compare the results here with the rmse30 vector to assess
%the improvement in the forecast skill compared to the 30-mean
fma_0_comp1 = zeros(1,29);
fma_0_comp2 = zeros(1,29);
fma_0_comp3 = zeros(1,29);
fma_0_comp4 = zeros(1,29);
for loc = 1:29;
   fma_0_comp1(loc) = (rmse30(loc) - fma_0_rmse1(loc)) / rmse30(loc);
   fma_0_comp2(loc) = (rmse30(loc) - fma_0_rmse2(loc)) / rmse30(loc);
```

```
   fma_0_comp3(loc) = (rmse30(loc) - fma_0_rmse3(loc)) / rmse30(loc);
   fma_0_comp4(loc) = (rmse30(loc) - fma_0_rmse4(loc)) / rmse30(loc);
end

fma_0_sk = 100*[fma_0_comp1' fma_0_comp2' fma_0_comp3' fma_0_comp4'];

%--------------------------------------------
% Recalculate for FMA | Lag = 1 Year
%--------------------------------------------
%Divide out the forecast values into each alternative for this lag time
fma_1_qf1 = fma_fall(117:145,:)';
fma_1_qf2 = fma_fall(146:174,:)';
fma_1_qf3 = fma_fall(175:203,:)';
fma_1_qf4 = fma_fall(204:232,:)';

% Find difference between forecast values and observed values at
% each station (the error matrix).
fma_1_e1 = qo - fma_1_qf1;
fma_1_e2 = qo - fma_1_qf2;
fma_1_e3 = qo - fma_1_qf3;
fma_1_e4 = qo - fma_1_qf4;

%Find the square of each element in the error matrix
fma_1_se1 = zeros(70,29);
fma_1_se2 = zeros(70,29);
fma_1_se3 = zeros(70,29);
fma_1_se4 = zeros(70,29);
for loc = 1:29
   for yr = 1:70
      fma_1_se1(yr,loc) = fma_1_e1(yr,loc)^2;
      fma_1_se2(yr,loc) = fma_1_e2(yr,loc)^2;
      fma_1_se3(yr,loc) = fma_1_e3(yr,loc)^2;
      fma_1_se4(yr,loc) = fma_1_e4(yr,loc)^2;
   end
end

%Find the mean of the squared errors at each qauge location
fma_1_mse1 = mean(fma_1_se1,1);
fma_1_mse2 = mean(fma_1_se2,1);
fma_1_mse3 = mean(fma_1_se3,1);
fma_1_mse4 = mean(fma_1_se4,1);

%Find the root of the mean squared error at each location
fma_1_rmse1 = sqrt(fma_1_mse1);
fma_1_rmse2 = sqrt(fma_1_mse2);
fma_1_rmse3 = sqrt(fma_1_mse3);
```

```
fma_1_rmse4 = sqrt(fma_1_mse4);

%Compare the results here with the rmse30 vector to assess
%the improvement in the forecast skill compared to the 30-mean
fma_1_comp1 = zeros(1,29);
fma_1_comp2 = zeros(1,29);
fma_1_comp3 = zeros(1,29);
fma_1_comp4 = zeros(1,29);
for loc = 1:29;
   fma_1_comp1(loc) = (rmse30(loc) - fma_1_rmse1(loc)) / rmse30(loc);
   fma_1_comp2(loc) = (rmse30(loc) - fma_1_rmse2(loc)) / rmse30(loc);
   fma_1_comp3(loc) = (rmse30(loc) - fma_1_rmse3(loc)) / rmse30(loc);
   fma_1_comp4(loc) = (rmse30(loc) - fma_1_rmse4(loc)) / rmse30(loc);
end
fma_1_sk = 100*[fma_1_comp1' fma_1_comp2' fma_1_comp3' fma_1_comp4'];

%---------------------------------------------
% Recalculate for FMA | Lag = 2 Year
%---------------------------------------------
%Divide out the forecast values into each alternative for this lag time
fma_2_qf1 = fma_fall(233:261,:)';
fma_2_qf2 = fma_fall(262:290,:)';
fma_2_qf3 = fma_fall(291:319,:)';
fma_2_qf4 = fma_fall(320:348,:)';

% Find difference between forecast values and observed values at
% each station (the error matrix).
fma_2_e1 = qo - fma_2_qf1;
fma_2_e2 = qo - fma_2_qf2;
fma_2_e3 = qo - fma_2_qf3;
fma_2_e4 = qo - fma_2_qf4;

%Find the square of each element in the error matrix
fma_2_se1 = zeros(70,29);
fma_2_se2 = zeros(70,29);
fma_2_se3 = zeros(70,29);
fma_2_se4 = zeros(70,29);
for loc = 1:29
   for yr = 1:70
      fma_2_se1(yr,loc) = fma_2_e1(yr,loc)^2;
      fma_2_se2(yr,loc) = fma_2_e2(yr,loc)^2;
      fma_2_se3(yr,loc) = fma_2_e3(yr,loc)^2;
      fma_2_se4(yr,loc) = fma_2_e4(yr,loc)^2;
   end
end
```

```
%Find the mean of the squared errors at each qauge location
fma_2_mse1 = mean(fma_2_se1,1);
fma_2_mse2 = mean(fma_2_se2,1);
fma_2_mse3 = mean(fma_2_se3,1);
fma_2_mse4 = mean(fma_2_se4,1);

%Find the root of the mean squared error at each location
fma_2_rmse1 = sqrt(fma_2_mse1);
fma_2_rmse2 = sqrt(fma_2_mse2);
fma_2_rmse3 = sqrt(fma_2_mse3);
fma_2_rmse4 = sqrt(fma_2_mse4);

%Compare the results here with the rmse30 vector to assess
%the improvement in the forecast skill compared to the 30-mean
fma_2_comp1 = zeros(1,29);
fma_2_comp2 = zeros(1,29);
fma_2_comp3 = zeros(1,29);
fma_2_comp4 = zeros(1,29);
for loc = 1:29;
   fma_2_comp1(loc) = (rmse30(loc) - fma_2_rmse1(loc)) / rmse30(loc);
   fma_2_comp2(loc) = (rmse30(loc) - fma_2_rmse2(loc)) / rmse30(loc);
   fma_2_comp3(loc) = (rmse30(loc) - fma_2_rmse3(loc)) / rmse30(loc);
   fma_2_comp4(loc) = (rmse30(loc) - fma_2_rmse4(loc)) / rmse30(loc);
end

fma_2_sk = 100*[fma_2_comp1' fma_2_comp2' fma_2_comp3' fma_2_comp4'];
toc

rmse_0675 = [djf_0_sk jfm_0_sk fma_0_sk djf_1_sk jfm_1_sk fma_1_sk djf_2_sk
jfm_2_sk fma_2_sk];
xlswrite('L:/Kenneth Data/Matlab/Phase2/Hondo.xls',rmse_0675, 'RMSE','B2');
save rmse_0675 rmse_0675
toc
```

A1.5.6 Forecast and Error Plotting Code

```
%------------------------------------------------------------------------
%Code to plot the forecast and observed values at certain stations
%------------------------------------------------------------------------

%Read in the proper values from the forecast array, and the relative error
%arrays
load f_0655; load re_0655_all; load qoyr_all
load f_5605; load re_5605_all;
load f_clim;
```

```
%Pull out the observed flow for the eight gauges used for plotting:
o = qoyr_all;
obs = [o(1:100,1) o(1:100,3) o(1:100,4) o(1:100,9) ...
   o(1:100,12) o(1:100,18) o(1:100,20) o(1:100,27)];
clear o

%Pull out the 8 gauges that will be displayed from the RE array.
a = re_0655_all;
aa = [a(:,59,2) a(:,61,2) a(:,62,2) a(:,67,2) a(:,70,2) a(:,76,2) a(:,78,2) a(:,85,2) ...
   a(:,175,2) a(:,177,2) a(:,178,2) a(:,183,2) a(:,186,2) a(:,192,2) a(:,194,2) a(:,201,2) ...
   a(:,291,2) a(:,293,2) a(:,294,2) a(:,299,2) a(:,302,2) a(:,308,2) a(:,310,2) a(:,317,2)];
re1 = 100*reshape(aa,50,8,3); clear a; clear aa

b = re_5605_all;
bb = [b(:,59,2) b(:,61,2) b(:,62,2) b(:,67,2) b(:,70,2) b(:,76,2) b(:,78,2) b(:,85,2) ...
   b(:,175,2) b(:,177,2) b(:,178,2) b(:,183,2) b(:,186,2) b(:,192,2) b(:,194,2) b(:,201,2) ...
   b(:,291,2) b(:,293,2) b(:,294,2) b(:,299,2) b(:,302,2) b(:,308,2) b(:,310,2) b(:,317,2)];
re2 = 100*reshape(bb,50,8,3); clear b; clear bb;

%Pull out the eight guages that will be used for the forecast matrix
fa = f_0655;
faa = [fa(:,59,2) fa(:,61,2) fa(:,62,2) fa(:,67,2) fa(:,70,2) fa(:,76,2) fa(:,78,2) fa(:,85,2) ...
   fa(:,175,2) fa(:,177,2) fa(:,178,2) fa(:,183,2) fa(:,186,2) fa(:,192,2) fa(:,194,2)
fa(:,201,2) ...
   fa(:,291,2) fa(:,293,2) fa(:,294,2) fa(:,299,2) fa(:,302,2) fa(:,308,2) fa(:,310,2)
fa(:,317,2)];
fcast1 = reshape(faa,50,8,3); clear fa; clear faa;

fb = f_5605;
fbb = [fb(:,59,2) fb(:,61,2) fb(:,62,2) fb(:,67,2) fb(:,70,2) fb(:,76,2) fb(:,78,2) fb(:,85,2) ...
   fb(:,175,2) fb(:,177,2) fb(:,178,2) fb(:,183,2) fb(:,186,2) fb(:,192,2) fb(:,194,2)
fb(:,201,2) ...
   fb(:,291,2) fb(:,293,2) fb(:,294,2) fb(:,299,2) fb(:,302,2) fb(:,308,2) fb(:,310,2)
fb(:,317,2)];
fcast2 = reshape(fbb,50,8,3); clear fb; clear fbb;

fcast3 = [f_clim(:,1) f_clim(:,3) f_clim(:,4) f_clim(:,9) f_clim(:,12) ...
   f_clim(:,18) f_clim(:,20) f_clim(:,27)];

%Create the index labels and the -0.5 and 0.5 lines for the RE plots
x1 = 1906:1:1955; x2 = 1956:1:2005; x3 = 1906:1:2005;
line2 = zeros(100,1);
line1 = line2-50;
line3 = line2+50;
lines = [line1 line2 line3];
```

```
titlesa = {'09072500','09109000','09124700','09211200',...
   '09251000','09355500','09380000','09426000'};
titlesb = {'Colorado at Glenwood Springs, CO','Taylor below Taylor Park Res',...
   'Gunnison above Blue Mesa Res','Green below Fontenelle Res',...
   'Yampa near Maybell, CO','San Juan near Archuleta, NM', ...
   'Colorado at Lees Ferry, AZ','Bill Williams below Alamo Dam'};
figs = {'(a)','(b)','(c)','(d)','(e)','(f)','(g)','(h)'};

%create plots at each station of the forecast and observed values
%Create position array
l = 0.1; b = 0.05; h = 0.15; w = 0.39;
p1 = [l .5+l l .5+l l .5+l l .5+l];
p2 = [b+.75 b+.75 b+.5 b+.5 b+.25 b+.25 b b];
p3 = [w w w w w w w w];
p4 = [h h h h h h h h];

pos = [p1' p2' p3' p4'];

figure
set(gcf,'PaperPosition',[.75 1 7 9])
for j = 1:8
subplot(4,2,j,'Position',pos(j,:));
%plot(x1,fcast1(:,j,1),'g-'); hold on
plot(x1,fcast1(:,j,2),'b-'); hold on
%plot(x1,fcast1(:,j,3),'r-'); hold on
%plot(x2,fcast2(:,j,1),'g-'); hold on
plot(x2,fcast2(:,j,2),'b-'); hold on
%plot(x2,fcast2(:,j,3),'r-'); hold on
plot(x3,obs(:,j),'k-'); hold on;
plot(x3,fcast3(:,j),'k--');
title({titlesa{j},titlesb{j}},'FontName','Times');
xlabel(figs{j},'FontName','Times');
ylabel({'Streamflow','Vol (MAF)'},'FontName','Times')
end

%create plots of the relative errors at each gauge location
figure
set(gcf,'PaperPosition',[.75 1 7 9])
for k = 1:8
   subplot(4,2,k,'Position',pos(k,:));
patch([1931 1931 1940 1940],[-100 100 100 -100],...
   [255/255 234/255 170/255], 'EdgeColor','none'); hold on
%patch([1943 1943 1946 1946],[-100 100 100 -100],...
%    [255/255 234/255 170/255], 'EdgeColor','none');
patch([1950 1950 1956 1956],[-100 100 100 -100],...
   [255/255 234/255 170/255],'EdgeColor','none');
```

```
patch([1959 1959 1969 1969],[-100 100 100 -100],...
   [255/255 234/255 170/255],'EdgeColor','none');
%patch([1972 1972 1977 1977],[-100 100 100 -100],...
%    [255/255 234/255 170/255],'EdgeColor','none');
patch([1988 1988 1996 1996],[-100 100 100 -100],...
   [255/255 234/255 170/255],'EdgeColor','none');
patch([2000 2000 2005 2005],[-100 100 100 -100],...
   [255/255 234/255 170/255],'EdgeColor','none');
%plot(x1,re1(:,k,1),'r-'); hold on;
plot(x1,re1(:,k,2),'b-'); hold on;
%plot(x1,re1(:,k,3),'g-'); hold on;
%plot(x2,re2(:,k,1),'r-'); hold on;
plot(x2,re2(:,k,2),'b-'); hold on;
%plot(x2,re2(:,k,3),'g-'); hold on;
plot(x3,lines(:,1),'k:'); hold on;
plot(x3,lines(:,2),'k-'); hold on;
plot(x3,lines(:,3),'k:'); hold on;
axis([1905 2005 -100 100]);
title({titlesa{k},titlesb{k}},'FontName','Times');
xlabel(figs{k},'FontName','Times');
ylabel('% Rel. Error','FontName','Times')
end
```

APPENDIX 2

SUPPLEMENTAL FIGURES

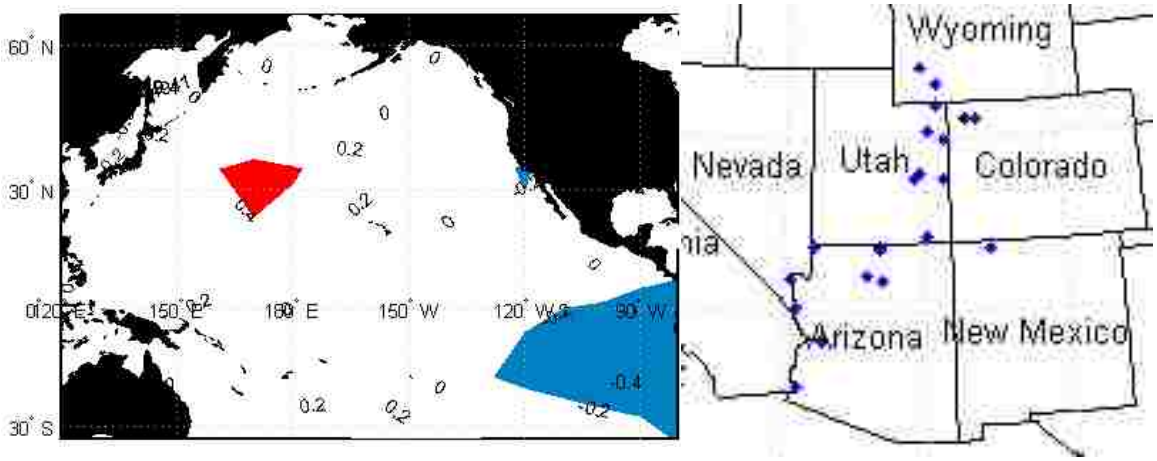

Heterogeneous correlation map created form the SVD analysis between yearly SST values from one water year compared with yearly streamflow volume for the following water year.

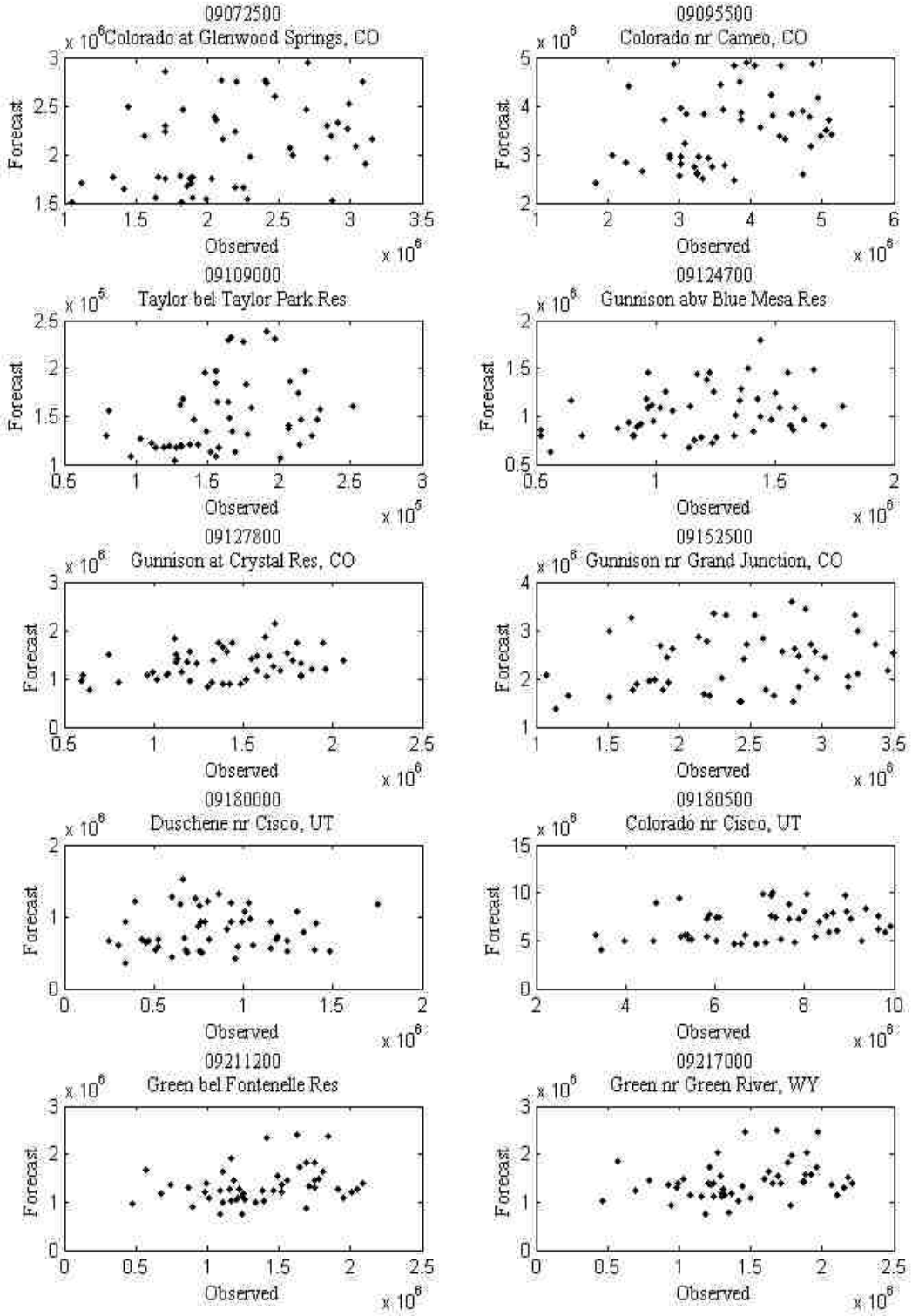

0-Year lag scatter plots of forecast and observed values (gauges 1 – 10)

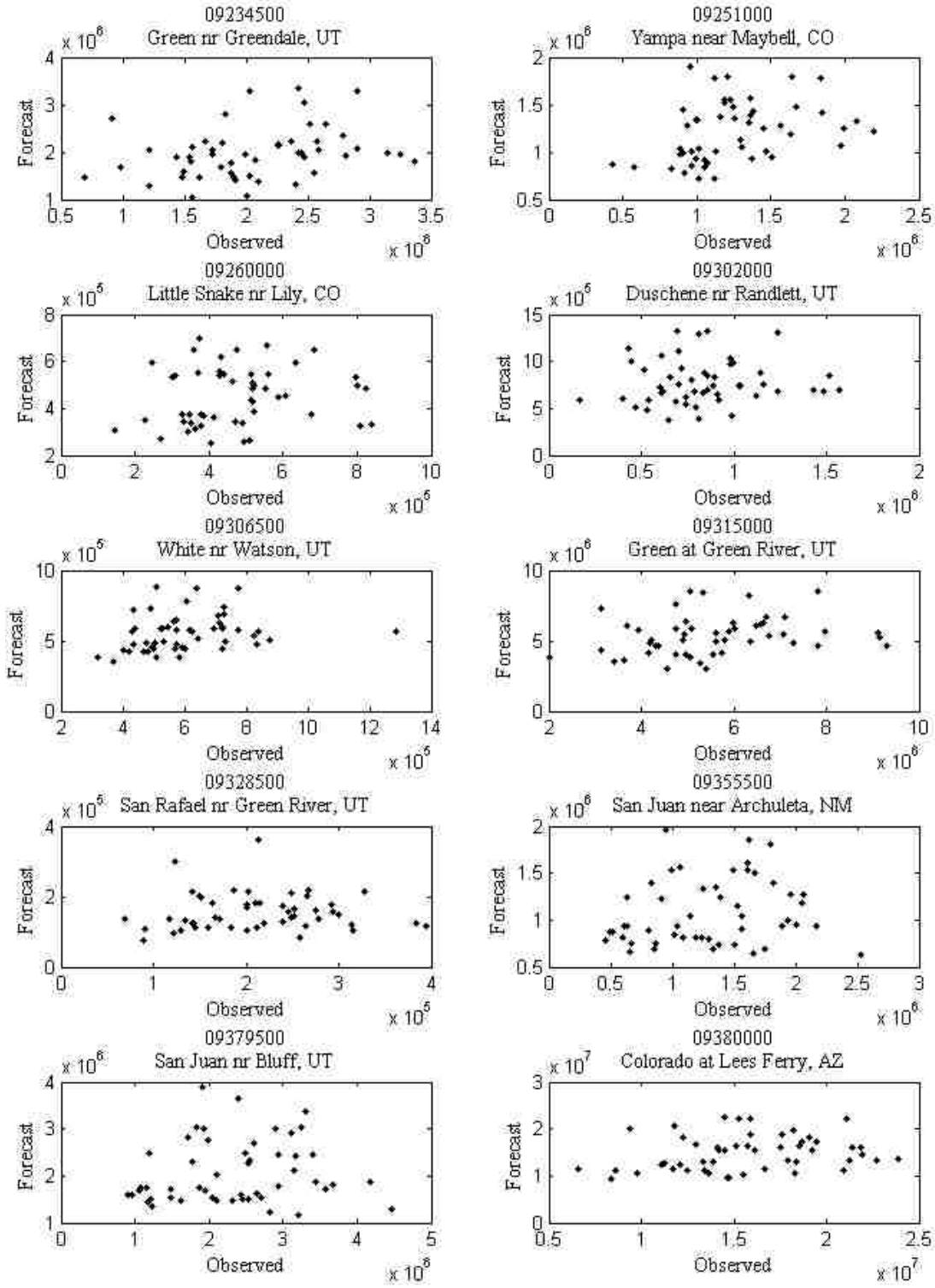

0-Year lag scatter plots of forecast and observed values (gauges 11 – 20)

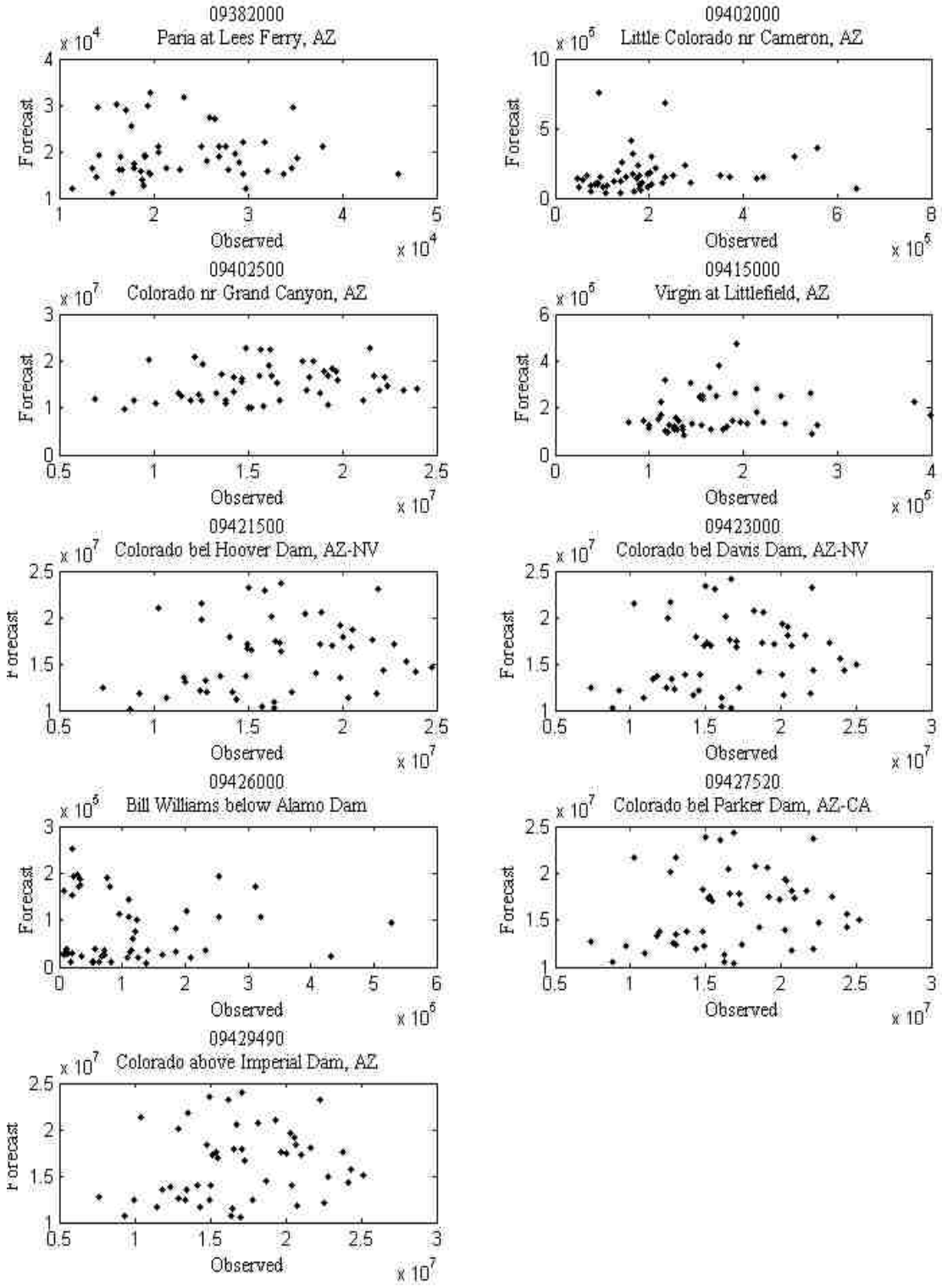

0-Year lag scatter plots of forecast and observed values (gauges 21 – 30)

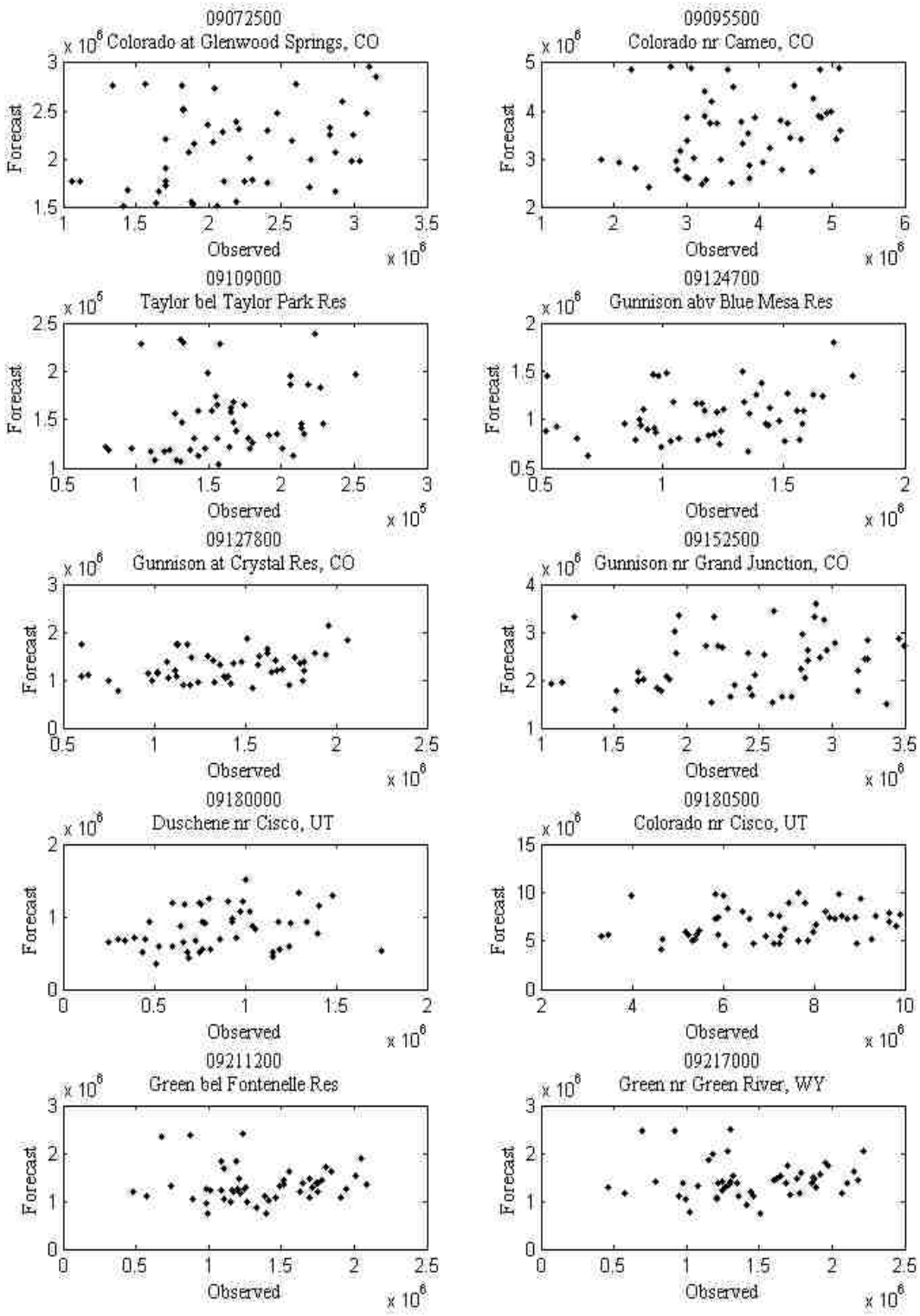

1-Year lag scatter plots of forecast and observed values (gauges 1 – 10)

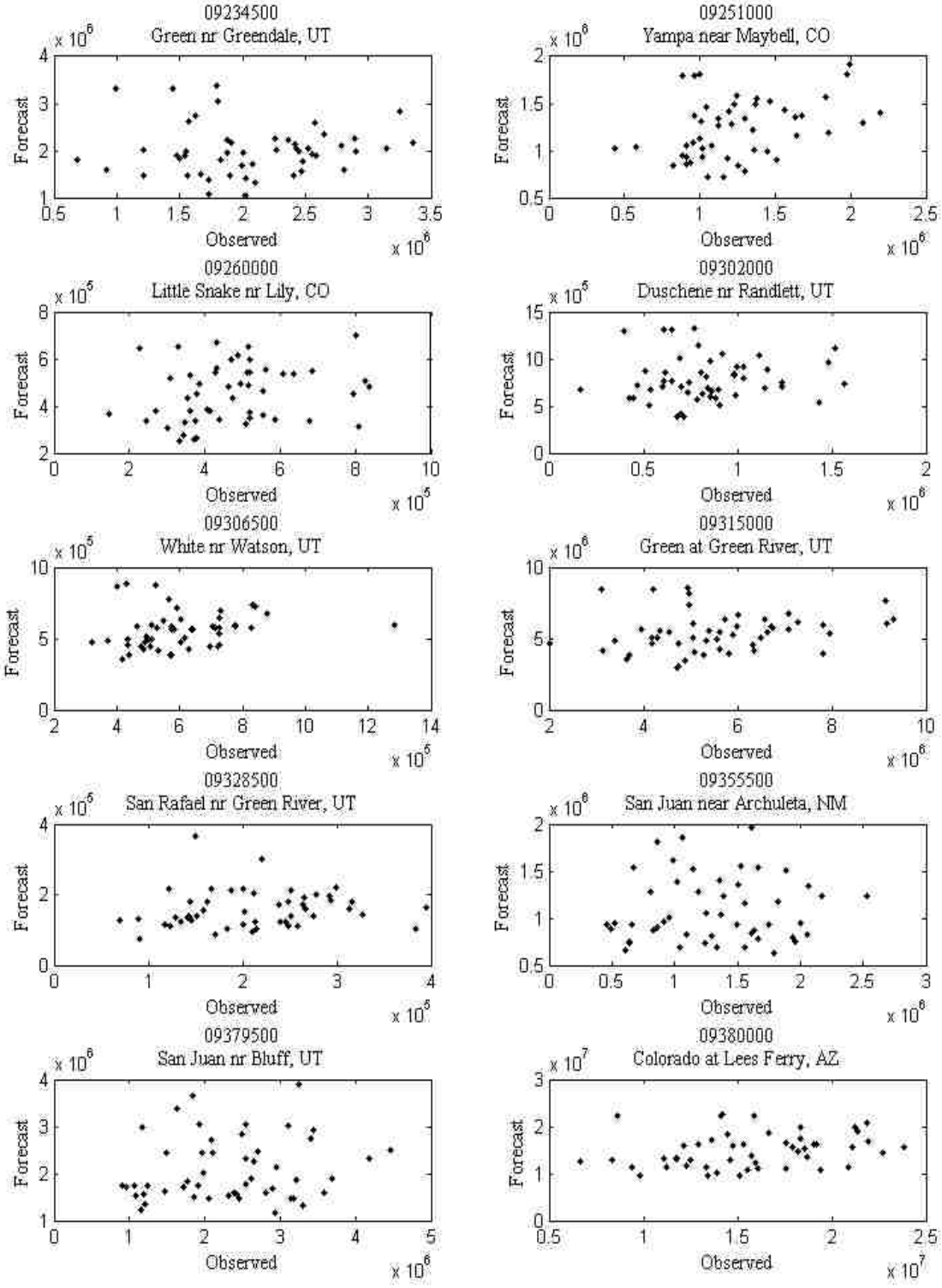

1-Year lag scatter plots of forecast and observed values (gauges 11 – 20)

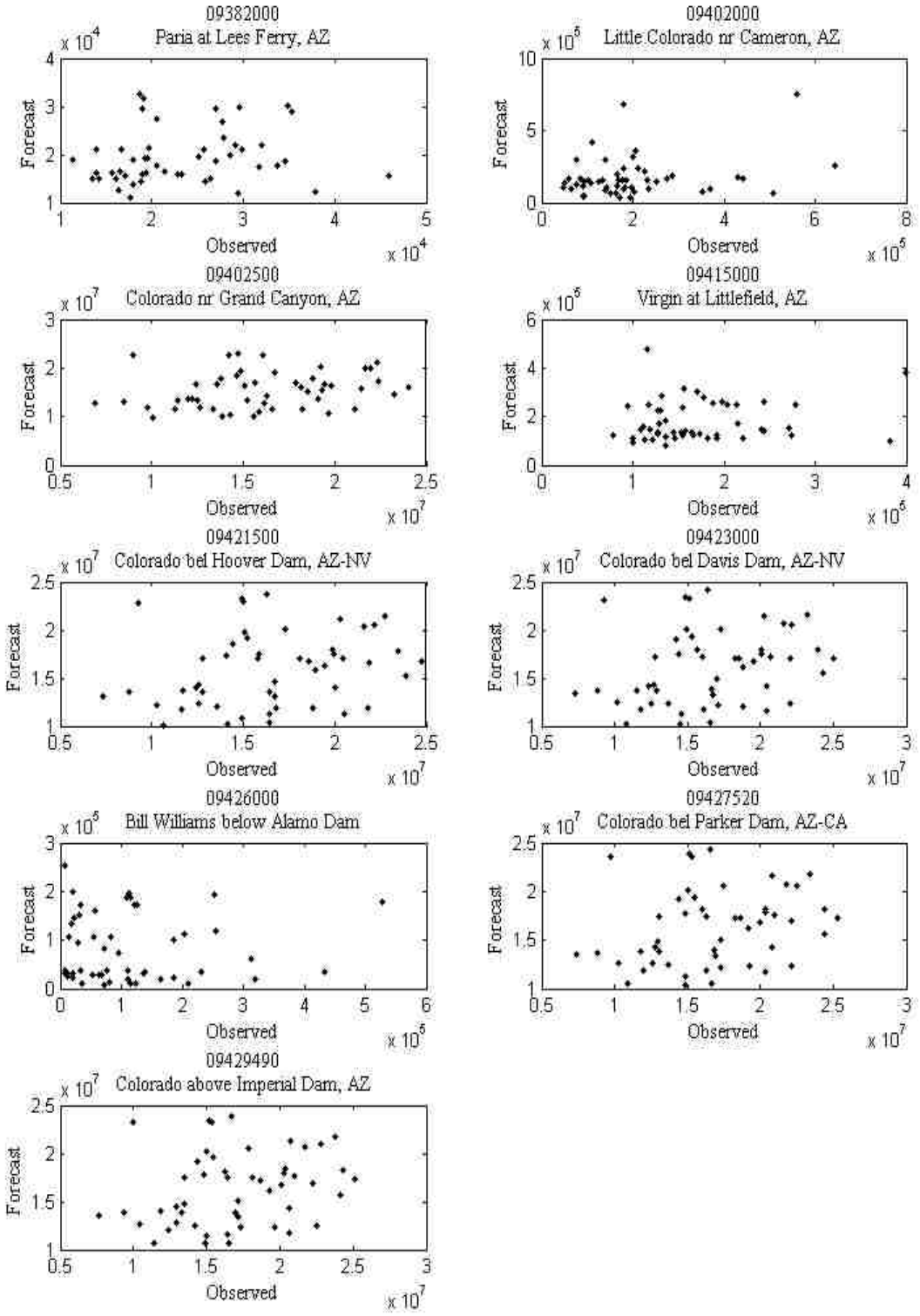

1-Year lag scatter plots of forecast and observed values (gauges 21 – 39)

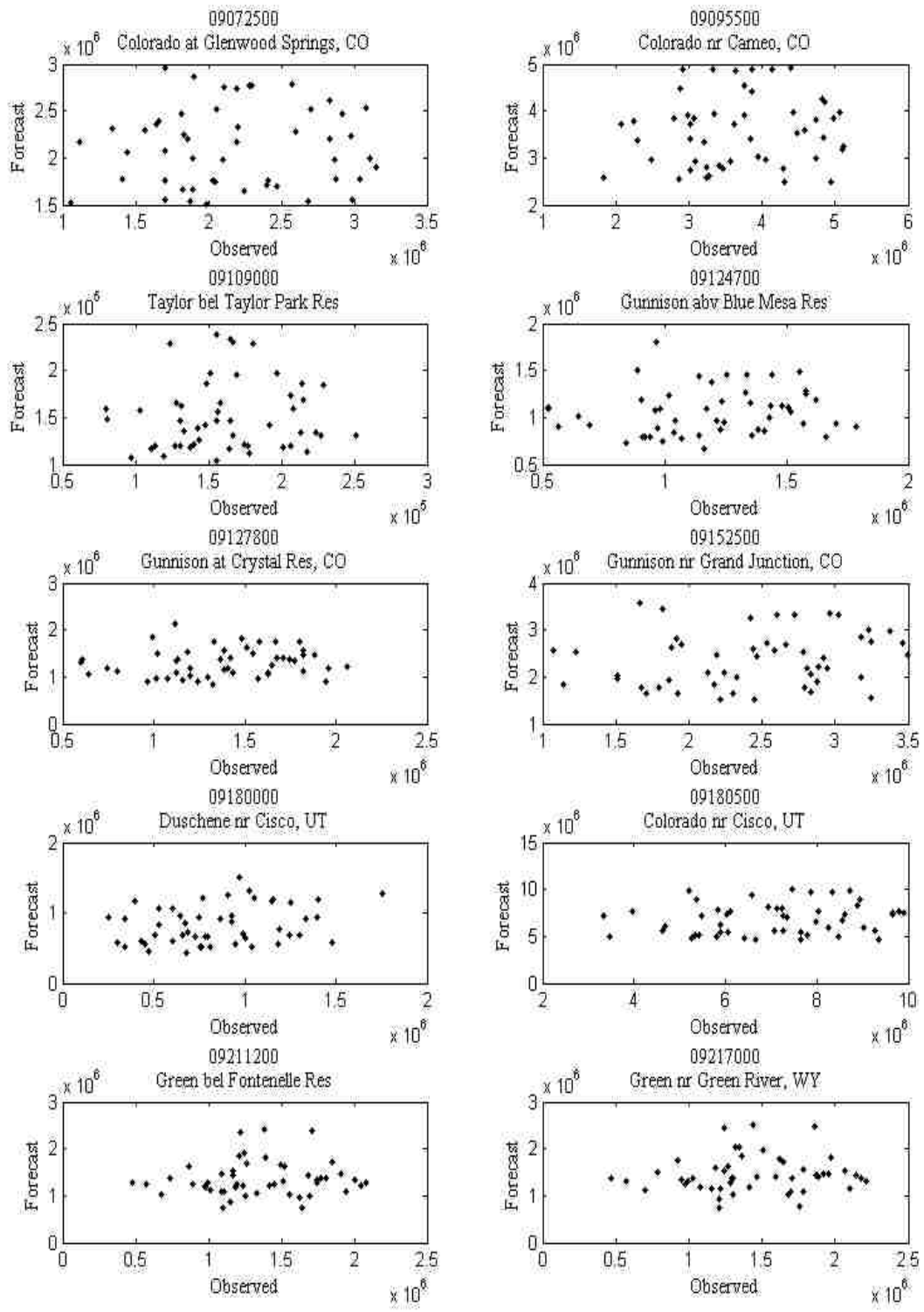

2-Year lag scatter plots of forecast and observed values (gauges 1 – 10)

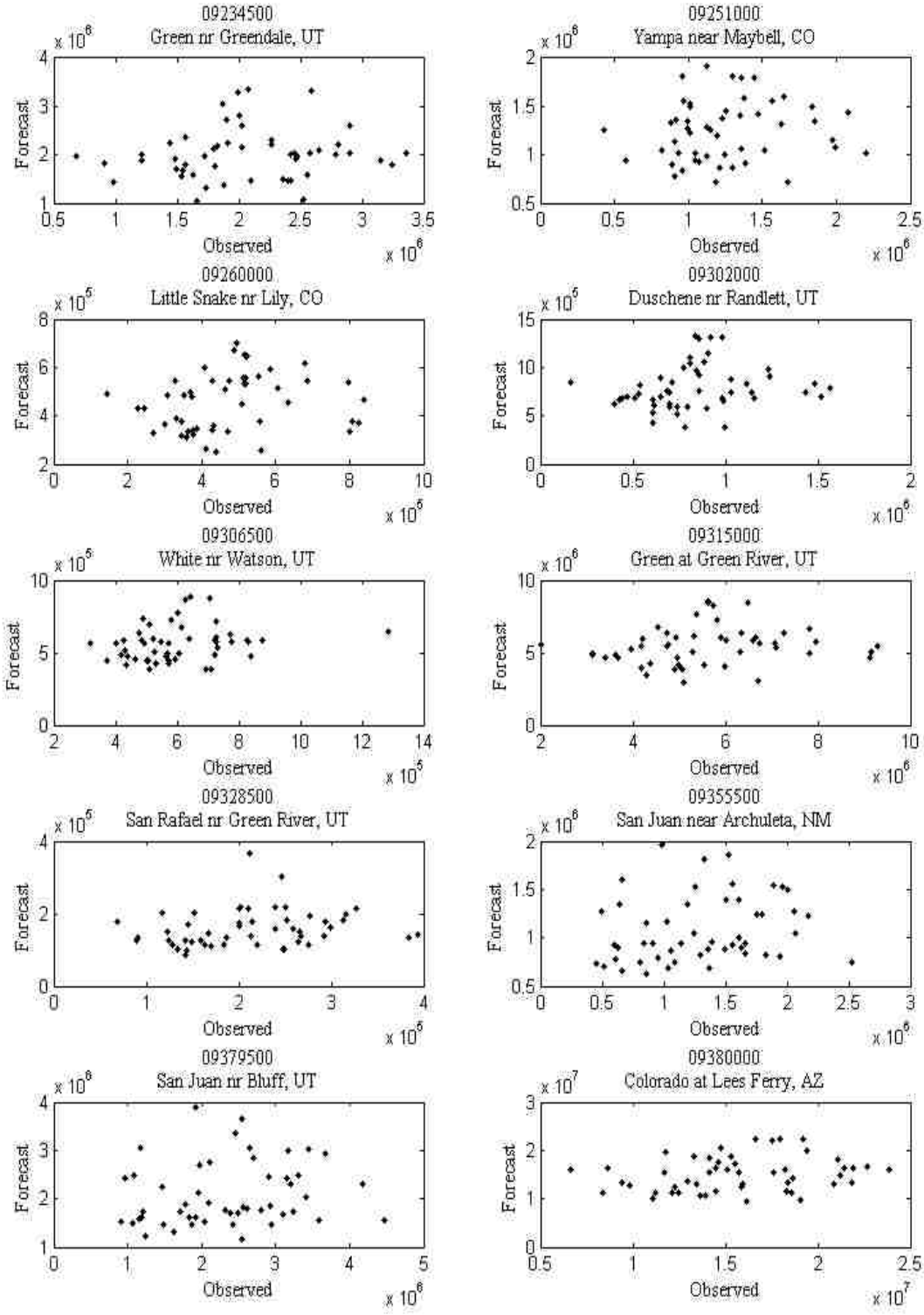

2-Year lag scatter plots of forecast and observed values (gauges 11 – 20)

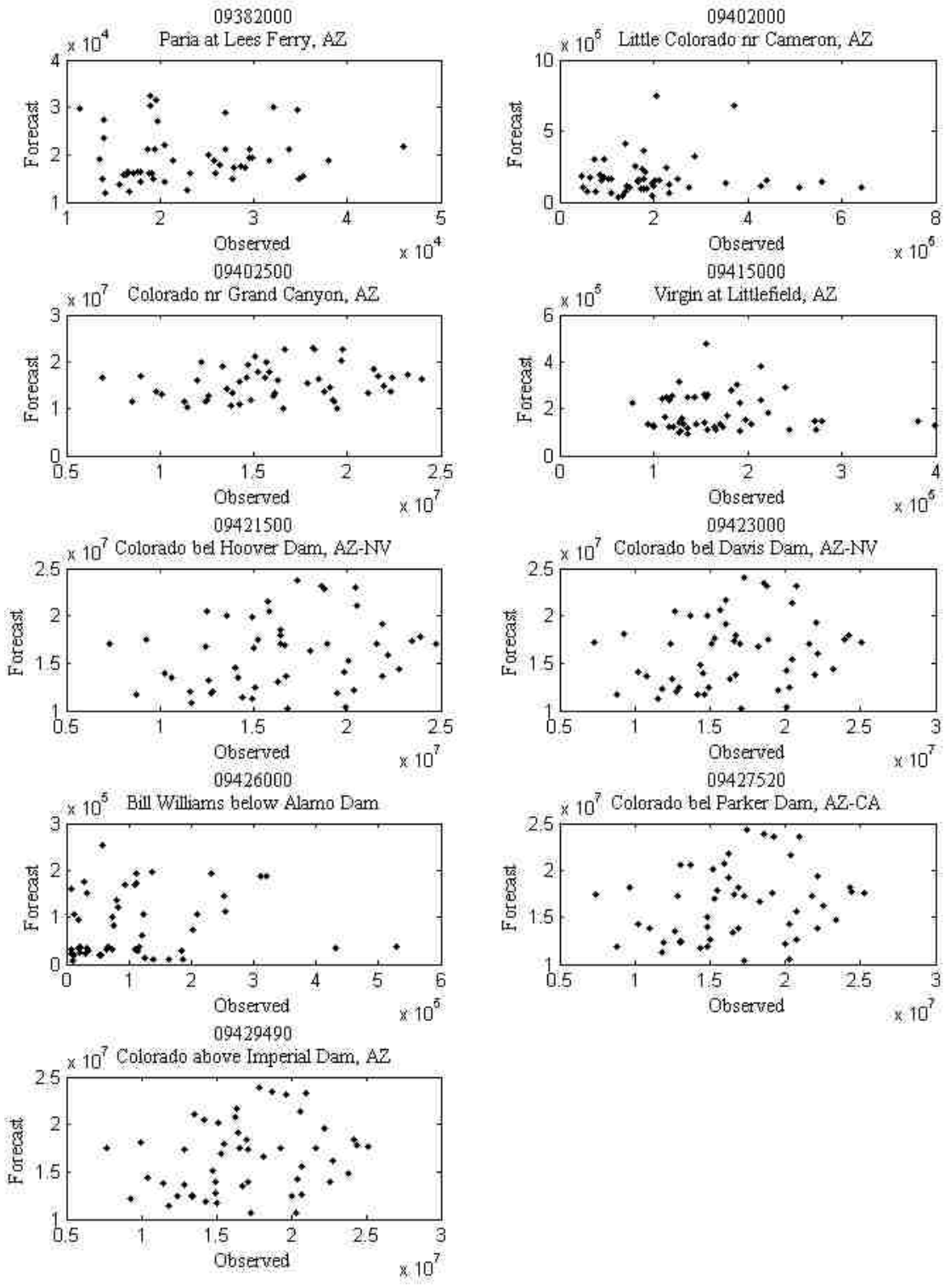

2-Year lag scatter plots of forecast and observed values (gauges 21 – 29)

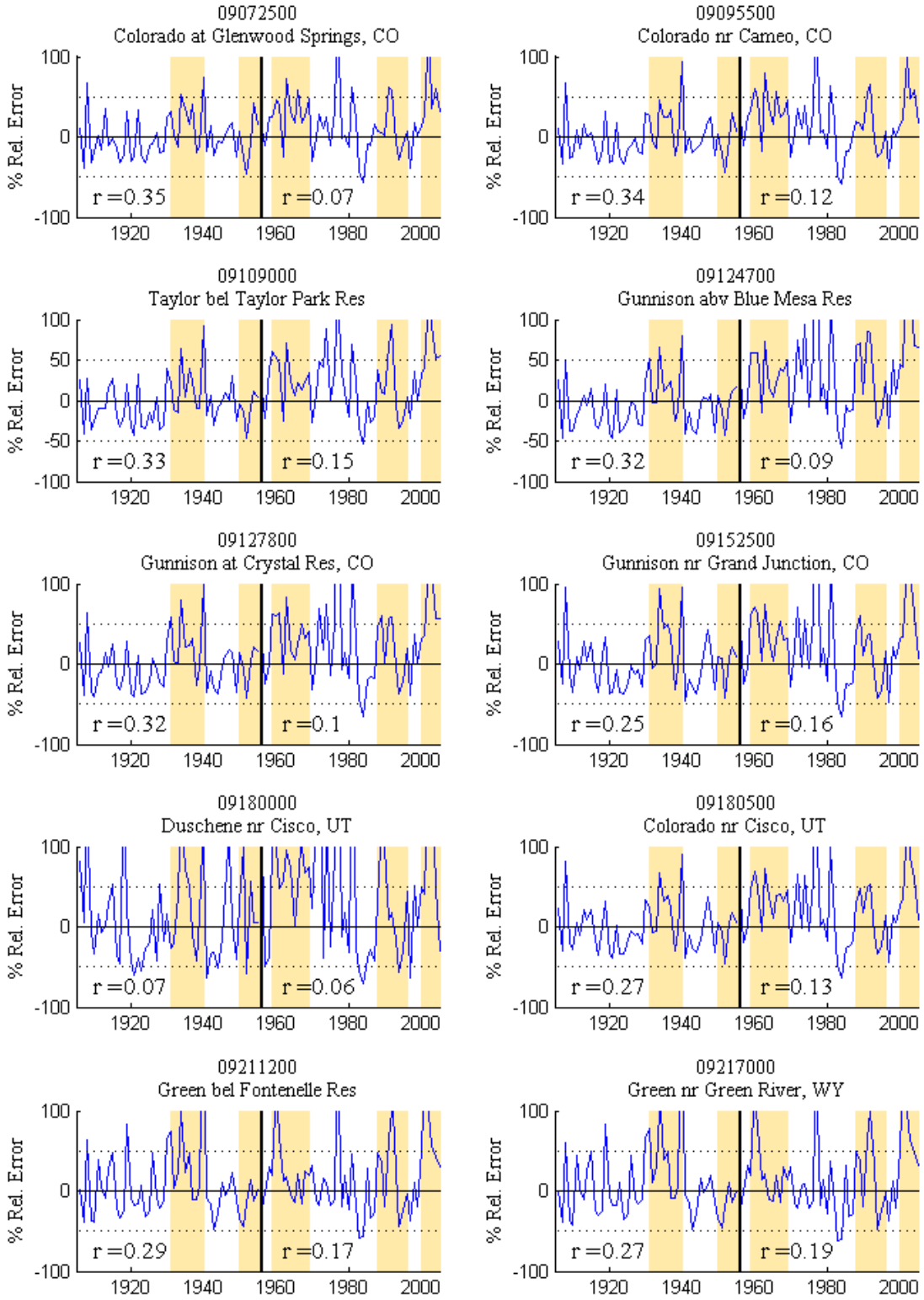

0-Year lag relative error plots for forecasts (gauges 1 – 10) whosing the correlation values between the forecast and observed

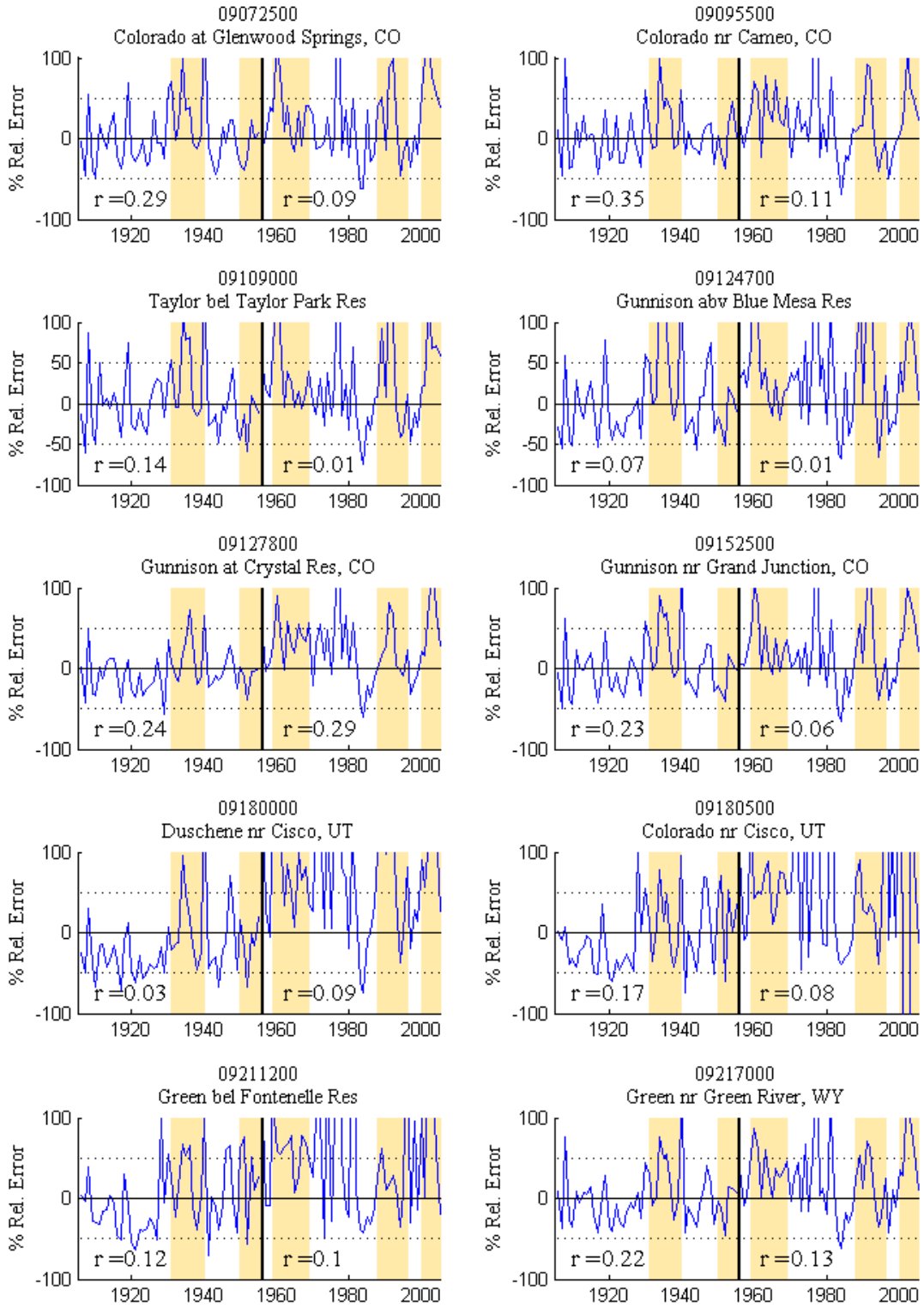

0-Year lag relative error plots for forecasts (gauges 11 – 20) whosing the correlation values between the forecast and observed

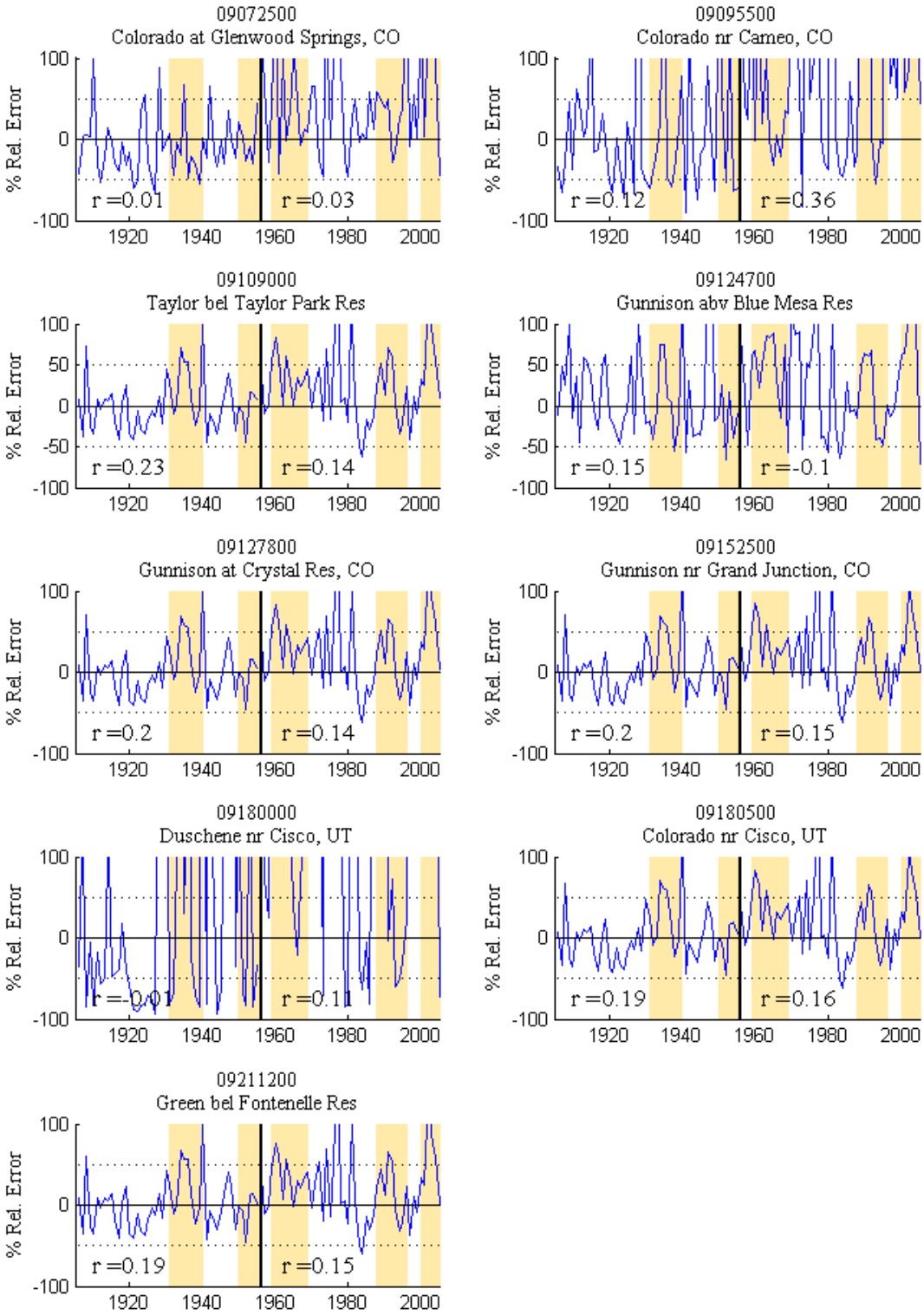

0-Year lag relative error plots for forecasts (gauges 21 – 29) whosing the correlation values between the forecast and observed

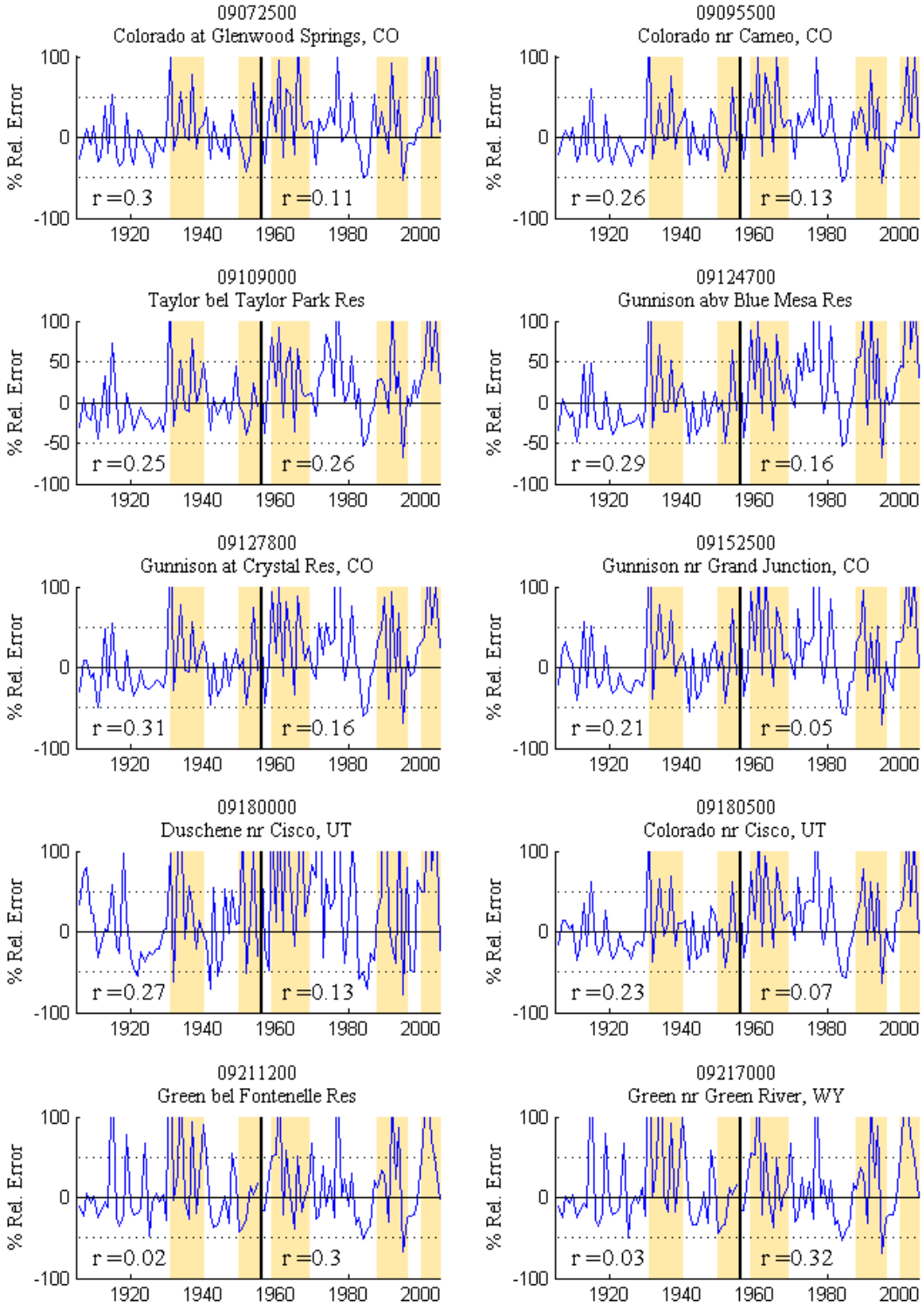

1-Year lag relative error plots for forecasts (gauges 1 – 10) whosing the correlation values between the forecast and observed

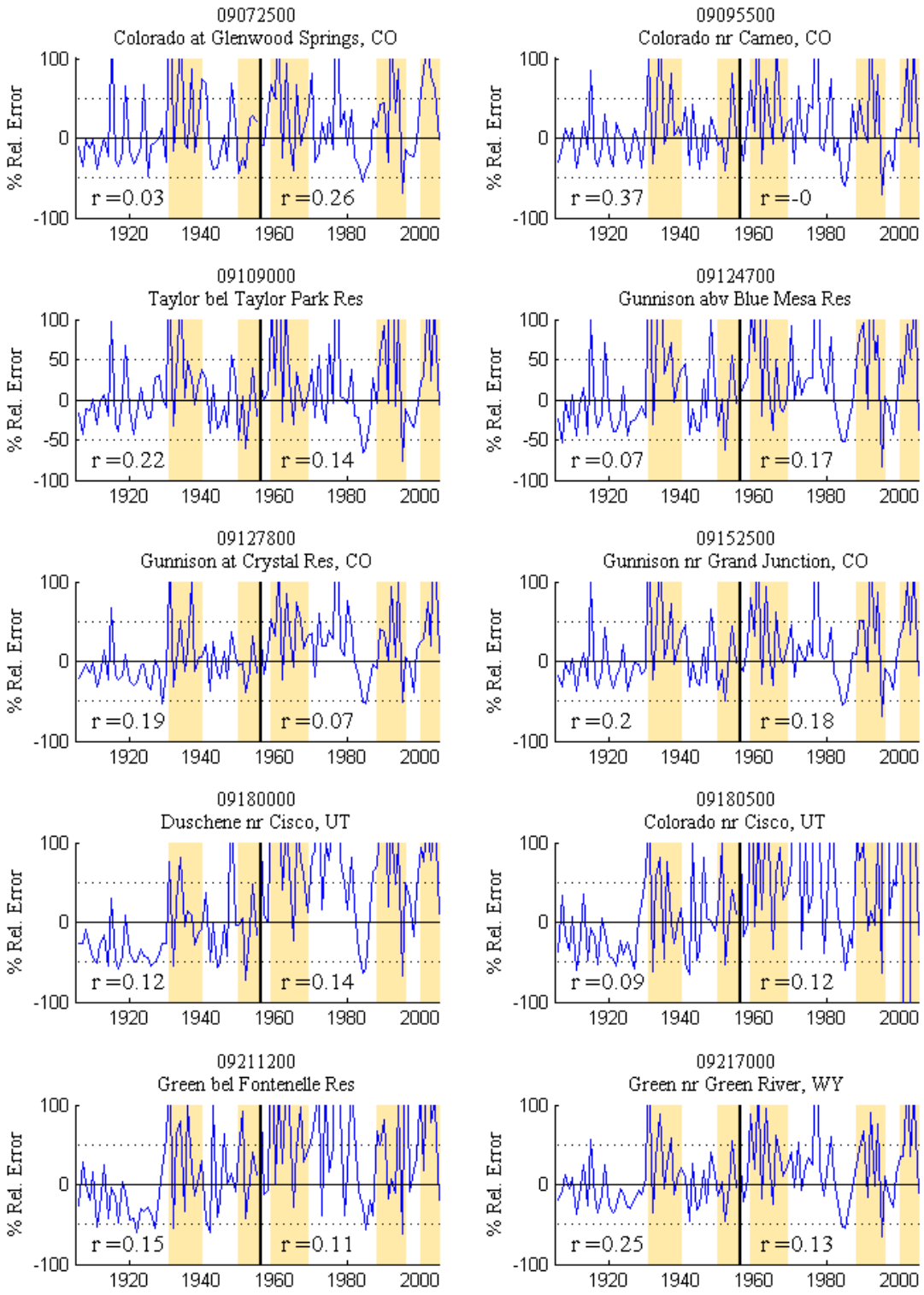

1-Year lag relative error plots for forecasts (gauges 11 – 20) whosing the correlation values between the forecast and observed

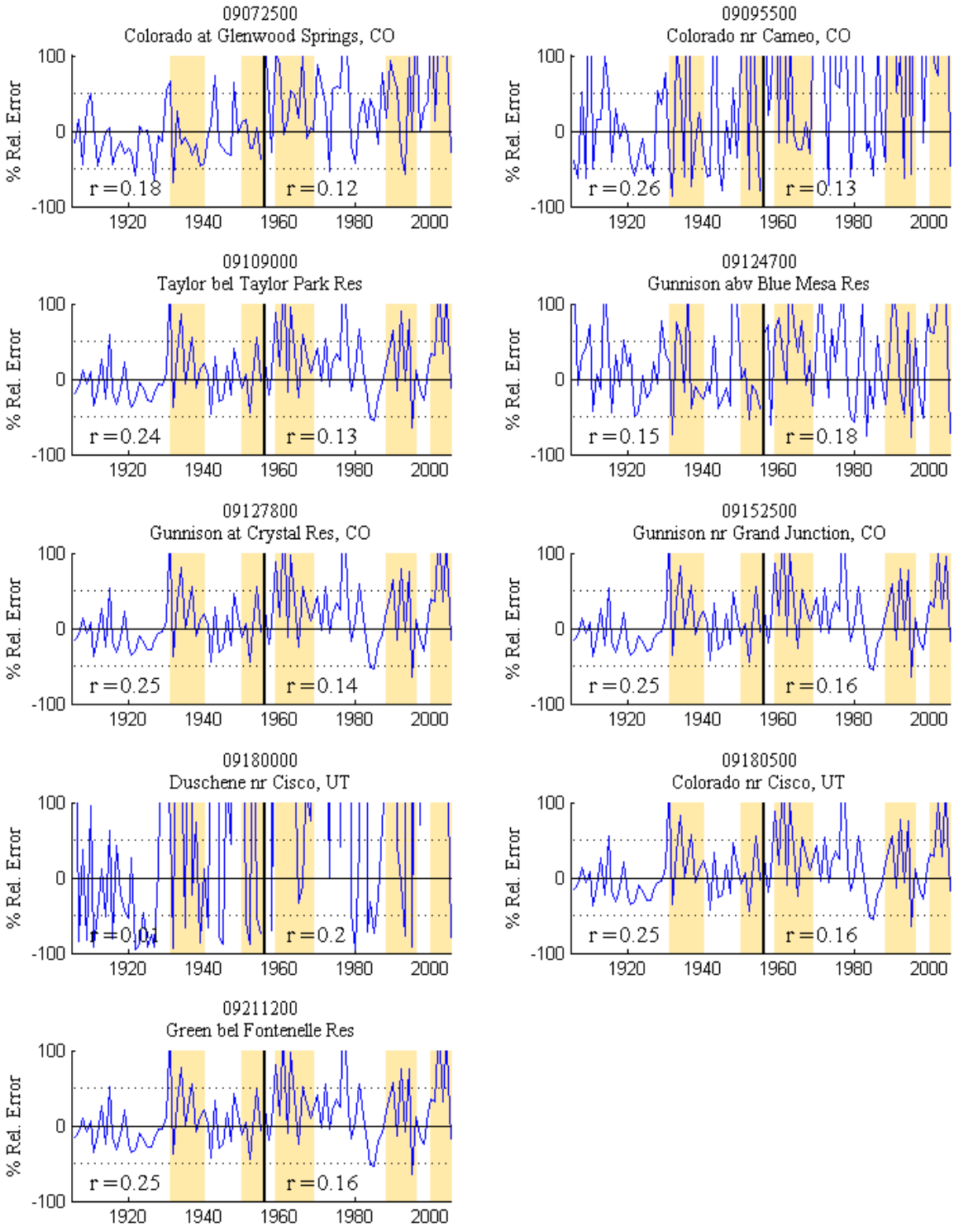

1-Year lag relative error plots for forecasts (gauges 21 – 29) whosing the correlation values between the forecast and observed

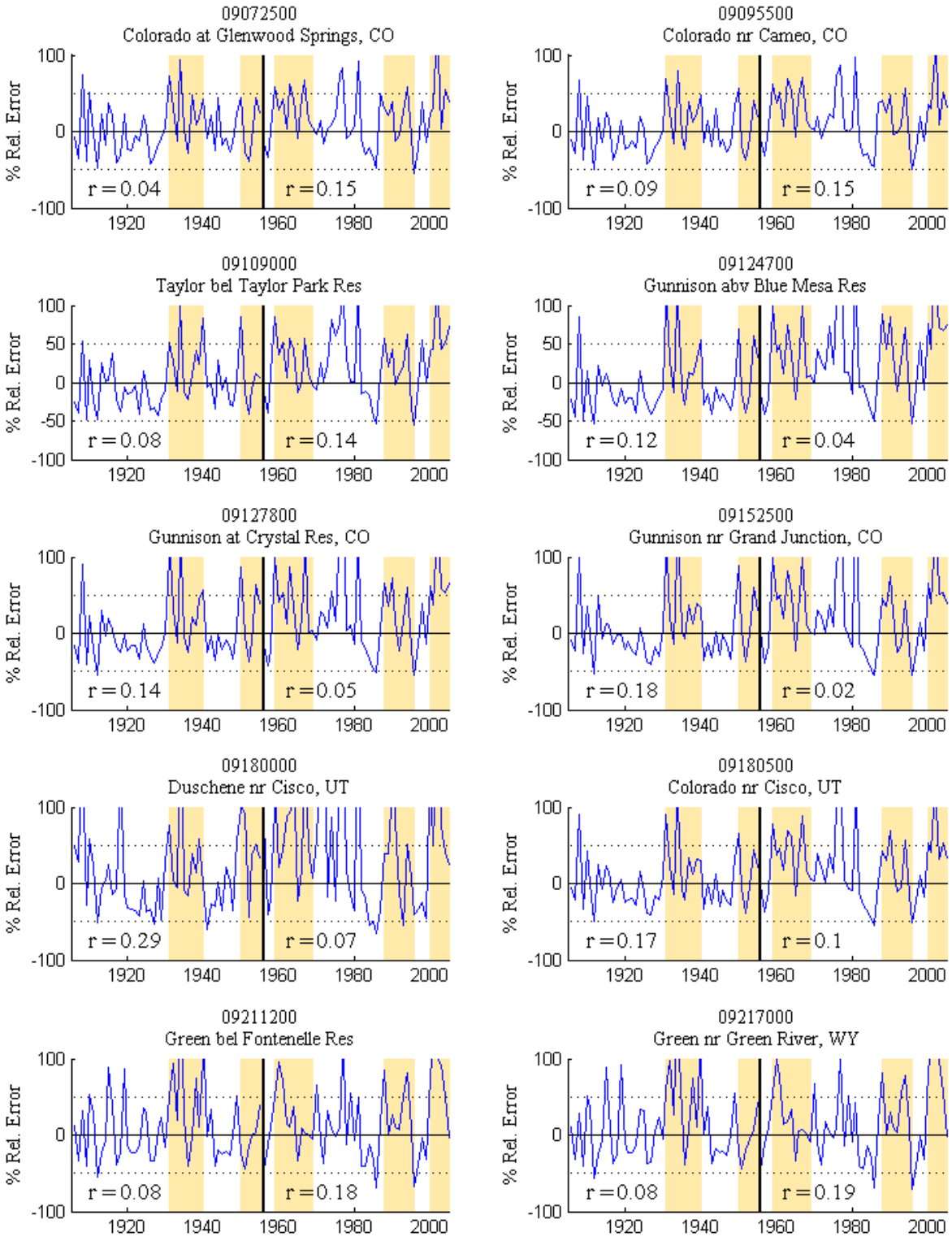

2-Year lag relative error plots for forecasts (gauges 1 – 10) whosing the correlation values between the forecast and observed

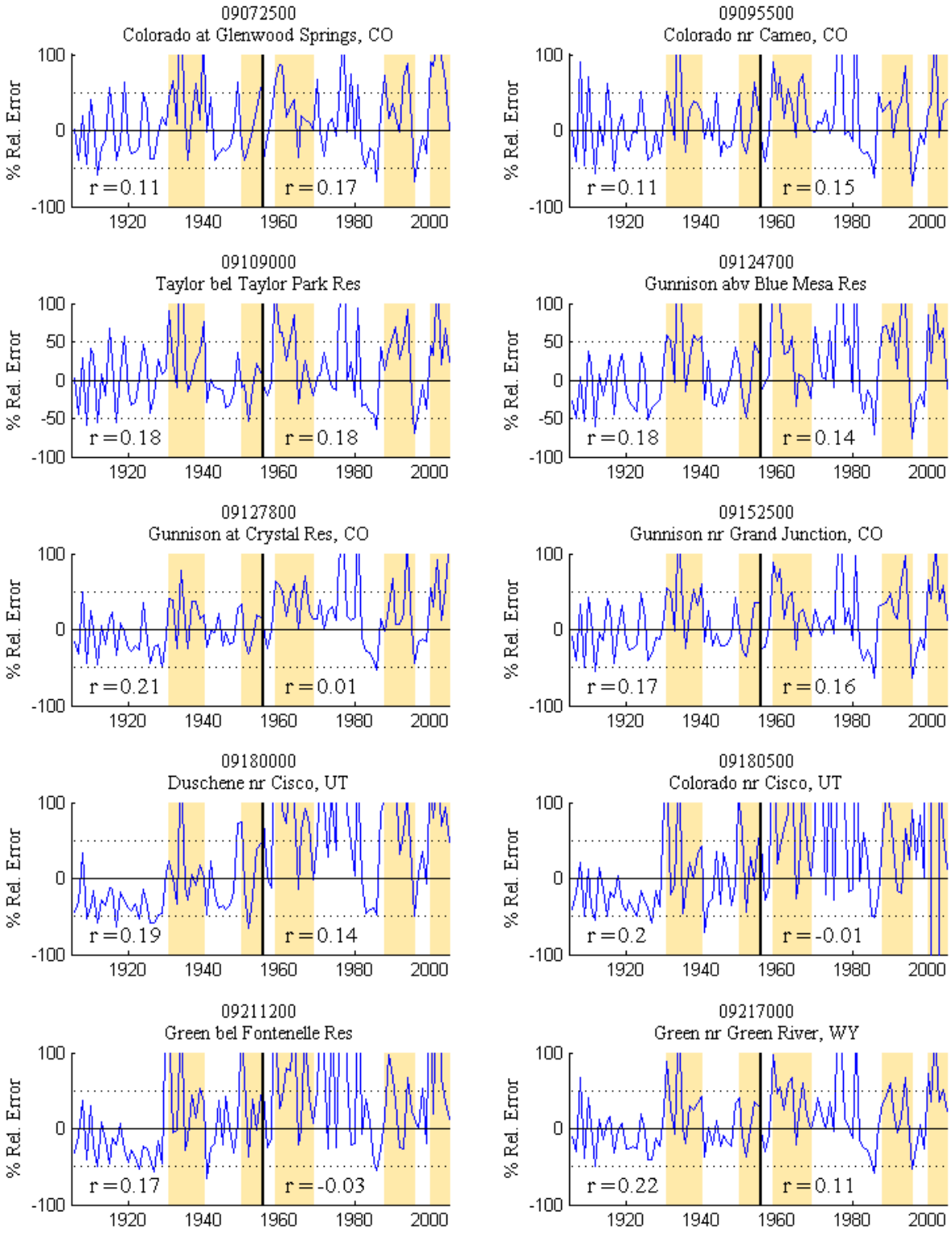

2-Year lag relative error plots for forecasts (gauges 11 – 20) whosing the correlation values between the forecast and observed

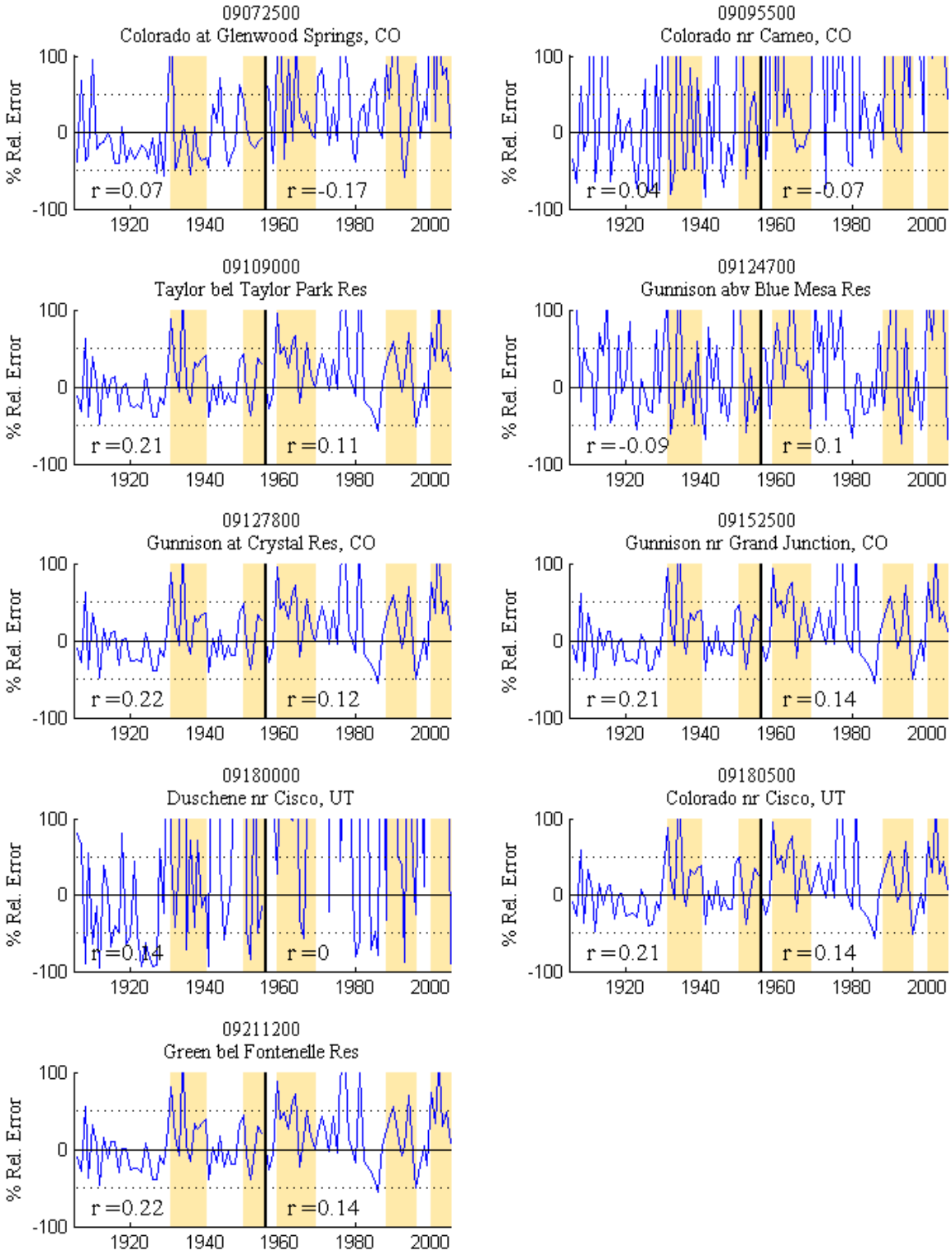

2-Year lag relative error plots for forecasts (gauges 21 – 29) whosing the correlation values between the forecast and observed

REFERENCES

Abramowitz, M. and I.A. Stegun, 1972. *Handbook of Mathematical Functions*. Dover Publications, New York

Adam, J.C., A.F. Hamlet, D.P. Lettenmaier, 2009. Implications of global climate change for snowmelt hydrology in the twenty-first century. Hydrological Processes 23(7): 962-97

Alder, H.L., E.B. Roessler 1977. *Introduction To Probability And Statistics,* Edition: 6, Revised. W H Freeman & Company Limited

An, S.I. 2004. Interdecadal Changes In The El Niño–La Nina Asymmetry. *Geophys. Res. Letters*, **31**(L23210)

Apipattanavis, S., G.J. McCabe, B. Rajagopalan, and S. Gangopadhyay, 2009. Joint Spatiotemporal Variability of Global Sea Surface Temperatures and Global Palmer Drought Severity Index Values. 22(23): 6251-6267.

Athanasiadis, P.J., J.M. Wallace and J.J. Wettstein, 2010. Patterns of Wintertime Jet Stream Variability and Their Relation to the Storm Tracks. J. Atmos. Sci., 67, 1361–1381.

Aziz, O.A., G.A. Tootle, S.T. Gray, And T.C. Piechota 2010. Identification Of Pacific Ocean Sea Surface Temperature Influences Of Upper Colorado River Basin Snowpack. *J Of Water Resour. Res.* (In Publication)

Barbe, P., And P. Bertail, 1995. *The Weighted Bootstrap*. Springer-Verlag, New York, NY

Barnston, A.G., R.E. Livezey 1987. Classification, Seasonality And Persistence Of Low-Frequency Atmospheric Circulation Patterns. *Month. Weather Rev.*115(6) 1083.

Baughman, R.G., D.M. Fuquay, And P.W. Mielke Jr., 1976. Statistical Analysis Of A Randomized Lightning Modification Experiment. *Journal Of Applied Meterology*, **15**, 790-794.

Beamish, R. J. 1993. Climate And Exceptional Fish Production Off The West Coast Of North America. *Can. J. Fish. Aquat. Sci.*, 50, 2270–2291.

Beebee, R.A. And M. Manga 2004. Variation In The Relationship Between Snowmelt Runoff In Oregon And ENSO And PDO. Journal American Water Resources Association, **40**(4):1011-1024.

Bjerknes, J., 1964. Atlantic Air–Sea Interaction. *Advances In Geophysics,* **10**:1–82.

Blackmon, M.L., 1976. A Climatological Spectral Study of the 500 mb Geopotential Height of the Northern Hemisphere. *J. of Atmospheric Sciences* 33(8):1607-1623.

Booker, J.F. 1995. Hydrologic And Economic Impacts Of Drought Under Alternative Policy Responses. *Water Resourc. Bull.,* **31**(5), 889-906

Bracken, C., B. Rajagopalan, J. Prairie. 2010. A multisite seasonal ensemble streamflow forecasting technique. Water Resour. Res. 46:3,

Brandon, D.G., 1998. Forecasting Streamflow In The Colorado And Great Basins Using El Niño Indices As Predictors In A Statistical Water Supply Forecast System. Floodplain Management Association, San Diego, CA.

Bretherton, C. S., C. Smith, And J. M. Wallace 1992. An Intercomparison Of Methods For Finding Coupled Patterns In Climate Data, *J. Of Climate.*, 5, 541– 560.

Cayan, D.R., And D.H. Peterson, 1989. The Influence Of North Pacific Atmospheric Circulation On Streamflow In The West. Aspects Of Climate Variability In The Pacific And The Western Americas, American Geophysical Union, Geophysical Monograph Series, 55:375-397.

Cayan, D.R., And R.H. Webb, 1992. El Niño/Southern Oscillation And Streamflow In The Western United States. El Niño: Historical And Paleoclimatic Aspects Of The Southern Oscillation. Cambridge University Press, New York, NY.

Casola, J.H. and J.M. Wallace. 2007. Identifying Weather Regimes in the Wintertime 500-hPa Geopotential Height Field for the Pacific–North American Sector Using a Limited-Contour Clustering Technique. *J. of App. Meteorol. and Climatol.* 46:10, 1619-1630

Chao, Y., M. Ghil And J.C. Mcwilliams 2000. Pacific Interdecadal Variability In The Century's Sea Surface Temperatures. *Geophys. Res. Lett.,* 27, 2261-2264.

Chen, T.-C., 1985. Global Water Vapor Flux and Maintenance During FGGE. *Mon. Wea. Rev.,* 113**:** 1801-1819.

Cholaw B., J. Liren 1999. The Ocean-Atmosphere Coupled Regimes And East Asian Winter Monsoon (EAWM) Activity. *Advances In Atmospheric Sciences* 16(1): 91.

Clark, W. G., S. R. Hare, A. M. Parma, P. J. Sullivan And R. J. Trumble 1999. Decadal Changes In Growth And Recruitment Of Pacific Halibut (Hippoglossus Stenolepis). *Can. J. Fish. Aquat. Sci.*, 56, 173–183.

Clark, M. P., M. C. Serreze, And G. J. Mccabe 2001. Historical Effects Of El Niño And La Nina Events On The Seasonal Evolution Of The Montane Snowpack In The Columbia And Colorado River Basins, *Water Resour. Res.*, 37(3), 741–757.

Day, G.A. 1985. Extended Streamflow Forecasting Using NWSRFS *J. Of Water Resour Plng And Mgmt.* 111(2) 157 – 170

Deser, C., And M. L. Blackmon 1993. Surface Climate Variations Over The North Atlantic Ocean During Winter: 1900–1989. *J.Climate,* 6:1743–1753.

Dettinger, M.D., D.R. Cayan, H.F. Diaz, and D. M. Meko, 1998. North-South Precipitation Patterns in Western North America on Interrannual-to-Decadal Timescales. *J.Clim.* 11:3095-3111

Diaz, H.F., And V. Markgraf (Eds.) 1992. *El Niño: Historical And Paleoclimatic Aspects Of The Southern Oscillation.* Cambridge University Press, New York, NY

Diaz, H.F., And V. Markgraf (Eds.) 2000. "El Niño And The Southern Oscillation: Multiscale Variability And Global And Regional Impacts" Cambridge University Press, New York, NY

Dijkstra, H.A., L. Raa, M. Schmeits, And J. Gerrits 2006. On The Physics Of The Atlantic Multidecadal Oscillation. *Ocean Dynamics* 56:36-50

Dima, M., And G.Lohmann 2007. A Hemispheric Mechanism For The Atlantic Multidecadal Oscillation. *J. Clim* 20, 2706-2719

Dracup, J.A., And E. Kahya, 1992. The Potential For Long-Range Streamflow Forecasting Based On ENSO. Proceedings Of The Sixteenth Annual Climate Diagnostics Workshop, Los Angeles, CA.

Druce, D.J. 2001 Insights From a History of Seasonal Inflow Forecasting With a Conceptual Hydrologic Model. *J. Hydrology*. 249:102-112

Dugam SS, Kakade SB,Verma RK 1997. Interannual And Long-Term Variability In The North Atlantic Oscillation And Indian Summer Monsoon Rainfall. *Theoretical And Applied Climatology* 58(1-2): 21.

Durkee JD, J.D. Frye, C.M. Fuhrmann, M.C. Lacke, H.G. Jeong, And T.L. Mote 2008. Effects Of The North Atlantic Oscillation On Precipitation-Type Frequency And Distribution In The Eastern United States. *Theoretical And Applied Climatology* 94(1-2): 51.

Epstein, E.S. 1969 Stochastic Dynamic Prediction. *Tellus*, 21:739-759

Efron, B. 1979. Bootsrap Methods: Antoher Look At The Jacknife. *Ann. Statist.* 7:1-26

Efron, B. 1982. The Jacknife, The Bootsrap, And Other Resampling Plans. *CBMS-NSF Regional Conference Series In Applied Mathematics No. 38. Society For Industrial And Applied Mathematics.* Philadelphia, P.A.

Ely, L. L., Y. Enzel, and D.R. Cayan, 1994. Anamalous North Pacific Atmospheric Circulation and Large Winter Floods in the Southwestern United States, *J. Climate*, 7: 977-987.

Enfield, D.B., A.M Mestas-Nuñez, And P.J. Trimble, 2001. The Atlantic Multidecadal Oscillation And Its Relation To Rainfall And River Flows In The Continental U.S. *Geophysical Research Letters,* 28(10):2077-2080.

Faber, B.A. and J.R. Stedinger 2001. Reservoir Optimization Using Sampling SDP With Ensemble Streamflow Prediction (ESP) Forecasts. *J. Hydrology*.

Frei A, And D.A. Robinson 1999. Northern Hemisphere Snow Extent: Regional Variability 1972-1994. *International Journal Of Climatology* 19(14): 1535.

Fulp, T.J., Theobald, D.M., Williams, B., And Vickers, B 1991. "Decision Support For Colorado River Operations." In: *Waterpower '91: A New View Of Hydro Resources, Proc. Of The Intl. Conf. On Hydropower,* New York, NY. 2144-2151

García, J., T. Losada And B. Rodríguez-Fonseca 2006. Modulación De Las Teleconexiones Sobre Europa: Pacífico Y Atlántico Tropical. *5ª Asamblea Hispano-Portuguesa De Geodesia Y Geofísic, Sevilla 2006*.

Garrick, D., K. Jacobs, And G. Garfin. 2008. Models, Assumptions, And Stakeholders: Planning For Water Supply Variability In The Colorado River Basin. *JAWRA* 44(2), 381-398.

George S.E., M.A. Saunders 2001. North Atlantic Oscillation Impact On Tropical North Atlantic Winter Atmospheric Variability. *Geophysical Research Letters* 28(6): 1015.

Gerreaud, R.D. And D.S. Battisti 1999: Interannual ENSO And Interdecadal ENSO-Like Variability In The Southern Hemisphere Tropospheric Circulation. *J. Clim.* 12, 2113-2123.

Gershunov, A., And T.P. Barnett, 1998. Interdecal Modulation Of ENSO Teleconnections. Bulletin Of The American Meteorological Society (79):2715-2725.

Gilmore, A.; Magee, T.; Fulp, T.; And Strzepek, K 2000. Multiobjective Optimization Of The Colorado River. In: *Joint Conf. Of Water Resourc. Eng. And Water Resourc. Plng. And Mgmt.* 104(5).

Girardin, M.P. J.C. Tardif, M.D. Flanningan, And Y. Bergeron 2006. Synoptic-Scale Atmospheric Circulation And Boreal Canada Summer Drought Variability Of The Past Three Centuries, *J. Clim.* 19:1922-1947

Gleeson, T.A. 1961 A Statistical Theory of Meterological Measurements and Predictions. *J. of Meteorology.* 18:192-198

Gleeson, T.A. 1970. Statistical-dynamical Predictions. *J. of Applied Meteorology.* 9:333-344

Gochis, D.J., L. Brito-Castillo, W.J. Shuttleworth. 2007. Correlations between sea-surface temperatures and warm season streamflow in northwest Mexico. International Journal of Climatology 27(7): 883-901

Goebbert, K.H., L.M. Leslie, 2010. Interannual Variability of Northwest Australian Tropical Cyclones. *J. Climate*, 23: 4538–4555.

Goldenberg, S.B., C.W. Landsea, A.M. Mestas-Nunez, And W.M. Gray 2001. The Recent Increase In Atlantic Hurricane Activity: Causes And Implications. *Science.* 293(5529) 474-479.

Grantz, K., B. Rajagopalan, M. Clark, And E. Zagona 2005. A Technique For Incorporating Large-Scale Climate Information In Basin-Scale Ensemble Streamflow Forecasts, *Water Resour. Res.*, 41, W10410, Doi:10.1029/2004WR003467.

Grassi B, G. Redaelli, And G. Visconti 2009. Evidence For Tropical SST Influence On Antarctic Polar Atmospheric Dynamics. *Geophysical Research Letters* 36(9): L09703.

Gray, S.T., L.J. Graumlich, J.L. Betancourt, And G.T. Pederson 2004. A Tree-Ring Based Reconstruction Of The Atlantic Multidecadal Oscillation Since 1567 A.D. *Geophys. Res. Letters.* 31(L12205)

Grise, K.M., D.W. J. Thompson, T. Birner. 2010. A Global Survey of Static Stability in the Stratosphere and Upper Troposphere. J. of Clim 23:9, 2275-2292

Hamlet, A.F., And D.P. Lettenmaier, 1999. Columbia River Streamflow Forecasting Based On ENSO And PDO Climate Signals. *J. Of Water Res. Plan. And Mgmt.*, 125(6), 333-341.

Hamlet A.F., D. Huppert, and D.P. Lettenmaier 2002. Economic Value of Long-Lead Streamflow Forecasts for Columbia River Hydropower. *J. of Water Resourc. Plng and Mgmt.* 128(2): 91 – 101.

Hanson, K., And C.A. Maul, 1991. Florida Precipitation And The Pacific El Niño, 1895-1989. Florida Scientist 54:160-168.

Hare, S. R., N. J. Mantua And R. C. Francis 1999. Inverse Production Regimes: Alaskan And West Coast Salmon. *Fisheries*, 24, 6–14.

Harnack, R.P., D.T. Jensen, and J.R.Cermak, 1998. Investigation of upper-air conditions occurring with heavy summer rain in Utah. *Int. J. Climatol.,* 18: 701-723.

Harshburger, B., H. Ye, And J. Dzialoski, 2002. Obervational Evidence Of The Influence Of Pacific Sea Surface Temperatures On Winter Precipitation And Spring Stream Discharge In Idaho. Journal Of Hydrology 264(1-4):157-169.

Haylock, M. R., P. D. Jones, R. J. Allan, and T. J. Ansell, 2007. Decadal changes in 1870–2004 Northern Hemisphere winter sea level pressure variability and its relationship with surface temperature. J. of Geophys. Res. 112, D11103

Hidalgo, H.G., 2004. Climate Precursors Of Multidecadal Drought Variability In The Western United States, Journal Of Water Resources Research 40(12).

Hidalgo, H.G., & J.A. Dracup 2003. ENSO & PDO Effects On Hydrclimactic Variations Of The Upper Colorado River Basin. *J. Of Hydrometeorology*, Vol 4.(1)

Hidalgo, H.G. And J.A. Dracup, 2004. Evidence Of The Signature Of North Pacific Multidecadal Processes On Precipitation And Streamflow Variations In The Upper Colorado River Basin, Pending Publication.

Higuchi K., J. Huang And A. Shabbar 1999. A Wavelet Characterization Of The North Atlantic Oscillation Variation And Its Relationship To The North Atlantic Sea Surface Temperature. *International Journal Of Climatology* 19(10): 1119.

Hodson, D.L.R., et al. 2009. Climate Impacts Of Recent Multidecadal Changes In Atlantic Ocean Sea Surface Temperature: A Multi-Model Comparison. *Clim. Dynam.* 14 Apr 2009.

Holland, G.J. And P.J. Webster 2007. Heightened Tropical Cyclone Activity In The North Atlantic: Natural Variability Or Climate Trend? *Phil. Trans. R. Soc. A* 15 November 2007 365(1860):2695-2716

Hurell, J.W., 1995. Decedal Trends in the North Atlantic Oscillation: Regional Temperatures and Precipitation. *Science*. 269:676-679

Ionita M., N. Rimbu, And G. Lohmann 2009. Decadal Variability Of The Elbe River Streamflow. *International Journal Of Climatology*. Under Review.

Jeong, D, Kim, Y 2005. Rainfall-Runoff Models Using Artificial Neural Networks for Ensemble Streamflow Prediction. *Hydrological Processes*. 19(19):3819-3835.

Johnstone, J.A. 2010 A quasi-biennial signal in western US hydroclimate and its global teleconnections. Climate Dynamics

Kahya, E., And J.A. Dracup 1993. U.S. Streamflow Patterns In Relation To The El Niño / Southern Oscillation. Journal Of Water Resources Research, 29(8):2491-2503.

Kahya, E., And J.A. Dracup 1994a. The Influences Of Type 1 El Niño And La Niña Events On Streamflows In The Pacific Southwest Of The United States. Journal Of Climate 7(6):965-976.

Kahya, E., And J.A. Dracup 1994b. The Relationships Between U.S. Streamflow And La Niña Events. Journal Of Water Resources Research, 30(7):2133-2141.

Kalra, A. and S. Ahmad 2009. Using Oceanic-Atmospheric Oscillations for Long Lead Time Streamflow Forecasting. *Water Resourc. Res.* 45: W03413

Karcher M, F. Kauker, R. Gerdes, E. Hunke, And J. Zhang 2007. On The Dynamics Of Atlantic Water Circulation In The Arctic Ocean. *Journal Of Geophysical Research.* 112(C4): C04S02

Kalnay et al.,1996. "The NCEP/NCAR 40-year Reanalysis Project" Bull. Amer. Meteor. Soc., 77, 437-470

Keenlyside, N.S., et al 2008. Advancing Decadal-Scale Climate Prediction In The North Atlantic Sector. *Nature* 453:84-88.

Kelley, M.H. And J.A. Gore 2008. Florida River Flow Patterns And The Atlantic Multidecadal Oscillation. *River. Res. Applic.* 24:598-616

Kerr, R. A., 2000. A North Atlantic Climate Pacemaker For The Centuries. *Science*, 288:1984-1986.

Kiladis, G.N., And H.F. Diaz 1989. Global Climatic Anomalies Associated With Extremes In The Southern Oscillation. *J. Clim* 2(1):69-90.

Kim B, S. Moon, L. Riyu, R.H. Kripalani 2002. Teleconnections: Summer Monsoon Over Korea And India. *Advances In Atmospheric Sciences* 19(4): 665.

Kim, T, J.B. Valdes, B. Nijssen, & D. Roncayolo 2006. Quantification Of Linkages Between Large-Scale Climatic Patterns And Precipitation In The Colorado River Basin" *J. Of Hydrology*. 321: 173-186

Kim, T., C. Yoo., & J. Ahn 2007. Influence Of Climate Variation On Seasonl Precipitation In The Colorado River Basin" *Stochastic Environmental Research And Risk Assessment,* 22(3):411-420

Knight, J.R., R.J. Allan, C.K. Folland, M. Vellinga, And M.E. Mann 2005. A Signature Of Persistent Natural Thermohaline Circulation Cycles In Observed Climate. *Geophys. Res. Letters* 32(L20708)

Knight, J. R., C. K. Folland, And A. A. Scaife 2006. Climate Impacts Of The Atlantic Multidecadal Oscillation, *Geophys. Res. Letters,* 33, L17706

Krzysztofowicz, R. 1999. Bayesian Theory of Probabilistic Forecasting Via Deterministic Hydrologic Model. *Water Resour. Res.* 35(9):2739 - 2750

Krzysztofowicz, R. 2001. The Case for Probabilistic Forecasting in Hydrology. *J. Hydrology*. 249: 2 – 9

Kushnir, Y., 1994. Interdecadal Variations in North Atlantic Sea Surface Temperature and Associated Atmospheric Conditions. *J. Clim*. 7:141-157

Kushnir Y., W.A Robinson, P. Chang, And A.W. Robertson 2006. The Physical Basis For Predicting Atlantic Sector Seasonal-To-Interannual Climate Variability. *Journal Of Climate* 19(23): 5949.

Kvam, P.H. And B. Vidakovic 2007. *Nonparametric Statistics With Applications To Science And Engineering*. Hoboken, N.J. Wiley-Interscience, C2007

Lamb, K.W., T.C. Piechota, O.A. Azizz, and G.A. Tootle, 2010. Establishing a Basis for Extending Long-Term Forecasts in the Colorado River Basin. J of Hydrologic Engineering (In Press)

Latif, M And T.P. Barnett 1994. Causes Of Decadal Climate Variability Over The North Pacific And North America. *Science* 266: 634-637

Leith, C.E. 1974. Theoretical Skill of Monte-Carlo Forecasts. *Monthly Weather Review*, 102:409-418

Lin, H. 2009. Global Extratropical Response to Diabatic Heating Variability of the Asian Summer Monsoon. J. of the Atmospheric Sciences 66:9, 2697-2713

Lu, R., B. Dong, And H.Ding 2006. Impact Of The Atlantic Multidecadal Oscillation On The Asian Summer Monsoon. *Geophys. Res. Letters* 33(L24701)

Lundquist, J.D. A.L. Flint. 2006. Onset of Snowmelt and Streamflow in 2004 in the Western United States: How Shading May Affect Spring Streamflow Timing in a Warmer World. J. of Hydrometeorology 7(6): 1199-1217

Macklin M.G. And B.T. Rumsby 2007. Changing Climate And Extreme Floods In The British Uplands. *Transactions Of The Institute Of British Geographers* 32(2): 168.

Mann, H.B. And D.R. Whitney 1947. On A Test Of Whether One Of Two Random Variables Is Stochastically Larger Than The Other. *The Annals Of Mathematical Statistics*. 18(1), 50-60

Mantua, N. J., And S. R. Hare 2002. The Pacific Decadal Oscillation, J. Oceanography, 59(1), 35– 44.

Maurer, E.P., D.P. Lettenmaier, 2003. Predictability of Seasonal Runoff in the Mississippi River Basin, *J. Geophys. Res.* 108(D16) 8607

Mauer, E.P., D.P. Lettenmaier And N.J. Mantua, 2004. Variability And Potential Sources Of Predictability Of North American Runoff, Pending Publication.

Marshall, J., Y. et al. 2001. North Atlantic Climate Variability: Phenomena, Impacts And Mechanisms. *Int J Of Climatology* 21:1863-1898

Mccabe, G. J. And M. D. Dettinger 1999. Decadal Variations In The Strength Of Enso Teleconnections With Precipitation In The Western United States. *Int J Of Climatology* 19 1399-1410 (1999)

Mccabe, G.J. And M.D. Dettinger, 2002. Primary Modes And Predictability Of Year-To-Year Snowpack Variations In The Western United States From Teleconnections With Pacific Ocean Climate. Journal Of Hydrometeorology, 3(1):13-25.

Mccabe, Gregory J., Julio L. Betancourt, And Hugo G. Hidalgo, 2007. Associations Of Decadal To Multidecadal Sea-Surface Temperature Variability With Upper Colorado River Flow. *J Of The Amer Water Res. Assoc.* 43:183-192.

Mcfarlane, G. And R. J. Beamish 1992. Climatic Influence Linking Copepod Production With Strong Year-Classes In Sablefish, Anaplopoma Fimbria. *Can. J. Fish. Aquat. Sci.,* 49, 743–753.

Miller, N.L., J. Kim, J.Y. Zhang, J. Oh. 2001. Coupled Precipitation-Streamflow Simulations at the GAME/HUBEX Site: Sixian Basin. J. of the Meteorological Society of Japan 79(5): 985-998

Miller W.D., D.G. Kimmel, And L.W. Harding 2006. Predicting Spring Discharge Of The Susquehanna River From A Winter Synoptic Climatology For The Eastern United States. *Water Resources Research* 42(5): W05414.

Miller, W.P. and T.C. Piechota 2008. Regional Analysis Of Trend And Step Changes Observed In Hydroclimatic Variables Around The Colorado River Basin. *J. Of Hydrometeorology*. 9, 1020.

Milly, C., et al. (2008), Stationary is dead: Whither water management, Science, 318, 573–574.

Minobe, S. 1997. A 50-70 Year Climatic Oscillation Over The North Pacific And North America. *Geophys. Re. Lett.,* 24, 683-686.

Mo, K.C., G.H. White, 1985. Teleconnections in the Southern Hemisphere. *Mon. Wea. Rev.*, 113: 22–37.

Monahan, A.H., And A. Dai 2004. The Spatial And Temporal Structure Of ENSO Nonlinearity. *J. Clim.* 17(15):3026-3036.

Morin J, P. Block, B. Rajagopalan, And M. Clark 2008. Identification Of Large Scale Climate Patterns Affecting Snow Variability In The Eastern United States. *International Journal Of Climatology* 28(3): 315.

Muñoz E., And D. Enfield 2009. The Boreal Spring Variability Of The Intra-Americas Low-Level Jet And Its Relation With Precipitation And Tornadoes In The Eastern United States, *Clim. Dynam.*

Nakamura, H 1996. Year-To-Year And Interdecadal Variability In The Activity Of Intraseasonal Fluctuations In The Northern Hemisphere Wintertime Circulation. *Theoretical And Applied Climatology* 55(1-4): 19

National Resources Conservation Service (NRCS), National Water And Climate Center, 1997. Southern Oscillation Index Statistical Correlation With Spring Runoff In The Western United States – Report.

Nitta, T. And S. Yamada 1989: Recent Warming Of Tropical Sea Surface Temperatures And Its Relationship To The Northern Hemisphere Circulation. *J. Meteor. Soc. Japan,* 67, 375-383.

Oikonomou C., H.A. Flocas, M. Hatzaki, A. Nisantzi, D.N. Asimakopoulos 2010. Relationship Of Extreme Dry Spells In Eastern Mediterranean With Large-Scale Circulation. *Theoretical And Applied Climatology* 100(1-2): 137

Ottersen G., B. Ãdlandsvik, And H. Loeng 2000. Predicting The Temperature Of The Barents Sea. *Fisheries Oceanography* 9(2): 121.

Pauluis, O., A. Czaja, R. Korty, 2010. The Global Atmospheric Circulation in Moist Isentropic Coordinates. J. of Climate 23(11): 3077-3093

Patricola, C.M., K.H. Cook. 2009 Northern African climate at the end of the twenty-first century: an integrated application of regional and global climate models. Climate Dynamics

Piechota, T.C., And J.A. Dracup, 1996. Drought And Regional Hydrologic Variation In The United States: Associations With El Niño-Southern Oscillation. Journal Of Water Resources Research, 32(5):1359-1373.

Piechota T.C., And J.A. Dracup, And R.G. Fovell, 1997. Western U.S. Streamflow And Atmospheric Circulation Patterns During El Niño-Southern Oscillation. Journal Of Hydrology, 201:249-271.

Piechota, T.C., F.H.S. Chiew, J.A. Dracup, And T.A. Mcmahon 1998. Seasonal Streamflow Forecasting In Eastern Australia And The El Niño-Southern Oscillation. *Journal Of Water Resources Research*, 34(11), 3035-3044.

Potts, J.M., C.K. Folland, I.T. Jolliffe, And D. Sexton, 1996. Revised "LEPS" Scores For Assessing Climate Model Simulations And Long-Range Forecasts. *J. Climate,* 9, 34-53.

Power, S., F. Tseitkin, S. Totrok, B. Lavery, R. Dahni And B. Mcavaney 1997. Australian Temperature, Australian Rainfall And The Southern Oscillation, 1910-1992: Coherent Variability And Recent Changes. *Austr. Meteorol. Mag.* 47:85-101

Power, S., F. Tseitkin, V. Mehta, B. Lavery, S. Torok And N. Holbrook 1999a. Decadal Cliamte Variability In Australia During The Twentieth Century. *Int J. Climatol.,* 19:169-184

Power, S., T. Casey, C. Folland, A. Coleman, And V. Mehta 1999b. Interdecadal Modulation Of The Impact Of ENSO On Australia. *Clim. Dyn.,* 15:319-324

Prohaska, J. 1976. A Technique For Analyzing The Linear Relationships Between Two Meterological Fields. *Monthly Weather Review.* 104 , 1345 – 1353.

Rajagopalan, B., And U. Lall, 1999. A K-Nearest Neighbor Simulator For Daily Precipitation And Other Weather Variables, *J. Of Water. Resour. Res.* 35(10):3089-3101

Rajagopalan, B., E. Cook, U. Lall, And B. K. Ray 2000, Spatiotemporal Variability Of ENSO And SST Teleconnections To Summer Drought Over The United States During The Twentieth Century, *J. Clim*, 13, 4244– 4255.

Rasmussen EM, Wallace JM. 1983. Meteorological Aspects Of The El Niño/Southern Oscillation. *Science* 222: 1195–1202.

Redmond, K.T., And R.W. Koch, 1991. Surface Climate And Streamflow Variability In The Western United States And Their Relationship To Large-Scale Circulation Indices. Water Resources Research, 27(9):2381-2399.

Richter, I., S.-P. Xie, 2009. Moisture transport from the Atlantic to the Pacific basin and its response to North Atlantic cooling and global warming. Climate Dynamics

Rogers, Jeffery C., 1990. Patterns of Low-Frequency Monthly Sea Level Pressure Variability (1899–1986) and Associated Wave Cyclone Frequencies. *J. Climate*, 3: 1364–1379.

Rogers, J.C And J.S.M.Coleman 2003. Interactions Between The Atlantic Multidecadal Oscillation, El Niño/Laniña, And The PNA In Winter Mississippi Valley Stream Flow, *Geophys. Res. Lett.,* 30(10):1518

Ropelewski, C.F., And M.S. Halpert, 1986. North American Precipitation And Temperature Patterns Associated With The El Niño / Southern Oscillation. *Monthly Weather Review*, 114(2):2352-2362.

Ropelewski, C.F., And M.S. Halpert, 1989. Precipitation Patterns Associated With The High Index Phase Of The Southern Oscillation. *J. Of Clim.* 2:268-284.

Roundy, P.E., L.M. Gribble-Verhagen, 2010. Variations in the Flow of the Global Atmosphere Associated with a Composite Convectively Coupled Oceanic Kelvin Wave. Journal of Climate 23:15, 4192-4201

Roundy, P.E., K. MacRitchie, J. Asuma, T. Melino. 2010. Modulation of the Global Atmospheric Circulation by Combined Activity in the Madden–Julian Oscillation and the El Niño–Southern Oscillation during Boreal Winter. Journal of Climate 23:15, 4045-4059

Sangoyomi, T.B., And Harding, B.L. 1995. "Mitigating Impacts Of A Severe Sustained Drought On Colorado River Water Resources." *Water Resour. Bull.* 31(5) 925-938

Santos, J. A., J. Corte-Real, U. Ulbrich and J. Palutikof, 2007. European Winter Precipitation Extremes and Large-Scale Circulation: A Coupled Model and its Scenarios. Theor. Appl. Climatol. 87, 85–102

Schlesinger, M.E. And N. Ramankutty 1994. An Oscillation In The Global Climate System Of Period 65–70 Years. *Nature* **367**:723 - 726

Schmidt, N., And E.K. Lipp, J.B. Rose, And M.E. Luther, 2001. ENSO Influences On Seasonal Rainfall And River Discharge In Florida. Journal Of Climate – Notes And Correspondence **14**:615-628.

Schuster, R.J. 1989 "The Colorado River Simulation System." *Hydraulic Engineering,* ASCE New York, NY, M. Ports, Ed. 473-478

Serrano Mendoza, E., And B. Rodriguez De Fonseca 2004 Dinámica De La Columna Atmosférica En La Teleconexión Entre Anomalías Superficiales Oceánicas En El Atlántico Subtropical Y La Variabilidad Climática En El Sector Euro-Atlántico. *Física De La Tierra*, **16**:49-59

Shabbar, A., B. Bonsal, And M. Khandekar, 1997. Canadian Precipitation Patterns Associated With The Southern Oscillation. *J. Clim.* 10, 3016-3027

Shabbar A, And W. Skinner, 2004. Summer Drought Patterns In Canada And The Relationship To Global Sea Surface Temperatures. *J. Clim.* 17(14): 2866.

Shafer, J.C. and W.J. Steenburgh, 2008. Climatology of Strong Intermountain Cold Fronts, *Mon. Wea. Rev.,* **136**:784-807.

Shentsis, I., A. Ben-Zvi 2001 Considering Diversity in Precipitation Variability When Updating Seasonal Flow Forecasts. *J. Hydrology* **249**: 87 - 101

Shuanglin, L., And G.T. Bates 2003 Influence Of The Atlantic Multidecadal Oscillation On The Winter Climate Of East China, *Adv. In Atmos. Sci.*, **24**(1):126–135

Shi, X., A.W. Wood, D.P. Lettenmaier, 2008. How Essential is Hydrologic Model Calibration to Seasonal Streamflow Forecasting? J. of Hydrometeorology 9(6): 1350-1363

Simpson, J.J., M.D. Dettinger, F.Gehrke, T.J. McIntire, G.L. Hufford, 2004. Hydrologic Scales, Cloud Variability, Remote Sensing, and Models: Implications for Forecasting Snowmelt and Streamflow. Weather and Forecasting 19(2): 251-276

Skinner W.R., A. Shabbar, M.D. Flannigan, And K. Logan 2006 Large Forest Fires In Canada And The Relationship To Global Sea Surface Temperatures. *Journal Of Geophysical Research* **111**(D14): D14106.

Smith, T.M., And R.W. Reynolds 2003. Extended Reconstruction Of Global Sea Surface Temperatures Based On COADS Data (1854-1997). *J. Clim.*, **16:**1495-1510.

Smith, T.M., And R.W. Reynolds, 2004. Improved Extended Reconstruction Of SST (1854-1997). *J Of Clim.*, **17**: 2466-2477.

Smith, T.M., R.W. Reynolds, Thomas C. Peterson, and Jay Lawrimore, 2008: Improvements to NOAA's Historical Merged Land-Ocean Surface Temperature Analysis (1880-2006). Journal of Climate,21, 2283-2296.

Soukup, T., O., Aziz, G. Tootle, S. Wulff And T. Piechota 2010. Incorporating Climate Into A Long Lead-Time Non-Parametric Streamflow Forecast. *J Of Hydrology* (In Press).

Souza Filho, F.A. and U. Lall 2003. Seasonal to Interannual Ensemble Streamflow Forecasts for Ceara, Brazil: Applications of a Multivariate, Semiparametric Algorithm. *J. Water Resourc. Res.* **39** (11): 1307

Stevens, D. 1986. "Computer Models In Lower Colorado River Operations". *J. Of Water Resour. Plng. And Mgmt.* 112 (3) Pp. 395-408

Sutton R.T. And D.L.R. Hodson, 2005. Atlantic Ocean Forcing Of North American And European Summer Climate. *Science*, 309:115-118.

Thompson, D.W.J. and J.M. Wallace, 1998. The Arctic Oscillation Signature in the Wintertime Geopotential Height and Temperature Fields, Geophys. Res. Letters, 25(9): 1297-1300. May 1, 1998

Timilsena, J.A., T.C. Piechota, H Hidalgo, G.A. Tootle 2007 "Five Hundred Years Of Hydrological Drought In The Upper Colorado River Basin" J Of Amer. Water Res. Assoc., 43(3): 798-812

Timilsena, J.A., T.C. Piechota, G.A. Tootle, And A.K. Singh 2009. Associations Of Interdecadal/Interannual Climate Variability And Long-Term Colorado River Basin Streamflow. *J. Of Hydrology*. 365(3-4), 289-301.

Tootle, G.A., And T.C. Piechota, 2004. Suwannee River Long-Range Streamflow Forecasts Based On Seasonal Climate Predictors. *Journal Of The American Water Resources Association,* 40(2), 523-532.

Tootle, G.A., T.C. Piechota, A.K. Singh 2005. Coupled Oceanic-Atmospheric Variability And US. Streamflow. *Water Resour. Res*, 41, W12408 Doi:10.1029/2005WR004381

Tootle, G. A., And T. C. Piechota 2006. Relationships Between Pacific And Atlantic Ocean Sea Surface Temperatures And U.S. Streamflow Variability, *Water Resour. Res.,* W07411, Doi:10.1029/2005WR004184.

Tootle, G.A., A.K. Singh, T.C. Piechota, And I. Farnham 2007. Long Lead-Time Forecasting Of U.S. Streamflow Using Partial Least Squares Regression. *J. Hydrologic Engrg.* 12(5):442-451.

Tootle, G.T. et al, 2009. 2009-2010 El Niño: Hydrologic Relief For Parts Of The U.S.?. EOS Transactions, 90(50), 481-292.

Trenberth, K.E. 1990. Recent Observed Interdecadal Climate Changes In The Northern Hemispheric. *Bull Amer. Meteor Soc.,* **71**, 988-993.

Trenberth, K.E. And J.W. Hurell, 1994. Decadal Atmosphere-Ocean Variations In The Pacific. *Clim. Dyn.,* **9**, 303-319

Trenberth, K.E. And D.J.Shea 2006 Atlantic Hurricanes And Natural Variability In 2005. *Geophys. Res. Letters* **33**(L12704)

Twine, T.E., C.J. Kucharik, J.A. Foley. 2005. Effects of El Niño–Southern Oscillation on the Climate, Water Balance, and Streamflow of the Mississippi River Basin. J. of Climate 18(22): 4840-4861

Ukita J., et al. 2007. Northern Hemisphere Sea Ice Variability: Lag Structure And Its Implications. *Tellus A* **59**(2): 261.

Van Loon, H. And J.C. Rogers 1978. The Seesaw In Winter Temperatures Between Greenland And Northern Europe. Part I: General Description. *Month. Weath. Rev.* **106**(3):296-310

Visbeck, M., et al 2002. The Ocean's Response To North Atlantic Oscillation Variability. The North Atlantic Oscillation: Climatic Significance And Environmental Impact, *Geophys. Monogr.*, **134**:113–145.

Walker, G.T. 1923. Correlation Inseasonal Variations Of Weather. Part VIII: A Preliminary Study Of World Weather. *Memoirs Of The Indian Meteorological Department,* **24**:75-131

Walker, G.T. And E.W. Bliss 1932. World Weather V. *Memoirs Of The Royal Meteorological Society* 4:53-84.

Wallace, J.M. and D.S. Gutzler, 1981. Teleconnections in the Geopotential Height Field During the Northern Hemisphere Winter, *Mon Wea. Rev.* **109**:784-812

Wallace, J. M., D. S. Gutzler, And C. S. Bretheron 1992, Singular Value Decomposition Of Wintertime Sea Surface Temperature And 500-Mb Height Anomalies, J. Clim., 5, 561–576.

Wang, H. And M. Ting 2000 Covariabilities Of Winter U.S. Precipitation And Pacific Sea Surface Temperatures. *J. Clim* Oct, 3711-3719.

Wang, S., R. R. Gillies, J. Jin, and L. E. Hipps, 2009. Recent Rainfall Cycle in the Intermountain Region as a Quadrature Amplitude Modulation From the Pacific Decadal Oscillation. Geophys Res Letters 36, L02705.

Wang, S., L.E. Hipps, R.R. Gillies, X. Jiang, A.L. Moller, 2010a. Circumglobal teleconnection and early summer rainfall in the US Intermountain West. Theoretical and Applied Climatology, DOI: 10.1007/s00704-010-0260-4

Wang, S., R. R. Gillies, J. Jin, and L. E. Hipps, 2010b. "Coherence Between the Great Salt Lake Level and the Pacific Quasi-Decadal Oscillation. J. Climate, 23, 2161-2177.

Wang, S., R. R. Gillies, L. E. Hipps, and J. Jin, 2010c. A Transition-Phase Teleconnection of the Pacific Quasi-Decadal Oscillation. Clim Dyn. DOI: 10.1007/s00382-009-0722-5

Ward M.N., Folland C.K. 1991. Prediction Of Seasonal Rainfall In The North Nordeste Of Brazil Using Eigenvectors Of Sea-Surface Temperature. *International Journal Of Climatology* 11: 711–743.

Werner, K., D. Brandon, M. Clark, S. Gangopadhyay 2004. Climate Index Weighting Schemes For NWS ESP-Based Seasonal Volume Forecasts. J. Hydrometerology. 5, 1076-1090.

Wilcoxon, F. 1945. "Individual Comparisons By Ranking Methods." *Biometrics Bulletin* 1(6), 80-83

Wilks, D.S. 2006. *Statistical Methods In The Atmospheric Sciences*, Academic Press (Elsevier) Burlington, MA

Willmott, C.J., K. Matsuura, 2005. Advantages of the mean absolute error (MAE) over the root mean square error (RMSE) in assessing average model performance. *Clim. Res.* 30:79-82

Wu W, R.E. Dickinson, H. Wang, Y. Liu, And M. Shaikh 2007. Covariabilities Of Spring Soil Moisture And Summertime United States Precipitation In A Climate Simulation. *International Journal Of Climatology* 27(4): 429

Wu, B., R. Zhang, B. Wang, and R. D'Arrigo, 2009. On the association between spring Arctic sea ice concentration and Chinese summer rainfall. Geophys. Res. Ltrs, 36, L09501

Xue Y., S. Sun, K. Lau, J. Ji, I. Poccard, R. Zhang, H. Kang, G. Wu, J.C. Schaake, And J.Y. Zhang 2005. Multiscale Variability Of The River Runoff System In China And Its Long-Term Link To Precipitation And Sea Surface Temperature. *Journal Of Hydrometeorology* **6**(4): 550.

Yang, S., K.-M. Lau, and K.-M. Kim, 2002. Variations of the East Asian Jet Stream and Asian-Pacific –American Winter Cliamte Anomalies. *J. Climate,* **15**(3):306-325

Yang Q. (2009). Impact Of The Indian Ocean Subtropical Dipole On The Precipitation Of East China During Winter Monsoons. *Journal Of Geophysical Research* **114**(D14): D14110.

Yarnal B., And H. F. Diaz, 1986. Relationships Between Extremes Of The Southern Oscillation And The Winter Climate Of The Anglo-American Pacific Coast. *Journal Of Climatology*, 6, 197-219.

Yu, B. 2007. The Pacific–North American pattern associated diabatic heating and its relationship to ENSO. Atmospheric Science Letters, 8: 107–112. doi: 10.1002/asl.160

Yuan, X. and C. Li, 2008. Climate Modes in Southern High Latitudes and Their Impacts on Antarctic Sea Ice. J. of Geophys. Res. Ltrs. 113. C06S91

Zagona, E.A., T.J. Fulp, R. Shane, T. Magee, And H.M. Goranflo 2001. Riverware: A Generalized Tool For Complex Reservoir System Modelling." *JAWRA*. 37(4) 913-929

Zhang, Y., K.R. Sperber, J.S. Boyle 1997a. Climatology and Interannual Variation of the East Asian Winter Monsoon: Results from the 1979-95 NCEP/NCAR Reannalysis. Monthly Weather Review. Oct 1997

Zhang, Y., J.M. Wallace, and D.S. Battisti, 1997b. ENSO-like Interdecadal Variability: 1900-93, J. Clim., 10:1004-1020..

Zhang, R. And T.L. Delworth 2006. Impact Of Atlantic Multidecadal Oscillations On India/Sahel Rainfall And Atlantic Hurricanes. *Geophys. Res. Letters* **33**(L17712)

Zhang, R., And T. L. Delworth 2007. Impact Of The Atlantic Multidecadal Oscillation On North Pacific Climate Variability, *Geophys. Res. Lett.,* **34**(L23708)

Zhao, M., I.M. Held, S. Lin, G.A. Vecchi. 2009. Simulations of Global Hurricane Climatology, Interannual Variability, and Response to Global Warming Using a 50-km Resolution GCM. J. of Climate 22:24, 6653-6678

Zhifang F, And J.M. Wallace 1993. The Relationship Between The Wintertime Blocking Over Greenland And The Sea Ice Distribution Over North Atlantic. *Advances In Atmospheric Sciences* **10**(4): 453.

Zorn, M.R., And P.R. Waylen, 1997. Seasonal Response Of Mean Monthly Streamflow To El Niño / Southern Oscillation In North Central Florida. Professional Geographer 49:51-62.

VITA

Graduate College
University of Nevada, Las Vegas

Kenneth W. Lamb

Degrees:

Bachelor of Science, Civil Engineering, 2003
University of Nevada, Las Vegas

Masters in Civil Engineering, 2007
Norwich University

Publications:

A Basis for Extending Long-Term Streamflow Forecasts in the Colorado River. *Journal of Hydrologic Engineering*, in press, 2010.

Dissertation Title: Improving Ensemble Streamflow Prediction Using Interdecadal/Interannual Climate Variability

Dissertation Examination Committee:

Chairperson, Thomas C. Piechota, Ph.D, P.E.
Committee Member, Jacimaria Batista, Ph.D, P.E.
Committee Member, Sajjad Ahmad, Ph.D.
Committee Member, Ashok K. Singh, Ph.D
Graduate Faculty Representative, Susanna Priest, Ph.D.